Synthesis and Transdermal Penetration of Selected Lamivudine Derivatives

Minja Gerber

B.Pharm., M.Sc. (Pharmaceutical Chemistry)

Thesis submitted in the fulfilment of the requirements for the degree

PHILOSOPHIAE DOCTOR

in the

Faculty of Health Sciences, School of Pharmacy (Pharmaceutical Chemistry)

at the

North-West University

Supervisor: Prof. J.C. Breytenbach

Co-supervisor: Prof. J. du Plessis

Potchefstroom

2007

ABSTRACT

The skin is the most extensive and readily accessible organ in the body. The outermost layer of the skin, the stratum corneum, functions as a barrier, limiting the transport of molecules into and across the skin. Transdermal drug delivery offers several advantages over oral and parenteral dosing that include a non-invasive treatment, improving bioavailability and patient compliance, bypassing of hepatic first pass metabolism, decreasing the administered dose and gastrointestinal adverse effects as well as the quick discontinuation of treatment. A hydrophilic compound will have trouble partitioning into the stratum corneum from its vehicle and a lipophilic compound may have difficulty leaving the stratum corneum. Optimal transport through the skin requires a drug to possess lipophilic as well as hydrophilic properties. Research suggests that a drug should have an aqueous solubility of more than 1 mg/ml and an octanol-water partition coefficient (log P) between 1 and 2 to optimally penetrate the skin.

Approximately 40.3 million people were living with HIV/AIDS at the end of 2005, which is generally treated with Nucleoside Reverse Transcriptase Inhibitors (NRTIs), like zalcitabine and lamivudine. NRTIs have a bitter taste and the most common adverse effects occurring with these two compounds are abdominal pain, nausea, vomiting, diarrhoea and mouth ulcers.

The aim of this study was primarily to determine the transdermal permeation of zalcitabine, lamivudine and the synthesised amide esters of lamivudine, with and without the use of Pheroid™ as delivery system and to establish a correlation, if any, with selected physicochemical properties.

The six amide ester derivatives of lamivudine were prepared by acylation esterification of lamivudine with six different acid chlorides. The structures of the products were confirmed by mass spectrometry (MS), nuclear magnetic resonance spectroscopy (NMR) and infrared spectroscopy (IR).

The aqueous solubility of all compounds was higher at pH 5 than at pH 7. The aqueous solubility of lamivudine at both pH 5 and 7 (114.36 mg/ml and 91.57 mg/ml, respectively) was lower than that of zalcitabine (144.78 mg/ml and 110.16 mg/ml, respectively), but was distinctly higher than that of the synthesised amide esters of lamivudine (ranging from 1.00×10^{-4} to 8.34 mg/ml and 1.00×10^{-4} to 6.16 mg/ml, respectively).

The octanol-PBS partition coefficient (log D) of lamivudine and its amide esters was lower at pH 5 than at pH 7. Of all compounds zalcitabine had the lowest log D at both pH 5 and 7 (-1.50

and -1.78, respectively). The log D of lamivudine at both pH 5 and 7 (-1.19 and -1.15, respectively) was lower than that of the amide esters (ranging from 0.12 to 4.55 and 0.25 to 4.88, respectively). Hence, there was a direct correlation between the aqueous solubility and the log D at both pH 5 and 7 for all compounds.

A comparison between average and median flux of the amide esters of lamivudine show that there is a good correlation between the flux values in PBS and in Pheroid^{TM}, (except for N-butyryllamivudine-5'-buterate). Compounds with higher flux, like zalcitabine and lamivudine, seem to be prone to larger differences between average and median flux. In the occurrence of large variation and skewed distributions of experimental values, the median flux is a more robust measurement. Therefore median flux was used as a more accurate method for determining flux.

In vitro penetration was measured through excised female human abdominal skin in Franz diffusion cells. The median flux of lamivudine (4.289 $\mu mol.cm^{-2}.h^{-1}$) in PBS was higher than that of zalcitabine (0.442 $\mu mol.cm^{-2}.h^{-1}$), but in Pheroid^{TM}, zalcitabine had a slightly higher median flux (0.015 $\mu mol.cm^{-2}.h^{-1}$) than lamivudine (0.011 $\mu mol.cm^{-2}.h^{-1}$). In both PBS and Pheroid^{TM}, the median flux of lamivudine was higher than that of the amide esters (2.0×10^{-4} to 0.046 $\mu mol.cm^{-2}.h^{-1}$ in PBS and 2.0×10^{-4} to 9.3×10^{-3} $\mu mol.cm^{-2}.h^{-1}$ in Pheroid^{TM}). Of all the amide esters of lamivudine, N-acetyllamivudine-5'-acetate (in PBS) and N-propionyllamivudine-5'-propionate (in Pheroid^{TM}) presented the highest flux.

When comparing flux in PBS with that in Pheroid^{TM} it is observed that all the compounds have lower flux in Pheroid^{TM} except N-hexanoyllamivudine-5'-hexanoate. Hence, Pheroid^{TM} does not improve transdermal flux of this series of compounds.

In this study a direct correlation between the aqueous solubility and transdermal flux was found.

A strong statistically significant correlation was observed between flux in both PBS and in Pheroid^{TM} and each of molecular weight, aqueous solubility (at pH 5 and 7), and log D (at pH 5 and 7); as was determined with a 5 % level of confidence using the Spearman correlation.

Yellow spots were observed in the confocal laser scanning microscopy (CLSM) micrographs which confirmed that the compounds were entrapped in Pheroid^{TM}. The more hydrophilic compounds had a decrease in microsponge size as they became more lipophilic from zalcitabine to N-butyryllamivudine-5'-buterate and thereafter an increase was noticed from N-butyryllamivudine-5'-buterate to N-decanoyllamivudine-5'-decanoate. Hence, it seems that hydrophilic drugs permeate easier when entrapped in Pheroid^{TM} than lipophilic compounds.

OPSOMMING

Die vel is die mees omvangryke en geredelik toeganklike orgaan in die liggaam. Die heel buitenste laag van die vel, die stratum corneum, dien as 'n skans wat die beweging van molekules in en deur die vel beperk. Die transdermale toediening van 'n geneesmiddel het verskeie voordele bo orale en parenterale dosering wat insluit 'n nie-indringende behandeling wat biobeskikbaarheid en pasïentinskiklikheid bevorder, ontwyking van die hepatiese eerstedeurgangseffek, vermindering van toegediende dosis en gastro-intestinale newe-effekte sowel as vinnige staking van behandeling. 'n Hidrofiele geneesmiddel mag dit moeilik vind om vanaf sy draermedium in die stratum corneum in te beweeg, terwyl 'n lipofiele geneesmiddel die stratum corneum moeilik verlaat. Vir optimale transdermale deurgang moet die geneesmiddel oor lipofiele sowel as hidrofiele eienskappe beskik. Navorsing toon dat vir 'n geneesmiddel om optimaal deur die vel te penetreer dit 'n wateroplosbaarheid van meer as 1 mg/ml en 'n oktanol-water verdelingskoeffisiënt (log P) tussen 1 en 2 moet hê.

Teen die einde van 2005 was daar ongeveer 40.3 miljoen mense met HIV/VIGS, wat hoofsaaklik behandel word met nukleosied-omgekeerde-transkriptase-remmers (NOTR's), soos salsitabien en lamivudien. NOTR's het 'n bitter smaak en die mees algemene newe-effekte wat voorkom met die twee geneesmiddels is abdominale pyn, naarheid, braking, diarree en mondulkusse.

Die hoofdoel van hierdie studie was om die transdermale penetrasie van salsitabien, lamivudien en enkele gesintetiseerde amiedesters van lamivudien met of sonder die gebruik van Pheroid™ as afleweringsisteem te bepaal en om 'n korrelasie met sekere fisies-chemiese eienskappe, indien enige, te vind.

Die ses amiedesterderivate van lamivudien is deur selektiewe asilering van lamivudien met ses verskillende suurchloriede berei. Die strukture van die produkte van elke sintese is met behulp van massaspektroskopie (MS), kernmagnetieseresonansiespektroskopie (KMR) en infrarooi-spektroskopie (IR) bevestig.

Die eksperimentele wateroplosbaarheid vir al die verbindings was hoër by pH 5 as by pH 7. Die wateroplosbaarheid van lamivudien by sowel pH 5 as 7 (114.36 mg/ml en 91.57 mg/ml, onderskeidelik) was laer as dié van salsitabien (144.78 mg/ml en 110.16 mg/ml, onderskeidelik), maar was beduidend hoër as dié van die gesintetiseerde amiedesters van lamivudien (wissel van 1.00×10^{-4} tot 8.34 mg/ml en 1.00×10^{-4} tot 6.16 mg/ml, onderskeidelik).

Die oktanol-PBS verdelingskoeffisiënt (log D) van lamivudien en sy amiedesters by pH 5 was laer as by pH 7. Van al die verbindings het salsitabien by pH 5 en 7 die laagste log D gehad (-1.50 en -1.78, onderskeidelik). Die log D van lamivudien by sowel pH 5 as 7 (-1.19 en -1.15, onderskeidelik) was laer as dié van die amiedesters (wissel van 0.12 tot 4.55 en 0.25 tot 4.88, onderskeidelik). Daar bestaan dus 'n direkte korrelasie tussen die eksperimentele wateroplosbaarheid en die log D van al die verbindings by sowel pH 5 as 7.

'n Vergelyking tussen gemiddelde en mediaan vloed van die amiedesters van lamivudien toon goeie korrelasie tussen die vloedwaardes in PBS en Pheroid™, (behalwe vir N-butiriellamivudien-5'-buteraat). Dit lyk asof verbindings met hoër vloed , soos salsitabien en lamivudien, groter verskille tussen gemiddelde en mediaan vloed het. Mediaan vloed gee 'n meer akkurate maatstaf in gevalle soos hierdie waar groot variasie en skewe verspreiding in eksperimentele waardes gekry is.

In vitro-penetrasie deur vroulike abdominale mensvel is in Franz-diffusieselle gemeet. Die mediaan vloed van lamivudien (4.289 $\mu mol.cm^{-2}.h^{-1}$) in PBS was hoër as dié van salsitabien (0.442 $\mu mol.cm^{-2}.h^{-1}$), maar in Pheroid™ het salsitabien 'n effense hoër mediaan vloed (0.015 $\mu mol.cm^{-2}.h^{-1}$) as lamivudien (0.011 $\mu mol.cm^{-2}.h^{-1}$). Die mediaan vloed van lamivudine, in sowel PBS as in Pheroid™, was merkwaardig hoër as dié van die amiedesters (wissel van 2.0×10^{-4} tot 0.046 $\mu mol.cm^{-2}.h^{-1}$ in PBS en 2.0×10^{-4} tot 9.3×10^{-3} $\mu mol.cm^{-2}.h^{-1}$, in Pheroid™). Van al die amiedesters van lamivudien het N-asetiellamivudien-5'-asetaat (in PBS) en N-propioniellamivudien-5'-propionaat (in Pheroid™) die hoogste vloed gelewer.

As die vloed in PBS met dié in Pheroid™ vergelyk word, word opgemerk dat al die verbindings, behalwe N-heksanoïellamivudine-5'-heksanaat, laer vloedwaardes in Pheroid™ het. Pheroid™ bevorder dus nie transdermale vloed van hierdie reeks verbindings nie.

In hierdie studie is bevind dat daar 'n direkte verband tussen wateroplosbaarheid en transdermale vloed is.

'n Sterk statisties beduidende korrelasie tussen mediaan vloed in sowel PBS as in Pheroid™ aan die een kant en molekulêre massa, wateroplosbaarheid (in pH 5 en 7) en log D (in pH 5 en 7) aan die ander kant is waargeneem soos bepaal met 'n betroubaarheidsvlak van 5 % en die Spearman-korrelasie.

Geel kolle in mikrogramme van konfokale laserskanderingsmikroskopie (KLSM) bevestig dat die verbindings in Pheroid™ vasgevang word. Die grootte van die mikrosponse van die meer hidrofiele verbindings neem af soos die verbindings meer lipofilies word vanaf salsitabien tot N-butiriellamivudien-5'-buteraat en daarna het dit weer toegeneem vanaf N-dibutirielamivudien-5'-buteraat tot N-dekanoïelamivudien-5'-dekanoaat. Hieruit blyk dit dat die hidrofiele geneesmiddels wat in Pheroid™ vasgevang is, makliker as die lipofiele verbindings deurdring.

ACKNOWLEDGEMENTS

To **God, our loving Father and Saviour,** all the honour; for giving me strength and determination to complete this thesis successfully.

Jacobus J. Gerber & Miranda P. Gerber, my parents and **Anya Gerber,** my sister, thank you for all your love, support and faith in me. Knowing instinctively when times were tough to encourage me to keep on. I dedicate this thesis to all of you.

Professor Jaco C. Breytenbach, my supervisor, thank you for keeping me focused, all your support (financially and academically), guidance and sacrifices, words can't describe my gratitude. It was a great honour having you as a mentor during my thesis.

Professor Jeanetta du Plessis, my co-supervisor, thank you for all your advice, help and support. It was great working with you.

Professor Jonathan Hadgraft, thank you for all your help and objective advice during my thesis. It's been a great privilege to encounter a great researcher like yourself.

Liezl Badenhorst, thank you for your friendship, encouragement, sacrifices, support and being like a sister to me. You were my energy during the past few years of my life, keeping me on track and refuelling the tank to just keep swimming! I know a better friend than you I'll never find!

Esteé-Marie Holmes, thank you for being such a great friend, always providing entertainment in the lab, for listening while reasoning about my study and for being such a great student.

Tjaart N. Coetsee, thank you for always being there, being in the "technical team" and for being a wonderful friend.

Carita Marx, thank you for your friendship, support and objective nature and for being the best res-child one could ever ask for!

Ronel Bouwer, thank you for being general info, always knowing where to find anything in Potchefstroom or on Campus and being a great friend!

Mrs. Anriëtte Pretorius, thank you for being a friend, all your assistance and advice not only with the use of the library, but especially in my personal life. It's been an honour knowing you.

Dale Elgar, thank you for manufacturing the Pheroid™ and help in Confocal.

Anne Grobler, thank you for your help and advice with Confocal and Pheroid™.

Doctor Gerhard Koekemoer, thank you for all the assistance and advice with statistics, I really appreciate it.

Professor Jan du Preez, thank you for your help and expertise during my HPLC analysis.

Johan Hendriks, thank you for your help in the IR elucidation.

André Joubert, thank you for your help in the NMR elucidation.

Doctor Louis Fourie, thank you for your help in the MS elucidation.

All my **friends** and **family**, thank you for your faith, support and encouragement.

Pharmaceutical Chemistry and the **Transdermal Research Group,** for giving me the opportunity to work in your laboratories.

CENQAM (Centre for Quality Assurance of Medicine), thank you for the use of your laboratory.

NRF (National Research Foundation) and the **North-West University,** for the financial support during my post-graduate studies.

Roche Diagnostics GmbH, Mannheim, Germany, thank you for a generous gift of zalcitabine.

Aspen Pharmacare, Port Elizabeth, South Africa, thank you for a generous gift of lamivudine.

TABLE OF CONTENTS

ABSTRACT i

OPSOMMING iii

ACKNOWLEDGEMENTS v

TABLE OF CONTENTS vii

TABLE OF FIGURES xiii

TABLE OF TABLES xvi

ABBREVIATIONS xvii

CHAPTER 1 INTRODUCTION AND PROBLEM STATEMENT 1

1.1 Introduction 1

1.2 Aims and objectives of this study 3

CHAPTER 2 HIV / AIDS & NRTIs 4

2.1 Human Immunodeficiency Virus 4

2.1.1 Overview and statistics 4

2.1.2 Origin and discovery 4

2.1.3 Transmission of infection 5

2.1.4 Structure and genes 6

2.1.5 Mechanism of infection 8

2.1.5.1 Entry of HIV into the host cells 8

2.1.5.2 Replication and transcription 10

2.1.5.3 Assembly and budding 10

2.1.6 Symptoms & opportunistic infections 11

2.1.7 Treatment 11

2.2 Nucleoside Reverse Transcriptase Inhibitors 12

2.2.1 Mechanism of action 12

2.2.2 Zalcitabine 14

2.2.3 Lamivudine 14

2.2.4 Transdermal delivery of NRTIs 14

CHAPTER 3 TRANSDERMAL DRUG PERMEATION 17

3.1 Introduction 17

3.2 The skin structure 18

3.2.1 Stratum corneum 19

3.2.2 Viable epidermis 21

3.2.3 Dermis 22

3.2.4 Hypodermis 22

3.2.5 Skin appendages 22

3.3 The process of percutaneous absorption 23

3.4 Routes of transdermal delivery 24

3.4.1 Transappendageal 24

3.4.2 Transepidermal 24

3.4.2.1 Transcellular 24

3.4.2.2 Intercellular 25

3.5 Factors influencing transdermal permeation 25

3.5.1 Biological factors 25

3.5.1.1 Disease and skin conditions 25

3.5.1.2 Skin hydration 26

3.5.1.3 Skin age 26

3.5.1.4 Skin region 26

3.5.1.5 Skin metabolism of drugs 26

3.5.1.6 Temperature 27

3.5.2 Physicochemical factors 27

3.5.2.1 Drug solubility in the stratum corneum 27

3.5.2.1.1 Solubility parameter 28

3.5.2.1.2 Aqueous solubility 29

3.5.2.2 Partition coefficient 30

3.5.2.3 Diffusion coefficient 31

3.5.2.4 Ionisation 34

3.5.2.5 Melting point 35

3.5.2.6 Hydrogen bonding 36

3.5.2.7 Molecular size 38

3.5.2.8 Increased alkyl chain length 39

3.6 Skin integrity 40

3.7 Drug delivery systems 41

3.7.1 Liposomes 41

3.7.2 Pheroid™ 42

3.8 Confocal laser scanning microscopy 44

3.9 Summary 46

CHAPTER 4 EXPERIMENTAL 47

4.1 General experimental methods 47

4.1.1 Instrumentation 47

4.1.1.1 Nuclear magnetic resonance spectrometry (NMR) 47

4.1.1.2 Infrared spectroscopy (IR) 47

4.1.1.3 Mass spectroscopy (MS) 47

4.1.1.4 Melting points 47

4.1.1.5 Integrity 48

4.1.1.6 Confocal laser scanning microscopy (CLSM) 48

4.1.2 Chromatographic techniques 48

4.1.2.1 Thin-layer chromatography (TLC) 48

4.1.2.2 Column chromatography 48

4.1.2.3 High pressure liquid chromatography (HPLC) 49

4.1.3 Theoretical aqueous solubility 50

4.1.4 Theoretical partition coefficients 50

4.2 Synthesis and physical data of compounds 50

4.2.1 Synthesis of amide esters 50

4.2.1.1 N-acetyllamivudine-5'-acetate 51

4.2.1.2 N-propionyllamivudine-5'-propionate 51

4.2.1.3 N-butyryllamivudine-5'-buterate 51

4.2.1.4 N-hexanoyllamivudine-5'-hexanoate 52

4.2.1.5 N-octanoyllamivudine-5'-octanoate 52

4.2.1.6 N-decanoyllamivudine-5'-decanoate 53

4.3 Physicochemical properties and solubility 53

4.3.1 Solubility determination 53

4.3.2 Experimental partition coefficient 53

4.4 Transdermal permeation 54

4.4.1 Skin preparation 54

4.4.2 Preparation of donor solutions 54

4.4.3 Preparation of Pheroid™ 54

4.4.4 Skin permeation method 55

CHAPTER 5 RESULTS AND DISCUSSION 57

5.1 Amide ester synthesis 57

5.1.1 Structures of the products 57

5.1.1.1 N-acetyllamivudine-5'-acetate 57

5.1.1.2 N-propionyllamivudine-5'-propionate 58

5.1.1.3 N-butyryllamivudine-5'-buterate 59

5.1.1.4 N-hexanoyllamivudine-5'-hexanoate 59

5.1.1.5 N-octanoyllamivudine-5'-octanoate 60

5.1.1.6 N-decanoyllamivudine-5'-decanoate 61

5.1.2 Conclusion 62

5.2 Physicochemical properties 62

5.2.1 Aqueous solubility 62

5.2.2 Discussion 64

5.2.3 Partition coefficient 65

5.2.4 Discussion 66

5.3 Transdermal permeation of selected compounds 66

5.3.1 Transdermal permeation using average or median flux 66

5.3.2 Discussion 70

5.3.3 Experimental transdermal permeation vs. previous studies 72

5.3.4 Transdermal permeation: Experimental vs. predicted flux 74

5.3.5 Discussion 74

5.4 Flux vs. physicochemical properties 75

5.4.1 Median flux vs. molecular weight 76

5.4.2 Median flux vs. aqueous solubility 77

5.4.3 Median flux vs. partition coefficient 78

5.4.4 Median flux vs. melting point 80

5.4.5 Median flux vs. integrity 81

5.5 Confocal laser scanning microscopy 83

5.5.1 Size and morphology of microsponge Pheroid™ 83

5.5.2 Discussion 85

CHAPTER 6 SUMMARY AND FINAL CONCLUSIONS 86

REFERENCES 91

APPENDIX 1 126

TABLE OF FIGURES

Figure 1.1: Structures of zalcitabine **(1)** and lamivudine **(2)**. 2

Figure 2.1: The structure of HIV. 6

Figure 2.2: Structural representation of the HIV-1 genes. 7

Figure 2.3: The HIV-1 replication cycle showing the sites of action of available antiretrovirals. 9

Figure 2.4: Mechanism of action of lamivudine **(2)** (x = s) and zalcitabine **(1)** (x = CH_2). 13

Figure 3.1: A cross-section of the human skin. 19

Figure 3.2: Proposed "Brick and Mortar" Two-Compartment Model. 20

Figure 3.3: A schematic representation of the stratum corneum lipid bilayers. 20

Figure 3.4: Pathways of penetration through the skin: (1) via the sweat gland ducts; (2) across the stratum corneum; or (3) through the hair follicles. 24

Figure 3.5: Typical permeation profile for a molecule diffusing across human skin. 33

Figure 3.6: Schematic representation of different size and number of lamella of SUV, LUV, MLV and MVV. 41

Figure 3.7: The micrographs (CLSM) of several of the basic Pheroid™ types. 42

Figure 3.8: Schematic diagram of CLSM 45

Figure 4.1: Vertical Franz diffusion cell. 55

Figure 5.1: Experimental and predicted aqueous solubility values on a mass (mg/ml) and molar basis (mM) of compounds **(1)** to **(6)**. 63

Figure 5.2: Experimental and predicted partition coefficients of compounds **(1)** to **(8)**. 65

Figure 5.3: The average cumulative amount of **(1)** that penetrated through the skin as a function of time to illustrate the average flux of **(1)**. 67

Figure 5.4: The cumulative amount of **(1)** per area in each Franz cell experimentally determined together with the average cumulative amount of **(1)** that had penetrated through the skin as a function of time. 67

Figure 5.5: Box-plot of the flux of **(1)** in PBS to illustrate the median flux and the skewness of data. 68

Figure 5.6: Average and median flux values of compounds **(1)** to **(6)** in PBS. 69

Figure 5.7: Average and median flux values of compounds **(1)** to **(6)** in Pheroid™. 70

Figure 5.8: The relationship between median flux in PBS and molecular weight of compounds **(1)** to **(6)**. 76

Figure 5.9: The relationship between median flux in Pheroid™ and molecular weight of compounds **(1)** to **(6)**. 77

Figure 5.10: The relationship between median flux in PBS and aqueous solubility at pH 5 and 7 of compounds **(1)** to **(6)**. 77

Figure 5.11: The relationship between median flux in Pheroid™ and aqueous solubility at pH 5 and 7 of compounds **(1)** to **(6)**. 78

Figure 5.12: The relationship between median flux and log D in PBS at pH 5 and 7 of compounds **(1)** to **(6)**. 79

Figure 5.13: The relationship between median flux and log D in Pheroid™ at pH 5 and 7 of compounds **(1)** to **(6)**. 79

Figure 5.14: The relationship between median flux in PBS and melting point of compounds **(1)** to **(6)**. 80

Figure 5.15: The relationship between median flux in Pheroid™ and melting point of compounds **(1)** to **(6)**. 80

Figure 5.16: The relationship between melting point and aqueous solubility at pH 5 and 7 of compounds **(1)** to **(6)**. 81

Figure 5.17: The relationship between median flux in PBS and the integrity (before and after) of compounds **(1)** to **(6)**. 82

Figure 5.18: The relationship between median flux in Pheroid™ and the integrity (before and after) of compounds **(1)** to **(6)**. 82

Figure 5.19: A representation of the difference in microsponge size between the control and compounds **(1)** to **(8)** in microsponge Pheroid™ formulation. 83

Figure 5.20: The CLSM micrographs of the microsponge Pheroid™ (control) and compounds **(1)** to **(8)** in entrapped in Pheroid™ microsponges. 84

Figure 5.21: The digitally zoomed CLSM micrographs of **(3)**, **(6)** and **(7)** entrapped in the microsponges of the Pheroid™ formulation. 84

TABLE OF TABLES

Table 4.1: Data of the HPLC method. 49

Table 5.1: The aqueous solubility values of compounds **(1)** to **(8)**..... 63

Table 5.2: Partition coefficients of compounds **(1)** to **(8)**. 65

Table 5.3: Average and median flux data of compounds **(1)** to **(8)** in PBS and Pheroid™. 69

Table 5.4: Aqueous solubility, log D and median flux values in PBS and Pheroid™ of stavudine and its esters..... 73

Table 5.5: Predicted flux values using the Potts and Guy equation. 74

Table 5.6: Spearman correlations between median flux and the physicochemical properties of compounds **(1)** to **(6)** in PBS and Pheroid™. 75

ABBREVIATIONS

(1)	Zalcitabine
(2)	Lamivudine
(3)	N-acetyllamivudine-5'-acetate
(4)	N-propionyllamivudine-5'-propionate
(5)	N-butyryllamivudine-5'-buterate
(6)	N-hexanoyllamivudine-5'-hexanoate
(7)	N-octanoyllamivudine-5'-octanoate
(8)	N-decanoyllamivudine-5'-decanoate
AIDS	acquired immunodeficiency syndrome
br s	broad singlet
CDC	Centres for Disease Control and Prevention
CLSM	confocal laser scanning microscopy
CMP/dCMP-K	cytidylate/2'-deoxycytidylate kinase
CMV	cytomegalovirus
dCK	2'-deoxycytidine kinase
dNTPs	deoxynucleoside triphosphate
DCM	dichloromethane
ddI	didanosine
DSC	differential scanning calorimetry
DP	diphosphate
dsDNA	double-stranded DNA

d	doublet
dd	doublet of doublets
ddd	doublet of doublets of doublets
dt	doublet of triplets
p50	fifty percentile
EtOH	ethanol
EtOAc	ethyl acetate
FAB	fast atom bombardment
FDA	Food and Drug Administration
gp	glycoprotein
HBV	hepatitis B virus
HPLC	high pressure liquid chromatography
HIV	human immunodeficiency virus
HTLV-III	human T lymphotropic virus type III
IR	infrared spectroscopy
IPM	isopropyl myristate
KS	Kaposi's sarcoma
3TC	Lamivudine
LUV	large unilamellar vesicles
LTR	long terminal repeat
LAV	lymphadenopathy associated virus
M-tropic	macrophage-tropic
MS	mass spectrometry
mRNA	messenger RNA

MeOH	methanol
MP	monophosphate
MLV	multilamellar vesicles
m	multiplet
MVV	multivesicular vesicles
MAC	Mycobacterium avium complex
NCI	National Cancer Institute
NMP	N-methyl-2-pyrrolidone
NNRTIs	non-nucleoside reverse transcriptase inhibitors
NSI	non-syncytium-inducing
NF-κB	nuclear factor kappa B
NMR	nuclear magnetic resonance spectroscopy
NDP-K	nucleoside 5'-diphosphate kinase
NRTIs	nucleoside reverse transcriptase inhibitors
NtRTIs	nucleotide reverse transcriptase inhibitors
log D	octanol-PBS partition coefficient
log P	octanol-water partition coefficient
OA	oleic acid
OI	opportunistic infections
OPA	orthophosphoric acid
ppm	parts per million
PBS	phosphate buffer solution
PCP	Pneumocystis carinii pneumonia
PE	polyethylene

PIs	protease inhibitors
q	quartet
RT	reverse transcriptase
RNA	ribonucleic acid
§	see section
STD	sexually transmitted disease
ssRNA	single-strand (+) RNA
s	singlet
SUV	small unilamellar vesicles
d4T	stavudine
SI	syncytium-inducing
TLC	thin-layer chromatography
T-tropic	T-lymphocyte tropic strains
TDS	transdermal delivery system
TEM	transmission electron microscopy
TCP	tricaprylin
TP	triphosphate
t	triplet
VWD	variable wave detector
ddC	Zalcitabine
AZT	zidovudine

CHAPTER 1

INTRODUCTION AND PROBLEM STATEMENT

1.1 Introduction

The skin is a complex, highly effective barrier between the internal plasma and the harsh exterior. Its principal functions are concerned with temperature regulation, protection, sensation and control of water excretion. The skin covers an area of about 1.73 m^2 in an average adult and receives one third of circulating blood through the body at any given time. The potential of using intact skin as the site of administration for dermatological preparations to elicit pharmacological action in the skin tissue has been well recognised (Barr, 1962). The permeation of toxicants, chemicals and drugs are much slower across the skin when compared to other biological membranes in the body, due to the outermost layer of the skin, the stratum corneum. The lipophilic stratum corneum is responsible for the primary barrier function of the skin and provides an extensive challenge to scientists in their pursuit to develop drugs for transdermal delivery (Pefile & Smith, 1997). A great deal of research has been performed to enhance transdermal flux by reducing the barrier function of the stratum corneum. Synthesising prodrugs or increasing the alkyl chain length are other methods in the attempt to improve flux, as well as the use of penetration enhancers and delivery systems.

In addition to the structure of the stratum corneum through which percutaneous absorption occurs, the physicochemical properties of both the drug and the vehicle play an important role in determining the transdermal absorption (Blank *et al.*, 1967; Abraham *et al.*, 1995). These factors include the molecular properties of the drug and the vehicle (Ritschel & Hussain, 1988; Blank *et al.*, 1967). Transdermal absorption is also dependent on the partition coefficient, melting point, molecular size, pH of the drug solution in the vehicle and the concentration of the drug on the surface of the skin required to deliver a desired therapeutic effect (Barry, 1983; Bunge & Cleeck, 1995). Compounds are likely to have decent passive skin permeabilities if they have an aqueous solubility of more than 1 mg/ml and a log P value between 1 and 3, with relative low molecular weights and modest melting points (Guy, 1996). Compounds with lower melting points exhibit higher permeability coefficients (Roy & Flynn, 1988). The lipophilic stratum corneum is more permeable to drugs in their non-ionic state, because of their greater lipid solubility (Abdou, 1989). Small molecules penetrate more rapidly than large molecules (Liron & Cohen, 1984). Drugs utilised for transdermal delivery should have a high potency, as the concentration, which is usually delivered transdermally, is very low (Naik *et al.*, 2000).

AIDS (acquired immunodeficiency syndrome) is caused by an infection with a retrovirus known as HIV (human immunodeficiency virus). HIV invades cells of the immune system, particularly the CD4 T-helper lymphocytes and multiplies. Part of the process of viral multiplication, in the early stages of cell fusion, involves the conversion of the virus genetic material, RNA, into DNA, which is achieved by a compound essential to the virus, called reverse transcriptase (RT), which has been a major target for anti-AIDS therapy (Mohan, 1992).

Zalcitabine **(1)** (ddC) and lamivudine **(2)** (3TC) are both nucleoside reverse transcriptase inhibitors (NRTI). Zalcitabine **(1)** and lamivudine **(2)** enter cells by passive diffusion and are phosphorylated to their active metabolites, 2',3'-dideoxycytidine-5'-triphosphate and 2',3'-dideoxy,3'-thiacytidine-5'-triphosphate, respectively, which competes with naturally occurring deoxycytidine triphosphate for incorporation into viral DNA by reverse transcriptase (Gao *et al.,* 1993).

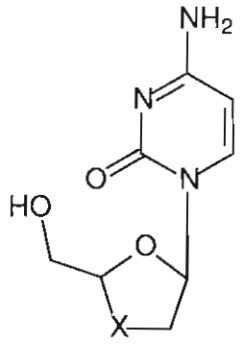

(1) Zalcitabine X = CH_2

(2) Lamivudine X = S

Figure 1.1: Structures of zalcitabine **(1)** and lamivudine **(2)**.

Nucleoside medications are perceived as having mainly a bitter taste (Schiffman *et al.,* 1999). Patients who receive long-term zalcitabine **(1)** treatment develop a painful peripheral neuropathy (Merigan *et al.,* 1989), while adverse effects commonly associated with lamivudine **(2)** include abdominal pain, nausea, vomiting and diarrhoea (Gregg, 1999; Sweetman, 2002).

Transdermal delivery of anti-HIV drugs is an appropriate method to overcome the problems of conventional delivery, since it is very helpful in maintaining suitable plasma concentration through zero-order delivery. Thus, it can enhance the anti-viral activity, and reduce the frequency and severity of side effects by optimising blood concentration levels within the therapeutic range for a longer duration, which, in turn, decreases the large quantity of oral medication in adult patients with advanced HIV and finally approves patient compliance. Transdermal delivery can be the solution for children or infants that have trouble drinking the lamivudine **(2)** formulation, due to its poor palatability (bitter taste) (Schiffman *et al.,* 1999). Transdermal application of zalcitabine **(1)** and lamivudine **(2)** may eliminate gastrointestinal intolerance, experienced with these drugs. Transdermal drug delivery offers other advantages

that include avoiding hepatic first-pass metabolism, improving bioavailability, decreasing the administered dose and it is easy to discontinue in case of toxic effects (Mitragotri, 2000).

1.2 Aims and objectives of this study

The aim of this study was to determine the transdermal penetration of zalcitabine, lamivudine and the synthesised amide esters of lamivudine, with and without the use of Pheroid™ as delivery system and to establish a correlation, if any, with selected physicochemical properties.

In order to achieve this goal, the following objectives were set:

- Synthesise amide esters of lamivudine and verify their structures by use of NMR, IR and MS.
- Experimentally determine the aqueous solubility and the partition coefficient of zalcitabine, lamivudine and the synthesised amide esters of lamivudine in both pH 5 and 7 and compare it with values calculated from commonly used prediction software.
- Experimentally determine the transdermal flux of zalcitabine, lamivudine and the amide esters of lamivudine in both phosphate buffer solution (pH 5) and Pheroid™ and compare it with values calculated from commonly used theoretical equations.
- Determine if transdermal application of these compounds will reach therapeutic drug concentrations with respect to transdermal flux.
- Determine whether a correlation exists between selected physicochemical properties and transdermal flux data of zalcitabine, lamivudine and the lamivudine derivatives.
- Determine whether zalcitabine, lamivudine and the synthesised amide esters of lamivudine have been entrapped in Pheroid™ by use of confocal laser scanning microscopy.

CHAPTER 2

HIV / AIDS & NRTIs

2.1 Human Immunodeficiency Virus

2.1.1 Overview and statistics

Human Immunodeficiency Virus (HIV), like all viruses cannot develop or reproduce on its own. In order to create new duplicates of itself it must infect the cells of a living organism. HIV is a retrovirus that causes Acquired Immunodeficiency Syndrome (AIDS) (Fauci, 1993), a condition in which the immune system start to break down, leading to severe opportunistic infections (OI). A person is diagnosed with AIDS when he or she has less than 200 CD4+ T cells per cubic millimetre of blood and/or one of 21 AIDS-defining OIs (HHS, 2005; CDC, 1992).

At the end of 2005 global HIV/AIDS statistics shown that an estimate of 40.3 million people are living with HIV/AIDS of which 38.0 million are adults, 17.5 million are women and 2.3 million are children. In 2005, 4.9 million people were newly infected with HIV and 3.1 million deaths have occurred due to AIDS. Since 1981, more than 23.1 million people have died of AIDS. Approximately 7 000 young people (10 – 24 years old) are infected with HIV every day. In developing and traditional countries 6.8 million people are in urgent need of life-saving AIDS drugs; of these, only 1.65 million are receiving it (UNAIDS, 2006).

2.1.2 Origin and discovery

The earliest documented cases of AIDS occurred in the summer of 1981 in America (Adler, 1993). Reports appeared of Kaposi's sarcoma (KS) and Pneumocystis carinii pneumonia (PCP) in young males, whom it was consequently recognised were both immunocompromised and homosexual (Adler, 1993; Brennan & Durack, 1981; Garcia *et al.*, 1981). Classic KS are rare multiple pigmented vascular tumours generally found on the legs of elderly, Jewish or east European, male patients (Smith & Spittle, 1993; Safai & Weiss, 1984).

By March 1981, no less than eight cases of an aggressive form of KS had occurred between young homosexual men in New York (Hymes *et al.*, 1981). During that time there was an increase, in both New York and California, in the number of cases of PCP (CDC, 1981). The U.S. Centres for Disease Control and Prevention (CDC) in June 1981 reported PCP in five

homosexual men in Los Angeles (CDC, 1982). In December 1981, PCP affected intravenous drug users and haemophiliacs (Davis *et al.,* 1983; Masur *et al.,* 1981).

At the beginning of 1983 reports of AIDS among females suggested that the infection might be passed on by heterosexual sex (CDC, 1983). In May 1983, Barré-Sinoussi, Montagnier, and colleagues at the Pasteur Institute, Paris discovered HIV and called it lymphadenopathy associated virus (LAV) (Barré-Sinoussi *et al.,* 1983).

In 1984, Dr. Robert Gallo of the United States described the development of cell lines, permanently and productively infected with the virus, and renamed it human T lymphotropic virus type III (HTLV-III) (Popovic *et al.,* 1984).

By March 1985 it was clear that LAV and HTLV-III was the same (Marx, 1985). Another retrovirus, dissimilar from HIV-1, was recognised 1985. This virus referred to by the Paris researchers as LAV-2 and more recently as HIV-2, is less transmittable and is largely confined to West Africa (Reeves & Doms, 2002). Accordingly it is also associated with AIDS, though it is more closely related to a simian retrovirus, SIV, carried by healthy African vervet monkeys, than it is to HIV-1 (Daniel *et al.,* 1985).

One of the foremost known cases of HIV-1 infection was from a plasma sample collected in 1959 from an adult male in Kinshasa, Democratic Republic of Congo. Genetic analysis of this blood sample (1998) suggested that HIV-1 might have stemmed from a single virus in the late 1940s or early 1950s (Zhu *et al.,* 1998).

2.1.3 Transmission of infection

The most common method of transmission of HIV is through sexual intercourse (anal or vaginal) (Nakashima & Fleming, 2003). The transmission of HIV between males is more efficient than from female to male (Padian *et al.,* 1991). Vulnerability to HIV infection enhances when the mucous membrane or a skin is torn or damaged. Sexual transmission of HIV is more probable if the individual has syphilis, herpes, or another sexually transmitted disease (STD) that produces inflammation of the genitals or ruptures in the skin (Fleming & Wasserheit, 1999). Although HIV transmission during oral sex may occur, it is far less common than during anal or vaginal intercourse (Winkelstein *et al.,* 1988).

Parenteral transmission of HIV generally includes infections due to contaminated blood exposure such as from organ transplants, delivery of blood products, intravenous injection with used needles, or needlesticks. Since 1985, all blood accumulated for transfusion is tested in the U.S.A. for HIV, and when feasible, some blood products are heat-treated to eradicate the risk of HIV infection (Donegan, 2003). These precaution measures have reduced the risk of HIV

infection from a single blood transfusion to less than one in half a million (Donegan, 2003). Health care workers who are accidentally pricked with an HIV-contaminated needle have approximately a 0.23 % chance of getting HIV (Baggaley *et al.*, 2006). The risk increases if visible contaminated blood is injected or with deep penetration of the needle (Baggaley *et al.*, 2006).

Perinatal infection (vertical transmission) is predominantly the origin of paediatric HIV infection (Garcia *et al.*, 1981). In nearly 25 – 35 % of all untreated HIV infected pregnancies, the virus is transmitted to the fetus in utero or, more frequently, at birth during passage through the birth canal (Coovadia, 2004). Infants can also contract HIV infection through breastfeeding from mothers with HIV (Rousseau *et al.*, 2003; Heymann & Brubaker, 1997). Cesarian section and drug treatment can reduce HIV infection in infants to 1 % (Coovadia, 2004).

Casual or nonsexual contact with HIV infected or AIDS patients are not a significant risk factor for HIV transmission (Friedland & Klein, 1987). Low concentrations of HIV have been found in urine, saliva and tears of infected individuals, but the probability of transmission by these secretions is insignificant. In addition, HIV is not spread through mosquito bites or the sharing of towels, food utensils, telephones, swimming pools or toilet seats (Friedland *et al.*, 1990).

2.1.4 Structure and genes

The structure of HIV is different from other retroviruses. It is nearly spherical and is approximately 120 nm in diameter (one seventieth of the diameter of a human CD4+ white cell and about 60 times smaller than a red blood cell) (McGovern *et al.*, 2002).

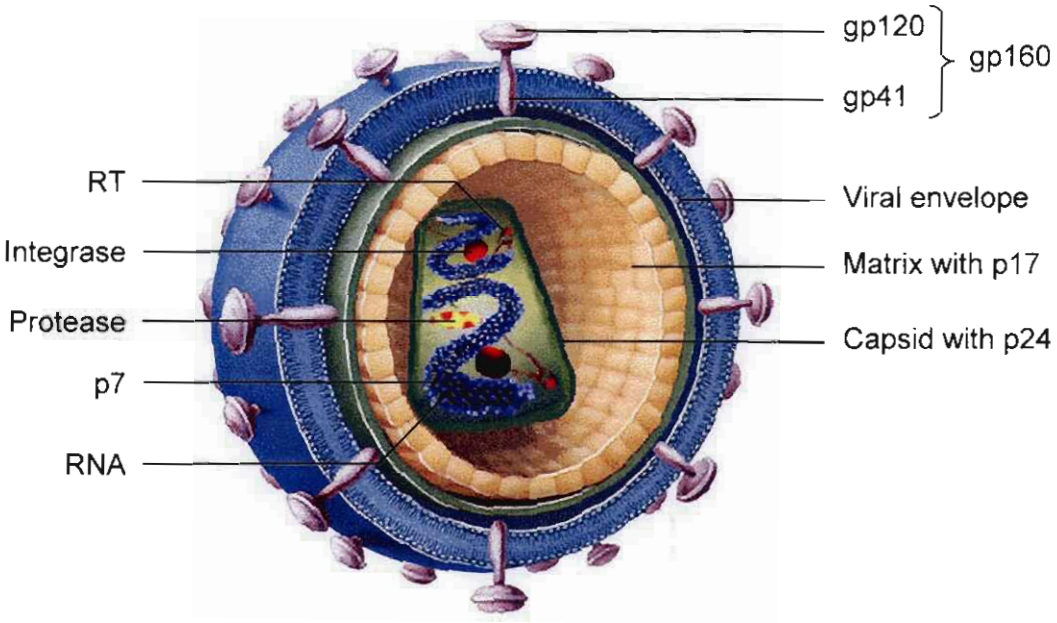

Figure 2.1: The structure of HIV.

The external viral membrane or envelope composes of bilayers of phospholipids, acquired by the virion during budding (Freed & Martin, 1995). Protruding through the surface of the viral envelope are 72 little spikes (Freed & Martin, 1995), which are formed from proteins of the host cell and almost 70 copies of a complex HIV protein. This protein (env) contains a cap consisting of three molecules called glycoprotein (gp) 120 (molecular weight of 120 kilodaltons), and a stem made of three gp41 molecules (molecular weight of 41 kilodaltons), which anchors the structure into the viral envelope (Poignard *et al.,* 2001; Chan *et al.,* 1997; Freed & Martin, 1995). The aforementioned glycoprotein complex permits the virus to connect to and combine with target cells to commence the infectious cycle (Chan *et al.,* 1997).

Just beneath the viral envelope is a layer known as the matrix (Lusso *et al.,* 1990; Gabuzda *et al.,* 1992). It contains the viral protein p17 and surrounds the viral core or capsid, ensuring the integrity of the virion particle. The HIV-1 matrix protein p17 is important in the life cycle of the retrovirus and is involved in viral RNA binding (Gallay *et al.,* 1995). The capsid is normally bullet-shaped and consists of 2 000 copies of viral protein, p24. It encloses two copies of single-stranded HIV Ribonucleic Acid (RNA) genome that codes the virus's nine genes. The single-stranded RNA is firmly adjacent to nucleocapsid proteins, p7 and enzymes, (Theilleux-Delande *et al.,* 2000; Jossinet *et al.,* 1999) essential for the development of the virion such as reverse transcriptase, integrase and proteases (Jet *et al.,* 2000).

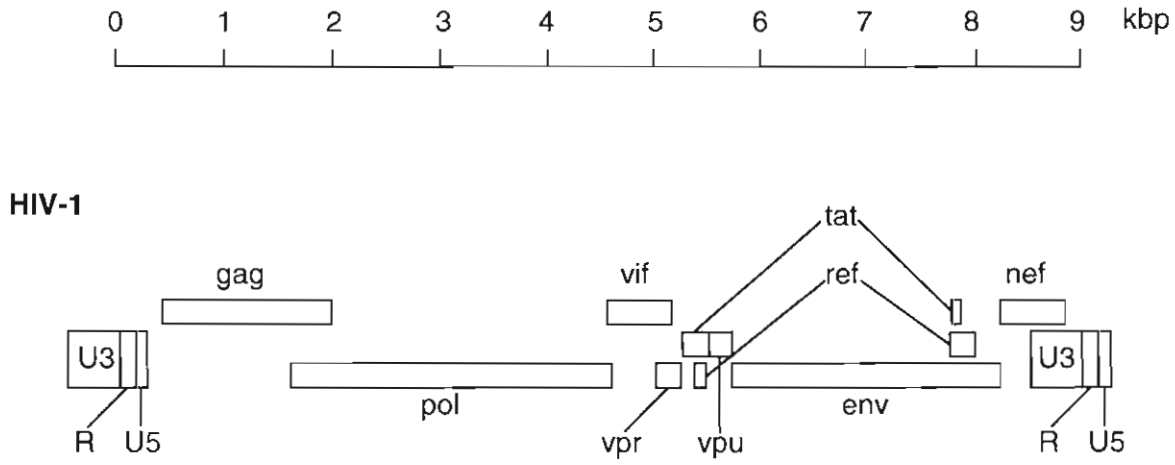

Figure 2.2: Structural representation of the HIV-1 genes (Myers *et al.,* 1996).

HIV has only nine genes (in contrast to bacteria with more than 500 genes and approximately 20 000 – 25 000 in a human). Three of these genes (pol, env and gag) comprise information required to produce structural proteins for new virus particles (Robey *et al.,* 1985). Env, for instance, codes for the protein known as gp160 that is cleaved by host cellular enzymes to form the major external gp120 and the trans-membrane gp41 (Veronese *et al.,* 1985).

The HIV genome also encodes several regulatory proteins (tat, rev, nef, vif, vpr and vpu or vpx in the case of HIV-2) from corresponding genes (Willard-Gallo *et al.,* 2001). The tat and rev proteins encode small nuclear proteins that regulate transcription of other HIV genes. The rev gene is required for the synthesis of structural proteins (Feinberg *et al.,* 1986). The nef-encoded protein assists in viral access into vulnerable cells consequently enhancing infectivity (Zhou & Aiken, 2001). The vif protein plays a role in production of the infectious virus (Sova *et al.,* 2001). The vpr proteins reveal in vitro CD4-mediated T-cell functions and the regulation of productive HIV-1 infection (Schaeffer *et al.,* 2001). The protein encoded by vpu, for example, have an effect on the extracellular release of new virus particles from infected cells (Deora & Ratner, 2001).

At either end of each strand of RNA is a sequence called the long terminal repeat (LTR), which acts as switches that helps to control HIV replication and can be initiated by proteins from either the host cell or HIV (Myers *et al.,* 1996).

2.1.5 Mechanism of infection

2.1.5.1 Entry of HIV into the host cells

When HIV enters the body, gp160 allows HIV to bind to CD4 receptors, which are proteins present on helper T-lymphocytes, macrophage, monocytes, brain microglia and dentric cells. The virion envelope gp120 subunit has a high affinity for CD4 receptors of the host cell and is accountable for the initial binding of the virus to the target cells and also with the chemokine co-receptors (Poignard *et al.,* 2001).

HIV uses two major chemokine receptors, i.e., CCR5 and CXCR4. HIV that preferentially uses CCR5, also known as R5 viruses, is macrophage-tropic (M-tropic) and non-syncytium-inducing (NSI). The X4 virus preferentially uses CXCR4 as a co-receptor for T-lymphocyte tropic strains (T-tropic) – this virus is often predominant in the later stage of disease and is syncytium-inducing (SI). These distinctions are not exclusive, as strains exhibiting dual tropism have been reported (R5X4 strains) (Morris *et al.,* 2001; Costa *et al.,* 2000). Genetic defects of the chemokine receptor seem to defend some individuals from developing AIDS regardless of them being exposed to the virus (Dean *et al.,* 1996).

Attachment of HIV to the cell permits the N-terminal fusion peptide gp41 to infiltrate the cell membrane; subsequently the extracellular portion of gp41 subsides into a hairpin, bringing the virus and cell membranes closer together; promoting fusion of the membranes and consequent entry of the viral capsid (Chan & Kim, 1998).

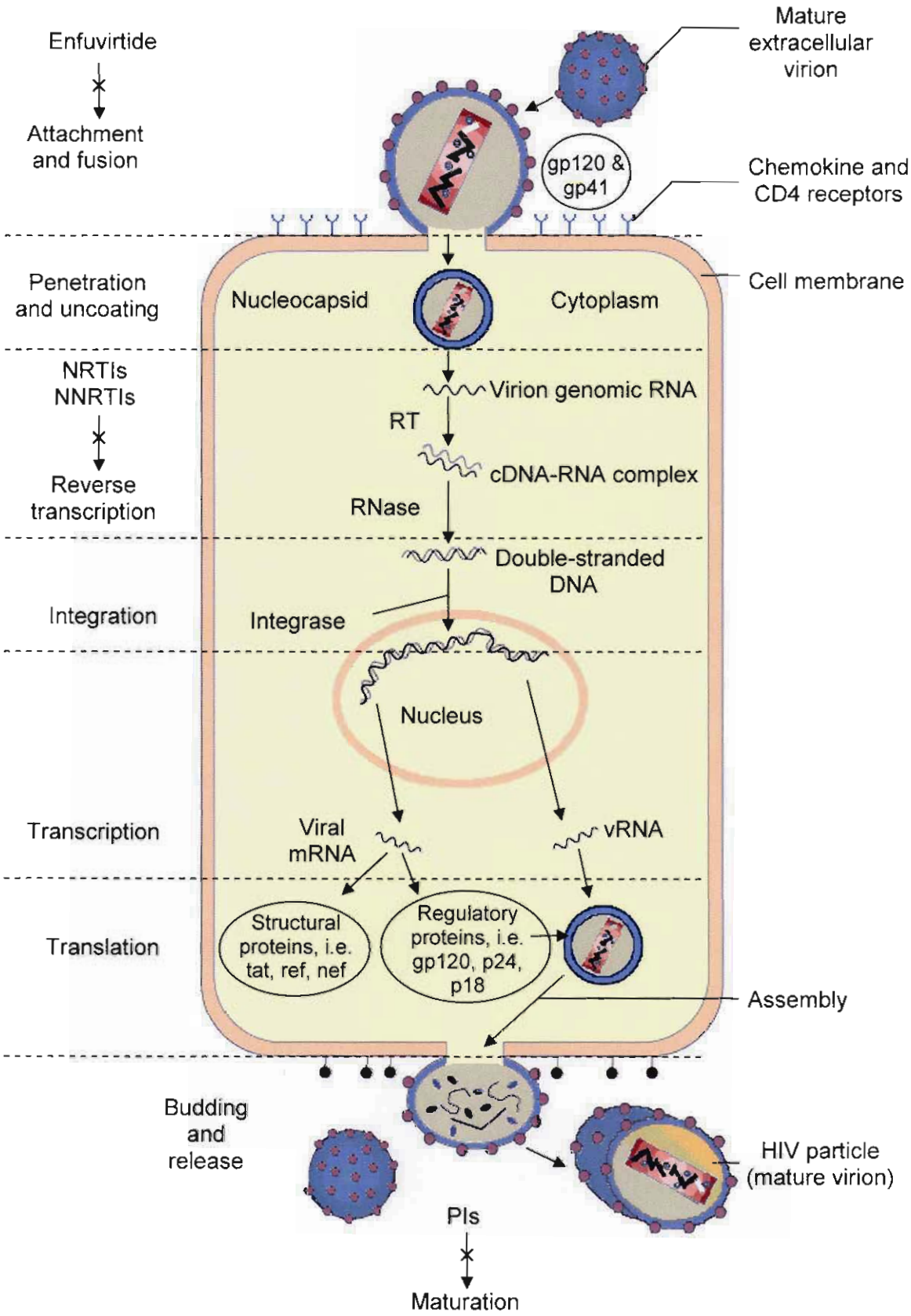

Figure 2.3: The HIV-1 replication cycle showing the sites of action of available antiretrovirals (Redrawn from Flexner, 2006).

2.1.5.2 Replication and transcription

The moment the viral capsid penetrates the cell; the virus is uncoated in preparation for replication. HIV enzyme, RNA-dependant DNA polymerase (reverse transcriptase (RT)), catalyses the incorporation of deoxynucleoside triphosphate (dNTPs), forming a (-) DNA strand, by using HIV single-strand (+) RNA (ssRNA) as a template to optimally replicate in human cells (transcription normally occurs from DNA to RNA – HIV work backwards, hence the name retrovirus). RT synthesises a second (+) DNA strand to form a double-stranded DNA (dsDNA) molecule (Loveday, 2001). Unfortunately, RT makes many mistakes during this process, which contributes to the rapid mutation of the virus, and allows drug resistance to evolve. The final dsDNA product of the viral sequence (provirus) migrates into the nucleus and is integrated into the host cell DNA by integrase, another virus-specific enzyme unique to HIV (Bouyac-Bertoia *et al.,* 2001).

The integrated provirus may be transcriptionally inactive (Zheng *et al.,* 2005). For the provirus to become active, certain cellular transcription factors are required, especially nuclear factor kappa B (NF-κB), an enhancer-binding protein. NF-κB usually regulates the T-lymphocyte genes involved in growth but also can unintentionally activate replication of HIV (Hiscott *et al.,* 2001). When HIV replication is induced, the host DNA polymerase transcribes the integrated proviral DNA into messenger RNA (mRNA) with subsequent translation of the mRNA into viral proteins. These viral proteins produce the regulatory HIV proteins such as tat, nef and rev. The tat protein encourages new virus production. There is no evident function for nef, although it seems to protect infected cells from cytotoxic T-lymphocytes (Frankel & Young, 1998). The rev protein is essential for HIV replication and fundamentally shifts synthesis of HIV regulatory proteins to structural proteins (i.e., gp120) by inhibiting viral mRNA splicing (Pollard & Malim, 1998) and exporting the mRNA outside the nucleus (Frankel & Young, 1998).

2.1.5.3 Assembly and budding

Structural proteins assemble around full-length genomic RNA to form a nucleocapsid subsequently formed with viral ssRNA. Gp160 is sliced by protease and processed into gp120 and gp41. Gp41 and other structural proteins accumulate at the cell surface, concentrated in cholesterol-rich rafts. The nucleocapsid is absorbed at these sites and bud through the lipid bilayer, creating a new HIV particle containing two genomic single-stranded RNA. After the virus buds, the maturation process begins.

During maturation, HIV proteases cleave the polyproteins into functional HIV proteins and enzymes that are necessary to produce a complete virus. Without this enzyme, the virion is immature and unable to adequately infect cells (Kohl *et al.,* 1988). The various structural

components then assemble to produce a mature HIV virion. The mature virus is then able to infect another cell. RT is integrated into this particle so that reproduction can begin directly after the virus enters a new cell (Greene and Peterlin, 2002).

2.1.6 Symptoms & opportunistic infections

Generally patients experience no obvious symptoms upon initial HIV infection. However, patients with the primary HIV experience symptoms of a viral illness, such as fatigue, fever, pharyngitis, rash and weight loss, as well as other non-specific symptoms, one to four weeks after infection (Kahn & Walker, 1998; Schacker *et al.*, 1996). Diagnosis of primary HIV infection could prevent transmission to others (i.e., sexually), because in the first stages of the disease, patients have a high viral load (the amount of virus in the blood) and persistent decrease in CD4 lymphocytes, even if there are no symptoms experienced (Cates *et al.*, 1997).

A person can have HIV infection for years before developing AIDS. The result of uncontrolled HIV replication is a steady decrease in CD4 cells, paradoxically; they have to prevent infections from occurring. HIV is an ominous disease in that persons infected often present with OIs, as result of an impaired immune system. Organisms that are common in the environment cause most OIs. The major OIs include: candidial esophagitis, PCP, toxoplasmosis, Mycobacterium avium complex (MAC), cytomegalovirus (CMV) and cryptococcal meningitis. The development of certain OIs is associated directly or indirectly to the level of CD4 and can be predicted with some degree of accuracy (CDC, 2001).

2.1.7 Treatment

There is currently no cure for HIV/AIDS; however, drugs have been developed to fight both HIV infection and its associated infections and cancers. Antiretrovirals inhibits viral entry (fusion inhibitors) and generally target two key enzymes that the virus requires in order to replicate, i.e., protease and RT (De Clercq, 2004b; De Clercq, 2001).

RT inhibitors target the RT enzymes, furthermore they are divided into three classes - nucleoside reverse transcriptase inhibitors (NRTIs), nucleotide reverse transcriptase inhibitors (NtRTIs) and non-nucleoside reverse transcriptase inhibitors (NNRTIs) - based on the mode of action and minor alterations in their chemical structure (De Clercq, 2004b; De Clercq, 2001).

NRTI and NtRTIs are analogues of deoxynucleotides and are classified as competitive substrate inhibitors. They function by inhibiting RT (see section (§) 2.2.1). NRTIs undergo three phosphorylations to become active, where NtRTIs requires only one (Flexner, 2006). Examples of NRTIs include zalcitabine **(1)** (ddC), lamivudine **(2)** (3TC), zidovudine (AZT), didanosine (ddI),

stavudine (d4T), abacavir and emtricitabine, while tenofovir is classified as a NtRTIs (De Clercq, 2004b; De Clercq, 2001).

NNRTIs also inhibit the synthesis of viral DNA by connecting to and modifying the structure of the RT enzyme, so that it is incapable to function properly. They are non-competitive inhibitors of RT. Delavirdine, nevirapine and efavirenz are examples of NNRTIs (De Clercq, 2004b; De Clercq, 2001).

Protease inhibitors (PIs) act on the viral protease enzyme, which is essential for the final assembly and maturation of new virus particles as they leave the host cell and infect other cells. By binding to the active site of the viral protease enzyme, PIs prevent the processing of viral proteins into functional forms. Viral particles are still produced when the protease is inhibited, but these particles are immature and unable to infect new cells (Lewis *et al.,* 1997). Examples of PIs include ritonavir, saquinivir, indinavir, amprenivir, nelfinavir, lopinavir, atazanavir and fosamprenavir (De Clercq, 2004b; De Clercq, 2001).

Enfuvirtide, the first approved fusion inhibitor, interferes with HIV-1's ability to enter cells by blocking the integration of the virus with the cell membranes, consequently preventing infection of the CD4 cells. This reduces the level of HIV infection in the blood (Young *et al.,* 1995; Wild *et al.,* 1994).

New drugs that have progressed through clinical and/or preclinical development are CCR5 antagonists (i.e., SCH-C), CXCR4 antagonists (i.e., AMD070), NRTIs (i.e., amdoxovir), integrase inhibitors (i.e., S-1360), NNRTIs (i.e., etravirine) and PIs (i.e., tipranavir). Other compounds that appear valuable as anti-HIV agents are viral envelope gp120-binding agents (i.e., gp antibiotics and plant lectins), HIV integrase inhibitors (i.e., the pyranodipyrimidine V-165), cell receptor CD4 down-modulators (i.e., cyclotriazadisulfonamides) and compounds that appear to hinder with a post-integration, transcription transactivation event (i.e., N-aminoimidazoles and pyridine oxide derivatives) (De Clercq, 2004a).

2.2 Nucleoside Reverse Transcriptase Inhibitors

2.2.1 Mechanism of action

NRTIs need to be converted by cellular enzymes to the corresponding 5'-triphosphate (TP) before they can inhibit RT (Figure 2.4). NRTIs structurally resemble natural dNTPs, interacting with RTs substrate binding site; subsequently inhibiting the HIV replication through two mechanisms. Firstly, they competitively inhibit natural dNTPs for the RT enzyme. Secondly, by their own integration into the viral DNA chain, which leads to DNA chain termination, because

the NRTIs lack the 3'-hydroxyl group necessary for further DNA chain elongation (Flexner, 2006).

Lamivudine **(2)** enters cells by passive diffusion, where dCK (2'-deoxycytidine kinase) converts it to lamivudine-MP (monophosphate), subsequently CMP/dCMP-K (cytidylate/2'-deoxycytidylate kinase) phosphorylates lamivudine-MP to lamivudine-DP (diphosphate), thereafter NDP-K (nucleoside 5'-diphosphate kinase) converts lamivudine-DP to lamivudine-TP, which is the active anabolite (Perry & Faulds, 1997).

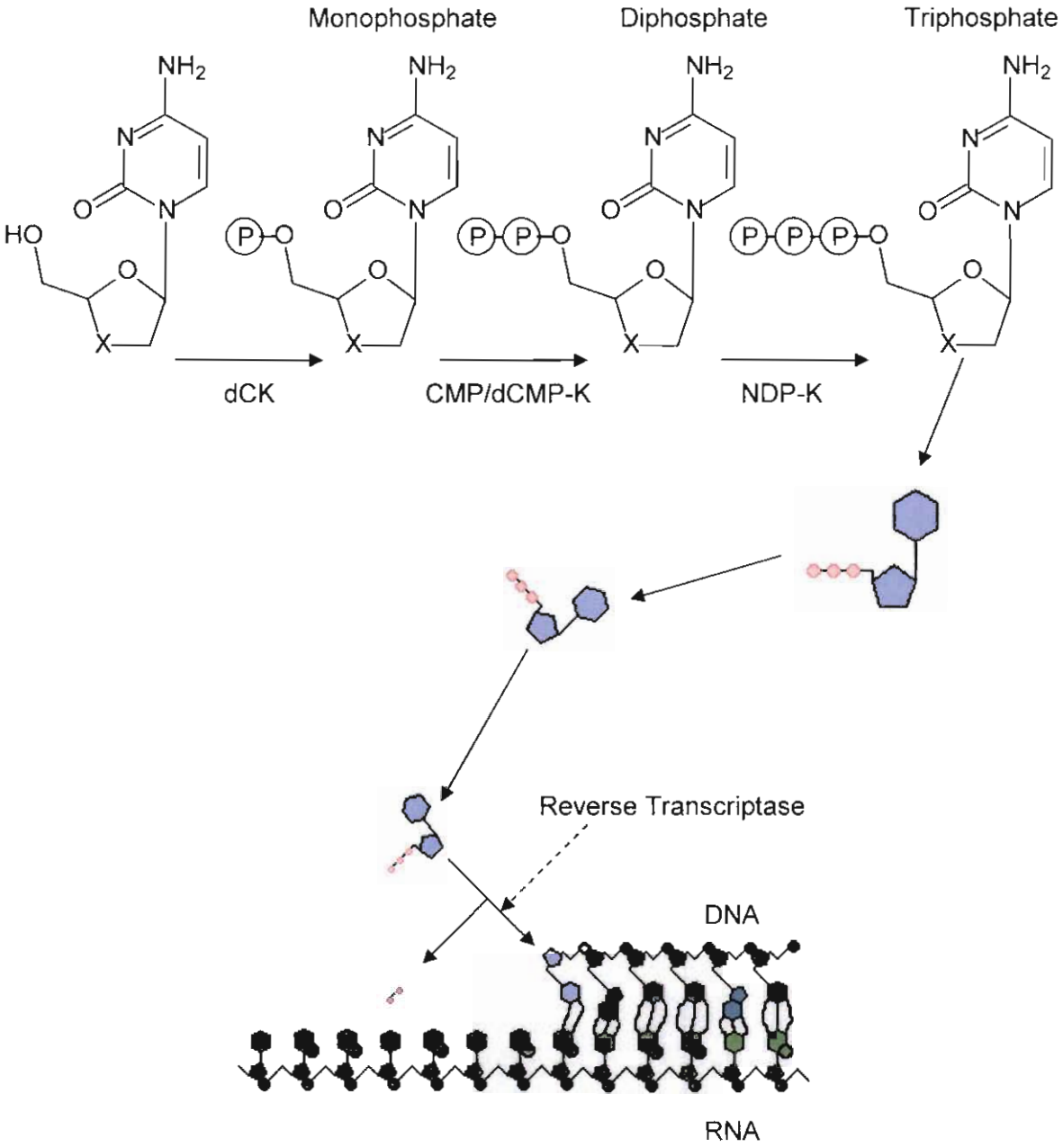

Figure 2.4: Mechanism of action of lamivudine **(2)** (X = S) and zalcitabine **(1)** (X = CH_2) (De Clercq, 2004b).

Zalcitabine **(1)** enters cells by passive diffusion and carrier-mediated transport (Adkins *et al.*, 1997). dCK phosphorylates zalcitabine **(1)** to zalcitabine-MP, subsequently CMP/dCMP-K converts zalcitabine-MP to zalcitabine-DP, afterwards NDP-K converts zalcitabine-DP to the active anabolite zalcitabine-TP (Adkins *et al.*, 1997).

2.2.2 Zalcitabine

Samuel Broder, Hiroaki Mitsuya and Robert Yarchoan at the National Cancer Institute (NCI) developed zalcitabine **(1)** and were later licensed to Hoffman LaRoche. In 1992, the Food and Drug Administration (FDA) approved the third antiretroviral on the market, monotherapy zalcitabine **(1)**, and in 1996, zalcitabine **(1)** in combination with AZT. Zalcitabine **(1)** ([4-amino-1-[5-(hydroxymethyl)tetrahydrofuran-2-yl]-1H-pyrimidin-2-one or 2',3'-dideoxycytidine) is a synthetic pyrimidine nucleoside derivative of the naturally occurring 2'-deoxycytidine in which the 3' hydroxy group is replaced by a hydrogen (Hayden, 2001).

Zalcitabine **(1)** are therapeutically used against HIV-1 and HIV-2. The major clinical toxicities of zalcitabine **(1)** are peripheral neuropathy, stomatitis and pancreatitis (Hayden, 2001); some other adverse effects are mouth ulcers, fatigue, diarrhoea, rash, fever, insomnia, nausea and cardiomyopathy (Brinkman & Ter Hofstede, 1999; Flexner, 2006).

2.2.3 Lamivudine

Bernard Belleau and Nghe Nguyen-Ba at the Montreal-based IAF BioChem International, Inc. laboratories invented lamivudine **(2)** in 1989 and were later licensed to Glaxo. In 1995, the FDA approved the fifth antiretroviral on the market, lamivudine **(2)** in combination with AZT and as a single dosed medication in 2002. Lamivudine **(2)** (4-amino-1-[2-(hydroxymethyl)-1,3-oxathiolan-5-yl]-1H-pyrimidin-2-one) is the (-)-enantiomer of 2',3'-dideoxy-3'-thiacytidine, in which the 3' carbon of the ribose of cytidine has been replaced with sulphur, forming an oxathiolane ring (Hayden, 2001). The (-)-enantiomer of the drug shows much less cytotoxicity and greater antiviral activity than the (+)-enantiomer (Skalski *et al.*, 1993).

Lamivudine **(2)** can therapeutically be used against HIV-1, HIV-2 and hepatitis B virus (HBV) and is one of the least toxic antiretrovirals; several of the major adverse effects are fatigue, vomiting, diarrhoea, rash, abdominal pain, insomnia, nausea and headache (Flexner, 2006; Bartlett *et al.*, 1996).

2.2.4 Transdermal delivery of NRTIs

Sawanpidokkul *et al.* (2004) investigated and compared the effects that different vehicles, enhancers and polymer membranes have on AZT across cadaver pig skin. Four dual vehicles

were used, i.e., polyethylene glycol 400 / water, isopropyl alcohol / water, ethanol (EtOH) / water and EtOH / isopropyl myristate (IPM). The highest flux (185.23 μg/cm^2/h) was established with the EtOH / IPM (50 : 50 (v/v)) vehicle. Different volume ratios of EtOH / IPM with various concentrations of different enhancers, i.e., oleic acid (OA), N-methyl-2-pyrrolidone (NMP) and lauric acid was studied on the solubility and permeation of AZT. EtOH / IPM (30 : 70) plus 10 % NMP and EtOH / IPM (20 : 80) plus 10 % NMP gave increased AZT solubility (56.27 and 42.6 mg/ml, respectively) and high flux values (460.34 and 284.92 μg/cm^2/h, respectively). AZT permeation was investigated if microporous polyethylene (PE) membranes were used to cover the pig skin. It was established that AZT flux values with PE membranes was approximately 50 % lower than the flux value of AZT with pig skin alone. Although, the flux of AZT (215.31 μg/cm^2/h) for PE membranes with EtOH / IPM (30 : 70) plus 10 % NMP, was greater than the AZT target flux (208 μg/cm^2/h) needed to maintain steady-state plasma concentration in humans.

Narishetty & Panchagnula (2004) investigated and evaluated *in vivo* and *ex vivo* penetration of AZT across rat skin, as well as a transdermal delivery system (TDS) for AZT with penetration enhancers, i.e., a combination of OA and menthol, integrated with hydroxypropyl methylcellulose. Drug release from the gel formulation was studied *in vitro* across PE membranes and *ex vivo* through full thickness rat skin. An AZT formulation was injected into rats and blood samples collected for *in vivo* studies. AZT in gel formulation TDS was stable at both 2 – 8 °C and 40 °C for 3 months and more. Compared with the solution formulation the gel did not notably slow down the penetration of AZT across the skin. Penetration enhancers (2.5 % (w/w)) improved the transdermal penetration of AZT across rat skin.

Oh *et al.* (1998) studied the transdermal delivery of AZT across hairless mouse skin by using iontophoresis and a penetration enhancer, i.e., propylene glycol / OA. The *in vitro* AZT solution flux increased approximately 5 – 40 times iontophoretically. When the solution was replaced with karaya gum matrix, the iontophoretic flux was much smaller for AZT. Inclusion of the penetration enhancer in the matrix increased the flux about 2 – 50 times. Using iontophoresis with the penetration enhancer in the matrix lead to a much higher flux for AZT than expected.

Kim & Chien (1996a) investigated the effects that an enhancer (OA) and vehicles (EtOH / tricaprylin (TCP) or EtOH / water) have on the simultaneous transdermal delivery of three NRTIs (zalcitabine **(1)**, ddI and AZT) using hairless rat skin at 37 °C. Different volume fractions of the co-solvent in the vehicles were used to saturate the drugs. As the EtOH volume increased, the skin permeation rates of the three NRTIs increased. Maximum values at 70 – 80 % (EtOH / water) and 50 % (EtOH / TCP) were reached, subsequently the skin permeation rates decreased with an increase in EtOH. 5 % (v/v) OA were added to EtOH / water (80 : 20) and EtOH / TCP (50 : 50). As the OA concentration increased the

permeation of AZT increased. Thus EtOH and OA increase skin permeation of AZT. Flux values obtained for zalcitabine **(1)**, ddI and AZT in 100 % water through hairless rat skin at 37 °C were 3.19, 1.73 and 1.99 μg/cm^2 per h, respectively.

Kim & Chien (1996b) did the same study as they did in 1996a, except for using two 1 % (v/v) penetration enhancers, i.e., NMP and OA. The permeation rate for the three NRTIs could not be enhanced appreciably with 1 % (v/v) NMP or OA in the EtOH / TCP vehicle, even though the permeation rate for these drugs were radically enhanced with 1 % (v/v) OA in the EtOH / water (60 : 40) vehicle. Flux values obtained for zalcitabine **(1)**, ddI and AZT in EtOH / water (60 : 40) containing 1 % (v/v) OA through human cadaver skin at 37 °C are were 0.61, 0.47 and 0.67 (mg/cm^2)/h, respectively and through hairless rat skin 1.88, 1.66 and 2.68 (mg/cm^2)/h, respectively.

Kim & Chien (1995a) investigated the transdermal delivery of zalcitabine **(1)** in both vehicles previously stated (1996a and 1996b) and used the same penetration enhancers as in 1996b. They found that increasing the volume fraction of EtOH to a maximum of 50 – 60 % in both vehicles increased the permeation rate for zalcitabine **(1)**. The same flux values for EtOH / water (60 : 40) containing 1 % (v/v) OA were reached as in 1996b and was 4 – 5 times higher than the target rate for maintaining therapeutic blood level for zalcitabine **(1)** (0.14 mg/cm^2/h).

Kim & Chien (1995b) investigated the stability of zalcitabine **(1)**, ddI and AZT in phosphate buffer solution (PBS) (pH 7.5) at 37 °C for transdermal use by means of hairless rat skin. Zalcitabine **(1)** and ddI degraded in the extract of the dermis, although all three NRTIs were stable for at least 30 h in the extract of the epidermis. An unidentified peak appeared on the chromatograms for zalcitabine **(1)** in the extract of the dermis. When zalcitabine **(1)** was added to the filtered extract the peak vanished, this suggested bacterial degradation. A 0.01 % (w/v) antibacterial, i.e., gentamicin was added in the receptor solution and stabilised zalcitabine **(1)**, whereas a 0.01 % (w/v) purine nucleoside phosphorylase inhibitor, such as p-chloromercuri-benzoic acid was added to stabilise ddI.

Seki *et al.* (1990) synthesised five esters of AZT, to try and improve the delivery of AZT. The aqueous solubility in water and IPM, partition coefficients and flux values in water and IPM were determined for AZT and its esters. The aliphatic esters with their flux values calculated in nmol/cm^2-hr, obtained in water after 23.5 - 24.5 h were acetate, 38.3 ± 10.2; butyrate, 13.6 ± 2.3; hexanoate,17.4 ± 6.2; octanoate, 2.0 ± 0.9 and decanoate, 0.4 ± 0.1.

CHAPTER 3

TRANSDERMAL DRUG PERMEATION

3.1 Introduction

There has been an increasing interest in percutaneous drug absorption over the past few years, especially in conditions where the most convenient method of drug intake (orally) is not possible and an alternative route must be sought (Naik *et al.*, 2000). Topical application of drugs for systemic therapy may have several advantages over the conventional oral route. It circumvents two of the main problems from oral drug administration:

1. It eliminates variables that may influence the gastro-intestinal absorption, such as food intake, the drastic change in pH along the gastro-intestinal tract, intestinal motility and illness such as nausea, which disables the patient to contain the drug for a long enough period, thus inhibiting absorption.
2. It may eliminate systemic first-pass metabolism as it circumvents the liver. This may result in an increased bioavailability of the drugs susceptible to this bioconversion (Wiechers, 1989).

Except for these two main advantages, we can add that transdermal drug delivery avoids peaks and valleys in serum levels often seen with discrete oral dosages and which can often cause undesirable side effects (Roy, 1997), furthermore, it maintains zero-order delivery in many instances and can be sustained for longer periods of time, leading to less frequent dosing regimens. This would, in turn, improve patient compliance, since frequent drug intake is no longer necessary (Kai *et al.*, 1992; Naik *et al.*, 2000; Ouriemchi & Vergnaud, 2000).

As the largest and most external organ, the skin is constantly exposed to the hazards of the environment and is often viewed as a living protective envelope surrounding the body. Histologically, the skin is a complex multilayered organ (Holbrook & Wolff, 1993) with a total thickness of $2-3$ mm. The stratum corneum has physical barrier functions to most compounds, including drugs, while the viable skin is responsible for enzymatic bioconversion. Transdermal permeation involves drug molecules first partitioning onto the surface of the skin and subsequently diffuses across the stratum corneum toward the viable tissue. The diffusion into the stratum corneum is believed to be a rate-limiting step on transdermal absorption of most drugs that are stable in the skin. After penetration across the skin, drug molecules are

efficiently taken away into the microcirculation located beneath the basal layer of the skin (Tojo, 1997).

Transdermal therapy, however, has its limitations. Firstly, and most obviously, the skin acts as a two-way barrier, preventing the entry of harmful or unwanted molecules from the external environment, while controlling the loss of water, electrolytes and other body constituents. Secondly, there may be pharmacodynamic, physiological and/or physicochemical limitations. Compounds may act as irritants, cause allergic sensitisation, be keratolytic or cause hyperpigmentation. These pharmacodynamic effects are dependent on the extent of the percutaneous absorption of the substance in question, which, in turn, depends on the physiological characteristics of the skin and the physicochemical properties of the penetrant. Thus, the physicochemical properties of the drug have an influence on the rate and extent to which a number of drugs pass through the skin readily (Beckett, 1982).

The percutaneous delivery of drugs is an effective way of achieving controlled drug delivery. Unfortunately it is only suitable for a limited number of drugs that possesses the appropriate physicochemical characteristics to allow them to cross the excellent barrier provided by the outermost layer of the skin, the stratum corneum (Foldvari, 2000; Harrison *et al.,* 1996; Naik *et al.,* 2000).

3.2 The skin structure

The largest organ of the body, the skin, covers an area of approximately 1.73 m^2 (Barr, 1962) and weighs an average of 3 – 4 kg (Schalla & Schaefer, 1982; Stüttgen, 1982). The average thickness of the skin is about 0.5 mm (ranging from 0.05 – 2.0 mm) (Foldvari, 2000). A square centimetre of skin contains 3 blood vessels, 10 hair follicles, 12 nerves, 15 sebaceous glands and 100 sweat glands (Asbill & Michniak, 2000).

A cross-section of the skin (Figure 3.1) shows the anatomically distinguishable regions, from the outside of the skin inwards (Flynn, 1990).

- The ~ 10 µm thin nonviable epidermis or stratum corneum;
- The ~ 100 µm thin viable epidermis, which includes the germinal (basal) layer and everything living above up to the stratum corneum;
- The ~ 1000 µm thick dermis, and
- The hypodermis or subcutaneous fat layer.

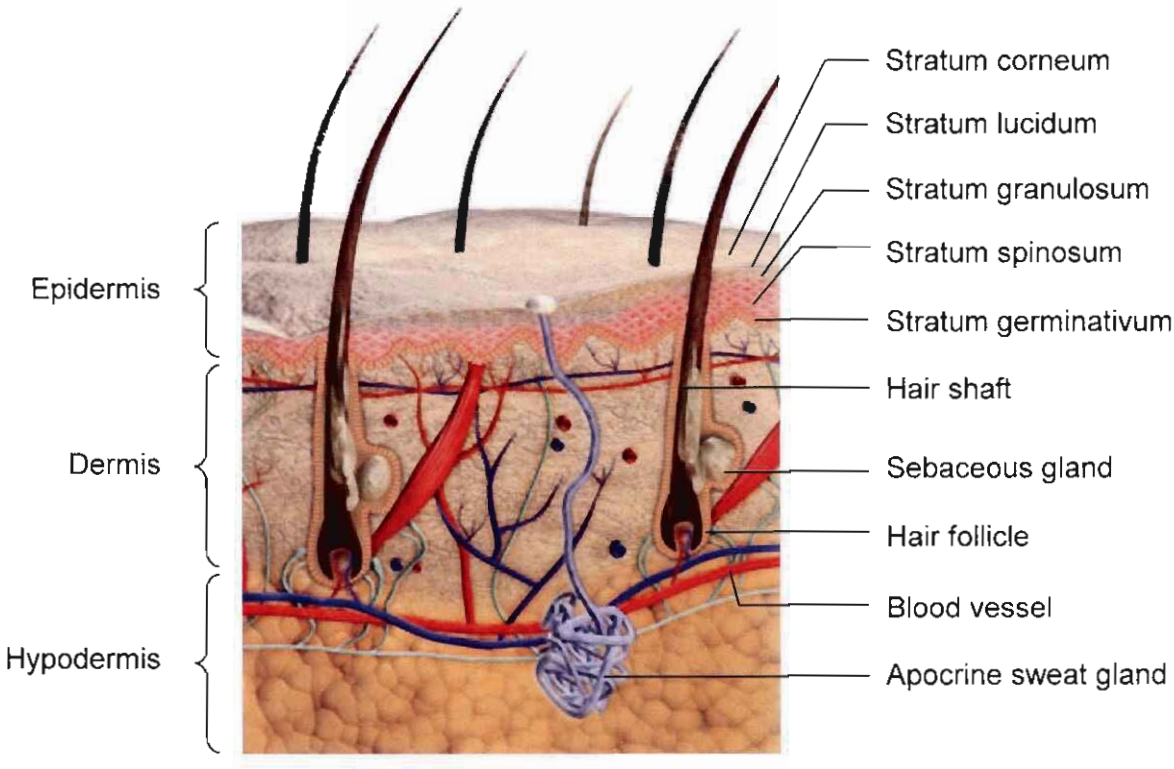

Figure 3.1: A cross-section of the human skin (West & Nowakowski, 1996).

Before reaching the systemic circulation, a penetrating chemical has to cross several potential barriers. These include the epidermis (consisting of the stratum corneum or horny layer and the viable layers of the epidermis) and the dermis (Foldvari, 2000; Schalla & Schaefer, 1982) and will be discussed in the succeeding sections.

3.2.1 Stratum corneum

The outmost layer of the skin, the stratum corneum or "cornified layer", is extremely hydrophobic and consists of keratinised epithelial cells (corneocytes), physically isolated from one another by extracellular lipids arranged in multiple lamellae, which produces the primary barrier to drug delivery into the skin (Prausnitz *et al.*, 2004). Epidermal cells are continuously formed in the basal layer and gradually move upwards and away from their supply of nourishment and oxygen (Roy, 1997; Schaefer and Hensby, 1990). This process takes almost four weeks and results in the formation of the stratum corneum (Schaefer and Hensby, 1990).

The total thickness of the stratum corneum under normal non-hydrated conditions ranges from 10 – 20 µm and contains 10 – 25 layers of corneocytes (Flynn, 1979; Foldvari, 2000) that are continuously shed (desquamated). On the palms of the hands and on the foot soles, the stratum corneum has an average thickness of 400 – 600 µm, with vertically stacked cells.

The stratum corneum tissue is often schematically represented as a brick wall (as shown in Figure 3.2). The terminally differentiated, keratin-filled corneocytes are the "bricks" while the lamellar, intercellular lipid domain represents the "mortar" (Williams, 2003). The corneocytes are joined together by desmosomes, which provide the stratum corneum with structural stability and strength (Prausnitz *et al.*, 2004).

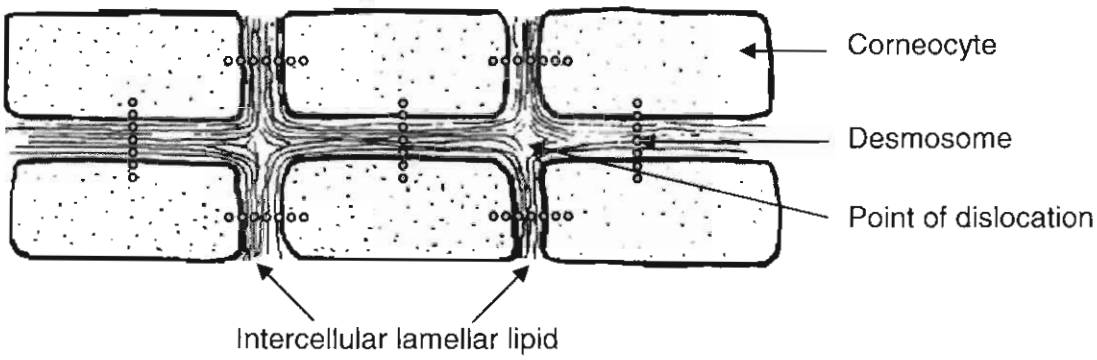

Figure 3.2: Proposed "Brick and Mortar" Two-Compartment Model (Elias, 1983; Williams, 2003).

The stratum corneum lipids are selectively enriched in ceramides, free acids, free sterols and lesser quantities of glycolipids, triglycerides, hydrocarbons, sterol esters and cholesterol sulphate, but contains no phospholipids (Elias, 1983). It is postulated that despite an absence of phospholipids, these lipids apparently can arrange themselves into membrane bilayers (Figure 3.3) (Roy, 1997). All of the compounds of interstitial lipids, except for water-soluble proteins, essentially contribute to the variable function of the stratum corneum (Scheuplein & Blank, 1971).

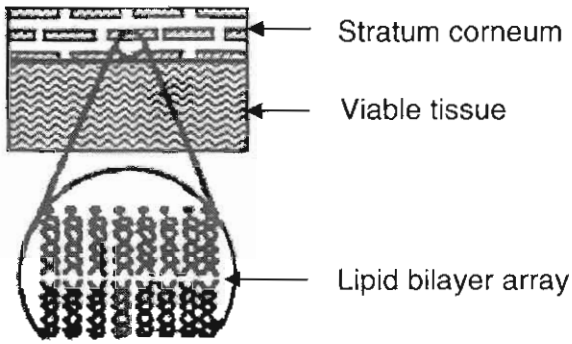

Figure 3.3: A schematic representation of the stratum corneum lipid bilayers (Hadgraft & Wolff, 1993).

The stratum corneum can be considered as a hydrophilic-lipophilic multilayered formation, due to the lipophilic cell membranes and the protein rich intercellular spaces between the corneocytes. Consequently, substances will not easily penetrate the stratum corneum if they do

not contain both lipophilic and hydrophilic properties, even though exceptions to this rule do exist (Foldvari, 2000; Schalla & Schaefer, 1982). The stratum corneum is generally regarded as the rate-limiting barrier for transport, of most solutes of pharmaceutical interest, across the skin. In spite of this well-documented heterogeneity, most studies of drug transport treat the stratum corneum as a homogeneous membrane. Thus, solute fluxes are assumed to be directly proportional to stratum corneum/water partition coefficients and diffusivities and inversely proportional to the macroscopic thickness of the stratum corneum (Raykar *et al.*, 1988).

Some experimental observations appear to conflict with predictions arising from the assumption of homogeneity. For example, the thickness of the stratum corneum and the rates of percutaneous transport across human skin, are not influenced by the number of cell layers but, instead, correlate inversely with the lipid content. These stratum corneum lipids may be pooled in the intercellular spaces, forming broad, multilamellar sheets, which constitute the barrier to diffusion. Similarly, in reaggregrated stratum corneum cell systems the effectiveness of the barrier function is directly proportional to the lipid content rather than the barrier thickness (Raykar *et al.*, 1988).

3.2.2 Viable epidermis

As shown in Figure 3.1, the viable epidermis lies between the stratum corneum and the dermis, and it has shown readily definable interfaces with each. It consists primarily of an aqueous cytoplasm encapsulated in cellular compartments by delicate cell membranes - the cells are fused together by tonofibrils. In drug delivery considerations it is often regarded as a single stratum of living cellular tissue, although histologically it is multilayered.

It is about 75 – 150 μm thick and consists of various layers, characterised by various stages of differentiation (Rieger, 1993; Roy, 1997). A penetrating chemical has to cross the stratum lucidum, the stratum granulosum (granular layer), the stratum spinosum (spinous layer) and the stratum basale (or basal layer). These are metabolically active cells undergoing systematic transitions that eventuate in cell death, for as they move toward the surface, they move away from the microcirculation in the dermal layer and eventually lose their nuclei.

The viable epidermis and stratum corneum are dissimilar in that it possesses metabolically active enzymes and phospholipids. Phospholipids are predominantly located in the basal and spinous layers, but the content decreases as the cells differentiate to the surface and the cholesterol content simultaneously increases (Foldvari, 2000).

The cellular structure of the viable epidermis is primarily hydrophilic throughout its various layers, and substances can be transported in its intercellular fluids. Especially for polar substances, the resistance to penetrate is considerably lower than in the stratum corneum;

because the tightly packed alternating hydrophilic and lipophilic layers are no longer present (Wiechers, 1989).

3.2.3 Dermis

The dermis is depicted in Figure 3.1 as a nondescript region lying between the epidermis and the subcutaneous fatty region (Hunter *et al.,* 1996). It consists mainly of a dense network of structural protein fibres, collagen, reticulum (that supports and strengthens the epidermis) and elastin (providing flexibility) embedded in a semigel matrix of mucopolysaccharidic gel (Asbill & Michniak, 2000; Flynn, 1990). It is mostly acellular, rich in nerve endings, lymphatic and blood vessels (Schaefer & Hensby, 1990). Its thickness varies, being the least in the eyelids and the greatest in the soles and palms. The microcirculation that subserves the entire skin is located in the epidermis (Flynn, 1990). A broad network of dermal capillaries connects to the systemic circulation, with significant horizontal branching from the venules and arterioles in the papillary dermis to form plexuses, as well as supplying blood to glands and hair follicles (Foldvari, 2000).

The excellent blood supply in the dermis functions as a "sink" (constantly removing drugs from the absorption site) for diffusing molecules and keeps penetrating molecule concentrations very low, thereby amplifying concentration gradients across the skin layers and promoting percutaneous absorption (Danckwerts, 1991; Roy, 1997). Hence it is believed that the dermis offers no barrier for drug to permeate, except for molecules that might be substantive to specific dermal components (Rieger, 1993).

3.2.4 Hypodermis

The hypodermis or subcutaneous fatty layer is the innermost layer of the skin, provides a mechanical cushion for external blows and a thermal barrier from external variations in temperature. In general, if a substance is transported to this layer it is considered that it has entered the systemic circulation. The fat deposits may serve as a depot for a substance, possibly hindering entry into the blood circulation (Washington & Washington, 1989).

3.2.5 Skin appendages

In addition to the above three major layers of the skin, the skin has many other appendages that affect the percutaneous delivery of drug compounds (Danckwerts, 1991). The skin has interspersed hair follicles, nails and associated sebaceous glands, as well as in specific regions two types of sweat glands, the eccrine and apocrine glands (Hunter *et al.,* 1996; Stüttgen, 1982). Collectively these are all called the skin appendages (Flynn, 1990) of which all, except the nails, lie in the dermis (Hunter *et al.,* 1996). The sebum, which is produced by the

sebaceous glands, consists of a mixture of fatty acids, triglycerides, waxes, cholesterol and cellular debris (Montaga, 1965). The expanded lower part of the hair follicle contains the matrix from which new cells are formed. These cells move upward and cornify differently than the skin (Katz & Poulson, 1971).

3.3 The process of percutaneous absorption

Percutaneous absorption can be defined as the uptake of a compound into the systemic circulation after dermal application, and it describes the movement through the various layers of the skin with respect to both rate and extent.

This whole process of absorption can be divided into three steps:

1. Penetration (the entry of a substance into a particular layer or organ).
2. Permeation (the penetration through one layer into another, which is both functionally and structurally different from the first layer).
3. Absorption (the uptake of a substance into the vascular system, lymph and/or blood vessels, which act as the central compartment) (Schaefer *et al.,* 1982).

There are many factors that can alter the rate and extent of absorption into the skin. The mode of application, temperature and condition of the skin, influence of the vehicle, frequency and duration of application, concentration and physicochemical properties of the active ingredient are all examples that can affect the absorption (Lien & Tong, 1973).

Molecules moving from the environment across the intact skin of living humans must first penetrate the stratum corneum. They must then penetrate the viable epidermis, the papillary epidermis, and the capillary walls into the bloodstream or lymph channels, whereupon they are removed from the skin by flow of blood or lymph (Idson, 1975; Kalia & Guy, 2001). To move, molecules have to overcome a different resistance in each tissue (Idson, 1975).

A concentration gradient is established through the skin via passive diffusion. The concentration gradient is very steep in the horny layer because of its barrier function and less steep in the viable epidermis. As a consequence of the passive diffusion (there being no evidence for active transport mechanisms in the skin) a decreasing concentration gradient from the horny layer to the subcutaneous tissue is found. The driving force for absorption or transport of any drug is proportional to the concentration gradient of any drug within the skin (Flynn, 1989).

3.4 Routes of transdermal delivery

When molecules move onto the intact skin, the diffusant then have three potential penetration pathways through the skin as seen in Figure 3.4, i.e., through sebaceous glands, across the stratum corneum or through the hair follicles (Barry, 2001; Idson, 1975). The path through the follicles and glands are known as the transappendageal route. Two transdermal pathways exist within the stratum corneum, i.e., transcellular and intercellular routes (Barry, 2001; Guy & Hadgraft, 1989b).

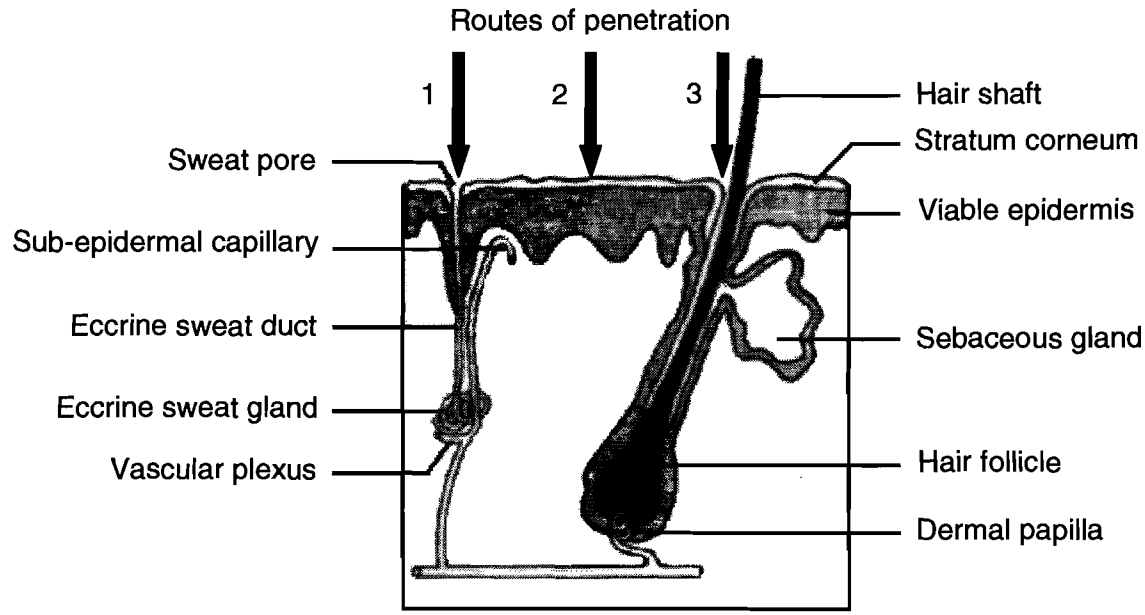

Figure 3.4: Pathways of penetration through the skin: (1) via the sweat gland ducts; (2) across the stratum corneum; or (3) through the hair follicles (Barry, 2001).

3.4.1 Transappendageal

This path permeates through the hair follicles and sweat gland ducts, bypassing the stratum corneum and is considered to be of substantially less importance as it accounts for a minimum of 0.1 % of the total surface area of the skin (Schaefer & Hensby, 1990), but may be important for ions, colloidal particles, polymers and large polar molecules that struggle to cross intact stratum corneum (Barry, 2001).

3.4.2 Transepidermal

3.4.2.1 Transcellular

The transcellular pathway involves crossing the stratum corneum by the most direct route and diffusing through the cornified cells, intracellular spaces and extracellular bilayers (Barry, 2001).

Although the intercellular bilayered domains surround the corneocytes, the aforementioned are basically aqueous in nature providing a polar route for the penetrant through the membrane (Wlliams, 2003).

3.4.2.2 Intercellular

The intercellular pathway involves passage through the lipids in the stratum corneum and therefore lipid compounds pass through this route with ease (Flynn & Weiner, 1993). It is considered that for most small, uncharged molecules, the intercellular route predominates (Guy & Hadgraft, 1989b, Williams, 2003).

Irrespective of which route is favoured, the drug eventually works its way to the edge of the viable tissue. Ordinarily the viable tissue is not much of a diffusion impediment and net drug passes with facility through the living layer towards the closest capillary bed (Flynn & Weiner, 1993).

3.5 Factors influencing transdermal permeation

The biological and physicochemical properties are the main factors influencing transdermal permeation (Mukhtar, 1992). These factors are only separated for practicality; useful for comprehensive purposes. However, if one variable changes, it usually causes several effects on drug flux (Barry, 2002).

3.5.1 Biological factors

The quantitative prediction of the rate and extent of transdermal penetration and absorption of topically applied drugs are complicated by the biological variability inherent to the skin. In order to gain perspective of this phenomenon, one should appreciate that mammalian skin is a dynamic organ with important biological factors, i.e., skin age, disease, the specific site of transdermal drug application, etc. that influence transdermal permeation.

3.5.1.1 Disease and skin conditions

Intact skin provides a barrier to absorption; therefore skin that is in a diseased state or damaged and inflamed has the potential to increase percutaneous absorption. Acne, psoriasis, atopic dermatitis, cracks, scratches or cuts enhance permeability (Jackson, 1993). Conditions that result in a thickened stratum corneum like eczema, ichthyosis, corns and warts reduce permeability (Barry, 2002; Pefile & Smith, 1997).

3.5.1.2 Skin hydration

In its normal state at ordinary relative humidity, the stratum corneum contains moisture to the extent of 15 – 20 % of its dry weight. The water content increases up to 300 – 400 % of the dry weight on some areas of the body when the skin becomes waterlogged through soaking. Hydrated skin plays an essential role in the extent and rate of transdermal absorption (Riviere, 1993) and is considered as a useful penetration enhancer (Idson, 1975; Wurster & Kramer, 1961). Hydrating the skin through moisturising, bathing, being in a humid area, etc. makes the skin swell and water is absorbed by the corneocytes, which increases the percutaneous absorption of certain substances into the skin (Jackson, 1993).

3.5.1.3 Skin age

The skin structure of infants and neonates is identical to that of an adult, but topically applied drugs can lead to very high blood concentrations. The dermis needs 3 – 5 months to mature after birth and it is approximately 60 % of its adult thickness. Furthermore, infants and children have a higher surface area to weight ratio and the epidermal enzymes may not be fully developed to metabolise applied drugs (Williams, 2003). This trend continues for infants until the end of gestation (Lund, 1994). In the elderly, the permeation of the skin can also be affected through the changes in the ultra structure, elasticity, barrier properties and chemical composition of the skin (Idson, 1975; Lund, 1994).

3.5.1.4 Skin region

Skin structure differs to some extent over the human body. There is an inverse relationship between the diffusion path length (h) and the permeability coefficient (k_p) of a penetrant through the stratum corneum. Consequently it can be expected that the permeability would decrease at skin sites where the stratum corneum is thicker. There is a significant variation (approximately 40 %) in permeation between the same body site on different individuals and also a significant variation (up to 30 %) across a given body site (for example the abdomen) of an individual (Williams, 2003). The region for transdermal application may influence the drug concentration reaching the systemic blood circulation and should consequently be taken into account when the transdermal permeant is applied (Schalla & Schaefer, 1982).

3.5.1.5 Skin metabolism of drugs

The skin consists of a great number of different, extremely specialised cells in various layers (Täuber, 1982); therefore if a penetrant passes through, it may lead to drug metabolism. Skin metabolism may become the rate-limiting step in percutaneous permeation of drugs, which undergo biotransformation. Bioconversion, in general, takes place in the viable epidermis;

which is the most metabolically active layer in the skin (Tojo, 1997). Dermal drug metabolism is not a common problem (Flynn & Weiner, 1993; Täuber, 1982) and is negligible in comparison to hepatic first-pass metabolism (Gupta *et al.,* 1997; Täuber, 1989).

3.5.1.6 Temperature

The human body's internal temperature is about 37 °C and the external skin surface is approximately 32 °C. Increasing the temperature, i.e., through applied heat, increases the blood flow and dilates blood vessels, thus leading to increased drug removal in the skin and finally enhanced drug permeation (Sun, 1997; Williams, 2003).

3.5.2 Physicochemical factors

The principal factors affecting penetration are the properties of the drug, the vehicle and the skin. The physical and chemical nature of each of these components and their collective interactions all influence the rate at which the drug penetrates the skin (Katz & Poulsen, 1971).

The physicochemical properties of a drug substance are very important determinants for its permeation through the skin. The most important processes to consider are the partitioning and diffusion steps that occur in the transport into, through and out of the stratum corneum (Hadgraft & Wolff, 1993).

3.5.2.1 Drug solubility in the stratum corneum

Compounds will partition into the outer layers of the stratum corneum once they are released from their vehicles. The degree to which this will happen is controlled by the amount applied and the solubility limit in the stratum corneum (Smith, 1990). The rate of partitioning from the vehicle to the skin will be more rapid than the diffusion into the skin (Hadgraft & Wolff, 1993).

The thermodynamic activity of a drug in a particular vehicle indicates the potential of the active substance to become available for therapeutic purposes (Kemken *et al.,* 1992). It has been shown that supersaturated solutions provide enhanced fluxes through model membranes and skin (Hadgraft, 1991). A saturated solution is therefore preferable for a topical drug delivery system as it represents maximum thermodynamic activity (Kemken *et al.,* 1992). The level of saturation is dependent on the solubility of the drug in the delivery formulation (Danckwerts, 1991). A smaller amount of drug is released from sub-saturated solvents than from saturated ones.

The importance of solubility was recognised early when it was found that compounds with both lipid and water solubilities penetrate better than substances with either high water or high lipid

solubility (Liron & Cohen, 1984; Naik *et al.,* 2000; Pefile & Smith, 1997). The solubility characteristics of a substance greatly influence its ability to penetrate biological membranes. The lipid-water solubility pattern of the applied material was recognised in the Meyer-Overton theory of absorption. This theory stated that, because the epidermal cell membrane consists of a mosaic pattern of lipid and protein molecules, substances soluble in lipids pass through the cell membrane owing to its lipid content; while, water soluble substances pass after the hydration of the protein particles in the cell wall, which leaves the cell permeable to water soluble substances (Naik *et al.,* 2000). In essence, the aqueous solubility of a drug, determines the concentration presented to the absorption site, and the partition coefficient strongly influences the rate of transport across the absorption site (Idson, 1975).

3.5.2.1.1 Solubility parameter

The solubility parameter is defined as the square root of the cohesive energy density. The cohesive energy of a material is the energy which holds that substance together and is therefore also the net effect of all the intermolecular interactions. It is the amount of energy required to separate the constituent atoms or molecules of the material to an infinite distance and therefore it is a direct measurement of the attraction that atoms of molecules have for one another (Hildebrand & Scott, 1950).

The solubility parameter, δ, is an intrinsic physicochemical property of a substance, which has been used to explain the drug action, structure-activity relationships, drug transport kinetics and *in situ* release of drugs. Hence, the precise value of the solubility parameter of the drug is of interest (Subrahmanyam & Sarasija, 1997).

The solubility parameter first defined by Hildebrand and Scott has been found to be a useful guide for solvent miscibility. The solubility parameter of an organic solute (δ_2) in the stratum corneum can be estimated using Equation 3.1, if the solubility of the solute in a non-polar organic solvent (like hexane) is known, as well as the solute's heat of fusion, the melting point, and the solubility parameter of the solvent (hexane) (Hildebrand *et al.,* 1970):

$$\ln X_2 = \frac{-\Delta H_f}{RT}\left(\frac{T_f - T}{T_f}\right) + \frac{\Delta C_p}{R}\left(\frac{T_f - T}{T} - \ln\frac{T_f}{T}\right) - \frac{V_2\phi_1^{\,2}}{RT(\delta_1 - \delta_2)^2} \qquad \textbf{Equation 3.1}$$

where X_2 is the solute's mole fraction solubility in hexane, ΔH_f is the heat of fusion of a solid, R is the gas constant, T_f is the melting point of the solid (Kelvin), T is experimental temperature $< T_f$, ΔC_p is the difference in heat capacity between the solid form and the hypothetical super cooled liquid form of the compound, both at the same temperature, V_2 is the molar volume of the liquid solute, Φ_1 is the volume fraction of the solvent, δ_1 is the solubility parameter or square

root of the cohesive energy density of the solvent (hexane) and δ_2 is the solubility parameter or square root of the cohesive energy density of the solute.

A low solubility parameter for a solute is synonymous with high lipophilicity (Roy & Flynn, 1989).

The solubility parameter of the skin has been estimated at approximately 10 (Liron & Cohen, 1984) and therefore drugs, which possess similar values would be expected to dissolve readily in the stratum corneum. Formulation components, which can diffuse into the skin, i.e., propylene glycol, will tend to and is expected to increase the value of the solubility parameter and would be expected to promote the solubility of polar drugs in the lipids (Hadgraft & Wolff, 1993).

3.5.2.1.2 Aqueous solubility

One of the most important factors influencing bioavailability is the drug's chemical structure, which in return influences the drug's aqueous solubility. Both the pH and the physical properties play a role in determining solubility. As a general rule, a drug substance with an aqueous solubility of less than 1 mg/ml may represent a potential bioavailability problem. In some instances, minor chemical modifications of the drug chemical, such as salt formation or esterification, are necessary (Abdou, 1989).

Aqueous solubilities of nonpolar organic compounds depend on their molecular surface areas, which are essentially hydrophobic in nature. Thus, the affinity for water decrease exponentially as molecular hydrophobic surface area increases (Barry, 2001). The following equation enables the estimation for the aqueous solubility, S*w*, of either liquid or crystalline organic or crystalline nonelectrolytes (Yalkowsky & Valvani, 1980):

$$\log Sw \approx 1.00 \log PC - 1.11 \frac{\Delta Sf\,(mp - 25)}{1364} + 0.54 \qquad \textbf{Equation 3.2}$$

where PC is the octanol-water partition coefficient, ΔSf is the entropy of fusion and are estimated from the chemical structure and mp is the melting point.

This equation provides a means of assessing the role of crystal structure (as reflected by the melting point and the entropy of fusion) and the activity coefficient (as reflected by the octanol-water partition coefficient) in controlling the aqueous solubility of a drug (Yalkowsky & Valvani, 1980).

Compounds with low melting points usually have high solubilities and consequently penetrate the skin better than compounds with high melting points (Hadgraft & Wolff, 1993).

3.5.2.2 Partition coefficient

Although only 10 – 15 % of the total stratum corneum mass comprise lipids, these lipids largely dictate the overall skin permeability properties. The transfer of a drug across the stratum corneum is by passive diffusion and, because of barriers imposed by the skin, this process occurs very slowly. The tissue consists of aggregates of closely packed cells and contains both lipid and aqueous regions. Lipid soluble substances readily pass through the intercellular bilayers of the cell membranes, whereas water soluble drugs are able to pass through the skin because of hydrated intracellular proteins. Charged and highly hydrophilic drugs may also use the appendageal route to permeate through the skin (Williams, 2003).

When a drug reaches the viable tissue it encounters a phase change. It has to transfer from the predominantly lipophilic intercellular channels of the stratum corneum into the living cells of the epidermis, which will be largely aqueous in nature and essentially buffered to pH 7.4 (Hadgraft & Wolff, 1993; Smith, 1990). Therefore, skin permeants must have reasonable solubilities in oil and water, but should favour the oil (Guy & Hadgraft, 1989a). For lipophilic drugs, transfer into the viable epidermis can be a slow process (Hadgraft & Wolff, 1993). That is why Hadgraft & Somers (1956) stated that maximal percutaneous absorption occurs when the medicament combines lipid solubility with a moderate solubility in water. A preferentially oil soluble drug may have difficulty leaving the stratum corneum and in contrast, an extremely polar drug will have trouble partitioning into the stratum corneum from its vehicle. Kai *et al.* (1992) found that the partition coefficient to the membrane showed a linear correlation with drug lipophilicity, which suggested that drug permeation through membranes is governed mainly by the process of drug partitioning to the membrane.

Compounds with a high partition coefficient, i.e., high lipophilicity, are likely to be the best penetrants of the skin. Since there are difficulties in determining the actual skin/water partition coefficients of drugs, olive oil/water (Scheuplein & Blank, 1971) and octanol/water ($K_{octanol/water}$) (Scheuplein, 1986) partition coefficients are used for ranking the lipophilicities of compounds for skin permeation (Takahashi *et al.,* 1993). The octanol/water partition coefficient is generally believed to be a good representation of the partitioning of the drug between the lipophilic stratum corneum and the underlying hydrophilic viable epidermis (Tenjarla *et al.,* 1996). Dissolving drugs in aqueous solution with an organic solvent, and thereafter assaying each of the two phases for drug content determine partition coefficients. The partition coefficient is the organic solvent to water drug concentration ratio (Ansel, 1981).

The vehicle to stratum corneum partitioning often contributes to the rate-limiting step in transdermal drug delivery. Partitioning of the drug to the stratum corneum is dependent upon

the affinity of the drug for the base formulation and the absorption of the drug through the skin (Watkinson *et al.*, 1995).

It is possible to make the following general comments regarding the optimal permeation of the drug. It should have reasonable solubility characteristics in both water and oils (this is generally associated with low melting point and molecular weight) and have a log P (octanol-water partition coefficient) in the range of 1 – 2 (Hadgraft, 1996; Roberts & Sloan, 2000). For compounds with log P > 2, there are potential problems in achieving steady plasma concentrations in a reasonable time span (Guy & Hadgraft, 1989a).

3.5.2.3 Diffusion coefficient

Diffusion can be defined as the transport of matter resulting from movement of the substance within a substrate (Rieger, 1993). The diffusion coefficient can therefore be defined as the number of moles of drug that diffuse across a membrane or within the various strata of a given area per time unit, and is influenced by the molecular size of the drug and the viscosity of the surrounding medium (Idson, 1983).

Particles move through membranes firstly by simple molecular permeation and secondly by movement through pores and channels (Martin *et al.*, 1983). Because of the dense nature of the stratum corneum, values of the diffusion coefficients in this tissue are 1000 times smaller than anywhere else in the skin. This factor contributes to a high resistance and low permeability (Flynn, 1990); hence a general rule is that molecules follow the path of least diffusional resistance (Flynn, 1989).

The three important factors influencing the penetration of drug into the skin are:

1. Concentration of dissolved drug, since penetration rate is proportional to concentration.
2. Partition coefficient, K - between the skin and the vehicle.
3. Diffusion coefficients, which represent the resistance of the drug molecule movement through the vehicle and the skin barriers (Martin *et al.*, 1983).

Fick's laws are generally viewed as the mathematical description of the diffusion process through the membranes. Fick's laws are applicable whenever the chemical or physical nature of the membrane controls the rate of diffusion. In order to pass from the solvent to the skin, the diffusing molecule must have some affinity for the stratum corneum. Once the molecule is within that membrane it can diffuse in any direction. Progress is not random, because the permeant tends to move readily from the higher concentration to the lower concentration. Fick's

first law can be applied to describe the diffusion processes in the stratum corneum (Wiechers, 1989; Schalla & Schaefer, 1982):

$$J = K_p \cdot \Delta C = \frac{D \cdot K \cdot \Delta C}{L}$$

Equation 3.3

where J is the steady-state flux of the permeant through the stratum corneum ($\mu g.cm^{-2}.h^{-1}$), K_p is the permeability coefficient of the permeant in the stratum corneum ($cm.h^{-1}$), ΔC is the concentration gradient of the permeant across the stratum corneum ($\mu g.cm^{-3}$), D is the diffusion coefficient of the permeant in the stratum corneum ($cm^2.h^{-1}$), K is the apparent partition coefficient of the permeant between the stratum corneum and the vehicle and L is the length of the pathway through the stratum corneum (cm).

It is apparent from Equation 3.3 that the flux is constant if the permeability coefficient and the concentration difference are constant.

The concentration gradient over the stratum corneum will depend primarily upon chemical characteristics of the permeant including solubility, lipophilicity, ionisation and stability (Smith, 1990; Wiechers, 1989). It is assumed that ΔC will be the same as the donor concentration if "perfect sink" conditions exist within the dermal membrane, together with the dermal drug concentration never exceeding 10 % of the donor concentration (Roy, 1997).

Fick's laws are more correctly expressed in terms of the chemical potential of the diffusant rather than its concentration. In an ideal system, there should be a linear relationship between the rate of diffusion and the concentration of the diffusant. The maximum flux will occur when the concentration reaches the solubility limit.

The diffusion coefficient or diffusivity, D, is a rough measure of the ease with which a molecule can move about within a medium, in this case the stratum corneum (Smith, 1990). It is dependent on the molecular weight and volume, and the degree of interaction between the permeant and the stratum corneum. The larger the molecule, the more difficult it is to move about, and the lower the diffusivity. Up to a molecular weight of at least 500 Daltons, and perhaps 5 000 Daltons, the molecular size plays no crucial role (Wiechers, 1989). For molecules with similar polarity, those having the lower molecular weight permeate faster. This might be explained by the observed decrease in diffusivity in liquid media with increasing molecular volume according to Equation 3.4:

$$D = A \cdot V_m^{-1/3}$$

Equation 3.4

where D is the diffusivity of a spherical penetrant, A is a constant and V_m is molar volume.

Non-specific and specific binding may occur in both the epidermis and dermis, reducing diffusivity and thereby decreasing skin permeability (Barry, 2002; Wiechers, 1989). Another important factor that influences the diffusion coefficient is the drug state, e.g., ionised or unionised, with unionised forms diffusing more freely than the ionised forms (Abdou, 1989).

Other parameters include the affinity of the drug for the vehicle, the temperature of the vehicle and the viscosity. The lower the affinity of the drug is for the vehicle, the higher the diffusion coefficient (Babar *et al.*, 1990). Diffusivity decreases with increasing viscosity and decreasing temperature of the vehicle. Equation 3.5 details the influence of the diffusion coefficient parameter on the permeability characteristics of the drug.

$$K = \frac{Ph}{D}$$

Equation 3.5

where K is the partition coefficient, P is the permeability coefficient, *h* is the thickness of the barrier and D is the diffusion coefficient.

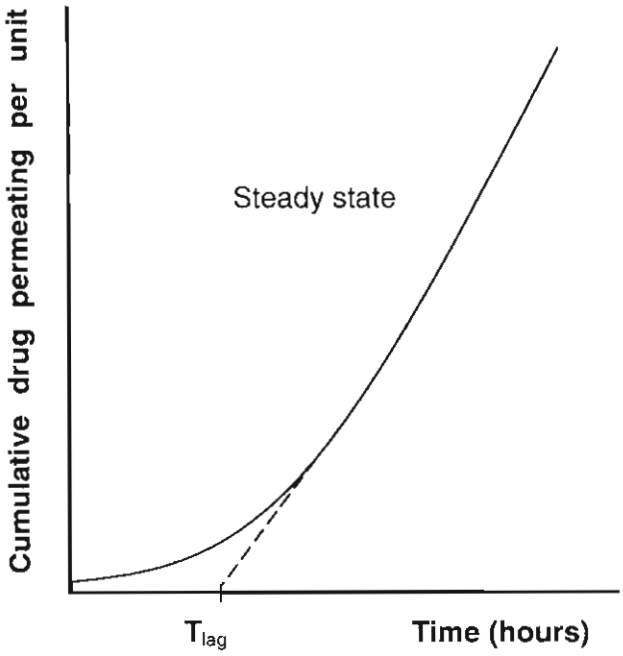

Figure 3.5: Typical permeation profile for a molecule diffusing across human skin (Smith, 1990; Williams & Barry, 1992).

The diffusivity, D, can be determined *in vitro* by simply measuring the transdermal flux at early times until a steady-state flux is reached using diffusion cells (§ 4.4.4). A representative plot of the cumulative amount of drug crossing the skin is shown in Figure 3.5. The time before steady-state is reached is characteristic for the diffusivity of the permeant in the membrane, and can be used to calculate the diffusivity (Smith, 1990; Williams & Barry, 1992). The lag time, T_{lag}, is the time obtained from extrapolation of the steady-state portion to the graph to the intercept

on the time axis, and is defined by Equation 3.6 (Bach & Lippold, 1998; Smith, 1990; Williams & Barry, 1992):

$$T_{lag} = \frac{L^2}{6\,D}$$

Equation 3.6

where L is the thickness of the membrane (cm) and D is the diffusivity ($cm.h^{-1}$).

It should be kept in mind, however, that L should represent the length of the pathway through the membrane, which most often does not correspond to the thickness of the membrane. Thus, in practice, this method for evaluating D has several disadvantages, as the exact length of pathway trough the membrane is difficult to measure. It may also vary with the constituents of the vehicle. Additionally, lag times obtained from permeation experiments with human skin tend to be very variable and may include a component arising from interactions between the stratum corneum and the permeant.

In order to increase the flux of drugs across the stratum corneum it is necessary to decrease the diffusional resistance across in the structured lipids by making them more fluid. This can be achieved by the use of penetration enhancers to impart disorder into the structured bilayers. It should be kept in mind that improving diffusion through the stratum corneum may not necessarily lead to improved absorption into the systemic circulation (Hadgraft & Wolff, 1993).

3.5.2.4 Ionisation

The lipoidal nature of cell membranes was first suggested in 1902. It was also found that membranes are selectively permeable by the free base or uncharged (unionised) form of the drug, as it tends to partition more rapidly than the charged (ionised) species, in the lipoidal membrane. The passage of drugs across the barrier, and hence there absorption, is dictated largely by physical processes and can be predicted from the dissociation constant and the lipid solubility of the undissociated drug moiety (Abdou, 1989).

Most drugs are weak acids or bases and according to the pH-partition theory, may exist in an ionised or unionised form, depending upon the pH of the vehicle. The activity coefficient of the molecular form of such drugs is rapidly changing as a function of pH, for pH values greater than pKa for acidic compounds, and less than pKw-pKb for alkaloid drugs (Barr, 1962). Membranes are more permeable by the unionised forms, because of their greater lipid solubility (Abdou, 1989; Smith, 1990). Thus, the unionised moiety of a drug is more lipid soluble and may dissolve more rapidly in the lipid material of the skin, thereby facilitating transport by passive diffusion (Abdou, 1989; Jack *et al.*, 1991). The ionised moiety, on the other hand, is usually less lipid soluble, limiting transdermal permeation (Ritschel, 1988). The pH of the vehicle in

which the penetrant is dosed, in combination with the penetrant ionisation constant, pKa, will determine the actual concentrations of the ionised and unionised species. The ionised molecule is believed to permeate by the intercellular route through the stratum corneum, whereas the unionised form is more likely to follow the intercellular spaces (Wiechers, 1989).

The drug concentration that exists in the unionised form is a function of both the dissociation constant of the drug and the pH at the absorption site (Abdou, 1989). The pH range of the stratum corneum is 4.2 – 5.6 and that of the viable epidermis is 7.3 – 7.4 (Pardo *et al.*, 1992). Therefore weak acids and weak bases are dissociated to different degrees, depending on the pH and the pKa or pKb of the diffusant. The concept of pKa is derived from the Henderson-Hasselbalch equation and is the following (Ansel, 1981):

For an acid:

$$pH = pKa + \log \frac{(salt)\ (ionised)}{(acid)\ (unionised)}$$ **Equation 3.7**

For a base:

$$pH = pKa + \log \frac{(base)\ (unionised)}{(salt)\ (ionised)}$$ **Equation 3.8**

Thus, the fraction of the unionised drug is a function of the pH (Barry, 1983).

This does not mean that ionic species are totally forbidden from passing through the skin, for ion pairing is possible and, in the form of ion pairs, a salt can be soluble, to some extent, within a lipid continuum and, thereby, can diffuse through it (Flynn, 1989; Hadgraft & Valenta, 2000).

Because of the effect of pH on the relative concentrations of unionised and ionised species, it would appear to be possible to control the total flux of compounds by varying the pH of the drug containing vehicle applied to the skin.

3.5.2.5 Melting point

From the equation of Hadgraft *et al.* (1990), it is clear that the solubility parameter in the stratum corneum, δ_{sc}, can be estimated more accurately if the melting point of that drug is also taken into account.

$$\log \delta_{sc} = 1.911 \frac{10^3}{mp} - 2.956$$ **Equation 3.9**

where δ_{sc} is the solubility parameter in the stratum corneum and mp is the melting point (Kelvin).

A high level of crystallinity is expressed in the form of a high melting point and heat of fusion. This limits solubility itself, and thus also sets a limit on mass transfer across the skin. Generally, the greater a drug's innate tendency to dissolve, the more likely it is that the drug can be delivered at an appropriate rate across the skin (Ostrenga *et al.*, 1971). Hence, in order to obtain the best candidate for transdermal drug delivery, the melting point should be kept as low as possible.

Permeant melting point has been shown to be inversely proportional to lipophilicity (log P) and, therefore, transdermal flux. The melting point of a substance is often considered as an indicator of the maximum flux attainable through the skin and the correlation between flux and the reciprocal of the melting point have been attempted. Since the entropy of fusion of the permeant (ΔS_f) slowly varies with melting point, the ideal solubility increases exponentially with decreasing melting point for any given molecular weight. It follows that there should be an exponential increase in transdermal flux with decreasing melting point (Guy & Hadgraft, 1989a; Stott *et al.*, 1998).

Roy & Flynn (1989) plotted the relationship between melting point and permeability coefficients of narcotic analgesics. They showed that the permeability coefficients systematically change with the melting point, with the compounds having the lowest melting points exhibiting the highest permeability coefficients.

Another study by Kommuru *et al.* (1998) showed that enantiomers with a lower melting point might exhibit higher solubility than that of the racemate, and consequently have higher skin permeation profiles. For example, the flux of the pure enantiomer of nivaldipine, a calcium channel blocker, across human cadaver skin was about 7 fold higher than that of the racemate. In this case, the melting point difference was about 34 °C.

It is therefore clear that reduction in melting point of a permeant will have a direct effect on its solubility in skin lipids and increase transdermal permeation (Cleary, 1993; Stott *et al.*, 1998).

3.5.2.6 Hydrogen bonding

The permeability coefficients of the solutes through the stratum corneum have been related to the presence of hydrogen bonding groups on the penetrant. It is suggested that, whereas lipophilicity of a solute is the major determinant for solute partitioning into the stratum corneum from aqueous solutions, the hydrogen bonding of the solute is the main determinant of solute diffusion across the stratum corneum (Roberts *et al.*, 1995).

The penetration of most compounds seems to be limited by the barrier function of the stratum corneum and in particular by the properties of the stratum corneum lipids (Potts & Guy, 1992;

Surber *et al.,* 1993). The stratum corneum consists of terminally differentiated keratinocytes embedded in continuous array of extracellular lipid lamellae. These lamellae consist primarily of ceramides, fatty acids and cholesterol. The polar heads of ceramides are known to facilitate lateral hydrogen bonding with adjacent molecules, and since these lipids have acyl chains more than 24 carbons long, these extracellular lamellae form a rigid structure at physiological temperatures. Ceramide 6 is the most dominant hydrogen bonding lipid and consists of one secondary amine group and four secondary alcohol groups (Hadgraft *et al.,* 1996). If a permeant possesses hydrogen bonding abilities it may interact with the lipid polar head groups. Therefore, hydrogen bonding may occur between the permeant and the alcohol and amide groups of the ceramides as well as the carboxylic group of the fatty acids (Hadgraft *et al.,* 1996).

Anderson & Raykar (1989) considered that the stratum corneum barrier could be modelled by hydrogen bonding organic solvent, and El Tayar *et al.* (1991) suggested the hydrogen bond donor potential of the penetrant to be the main determinant of permeability. Various proposals relating permeability coefficient of the stratum corneum to several penetrant properties (Roberts *et al.,* 1995) have been reviewed and concluded that both the donor (α) and acceptor (β) properties of the penetrant hydrogen bonding properties are important in determining the permeability coefficient. Pugh *et al.* (1996) showed that the stratum corneum is a predominantly hydrogen bond donor environment, with donor/acceptor properties in the ratio of 0.57 : 0.43.

In a study done by Potts & Guy (1995) on the effects of molecular size and hydrogen bond activity, the hydrogen bonding terms show that increased solute hydrogen bond acceptor and donor activity resulted in decreased partitioning into the organic phase; due to the free energy cost associated with the disruption of the hydrogen bonds in the aqueous phase. A smaller decrease was seen for octanol due to the limited hydrogen bonding ability and water solubility in this solvent. In short, hydrogen-bonding solutes are better accommodated in octanol than in alkene.

According to Williams (2003) the diffusion through epidermis is not only dependent on the number of hydrogen bonding groups in a molecule, but also dependent on the symmetry (distribution) of these hydrogen bonding groups within the molecule. Consequently, permeation across the stratum corneum might be inhibited by an increase in the number of hydrogen bonding groups on the permeant.

According to Roberts *et al.* (1995), the diffusion coefficient is dependent in terms of a maximal absorption of a solute to polar groups in the transport pathway of solutes through the stratum corneum. Accordingly, the diffusion coefficient of a solute decrease as the solute becomes bound to polar groups in the pathway until these groups are unable to associate with any

additional hydrogen bonding groups on the solute. Above the saturated number of groups, the diffusion coefficient of the solute appears to be relatively constant.

The hydrogen bonding properties of a penetrant have a dominant effect on the diffusion across the stratum corneum, but a smaller influence on the partitioning, where lipophilicity might be an important factor (Roberts *et al.,* 1995).

3.5.2.7 Molecular size

Considering that the horny layer is a compact membrane and that diffusing molecules follow a tortuous path through it, it might seem obvious that the diffusion coefficient would be inversely related to molecular weight or some other measure of molecular size (Naik *et al.,* 2000; Zatz, 1993). Compounds of small molecular size may penetrate through the aqueous pathway more easily than larger molecules, which penetrate through the lipoidal pathway more readily (Takahashi, 1993; Zatz, 1993).

An inverse relationship appears to exist between the absorption rate and the molecular weight of a compound (Idson, 1975; Tregear, 1966). According to Potts & Guy (1995) increasing the molecular volume increases the hydrophobic surface area and that this will increase partitioning into, and hence, permeability through a lipid membrane. Conversely larger molecules diffuse more slowly, since they require more "space" to be created in the medium, and this in turn leads to diminished permeability. Small molecules penetrate more rapidly than larger molecules, but within a narrow range of molecular size (100 – 500 Daltons), there is little correlation between size and penetration rate (Liron & Cohen, 1984). The molecular weight dependency on transdermal permeation is much more apparent when selecting larger molecules (Williams, 2003).

There seems to be an inverse relationship between the permeant diffusivity and the permeant size. For the stratum corneum and the other lipid membranes, it has been suggested that the functional dependence of permeant diffusivity on molecular volume is exponential. Potts & Guy (1992) introduced a model for compounds ranging in molecular weight from 18 to > 750 and log K_{oct} from -3 to +6. They found that Equation 3.10 could predict the permeability of a diffusant from an aqueous solution through the human skin:

$$\log K_p = -2.7 + 0.71 \log K_{oct} - 0.0061\ MW \qquad \textbf{Equation 3.10}$$

where K_p is the permeability coefficient ($cm.sec^{-1}$), K_{oct} is the octanol/water partition coefficient and MW is the molecular weight. By using this equation it is clear that as the molecule becomes more lipophilic its permeability increases due to better partitioning into the skin. However, as the molecule becomes larger its diffusion in the skin is reduced (Hadgraft, 2001).

Potts & Guy (1992) found that the substitution of molecular weight for molecular volume provides an equivalent fit in the model and that the apparently sigmoidal dependence of log K_p upon log K_{oct} suggested a non-linear relationship between these parameters. However, when molecular volume is taken in to account, the data lies on a three-dimensional surface defined by log K_p, log K_{oct} and molecular volume (Potts & Guy, 1992).

Pugh *et al.* (2000) confirmed the direct relationship between log K_p and log K_{oct}, but found that the relationships between log K_p and MW is also direct, and not inverse as was found by Potts & Guy (1992).

The upper limit of molecular weight for permeation is still a matter of discussion. There seems to be a limit of about 5000, although some authors even mention molecular weights of not more than 3000. Nevertheless, influx of compounds into the skin does decrease with increasing molecular weight due to the parallel decrease in the diffusion coefficient in water (Idson, 1975; Schalla & Schaefer, 1982).

3.5.2.8 Increased alkyl chain length

It has long been recognised that a drug's physicochemical properties are very important in determining its biological and pharmaceutical characteristics. The major determinants of drug dissolution, distribution and availability are the aqueous solubility and the partition coefficient (Yalkowsky *et al.*, 1972). An understanding of the manner in which these and other properties change within a homologous series, i.e., with additions of methylene units, can be of use in choosing a derivative with optimum properties. It is recognised that in a homologous series, by increasing the nonpolar portion of a molecule by extending the length of the chain produces certain characteristic features, such as elevating boiling point, decreasing aqueous solubility and increasing the partition coefficient (Abdou, 1989).

As seen by Flynn & Yalkowsky (1972), relationships can be drawn for the influence of chain length on the partition coefficient and solubility. Partition coefficients of membranes of a homologous series between the immiscible polar and nonpolar phases, increase by a constant factor as the series ascend. This relationship is expressed in Equation 3.11:

$$\log K_n = \log K_o + \pi_n \qquad \textbf{Equation 3.11}$$

This is an especially useful relationship because it expresses a universal dependency, thereby allowing chain length *n* to be used in lieu of partition coefficients (log K_n) in theoretical analysis. The value, π, is the log of the increase per methylene unit. They studied the permeation of several odd chain length p-aminobenzoates from saturated solutions.

Flynn & Yalkowsky (1972) founded that:

1 There is initially an increase in flux in the steady-state as the homologous series is ascended.

2 The flux drops off markedly at longer chain lengths. Additionally, lag times, which appear to be approximately constant initially, increase sharply for the longest esters.

As the alkyl chain length as well as the molecular weight increased, the aqueous solubility and the flux decreased. At the lower end of the range it takes an addition of three methylene units to produce a 10 fold increase in the partition coefficient. While partition coefficients are growing exponentially as the homologous series is ascended, there appears to be little current effect on diffusion coefficients (Flynn, 1989).

Yalkowsky *et al.* (1972) investigated the physicochemical properties of a homologous series of alkyl-p-aminobenzoates and found that as chain length is increased, the melting point decreases almost linearly to the butyl ester and then increases gradually and irregularly. Thus, a change in melting behaviour relative to increasing chain length up to the butyl ester is clearly evident.

Hence, this all comes down to that an increase in chain length up to about 4 carbon atoms result in a lower melting point, lower solubility and lower crystallinity.

3.6 Skin integrity

After preparation of the skin (§ 4.4.1) the epidermis was visually examined for any defects, after it has been set on Whatman® filter paper and left to air dry. Visual examination was done by placing a light behind the filter paper to see if it had holes in the epidermis (damaged). This wasn't an accurate method and another way of distinguishing between intact or damaged skin was needed. Davies *et al.* (2004) and Nugroho *et al.* (2005) used electrical resistance as an indicator for the integrity on a selection of skin membranes. Davies *et al.* (2004) found that an inverse relationship existed between the electrical resistance and the permeability coefficients of tritiated water.

Fasano *et al.* (2002) made use of testing the integrity of the skin by obtaining the electrical resistance (§ 4.1.1.5) over the epidermis. Glass static diffusion cells with a 0.64 cm^2 effective diffusion area was used for the permeation studies. Tritiated water was used to determine permeability coefficients and subsequently compared with electrical resistance data obtained. They found that an inverse relationship existed between the diffusion area and the electrical resistance and obtained a median tritiated water permeability coefficient single point threshold

value of 1.13 x 10^{-3} cm/h. Undamaged human skin should have a tritiated water permeability coefficient single point threshold value of less than 1.5 x 10^{-3} cm/h (Bronaugh *et al.*, 1986).

3.7 Drug delivery systems

3.7.1 Liposomes

A liposome is a small, amphiphilic, spherical vesicle consisting of concentric phospholipid and cholesterol bilayers that encapsulate part of the vehicle or active in the centre aqueous core (Rongen *et al.*, 1997). Liposomes are often characterised according to their size and number of lamella, i.e., small unilamellar vesicles (SUV), large unilamellar vesicles (LUV), multilamellar vesicles (MLV) and multivesicular vesicles (MVV). The size of liposomes ranges from 20 nm in diameter up to several microns. SUV and LUV have one bilayer, where MLV have five to twenty lipid bilayers and MVV have a multicompartment range (Rongen *et al.*, 1997).

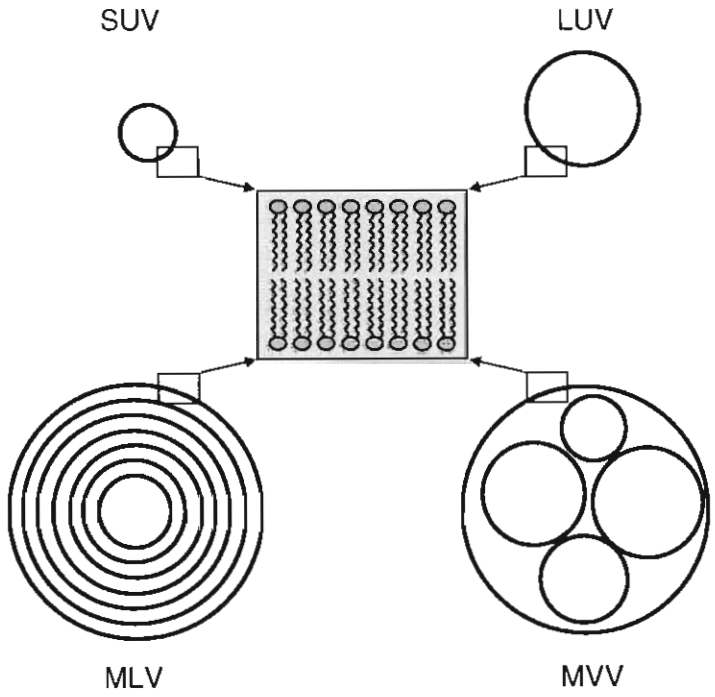

Figure 3.6: Schematic representation of different size and number of lamella of SUV, LUV, MLV and MVV (Rongen *et al.*, 1997).

Liposomes are used as vehicles in cosmetic and dermatological products and assist the dissolution and formulation of hydrophobic components. They also entrap hydrophilic drugs and can be used to moisturise and increase water retention in the skin that result in an enhanced skin elasticity and barrier function (Liu & Wisniewski, 1997).

3.7.2 Pheroid™

Pheroid™ (previously known as Emzaloids) is a patented system consisting of an exceptional submicron emulsion formulation. Although a Pheroid™ is stable within a system, manipulation is possible in terms of size, structure, morphology and function (Grobler, 2004). Pheroid™ as a basic formulation was first discovered when it was used to reduce psoriasis. One of the fundamental ingredients of this formulation was found in banana peel extract and was later recognised as essential fatty acids (Schlebusch, 2002).

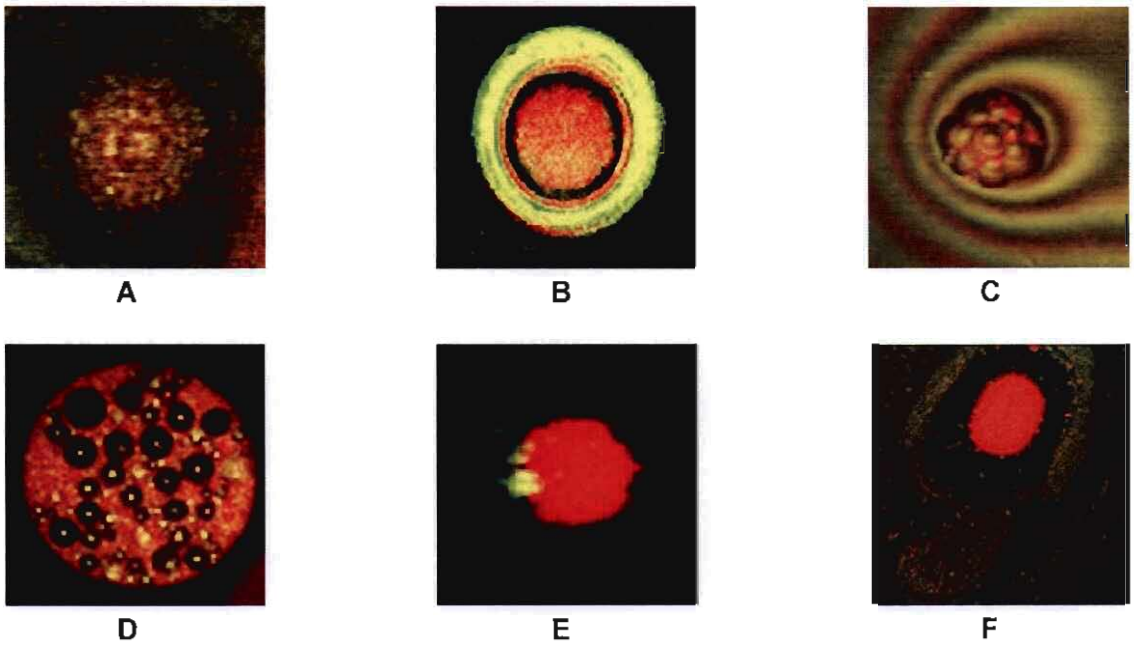

Figure 3.7: The micrographs (CLSM) of several of the basic Pheroid™ types. **(A)** A bilayer membrane vesicle containing rifampicin (100 nm in diameter). **(B)** A highly elastic or fluid bilayered vesicle with loose lipid packing containing rifampicin. **(C)** The formation of small pro-Pheroid™ that are used in oral delivery. **(D)** A reservoir (size: 1 – 10 µm) that contains multiple particles of coal tar. Reservoirs have large loading capacity to surface area ratios and are good entrappers of insoluble compounds. **(E)** This Pheroid™ is in the process of entrapping fluorescent labelled water-soluble diclofenac. It is very small (approximately 30 nm) and the membrane packing is sponge-like. **(F)** A depot (size: 5 – 100 µm) with a hydrophobic core containing pro-Pheroid™ formulation, a surrounding hydrophilic zone and an outer vesicle-containing zone. Selective addition of fluid results in the release of vesicles from a release zone. The depots are used for sustained release according to a concentration gradient. The sizes of Pheroid™ reflected above are not all to scale.

Currently Pheroid™ comprise mostly of essential and plant fatty acids i.e., ethyl esters of the essential fatty acids, oleic, linolenic and linoleic acids, which are emulsified in water and saturated with nitrous oxide. The essential fatty acids in the Pheroid™ system replenish the lack of lipids in the skin by means of merging with phospholipids and maintaining the integrity of the epidermal permeability barrier (Junginger *et al.,* 1991; Touitou *et al.,* 1994). Oleic acid increases transdermal permeation due to its kinked structure, by briefly disrupting the packed formation of the intercellular lipids (Touitou *et al.,* 1994). Pharmacologically active compounds and other beneficial molecules can be entrapped, transported and delivered by Pheroid™ (Saunders *et al.,* 1999), which in turn may increase therapeutic action (Grobler, 2004).

Effective drug delivery has numerous potential barriers. Drugs are entrapped and delivered by Pheroid™ to specific locations in the body. Pheroid™ permeate skin, keratinised tissue, intestinal lining, the vascular system, nasal epithelium, parasites, bacteria and fungi. Antivirals entrapped in Pheroid™ influence HIV viral load, perhaps by obstructing viral binding and/or budding (Grobler, 2004).

Figure 3.7 shows the micrographs of various formulations of the Pheroid™ obtained through confocal laser scanning microscopy (CLSM) (Grobler, 2004). Although several delivery systems exist; none compare to Pheroid™, which is exceptional in that its components are influenced in a particular way to guarantee elevated entrapment capabilities, swift transport, as well as delivery and stability.

A variety of Pheroid™ types exist, i.e., microsponges, lipid bilayer vesicles (in both the micro and nanometre size range) and depots or reservoirs that contain pro-Pheroid™ (ingested product entrapped with actives) (Grobler, 2004). Each type has a specific shape and size of vesicles due to specific formulation adjustments. For that reason the drug release characteristics and absorption potential of the Pheroid™ can be controlled (Schlebusch, 2002). Pheroid™ are generally made of three phases, i.e., an oil phase (unique blend of essential fatty acids), an aqueous phase (mainly water) and nitrous oxide (Grobler, 2004).

Human cells cannot produce these essential fatty acids that are required for numerous cell functions and therefore have to be ingested. There are several functions due to the fatty acid components in the Pheroid™ formulation, i.e., maintaining membrane integrity of cells, along with energy homeostasis and modulating the immune system through leukotriens and prostaglandins. Thus Pheroid™ are safer, more effective and have natural therapeutic qualities that offer considerable advantages over a variety of delivery systems (Grobler, 2004).

The following research has been done and clinically proven the advantages of Pheroid™:

- Ability to entrap and transfer genes to cell nuclei and expression of proteins
- Increased delivery of active compounds
- Increased therapeutic efficacy
- Penetration of most known barriers in the body and in cells
- Ability to target treatment areas
- Decreased time to onset of action
- Reduction of minimal effective concentration
- Reduction in cytotoxicity
- Reduction and suggested elimination of drug resistance (Grobler, 2004).

3.8 Confocal laser scanning microscopy

Electron and light microscopy have been valuable equipment for the examination of cellular structure and function of biological tissues. Transmission electron microscopy (TEM) presents outstanding resolution for skin images (ultrastructural details of 0.1 nm) but damages the sample. TEM offers static two-dimensional images (Wright *et al.,* 1993). Video-intensified fluorescence and video-enhanced microscopy increases detection and enhances contrast, but still the clarity and quality of the images are limited (Wright *et al.,* 1993). CLSM can solve this problem.

CLSM acquires high-resolution images (axial, 1 µm; lateral, 140 nm) from biological and other samples. CLSM has the capability to capture images (*in vivo* and *in vitro*) of optical segments in a non-invasive way, with time-resolution (Cullander & Guy, 1992) and an in depth visualising of samples with no mechanical slicing of the specimen. Visualising active changes in real time is accomplished by labelling the specimen with a fluorescent marker; subsequently if a molecule, through laser contact, enters an excited state it will emit light at a specific wavelength (Saunders *et al.,* 1999).

Illumination of the volume or depth of a sample together with the level in which the objective lens is focused, in traditional microscopy is done equally and simultaneously, which result in an out-of-focus blur below and above the focal level. The differentiation of cellular structures is complicated by the decreased resolution and contrast, due to out-of-focus light. In contrast, CLSM's illumination is sequential rather than simultaneous (Wright *et al.,* 1993). A single spot resulting in an illuminated area of the highest density is thus investigated. Excitation by laser is

directed from a CLSM towards the sample, in doing so attaining a micrograph (Alvarez-Román *et al.*, 2004).

The sample emits fluorescence that shines in every direction. From the focal level of the sample, fluorescence is returned by the objective and scanning system, reflecting off a dichroic mirror, finally focusing onto the detector. In the microscope's focal level, the speck's image is defined by the spatial filter, which is in front of a detector and contains an aperture (slit or pinhole diaphragm). Light is suppressed effectively from the non-focal levels by the spatial filter, which also constantly supplies the detector access for in-focus light (Shotton, 1989). An illustration of the CLSM is portrayed in Figure 3.8.

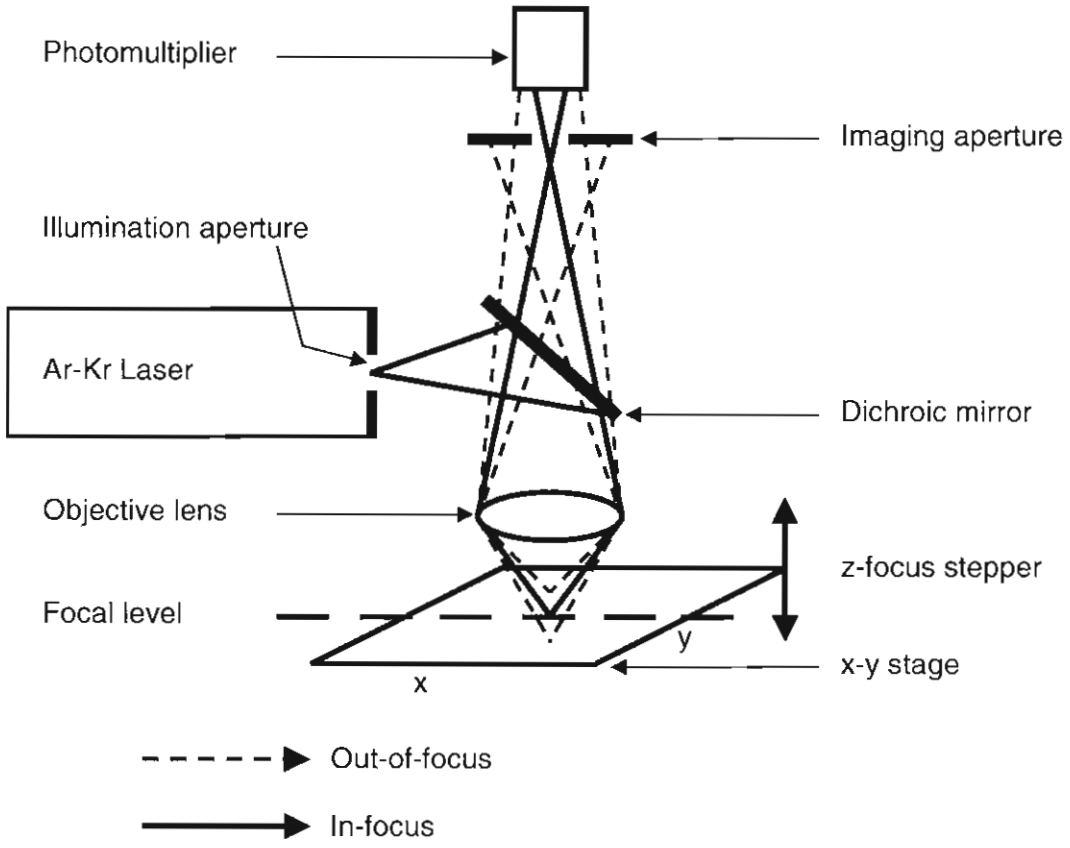

Figure 3.8: Schematic diagram of CLSM (Alvarez-Román *et al.*, 2004; Pedley, 1997).

The z-series is a sequence of optical divisions acquired for three-dimensional information of the skin. This series is successively taken at focal levels along the z-axis and can be examined as a plain image. Essentially a confocal image should be acquired within the x-y level (i.e., a level parallel to that of a membrane surface), in order for in depth information to be obtained from a particular surface. Using the laser as an optical knife and slicing through the successive x-y level produces an optical cross-section (x-z level) (Alvarez-Román *et al.*, 2004).

3.9 Summary

As the largest and most external organ, the skin is constantly exposed to the hazards of the environment and is often viewed as a living protective envelope surrounding the body. The permeation of chemicals, toxicants and drugs are much slower across the skin when compared to other biological membranes in the body, due to the outermost layer of the skin, the stratum corneum (Harrison *et al.,* 1996). The lipophilic stratum corneum is responsible for the primary barrier function of the skin and provides an extensive challenge to scientists in their pursuit to develop drugs for transdermal delivery (Pefile and Smith, 1997).

During transdermal delivery a drug has to partition from the donor vehicle into the stratum corneum, diffuse through the stratum corneum, permeate from the lipophilic stratum corneum into the hydrophilic epidermis, diffuse through the epidermis and finally be absorbed into the vascular system. The rate and extent to which a drug penetrates the skin is influenced by biological factors of the skin and physicochemical properties of the drug. A drug should be unionised and have an aqueous solubility of more than 1 mg/ml, a log D value between 1 and 2, a small molecular weight of less than 500 Daltons and a low melting point of less than 200 °C to ideally permeate the skin (Naik *et al.,* 2000).

Other methods of improving transdermal permeation can be used successfully, i.e., increasing the chain length (enhances lipophilicity) and by means of a delivery system (Pheroid™). Pheroid™ are made of natural fatty acids that entrap and deliver drugs to a specific site in the body and offer valuable advantages over a variety of delivery systems (Grobler, 2004).

Transdermal drug delivery offers a few advantages over oral and parenteral delivery. They include avoiding hepatic first pass metabolism, maintaining constant blood levels for longer periods of time, improving bioavailability, decreasing the administered dose, adverse effects and gastrointestinal side effects, easy discontinuation in case of toxic effects and improved patient compliance (Mitragotri, 2000).

CHAPTER 4

EXPERIMENTAL

This section will briefly describe the instrumentation, methods and techniques used to obtain the results presented in this thesis. The synthesis, physical data obtained of the compounds, the procedure to determine physicochemical properties, programs used to predict physicochemical data as well as the process to do permeation studies will be discussed.

4.1 General experimental methods

4.1.1 Instrumentation

4.1.1.1 Nuclear magnetic resonance spectroscopy (NMR)

The ^{1}H and ^{13}C NMR spectra were recorded on a Varian Gemini 300 spectrometer at a frequency of 300.075 MHz and 75.462 MHz, respectively. All the chemical shifts are reported in parts per million (ppm) relative to tetramethylsilane (δ = 0). The following abbreviations were used to describe the multiplicity of the ^{1}H signals: s = singlet, d = doublet, t = triplet, q = quartet, dd = doublet of doublets, dt = doublet of triplets, ddd = doublet of doublets of doublets, br s = broad singlet and m = multiplet.

4.1.1.2 Infrared spectroscopy (IR)

The IR spectra were recorded on a Nicolet Magna – IR 550 spectrometer using KBr pellets.

4.1.1.3 Mass spectrometry (MS)

The MS spectra were recorded on an analytical VG 7070E mass spectrometer using fast atom bombardment (FAB) at 70 eV as ionisation technique.

4.1.1.4 Melting points

Melting points were determined by differential scanning calorimetry (DSC). DSC thermograms were recorded with a Mettler Toledo DSC822e700 instrument (Mettler, Switzerland). The measurement conditions were as follows: sample weight, approximately 2 mg; sample holder, aluminium crimp cell; gas flow, nitrogen at 30 ml/min and heating rate, 10 °C/min.

4.1.1.5 Integrity

A Model 6401 LCR Databridge (H. Tinsley, Inc., Croydon, Surrey, UK) was used to determine the integrity of the skin before and after the transdermal procedure. Resistance readings (kΩ) were taken by immersing two stainless-steel test probe lead tips into the PBS filled donor and receptor compartments. The range of electrical resistance obtained in this study was between 2.2 and 31.0 kΩ.

4.1.1.6 Confocal laser scanning microscopy (CLSM)

The compounds containing Pheroid™ were viewed with the use of CLSM. The CLSM used was a PCM 2000 with Nikon inverted microscope and digital camera DXM 1200 (Nikon, Holland) equipped with a Helium/Neon Spectra-physics laser (red) with an excitation of 505 nm and emission of 568 nm and an Argon Spectra-physics laser (green) with an excitation of 488 nm and emission of 515 nm. An ApoPlanar oil immersion objective with a magnification of 60 x and numerical aperture of 1.4 was used to determine the size of the Pheroid™. The Pheroid™ was stained with Nile Red (Molecular Probes, Holland), placed on a glass slide and covered with a glass cover-slip. The glass slide and cover-slip were sealed together using adhesive to prevent the Pheroid™ from drying out. The slides were inverted and images were capture through the coverslip side of the prepared samples.

4.1.2 Chromatographic techniques

4.1.2.1 Thin-layer chromatography (TLC)

Analytical TLC was performed on 0.20 mm thick silica gel aluminium backed sheets (Merck® 5554 DC - Alufolien 60 F_{254}). Chromatograms were examined under UV-light (254 nm) for the detection of the individual compounds. The mobile phases used are: ethyl acetate (EtOAc), diethyl ether, methanol (MeOH) : dichloromethane (DCM) (8 : 2), ethanol (EtOH) : DCM (1 : 9) and EtOAc : DCM (9 : 1).

4.1.2.2 Column chromatography

Column chromatography was performed with a standard glass column with a length of 900 mm and an inner diameter of 30 mm. The stationary phase used was Merck® 7734 silica gel (0.063 – 0.200 mm). The mobile phases used are: EtOAc, diethyl ether, MeOH : DCM (8 : 2), EtOH : DCM (1 : 9) and EtOAc : DCM (9 : 1).

4.1.2.3 High pressure liquid chromatography (HPLC)

The HPLC system consisted of a HP (Hewlett Packard) Agilent 1100 series auto sampler, HP Agilent 1100 series variable wave detector (VWD) and HP Agilent 1100 series pump (Agilent, Polo Alto, CA). A Phenomenex (Luna C-18, 150 x 4.60 mm, 5 µm) column was used together with a Securityguard pre-column (C-18, 4 x 3 mm) insert (Phenomex, Terronce, CA) in order to prolong column life. The Agilent Chemstation for LC Systems software package was used for data analysis. The flow rate, UV wavelengths, mobile phase compositions and retention times for zalcitabine **(1)**, lamivudine **(2)** and each of the amide esters of **(2)** are presented in Table 4.1. Orthophosphoric acid (OPA) and 0.2 % triethylamine were used for **(1)** and **(2)** to adjust the pH of the mobile phase to 7.0. A different volume was injected for each of the compounds in order to compensate for the difference in concentration for each of the various derivatives and a correction calculation made. It was determined that the recycling of the mobile phase did not adversely affect the HPLC analysis. Calibration curves were constructed ranging from concentrations of 1.97 µg/ml to 475.0 µg/ml.

Table 4.1: Data of the HPLC method.

Compound	Flow rate (ml/min)	Wavelength (nm)	Mobile phase H_2O:acetonitrile	Retention time (min)
Zalcitabine **(1)**	1.0	270	95 : 5	4.36
Lamivudine **(2)**	1.0	270	90 : 10	2.91
N-acetyllamivudine-5'-acetate **(3)**	1.0	250	70 : 30	2.49
N-propionyllamivudine-5'-propionate **(4)**	1.0	250	60 : 40	3.90
N-butyryllamivudine-5'-buterate **(5)**	1.0	250	40 : 60	3.43
N-hexanoyllamivudine-5'-hexanoate **(6)**	1.0	250	30 : 70	5.32
N-octanoyllamivudine-5'-octanoate **(7)**	1.0	250	10 : 90	5.10
N-decanoyllamivudine-5'-decanoate **(8)**	1.0	250	10 : 90	12.53

4.1.3 Theoretical aqueous solubility

Interactive Analysis (http://www.logp.com/) prediction software was used to predict the water solubility for **(1)**, **(2)** and the amide esters of **(2)**. These values are compared to experimental values (§ 5.2.1).

4.1.4 Theoretical partition coefficients

ACD Labs, KowWin (http://www.syrres.com/esc/est_kowdemo.htm) and Interactive Analysis (http://www.logp.com/) prediction software were used to predict the partition coefficients for **(1)**, **(2)** and the amide esters of **(2)**. These values are compared to the experimental values (§ 5.2.3).

4.2 Synthesis and physical data of compounds

4.2.1 Synthesis of amide esters

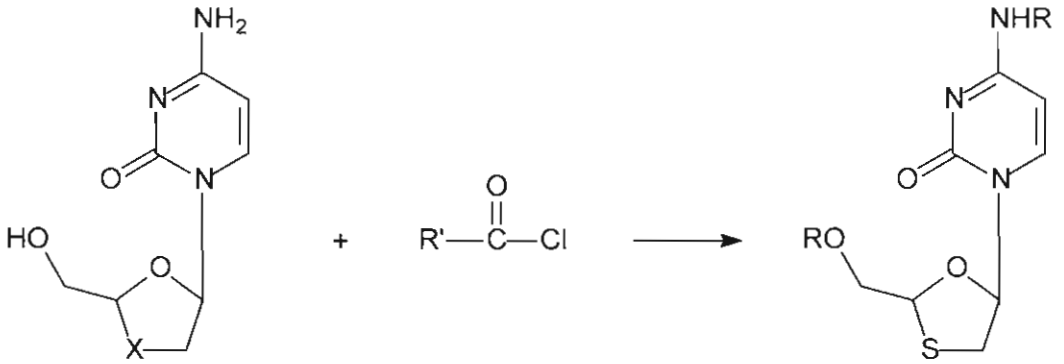

(2): X = S

(3): R = $COCH_3$
(4): R = $COCH_2CH_3$
(5): R = $CO(CH_2)_2CH_3$
(6): R = $CO(CH_2)_4CH_3$
(7): R = $CO(CH_2)_6CH_3$
(8): R = $CO(CH_2)_8CH_3$

Scheme 4.1: Synthesis of lamivudine amide esters.

To a well-stirred mixture of **(2)** (1.0 mol) in dry pyridine at room temperature was added acid chloride (5.0 mol) (Scheme 4.1) to form a clear solution. Stirring was continued for 2 h where after distilled water was added to stop the reaction followed by an excess of DCM. The organic phase was collected and washed with water at least three times to get rid of the pyridine. The organic phase was then dried over anhydrous $MgSO_4$, the DCM removed under vacuum and

the resulting product was collected. The prepared compounds were purified using column chromatography on silica gel (with EtOAc : DCM (9 : 1) for **(3)**, **(4)**, **(5)** and **(8)**; EtOAc for **(6)** and **(7)**; MeOH : DCM (8 : 2); for **(4)**; EtOH : DCM (1 : 9) for **(5)** and diethyl ether for **(7)**) followed by recrystallisation from EtOAc or MeOH.

4.2.1.1 N-acetyllamivudine-5'-acetate (3)

A yield of 2.0774 g (28.72 %) off-white crystalline compound was obtained; mp 168.06 °C (thermogram 1); Rf 0.25 (EtOAc : DCM (9 : 1)); $C_{12}H_{15}N_3O_5S$; M^+ 313; m/z (FAB, spectrum 1): 314 ((M+H$^+$) 35.5 %), 154 (100.0 %), 136 (56.0 %), 120 (9.5 %), 107 (22.5 %); ν_{max} (spectrum 7, KBr, cm^{-1}): 1059.81, 1134.49, 1184.38, 1656.81, 1715.40, 1741.19, 3256.47; δ_H (spectrum 13, 300.075 MHz, $CDCl_3$): 2.09 (s; 3H; H-b), 2.26 (s; 3H; H-b'), 3.16 (dd; 1H; J = 12.5, 3.3 Hz; H-5'b), 3.60 (dd; 1H; J = 12.5, 5.4 Hz; H-5'a), 4.40 (dd; 1H; J = 12.4, 3.1 Hz; H-2'b), 4.58 (dd; 1H; J = 12.5, 5.1 Hz; H-2'a), 5.37 (dd; 1H; J = 5.1, 3.1 Hz; H-1'), 6.29 (dd; 1H; J = 5.3, 3.3 Hz; H-4'), 7.43 (d; 1H; J = 7.6 Hz; H-5), 8.10 (d; 1H; J = 7.6 Hz; H-6), 10.07 (s; 1H; OH); δ_C (spectrum 19, 75.462 MHz, $CDCl_3$): 20.63 (C-b), 24.81 (C-b'), 38.78 (C-4), 63.57 (C-2), 84.69 (C-5'), 87.89 (C-4'), 96.47 (C-1'), 144.23 (C-5 / C-6), 154.79 (C-2'), 163.13 (C-6 / C-5), 170.14 (C-a), 171.08 (C-a').

4.2.1.2 N-propionyllamivudine-5'-propionate (4)

A yield of 4.7343 g (61.86 %) orange glass compound was obtained; mp 217.45 °C (thermogram 2); Rf 0.36 (EtOAc : DCM (9 : 1)), 0.83 (MeOH : DCM (8 : 2)); $C_{14}H_{19}N_3O_5S$; M^+ 341; m/z (FAB, spectrum 2): 342 ((M+H$^+$) 47.5 %), 168 (100.0 %), 154 (15.5 %), 136 (22.0 %), 112 (66.0 %); ν_{max} (spectrum 8, KBr, cm^{-1}): 1053.16, 1163.35, 1569.82, 1743.77, 3560.03; δ_H (spectrum 14, 300.075 MHz, $CDCl_3$): 1.16 (t; 6H; J = 7.6 Hz; H-c, H-c'), 2.38 (m; 2H; H-b), 2.51 (m; 2H; H-b'), 3.17 (dd; 1H; J = 12.5, 3.2 Hz; H-5'b), 3.61 (dd; 1H; J = 12.6, 5.4 Hz; H-5'a), 4.42 (dd; 1H; J = 12.5, 3.1 Hz; H-2'b), 4.59 (dd; 1H; J = 12.5, 4.7 Hz; H-2'a), 5.35 (dd; 1H; J = 4.8, 3.1 Hz; H-1'), 6.31 (dd; 1H; J = 5.4, 3.3 Hz; H-4'), 7.43 (d; 1H; J = 7.5 Hz; H-5), 8.12 (d; 1H; J = 7.6 Hz; H-6), 9.48 (br s; 1H; OH); δ_C (spectrum 20, 75.462 MHz, $CDCl_3$): 8.68 (C-c), 8.95 (C-c'), 27.30 (C-b), 30.67 (C-b'), 38.92 (C-4), 63.34 (C-2), 84.93 (C-5'), 87.86 (C-4'), 96.32 (C-1'), 144.24 (C-5 / C-6), 154.94 (C-2'), 162.84 (C-6 / C-5), 173.66 (C-a), 174.38 (C-a').

4.2.1.3 N-butyryllamivudine-5'-buterate (5)

A yield of 1.3389 g (16.30 %) white crystalline compound was obtained; mp 106.36 °C (thermogram 3); Rf 0.64 (EtOH : DCM (1 : 9)), 0.64 (EtOAc : DCM (9 : 1)); $C_{16}H_{23}N_3O_5S$; M^+ 370; m/z (FAB, spectrum 3): 371 ((M+H$^+$) 38.0 %), 189 (12.0 %), 182 (100.0 %), 138 (9.0 %), 112 (40.5 %); ν_{max} (spectrum 9, KBr, cm^{-1}): 1065.04, 1134.14, 1159.52, 1655.52,

1719.59, 1742.69, 3246.02; δ_H (spectrum 15, 300.075 MHz, $CDCl_3$): 0.91 (t; 6H; J = 7.4 Hz; H-d, H-d'), 1.66 (m; 4H; H-c, H-c'), 2.31 (t; 2H; J = 7.3 Hz; H-b), 2.47 (t; 2H; J = 7.2 Hz; H-b'), 3.15 (dd; 1H; J = 12.5, 3.2 Hz; H-5'b), 3.58 (dd; 1H; J = 12.5, 5.4 Hz; H-5'a), 4.38 (dd; 1H; J = 12.5, 3.2 Hz; H-2'b), 4.62 (dd; 1H; J = 12.5, 4.8 Hz; H-2'a), 5.35 (dd; 1H; J = 4.9, 3.1 Hz; H-1'), 6.29 (dd; 1H; J = 5.4, 3.3 Hz; H-4'), 7.45 (d; 1H; J = 7.6 Hz; H-5), 8.10 (d; 1H; J = 7.6 Hz; H-6), 9.34 (s; 1H; OH); δ_C (spectrum 21, 75.462 MHz, $CDCl_3$): 13.51 (C-d), 13.57 (C-d'), 18.24 (C-c), 18.27 (C-c'), 35.83 (C-b), 38.89 (C-b'), 39.35 (C-4), 63.31 (C-2), 84.86 (C-5'), 87.89 (C-4'), 96.27 (C-1'), 144.25 (C-5 / C-6), 154.82 (C-2'), 162.82 (C-6 / C-5), 172.84 (C-a), 173.54 (C-a').

4.2.1.4 N-hexanoyllamivudine-5'-hexanoate (6)

A yield of 0.9463 g (24.43 %) white crystalline compound was obtained; mp 133.84 °C (thermogram 4); Rf 0.78 (EtOAc); $C_{20}H_{31}N_3O_5S$; M^+ 425; m/z (FAB, spectrum 4): 426 ($(M+H^+)$ 40.5 %), 210 (100.0 %), 154 (17.0 %), 136 (22.5 %), 112 (70.0 %); ν_{max} (spectrum 10, KBr, cm^{-1}): 1110.53, 1152.38, 1183.82, 1663.06, 1703.02, 1732.37, 3337.89; δ_H (spectrum 16, 300.075 MHz, $CDCl_3$): 0.86 (t; 6H; J = 6.86 Hz; H-f, H-f'), 1.30 (m; 8H; H-e, H-e', H-d, H-d'), 1.64 (m; 4H; H-c, H-c'), 2.35 (t; 2H; J = 7.5 Hz; H-b), 2.46 (t; 2H; J = 7.5 Hz; H-b'), 3.16 (dd; 1H; J = 12.5, 3.3 Hz; H-5'b), 3.60 (dd; 1H; J = 12.5, 5.4 Hz; H-5'a), 4.39 (dd; 1H; J = 12.4, 3.2 Hz; H-2'b), 4.63 (dd; 1H; J = 12.5, 4.9 Hz; H-2'a), 5.36 (dd; 1H; J = 4.9, 3.1 Hz; H-1'), 6.30 (dd; 1H; J = 5.3, 3.2 Hz; H-4'), 7.44 (d; 1H; J = 7.5 Hz; H-5), 8.10 (d; 1H; J = 7.6 Hz; H-6), 9.14 (s; 1H; OH); δ_C (spectrum 22, 75.462 MHz, $CDCl_3$): 13.80 (C-f, C-f'), 22.23 (C-e), 22.29 (C-e'), 24.48 (C-d, C-d'), 31.14 (C-c), 31.18 (C-c'), 33.96 (C-b), 37.59 (C-b'), 38.88 (C-4), 63.37 (C-2), 84.84 (C-5'), 87.94 (C-4'), 96.21 (C-1'), 144.25 (C-5 / C-6), 154.82 (C-2'), 162.74 (C-6 / C-5), 173.04 (C-a), 173.53 (C-a').

4.2.1.5 N-octanoyllamivudine-5'-octanoate (7)

A yield of 2.1085 g (49.90 %) light yellow crystalline compound was obtained; mp 93.89 °C (thermogram 5); Rf 0.84 (EtOAc); $C_{24}H_{39}N_3O_5S$; M^+ 482; m/z (FAB, spectrum 5): 483 ($(M+H^+)$ 32.0 %), 239 (100.0 %), 138 (19.5 %), 127 (70.0 %), 112 (88.0 %); ν_{max} (spectrum 11, KBr, cm^{-1}): 1053.34, 1140.31, 1185.29, 1665.79, 1713.87, 1737.95, 3305.49; δ_H (spectrum 17, 300.075 MHz, $CDCl_3$): 0.82 (t; 6H; J = 6.3 Hz; H-h, H-h'), 1.27 (m; 16H; H-g, H-g', H-f, H-f', H-e, H-e', H-d, H-d'), 1.65 (m; 4H; H-c, H-c'), 2.36 (dt; 4H; J = 25.2, 7.5 Hz; H-b, H-b'), 3.16 (dd; 1H; J = 12.6, 3.2 Hz; H-5'b), 3.62 (dd; 1H; J = 12.5, 5.4 Hz; H-5'a), 4.38 (dd; 1H; J = 12.4, 3.1 Hz; H-2'b), 4.64 (dd; 1H; J = 12.5, 4.9 Hz; H-2'a), 5.37 (dd; 1H; J = 4.9, 3.1 Hz; H-1'), 6.31 (dd; 1H; J = 5.3, 3.2 Hz; H-4'), 7.45 (d; 1H; J = 7.6 Hz; H-5), 8.05 (d; 1H; J = 7.6 Hz; H-6), 9.42 (br s; 1H; OH); δ_C (spectrum 23, 75.462 MHz, $CDCl_3$): 13.98 (C-h, C-h'), 22.51 (C-g, C-g'), 22.53 (C-f, C-f'), 24.82 (C-e), 28.84 (C-e'), 28.90 (C-d), 28.97 (C-d'), 29.01 (C-c), 31.58 (C-c'), 34.02 (C-b),

37.62 (C-b'), 38.92 (C-4), 63.34 (C-2), 84.93 (C-5'), 87.95 (C-4'), 96.13 (C-1'), 144.43 (C-5 / C-6), 154.63 (C-2'), 162.78 (C-6 / C-5), 173.04 (C-a), 173.62 (C-a').

4.2.1.6 N-decanoyllamivudine-5'-decanoate (8)

A yield of 1.8530 g (38.99 %) off-white crystalline compound was obtained; mp 88.61 °C (thermogram 6); Rf 0.69 (EtOAc : DCM (9 : 1)), 0.46 (diethyl ether); $C_{28}H_{47}N_3O_5S$; M^+ 537; m/z (FAB, spectrum 6): 538 ($(M+H^+)$ 44.0 %), 266 (100.0 %), 155 (59.0 %), 138 (20.0 %), 112 (78.0 %); ν_{max} (spectrum 12, KBr, cm^{-1}): 1042.86, 1136.83, 1191.03, 1667.39, 1709.61, 1726.46, 3312.65; δ_H (spectrum 18, 300.075 MHz, $CDCl_3$): 0.84 (t; 6H; J = 6.73 Hz; H-j, H-j'), 1.25 (m; 24H; H-i, H-i', H-h, H-h', H-g, H-g', H-f, H-f', H-e, H-e', H-d, H-d'), 1.65 (m; 4H; H-c, H-c'), 2.39 (dt; 4H; J = 26.2, 7.5 Hz; H-b, H-b'), 3.17 (dd; 1H; J = 12.5, 3.3 Hz; H-5'b), 3.60 (dd; 1H; J = 12.5, 5.4 Hz; H-5'a), 4.40 (dd; 1H; J = 12.4, 3.2 Hz; H-2'b), 4.63 (dd; 1H; J = 12.5, 4.9 Hz; H-2'a), 5.36 (dd; 1H; J = 4.9, 3.2 Hz; H-1'), 6.30 (dd; 1H; J = 5.3, 3.2 Hz; H-4'), 7.45 (d; 1H; J = 7.6 Hz; H-5), 8.10 (d; 1H; J = 7.6 Hz; H-6), 9.06 (s; 1H; OH); δ_C (spectrum 24, 75.462 MHz, $CDCl_3$): 14.03 (C-j, C-j'), 22.60 (C-i, C-i'), 24.82 (C-h, C-h'), 29.03 (C-g, C-g'), 29.06 (C-f, C-f'), 29.17 (C-e, C-e'), 29.19 (C-d), 29.26 (C-d'), 29.35 (C-c), 31.80 (C-c'), 34.02 (C-b), 37.66 (C-b'), 38.91 (C-4), 63.38 (C-2), 84.88 (C-5'), 87.96 (C-4'), 96.20 (C-1'), 144.27 (C-5 / C-6), 154.83 (C-2'), 162.71 (C-6 / C-5), 173.05 (C-a), 173.46 (C-a').

4.3 Physicochemical properties and solubility

4.3.1 Solubility determination

The aqueous solubility of **(1)**, **(2)** and the amide esters of **(2)** were obtained by preparing saturated solutions in a phosphate buffer solution (PBS) at pH 5 and 7. The slurries were stirred with magnetic bars in a water bath at 32 °C for 24 h. An excess of solute was present at all times to provide saturated solutions. The solutions were filtered after 24 h, diluted (**(1)**, **(2)** and **(3)**) and analysed directly by HPLC to determine the concentration of solute dissolved in the solvent. The experiment was done in triplicate. Results are presented in section 5.2.1 and discussed in section 5.2.2.

4.3.2 Experimental partition coefficient

Equal volumes of *n*-octanol and PBS at pH 5 and 7 were saturated with one another under vigorous stirring for at least 24 hours and then separated. An excess of **(1)**, **(2)** and the amide esters of **(2)** was dissolved in 0.5 ml pre-saturated *n*-octanol and 0.5 ml pre-saturated PBS buffer, stoppered and agitated for 75 min, thereafter at 25 °C **(1)** and **(2)** were centrifuged at 4000 rpm for 20 min, **(3)**, **(4)** and **(5)** were centrifuged at 12000 rpm for 20 min and **(6)**, **(7)** and

(8) were centrifuged at 12000 rpm for 40 min. An excess solute was present at all times. The *n*-octanol and aqueous phases were separately analysed by HPLC. The aqueous and the *n*-octanol phase were diluted with PBS and MeOH, respectively, prior to being analysed by HPLC. The *n*-octanol-PBS partition coefficients (log D) were calculated as logarithmic ratios of the concentrations in the *n*-octanol phase to the concentrations in the PBS. The experiment was done in triplicate. Results are presented in section 5.2.3 and discussed in section 5.2.4.

4.4 Transdermal permeation

4.4.1 Skin preparation

Female human abdominal skin was used for the permeation studies and was obtained from Sunwardpark Clinic (Boksburg, South Africa) and Wilgers Private Hospital (Tswane, South Africa) after cosmetic procedures (Human ethics approval reference number 04D08). A scalpel was used to separate the skin from the fat layer; subsequently the epidermis was removed by means of immersion in 60 °C HPLC water for 60 sec (Kligman and Christophers, 1963). The epidermis was gently teased away from the skin with forceps. Special care was taken that the integrity of the epidermis was not ruptured, as this would compromise the validity of the results. The epidermis was placed in a bath filled with HPLC water and carefully set on Whatman® filter paper, left to air dry and was wrapped in foil. The foil containing the epidermis was stored in a freezer at -20 °C and was used within 3 months after being prepared. Prior to use, the epidermis was thawed and examined (visually and by measuring the electrical resistance) for any defects, before it was mounted on the Franz diffusion cells.

4.4.2 Preparation of donor solutions

Donor solutions of **(1)**, **(2)** and the amide esters of **(2)** were obtained by the equilibration of excess amounts of solvent in PBS at pH 5 in a water bath. The slurries were prepared in stoppered flasks; stirring in a water bath at 32 °C over a period of 24 hours, in order for solvent saturation to occur. An excess amount of solute was present at all times. The aforementioned method was used to prepare donor solutions in Pheroid™.

4.4.3 Preparation of Pheroid™

Pheroid™ in a microsponge formulation was formulated by Mr. Dale Elgar (Department of Pharmaceutics, School of Pharmacy, North-West University, Potchefstroom 2520, South Africa).

4.4.4 Skin permeation method

Vertical Franz diffusion cells (Figure 4.1) with 2.0 ml receptor compartments and 1.0751 cm^2 effective diffusion area was used for the permeation studies. The epidermal skin layer was carefully mounted on the lower half of the Franz cell with the stratum corneum facing upwards. Leakage of the diffusion cells were prevented by applying vacuum grease. A clamp was used to fasten the upper and lower parts of the Franz cell together, with the epidermis separating the donor and receptor compartments. The receptor compartments were filled with isotonic PBS (pH 7.4). Special care was taken that no air bubbles came between the buffer solution and the epidermis. The donor compartments filled with 1.0 ml PBS (pH 5) were equilibrated at 37 °C for one hour in the water bath and the integrity (electrical resistance) of the epidermis measured, prior to the addition of the saturated solutions. Only the receptor compartments were submerged in the water and were equipped with magnetic stirrers. After a period of one hour, 1.0 ml of freshly prepared saturated solution (in PBS (pH 5) or Pheroid™) was added to each donor compartment, which was immediately covered with Parafilm® to prevent the evaporation of any constituents within the saturated solution for the duration of the experiment. An excess amount of solute was present in the donor compartments at all times during the experimental procedure.

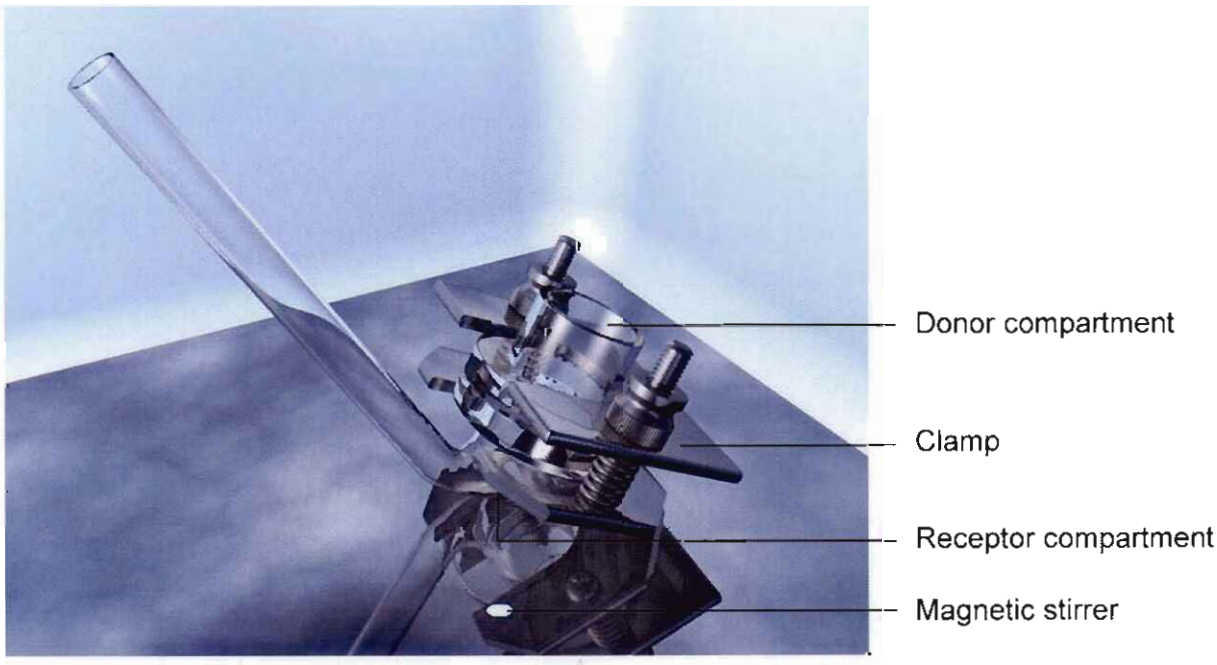

Figure 4.1: Vertical Franz diffusion cell.

The entire receptor volumes were withdrawn and replaced with 37 °C fresh buffer solution (pH 7.4) after 2, 4, 6, 8, 10, 12 and 24 hours to mimic sink conditions as they occur in the human body. The experiments were conducted over 24-hour periods.

In each case the withdrawn samples were assayed immediately by HPLC to determine the drug concentration of **(1)**, **(2)** and the amide esters of **(2)** that had permeated the epidermis. No extra peaks were observed in the chromatograms of the receptor phase of **(1)**, **(2)** or the amide esters of **(2)** in PBS. Except for the cells that leaked, all data obtained were used. At least six data points on the steady-state part of the curve were used. Average flux was calculated from the gradient of the cumulative concentration versus time graph and the median flux was statistically obtained (§ 5.3.1).

RESULTS AND DISCUSSION

5.1 Amide ester synthesis

Acylation and esterification of **(2)** with acid chloride (1.0 : 5.0 equivalent) yielded exclusively the amide esters. Selective esterification of the primary functional hydroxyl group was neither observed at different ratios of **(2)** : acid chloride, i.e., 1.0 : 0.5 and 1.0 : 1.0 equivalent, nor at different temperatures, i.e., room temperature (25 °C), elevated temperature (50 °C) and reduced temperature (-2 & 0 °C). The amide fraction will phosphorylate easier than the esters fraction. Although the esters of **(2)** will lose their chain in an aqueous solution to form the hydroxyl group, the amides will be available for phosphorylation almost immediately, due to the hydroxyl group being unbound.

The amide esters of **(2)** were synthesised, isolated and analysed by MS, IR and NMR, as well as DSC. It was clear from TLC that **(2)** and the six different acid chlorides reacted with each other to form the amide ester compounds. Purification by column chromatography was successful and the NMR analyses of these samples indicated that they were all pure amide compounds **(3)** – **(8)**. The ^{1}H and ^{13}C NMR data of all the amide esters of **(2)** are similar to that of **(2)** and thus only the differences will be discussed.

5.1.1 Structures of the products

5.1.1.1 N-acetyllamivudine-5'-acetate (3)

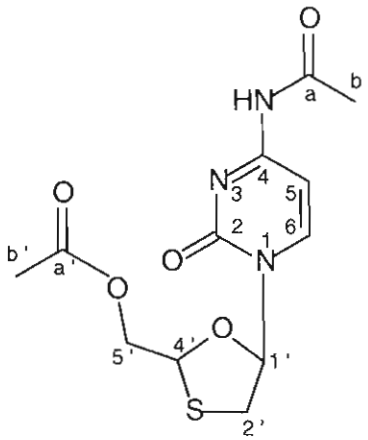

(3)

The MS data confirmed the presence of the molecular ion of **(3)** at m/z 314, corresponding to a molecular formula of $C_{12}H_{15}N_3O_5S$ and one proton. In the ^1H NMR spectrum the singlets at δ 2.09 and 2.26 represent H-b / H-b' and H-b' / H-b, respectively. The ^{13}C NMR data of **(3)** were similar to that of **(2)**, except that the following signals moved slightly: C-5' and C-6 / C-5 have shifted to a slightly higher magnetic field at δ 84.69 and 163.13, respectively and C-4, C-2 (carbonyl carbon atom), C-4', C-1' and C-5 / C-6 have shifted to a slightly lower magnetic field at δ 38.78, 63.57, 87.89, 96.47 and 144.23, respectively in the ^{13}C NMR spectrum. The presence of the methyl groups were indicated by the signals at δ 20.63 and 24.81 representing the carbon atoms C-b / C-b' and C-b' / C-b, respectively and the carbonyl carbon atoms were indicated by the signals at δ 170.14 and 171.08 representing the carbon atoms C-a / C-a' and C-a' / C-a, respectively. In the IR spectrum the ether (C-O) stretching vibration was at 1059.81 cm^{-1}, the stretching vibrations of two carbonyl groups (C=O) were at 1655.81 (mono amide) and 1741.19 cm^{-1} (acetate). These data verify the structure of **(3)**.

5.1.1.2 N-propionyllamivudine-5'-propionate (4)

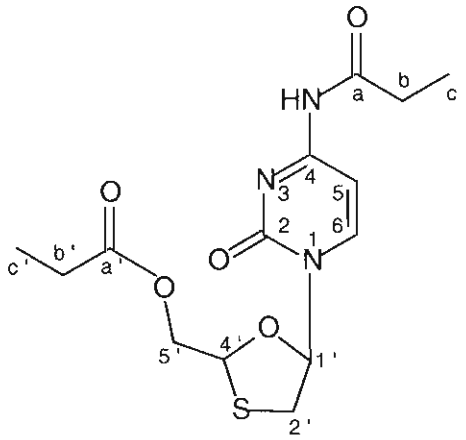

(4)

The MS data confirmed the presence of the molecular ion of **(4)** at m/z 342, corresponding to a molecular formula of $C_{14}H_{19}N_3O_5S$ and one proton. In the ^1H NMR spectrum the triplet at δ 1.16 represents H-c and H-c'. The multiplets δ 2.38 and 2.51 represent H-b / H-b' and H-b' / H-b, respectively. The ^{13}C NMR data of **(4)** were similar to that of **(2)**, except that the following signals moved slightly: C-5' and C-6 / C-5 have shifted to a slightly higher magnetic field at δ 84.93 and 162.84, respectively and C-4, C-2 (carbonyl carbon atom), C-4', C-1' and C-5 / C-6 have shifted to a slightly lower magnetic field at δ 38.92, 63.34, 87.86, 96.32 and 144.24, respectively in the ^{13}C NMR spectrum. The presence of the methyl groups were indicated by the signals at δ 8.68 and 8.95 representing the carbon atoms C-c / C-c' and C-c' / C-c, respectively, the methylene groups were indicated by the signals at δ 27.30 and 30.67 representing the carbon atoms C-b / C-b' and C-b' / C-b, respectively and the carbonyl carbon

atoms were indicated by the signals at δ 173.66 and 174.38 representing the carbon atoms C-a / C-a' and C-a' / C-a, respectively. In the IR spectrum the ether (C-O) stretching vibration was at 1053.16 cm^{-1} and the stretching vibrations of two carbonyl groups (C=O) were at 1659.82 (mono amide) and 1743.77 cm^{-1} (acetate). These data verify the structure of **(4)**.

5.1.1.3 N-butyryllamivudine-5'-buterate (5)

The MS data confirmed the presence of the molecular ion of **(5)** at m/z 371, corresponding to a molecular formula of $C_{16}H_{23}N_3O_5S$ and one proton. In the ^1H NMR spectrum the triplet at δ 0.91 represents H-d and H-d', the multiplet at δ 1.66 represents H-c and H-c' and the triplets at δ 2.31 and 2.47 represent H-b / H-b' and H-b' / H-b, respectively. The ^{13}C NMR data of **(5)** were similar to that of **(2)**, except that the following signals moved slightly: C-5' and C-6 / C-5 have shifted to a slightly higher magnetic field at δ 84.86 and 162.82, respectively and C-4, C-2 (carbonyl carbon atom), C-4', C-1' and C-5 / C-6 have shifted to a slightly lower magnetic field at δ 39.35, 63.31, 87.89, 96.27 and 144.25, respectively in the ^{13}C NMR spectrum. The presence of the methyl groups were indicated by the signals at δ 13.51 and 13.57 representing the carbon atoms C-d / C-d' and C-d' / C-d, respectively. The methylene groups were indicated by the signals at δ 18.24, 18.27, 35.83 and 38.89 representing the carbon atoms C-c / C-c', C-c' / C-c, C-b / C-b' and C-b' / C-b, respectively. The carbonyl carbon atoms were indicated by the signals at δ 172.84 and 173.54 representing the carbon atoms C-a / C-a' and C-a' / C-a, respectively. In the IR spectrum the ether (C-O) stretching vibration was at 1065.04 cm^{-1}, the stretching vibrations of two carbonyl groups (C=O) were at 1655.52 (mono amide) and 1742.69 cm^{-1} (acetate). These data verify the structure of **(5)**.

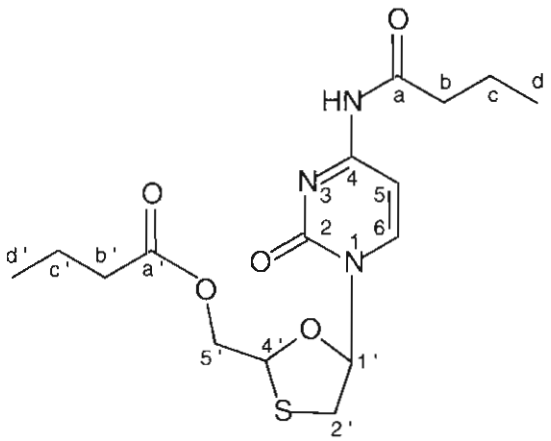

(5)

5.1.1.4 N-hexanoyllamivudine-5'-hexanoate (6)

The MS data confirmed the presence of the molecular ion of **(6)** at m/z 426, corresponding to a molecular formula of $C_{20}H_{31}N_3O_5S$ and one proton. In the ^1H NMR spectrum the triplet at δ 0.86

represents H-f and H-f', the multiplet at δ 1.30 represents H-e, H-e', H-d and H-d', the multiplet at δ 1.64 represents H-c and H-c' and the triplets at δ 2.35 and 2.46 represent H-b / H-b' and H-b' / H-b, respectively. The ^{13}C NMR data of **(6)** were similar to that of **(2)**, except that the following signals moved slightly: C-5' and C-6 / C-5 have shifted to a slightly higher magnetic field at δ 84.84 and 162.74, respectively and C-4, C-2 (carbonyl carbon atom), C-4', C-1' and C-5 / C-6 have shifted to a slightly lower magnetic field at δ 38.88, 63.37, 87.94, 96.21 and 144.25, respectively in the ^{13}C NMR spectrum. The presence of the methyl groups were indicated by one signal at δ 13.80 representing the carbon atoms C-f and C-f'. The methylene groups, C-d and C-d', were indicated by one signal at δ 24.48; the other methylene groups were indicated by the signals at δ 22.23, 22.29, 31.14, 31.18, 33.96 and 37.59 representing the carbon atoms C-e / C-e', C-e' / C-e, C-c / C-c', C-c' / C-c, C-b / C-b' and C-b' / C-b, respectively. The carbonyl carbon atoms were indicated by the signals at δ 173.04 and 173.53 representing the carbon atoms C-a / C-a' and C-a' / C-a, respectively. In the IR spectrum the ether (C-O) stretching vibration was at 1110.53 cm^{-1}, the stretching vibrations of two carbonyl groups (C=O) were at 1663.06 (mono amide) and 1732.37 cm^{-1} (acetate). These data verify the structure of **(6)**.

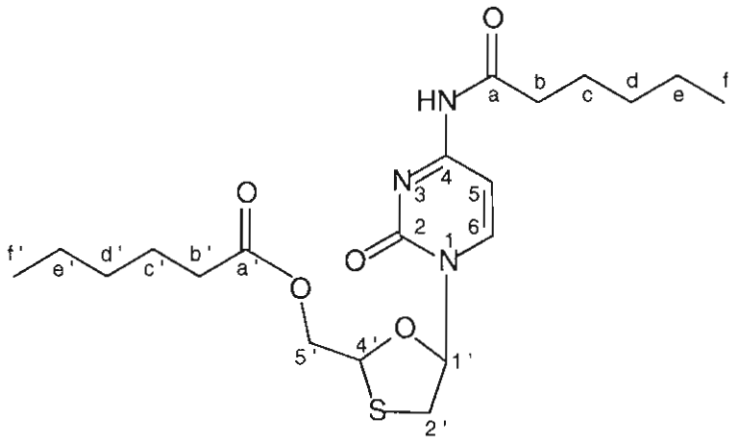

(6)

5.1.1.5 N-octanoyllamivudine-5'-octanoate (7)

The MS data confirmed the presence of the molecular ion of **(7)** at m/z 483, corresponding to a molecular formula of $C_{24}H_{39}N_3O_5S$ and one proton. In the ^1H NMR spectrum the triplet at δ 0.82 represents H-h and H-h', the multiplet at δ 1.27 represents H-g, H-g', H-f, H-f', H-e, H-e', H-d and H-d', the multiplet at δ 1.65 represents H-c and H-c' and the doublet of triplets at δ 2.36 represents H-b and H-b'. The ^{13}C NMR data of **(7)** were similar to that of **(2)**, except that the following signals moved slightly: C-5' and C-6 / C-5 have shifted to a slightly higher magnetic field at δ 84.93 and 162.78, respectively and C-4, C-2 (carbonyl carbon atom), C-4', C-1' and C-5 / C-6 have shifted to a slightly lower magnetic field at δ 38.92, 63.34, 87.95, 96.13 and

144.43, respectively in the ^{13}C NMR spectrum. The presence of the methyl groups were indicated by one signal at δ 13.98 representing the carbon atoms C-h and C-h'. The methylene

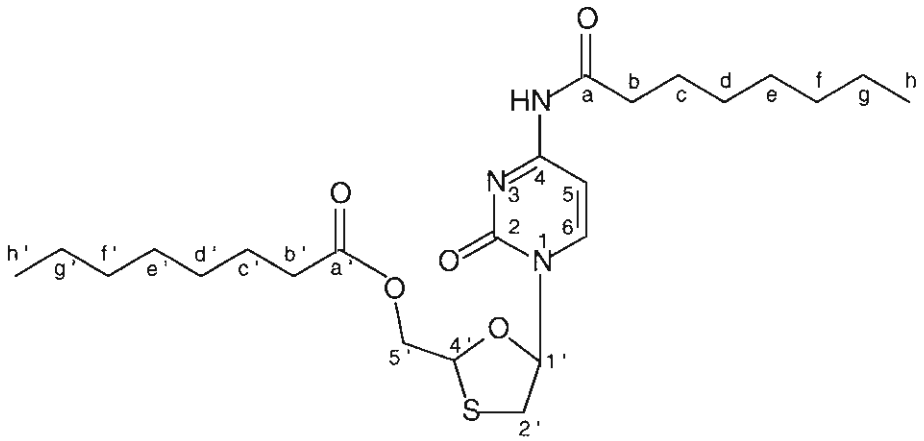

(7)

groups, C-g and C-g', were indicated by one signal at δ 22.51, as well as, C-f and C-f' at δ 22.53; the other methylene groups were indicated by the signals at δ 24.82, 28.84, 28.90, 28.97, 29.01, 31.56, 34.02 and 36.62 representing the carbon atoms C-e / C-e', C-e' / C-e, C-d / C-d', C-d' / C-d, C-c / C-c', C-c' / C-c, C-b / C-b' and C-b' / C-b, respectively. The carbonyl carbon atoms were indicated by the signals at δ 173.04 and 173.62 representing the carbon atoms C-a / C-a' and C-a' / C-a, respectively. In the IR spectrum the ether (C-O) stretching vibration was at 1053.34 cm^{-1}, the stretching vibrations of two carbonyl groups (C=O) were at 1665.79 (mono amide) and 1737.95 cm^{-1} (acetate). These data verify the structure of **(7)**.

5.1.1.6 N-decanoyllamivudine-5'-decanoate (8)

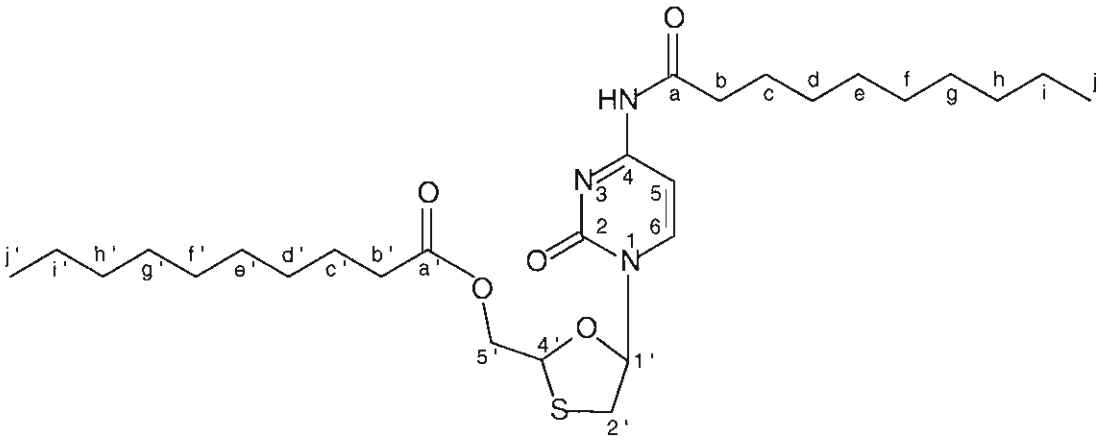

(8)

The MS data confirmed the presence of the molecular ion of **(8)** at m/z 538, corresponding to a molecular formula of $C_{28}H_{47}N_3O_5S$ and one proton. In the ^1H NMR spectrum the triplet at δ 0.84 represents H-j and H-j', the multiplet at δ 1.25 represents H-i, H-i', H-h, H-h', H-g, H-g', H-f, H-f',

H-e, H-e', H-d and H-d', the multiplet at δ 1.65 represents H-c and H-c' and the doublet of triplets at δ 2.39 represents H-b and H-b'. The ^{13}C NMR data of **(8)** were similar to that of **(2)**, except that the following signals moved slightly: C-5' and C-6 / C-5 have shifted to a slightly higher magnetic field at δ 84.88 and 162.71, respectively and C-4, C-2 (carbonyl carbon atom), C-4', C-1' and C-5 / C-6 have shifted to a slightly lower magnetic field at δ 38.91, 63.38, 87.96, 96.20 and 144.27, respectively in the ^{13}C NMR spectrum. The presence of the methyl groups were indicated by one signal at δ 14.03 representing the carbon atoms C-j and C-j'. The methylene groups, C-i and C-i', C-h and C-h', C-g and C-g', C-f and C-f', C-e and C-e', were all indicated by one signal at δ 22.60, 24.82, 29.03, 29.06 and 29.17, respectively; the other methylene groups were indicated by the signals at δ 29.19, 29.26, 29.35, 31.80, 34.02 and 37.66 representing the carbon atoms C-d / C-d', C-d' / C-d, C-c / C-c', C-c' / C-c, C-b / C-b' and C-b' / C-b, respectively. The carbonyl carbon atoms were indicated by the signals at δ 173.05 and 173.46 representing the carbon atoms C-a / C-a' and C-a' / C-a, respectively. In the IR spectrum the ether (C-O) stretching vibration was at 1042.86 cm^{-1}, the stretching vibrations of two carbonyl groups (C=O) were at 1667.39 (mono amide) and 1726.46 cm^{-1} (acetate). These data verify the structure of **(8)**.

5.1.2 Conclusion

The ^{1}H and ^{13}C NMR, MS and IR data confirmed that the amide esters **(3)** to **(8)** were successfully synthesised.

5.2 Physicochemical properties

5.2.1 Aqueous solubility

The experimentally determined aqueous solubility on a mass basis measured in mg/ml, as well as the aqueous solubility on a molar basis measured in μg/mol (mM) of **(1)**, **(2)** and the amide esters of **(2)** at pH 5 and 7 together with predicted aqueous solubility values (mg/ml and mM), obtained from IA (interactive analysis) prediction software (Parham, 2000), are presented in Table 5.1 and Figure 5.1.

Table 5.1: The aqueous solubility values of compounds **(1)** to **(8)**.

	Aqueous solubility (mg/ml)			Aqueous solubility (mM)		
Compound	**pH 5** [a]	**pH 7** [a]	**IA** [b]	**pH 5**	**pH 7**	**IA**
(1)	144.78	100.16	6.64	541.42	433.53	31.44
(2)	114.36	91.57	1.68	631.53	436.90	7.31
(3)	3.98	3.36	0.51	12.70	10.72	1.63
(4)	8.34	6.16	0.14	24.43	18.04	0.40
(5)	0.28	0.20	0.03	0.76	0.54	0.09
(6)	1.00×10^{-4}	1.00×10^{-4}	3.78×10^{-3}	2.00×10^{-4}	2.00×10^{-4}	8.90×10^{-3}
(7)	Insoluble	Insoluble	1.66×10^{-3}	Insoluble	Insoluble	3.50×10^{-3}
(8)	Insoluble	Insoluble	1.20×10^{-4}	Insoluble	Insoluble	2.00×10^{-4}

[a] experiments conducted in PBS at pH 5 and 7, respectively
[b] predicted values calculated using IA (interactive analysis) (Parham, 2000)

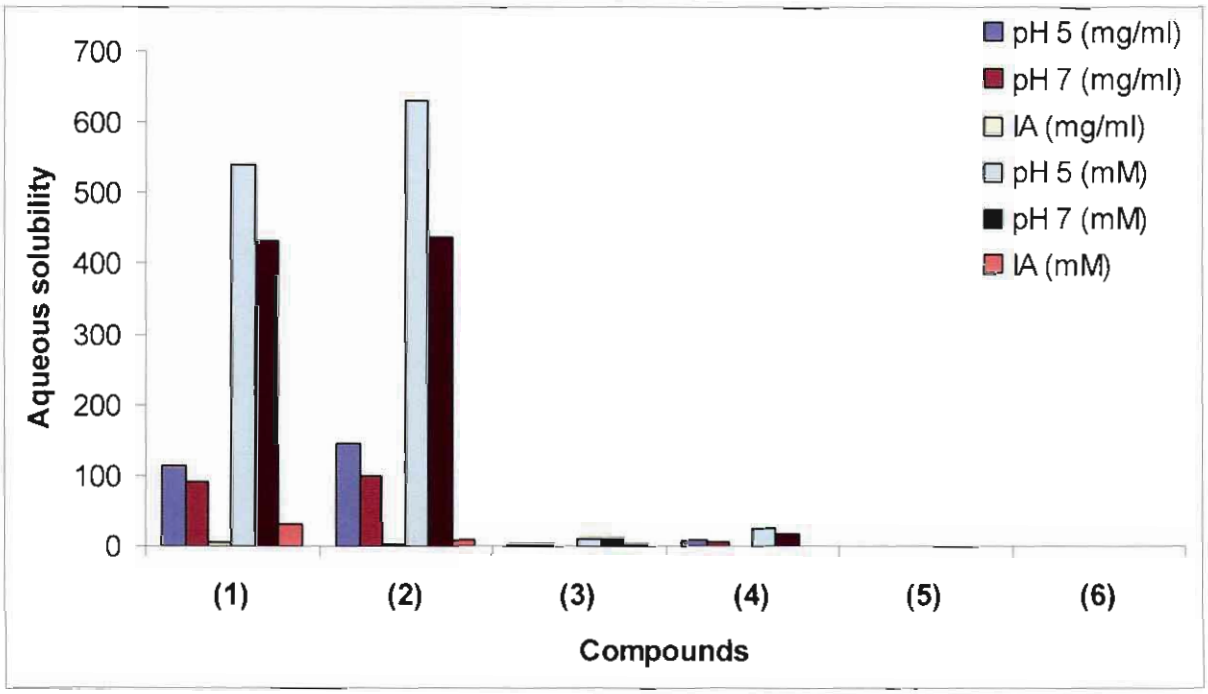

Figure 5.1: Experimental and predicted aqueous solubility values on a mass (mg/ml) and molar basis (mM) of compounds **(1)** to **(6)**.

5.2.2 Discussion

To compare the aqueous solubility of the amide esters with that of **(2)**, as well as the aqueous solubility of **(2)** with that of **(1)**, it was necessary to determine the aqueous solubility at the same pH. **(2)** has a pKa of 6.91, hence, for it to be 99.99 % unionised it should be dissolved in an acidic pH of 4.0. This provides a problem for transdermal application, for if the pH is lower than 4.5 it will irritate the skin. The aforementioned states the reason why a pH of 5.0 was chosen, where **(2)** was 98.78 % unionised. There is a negligible difference between a 99.99 and 98.78 % unionised species. A neutral pH of 7.0 (44.84 % unionised) was selected to compare the aqueous solubility values with those at pH 5.0 and to determine which pH to use for diffusion studies. It was established that, for all the compounds, the aqueous solubility values at pH 5.0 (the more unionised form) were higher than those at pH 7.0 (the less unionised species). Consequently, pH 5.0 was selected for permeation studies (§ 5.3.1), because compounds can only permeate the stratum corneum successfully if the proposed transdermal candidates are in a unionised state. Ionised molecules do not penetrate the lipophilic stratum corneum easily and have delayed transdermal permeation (§ 3.5.2.4).

The aqueous solubility of **(1)** on a mass basis (mg/ml) was higher than that of **(2)** at both pH 5 and 7, but on a molar basis it was found that the aqueous solubility (mM) of **(2)** was higher than that of **(1)** at both pHs. **(2)** has an aqueous solubility (mM) of approximately 90 mM higher than **(1)** at pH 5 and was slightly higher than **(1)** (less than 3 mM) at pH 7. The aqueous solubility values for all the compounds on a molar basis (mM) were higher than the aqueous solubility values on a mass basis (mg/ml).

As expected, the aqueous solubility of **(2)** is distinctly higher than that of the synthesised amide esters. The above results show that the solubility in general decreases with an increase in chain length in accordance with data in the literature (§ 3.5.2.8) (Abdou, 1989). Of all the amide esters synthesised **(4)** had the highest aqueous solubility values, where **(7)** and **(8)** were highly lipophilic and thus insoluble in PBS at pH 5 and 7. The aqueous solubility at both pH 5 and 7 of **(2)** was about half of that of **(4)**, and **(6)** had the lowest soluble aqueous solubility value of all the compounds.

Experimentally determined aqueous solubility values for **(1)**, **(2)**, **(3)** and **(4)** are higher than predicted values, **(5)** differed the least and for **(6)**, **(7)** and **(8)** the predicted aqueous solubility values were higher than the experimentally determined values. The difference between the data may be attributed to the method of calculation of the software.

5.2.3 Partition coefficient

Table 5.2: Partition coefficients of compounds **(1)** to **(8)**.

Compound	Experimental (log D) [a]		Predicted (log P)		
	pH 5	pH 7	ACD [b]	IA [c]	K_{ow}Win [d]
(1)	-1.50	-1.78	-1.50	-1.24	-1.72
(2)	-1.19	-1.15	-1.02	-0.89	-2.62
(3)	0.12	0.25	-2.20	-0.50	-2.99
(4)	1.70	1.88	-1.14	0.28	-2.01
(5)	2.51	2.55	-0.08	1.08	-1.02
(6)	4.55	4.88	2.05	2.79	0.94
(7)	Insoluble	Insoluble	4.17	4.53	2.90
(8)	Insoluble	Insoluble	6.30	6.20	4.87

[a] experiments conducted at pH 5 and 7 in PBS
[b] calculated using ACD software
[c] calculated using IA (interactive analysis) (Parham, 2000)
[d] calculated using K_{ow}Win (http://esc.syrres.com/interkow/kowdemo.htm)

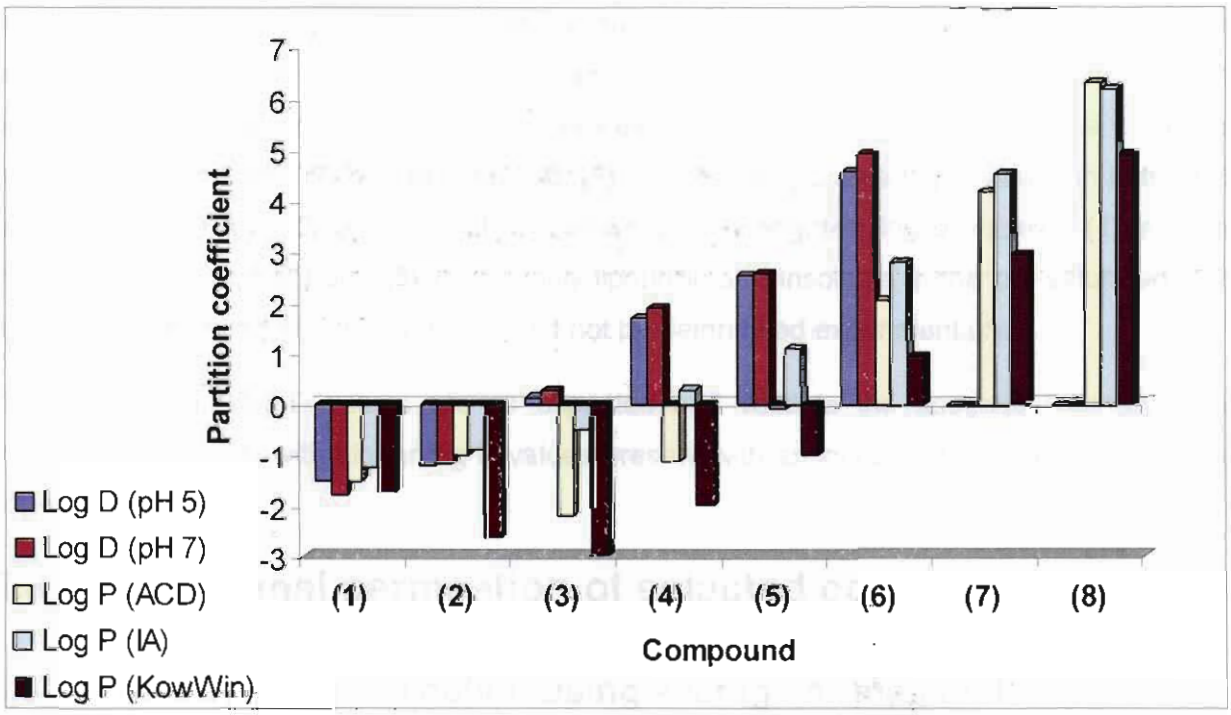

Figure 5.2: Experimental and predicted partition coefficients of compounds **(1)** to **(8)**.

The experimentally determined octanol-PBS partition coefficients at pH 5 and 7 (log D) together with predicted octanol-water partition coefficient values (log P), obtained from the ACD Labs, IA and K_{ow}Win prediction software, are presented in Table 5.2. A summary of the partition coefficient values for compounds **(1)** to **(8)** are given in Figure 5.2.

5.2.4 Discussion

When comparing the experimental log D with the predicted values (log P), obtained from ACD, IA and K_{ow}Win, it is observed that the predicted log P of the amide esters are lower for **(3)**, **(4)**, **(5)** and **(6)**, than the experimental log D values of these compounds. The experimentally determined log D of **(1)** at pH 5 and the predicted log P calculated by ACD of **(1)** had the same values, while the experimentally determined log D of **(1)** at pH 7 and the predicted log P calculated by K_{ow}Win of **(1)** had almost the same values. Of all the prediction software, ACD's log P and the experimental log D for **(2)** at both pH 5 and 7 were almost the same. ACD and K_{ow}Win predicted that only compound **(6)**, **(7)** and **(8)** were lipophilic, while IA calculated that only the first three compounds were hydrophilic. The difference between the log P values for the predicted data as well as the difference between the experimentally determined log D values and the predicted log P values may be attributed to the method the software calculates the data.

As expected, the log D of **(2)** is lower than those of the synthesised amide esters, due to the increase in alkyl chain length that leads to an increase in partition coefficients which is in accordance with data from the literature (§ 3.5.2.8) (Abdou, 1989). The experimentally determined log D values at pH 7 were higher than those at pH 5; this was the case for all the compounds except **(1)**, **(7)** and **(8)**. **(3)**, **(4)**, **(5)** and **(6)** had positive log D values in both pH 5 and 7, while **(1)** and **(2)** are hydrophilic, shown by the negative log D values. **(1)** is more hydrophilic than **(2)**. **(7)** and **(8)** were highly lipophilic and insoluble in the pre-saturated PBS buffer and therefore their log D values could not be determined experimentally.

The experimental log D values are as expected and validate the aqueous solubility data, whereby compounds with higher log D values present with an increased lipophilicity and lower aqueous solubility.

5.3 Transdermal permeation of selected compounds

5.3.1 Transdermal permeation using average or median flux

In general, during transdermal diffusion studies, the average (mean) flux is calculated for each compound as follows: the average cumulative amount per area is calculated and plotted against

time (§ Figure 5.3 and see APPENDIX 1). The slope of linear portion of the curve represents the average flux for each compound. The custom is to repeat the experiment until six values within 30 – 40 % of one another are obtained.

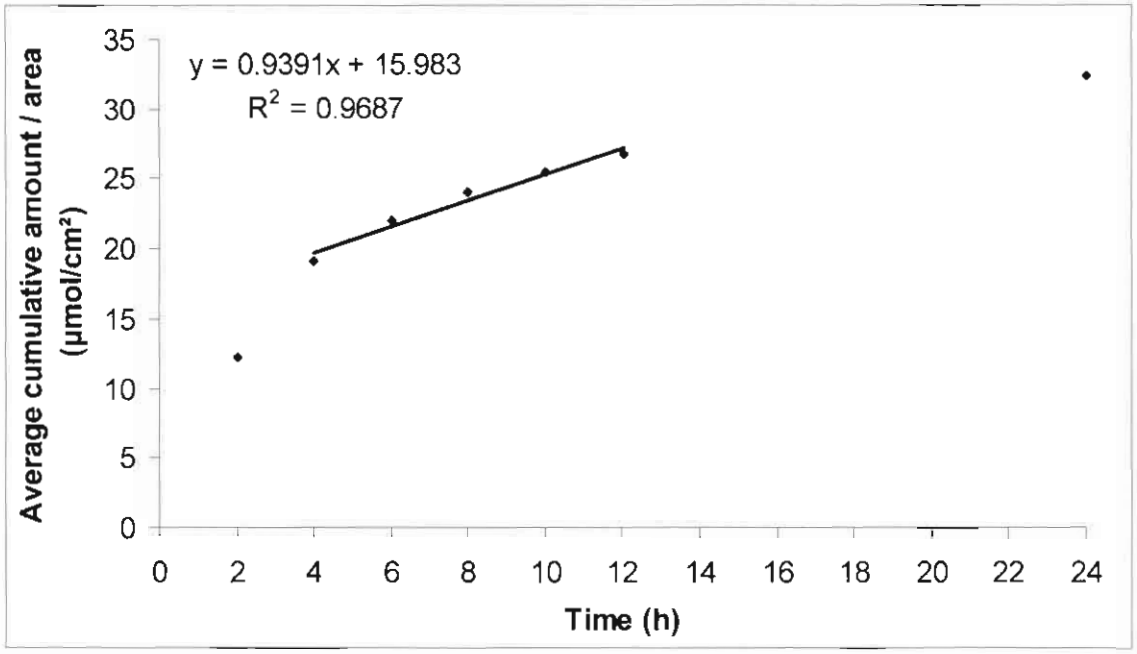

Figure 5.3: The average cumulative amount of **(1)** that penetrated through the skin as a function of time to illustrate the average flux of **(1)**.

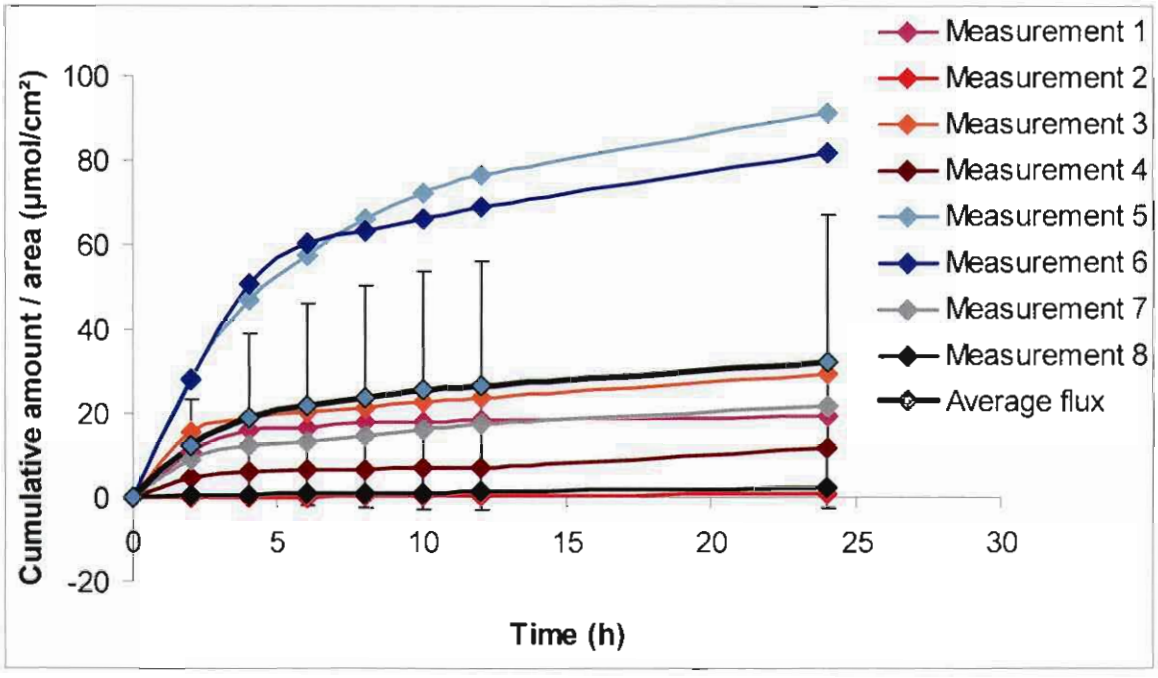

Figure 5.4: The cumulative amount of **(1)** per area in each Franz cell experimentally determined together with the average cumulative amount of **(1)** that had penetrated through the skin as a function of time.

The flux data obtained in the different Franz cells could, however, have a skew distribution around the central location (§ Figure 5.5). Thus, calculating the average flux could give an inaccurate value of the true flux of the compound and complicate further calculations (e.g., flux obtained in measurement 5 and 6 in Figure 5.4 were not in the same range as the rest of the data). Calculating the median flux would therefore give a better representation of the true flux for each compound.

The median flux is calculated as follows: the cumulative amount of compound that penetrated through the skin per area is plotted as a function of time (§ Figure 5.4) for each measurement. Steady-state flux is determined from the slope of the linear portion of each of these curves. Hence, this procedure is repeated for all the measurements for each compound, rendering a dataset of slope (flux) values (§ Figure 5.5). The median of the slope (flux) values represents the median flux for each compound.

The median flux (0.432 $\mu mol.cm^{-2}.h^{-1}$) is the 50 percentile (p50) or centre of all the flux data of **(1)**. In contrast, the average flux (0.939 $\mu mol.cm^{-2}.h^{-1}$) is higher due to measurements 5 and 6 having higher flux values than the rest of the data. By looking at the aforementioned and Figure 5.5 it is clear that the flux obtained has a positively skewed distribution. Hence, the average flux will be an over estimate. The box-plots of the flux values (see APPENDIX 1) confirm the positively skewed distributions for several compounds. Consequently the median will be used to determine the true flux, rather than the average, since the median is more robust to asymmetrical distribution of data.

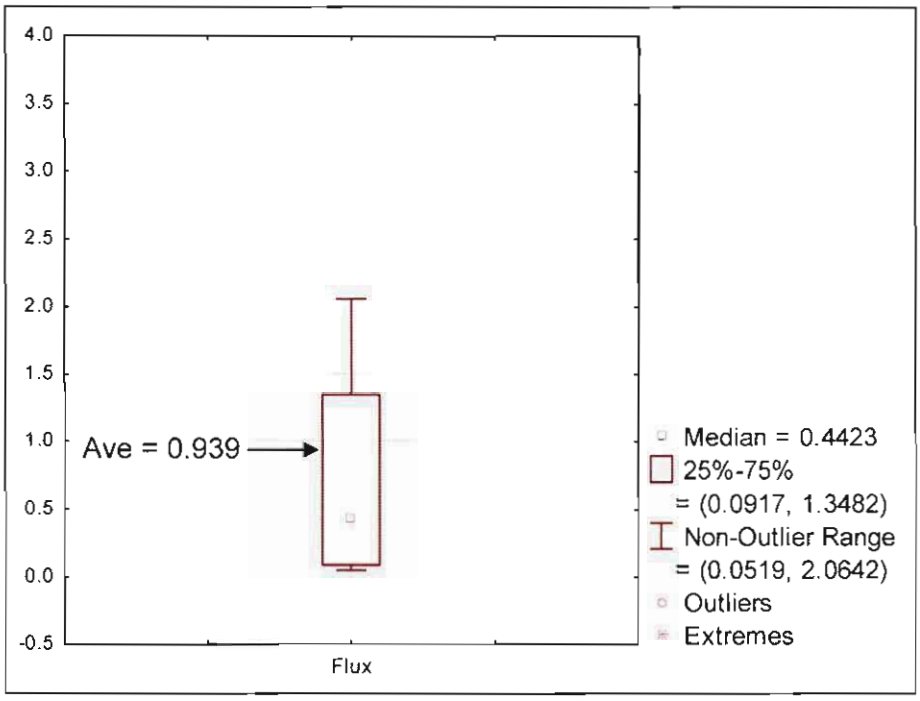

Figure 5.5: Box-plot of the flux of **(1)** in PBS to illustrate the median flux and the skewness of data.

A summary of the transdermal average and median flux values for compounds **(1)** to **(8)** are given in Table 5.3. The average vs. the median transdermal flux data for **(1)** to **(6)** in PBS and Pheroid™ are given in Figure 5.6 and Figure 5.7, respectively.

Table 5.3: Average and median flux data of compounds **(1)** to **(8)** in PBS and Pheroid™.

Compound	Flux ($\mu mol.cm^{-2}.h^{-1}$)			
	Average (in PBS)	**Average (in Pheroid™)**	**Median (in PBS)**	**Median (in Pheroid™)**
(1)	0.939 ± 1.30	0.020 ± 0.02	0.442	0.015
(2)	4.481 ± 3.96	0.013 ± 0.01	4.289	0.011
(3)	0.047 ± 0.04	1.3×10^{-3} ± 0.00	0.046	1.3×10^{-3}
(4)	0.013 ± 0.00	9.4×10^{-3} ± 0.00	0.013	9.3×10^{-3}
(5)	2.4×10^{-3} ± 0.00	7.0×10^{-4} ± 0.00	1.8×10^{-3}	7.0×10^{-4}
(6)	2.0×10^{-4} ± 0.00	2.0×10^{-4} ± 0.00	2.0×10^{-4}	2.0×10^{-4}
(7)	Insoluble	Insoluble	Insoluble	Insoluble
(8)	Insoluble	Insoluble	Insoluble	Insoluble

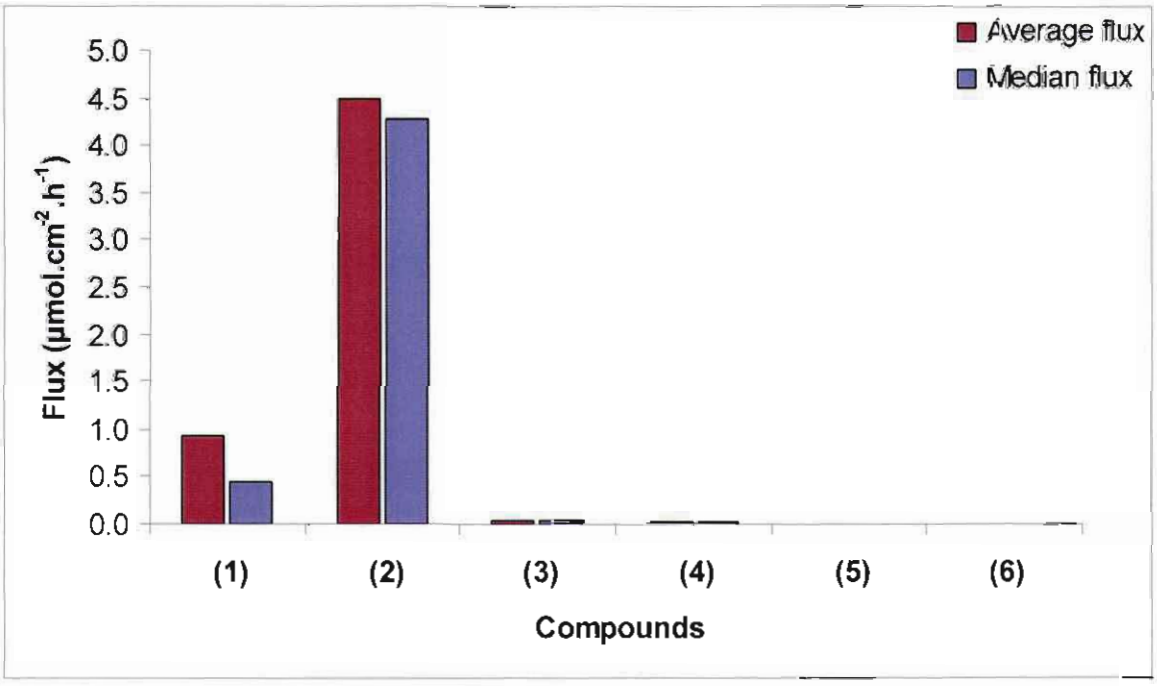

Figure 5.6: Average and median flux values of compounds **(1)** to **(6)** in PBS.

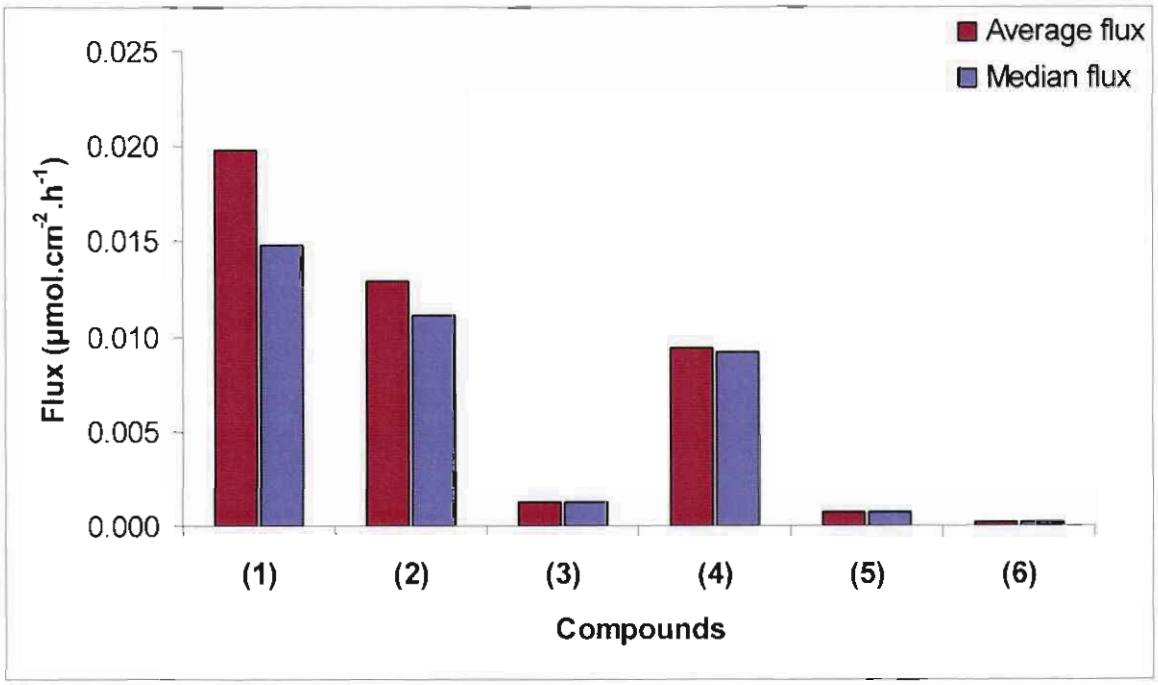

Figure 5.7: Average and median flux values of compounds **(1)** to **(6)** in Pheroid™.

5.3.2 Discussion

In PBS, the average flux of **(1)** (0.939 µmol.cm^{-2}.h^{-1}) was double the median flux of **(1)** (0.442 µmol.cm^{-2}.h^{-1}), but in Pheroid™, there wasn't much of a difference between average (0.020 µmol.cm^{-2}.h^{-1}) and median flux (0.015 µmol.cm^{-2}.h^{-1}). In PBS, the average flux of **(1)** is about 4.5 times lower than **(2)** (4.481 µmol.cm^{-2}.h^{-1}), but the median flux value of **(2)** (4.289 µmol.cm^{-2}.h^{-1}) is about 10 times higher than **(1)**. Hence, in Pheroid™ **(2)** had a lower average (0.013 µmol.cm^{-2}.h^{-1}) and median flux (0.011 µmol.cm^{-2}.h^{-1}) than **(1)**. The average flux in PBS of **(2)**, **(3)** and **(5)** was moderately higher than the median flux; all the other average and median flux values obtained for each compound in PBS and Pheroid™ were predominantly similar. The compounds that shown the greatest difference between average and median flux were **(1)** and **(2)** in PBS, they also had the highest standard deviation of all the compounds, as well as positively skewed flux distributions in the box-plots; **(1)** in PBS even contained an outlier. Hence, the median flux is a more accurate method to determine flux, because it is not influenced by skewed distributions that may result in possible over or under estimation of expected flux values. As a result, median instead of average flux values will be used further in this study.

In Pheroid™, **(1)** had the highest median flux value, but in PBS, **(2)** had the highest median flux value of all the compounds. The median transdermal flux of **(1)** and **(2)** was higher than the amide esters in both PBS and Pheroid™. Of all the amide esters **(3)** had the highest median flux value in PBS (0.046 µmol.cm^{-2}.h^{-1}) and **(4)** had the highest median flux value in Pheroid™

(9.3×10^{-3} µmol.cm^{-2}.h^{-1}). In both PBS and Pheroid™ **(6)** had the lowest median flux value (2.0×10^{-4} µmol.cm^{-2}.h^{-1}), since the aqueous solubility value (1.00×10^{-4} mg/ml) is lower than 1 mg/ml and the log D value (4.55) was higher than 2 (Guy & Hadgraft, 1989a).

In PBS, the flux values decreased for the amide esters of **(2)** as the alkyl chain length increased. Hence, as the alkyl chain length increased, the aqueous solubility values decreased, the log D increased and the compounds became more lipophilic and had trouble leaving the stratum corneum to permeate into the aqueous receptor, resulting in lower median flux values.

In Pheroid™ **(2)** and **(4)** have almost the same median flux value, **(1)** has a median flux value approximately 1.5 times higher than **(4)**. The log D value of **(4)** is between 1 and 2 (Hadgraft, 1996; Roberts and Sloan, 2000) and its aqueous solubility value is higher than 1 mg/ml, which of all the amide esters synthesised makes it the best candidate for transdermal delivery, this phenomenon was observed with Pheroid™ but not with PBS. This might be because it was entrapped better in Pheroid™, with the right particle size needed for permeation across the skin, than any of the other amide esters, which resulted in a higher concentration to permeate into the buffer.

When comparing flux values in Pheroid™ and in PBS it is observed that all the compounds had lower flux values in Pheroid™ except **(6)**, which had the same value. Hence, Pheroid™ did not improve transdermal flux.

Transdermal diffusion studies were done with **(7)** and **(8)**, but it did not dissolve in PBS and even if the Franz cells leaked (due to damaged skin) no peaks were seen on the chromatograms. In Pheroid™, **(7)** and **(8)** gave no peaks on the chromatograms during diffusion studies, except if the receptor phase was milky (leaking cells) and injected on the HPLC, small peaks in the first 2 – 6 h were observed with a maximum concentration of 0.005 µmol.cm^{-2} for **(7)** and 0.01 µmol.cm^{-2} for **(8)**, after 8 h no peaks were noticed on the HPLC. Therefore **(7)** and **(8)** were dissolved or entrapped in the Pheroid™ and due to these two compounds being so lipophilic and the fact that Pheroid™ are lipophilic they might have had trouble leaving the epidermis and did not want to permeate into the aqueous buffer phase. According to Guy & Hadgraft (1989a) there are potential problems in achieving steady plasma concentrations if compounds have log P values higher than 2.

The aqueous solubility values of **(1)** and **(2)** are much higher than the amide esters and even had negative log D values and therefore are more hydrophilic than the amide esters. Of all the amide esters **(4)** had the highest aqueous solubility value. Hence, these three compounds gave the best median flux values in Pheroid™. Consequently, when using Pheroid™, it seems that the more hydrophilic a compound, the higher the flux value. According to mosaic theory,

proteins in the skin may absorb water and the resulting swollen membranes may become permeable to hydrophilic substances (Rothman, 1954). **(1)** and **(2)** most probably penetrated through the protein rich spaces between the corneosytes of the stratum corneum (Foldvari, 2000; Schalla & Schaefer, 1982), resulting in higher flux values. This could be possible, because the stratum corneum is hydrated in an aqueous buffer for 24 hours making it easier for hydrophilic compounds to penetrate (Morganti *et al.*, 2001). Of all the compounds **(1)** and **(2)** had the smallest molecular weight and may penetrate through the aqueous pathway more easily than larger molecules (Takahashi, 1993; Zatz, 1993).

In this study, it seems that a high aqueous solubility has a greater influence on increasing transdermal permeation than any of the other physicochemical properties; this phenomenon was also found in studies done by Fourie (2002), Gerber *et al.* (2006) and Goosen *et al.* (2002).

5.3.3 Experimental transdermal permeation vs. previous studies

Holmes (2006) prepared six esters of stavudine, i.e., stavudine-5'-acetate, stavudine-5'-propionate, stavudine-5'-buterate, stavudine-5'-hexanoate, stavudine-5'-octanoate and stavudine-5'-decanoate. A summary of aqueous solubility in PBS at pH 7, log D at pH 7 and median flux in both PBS and Pheroid™ are given in Table 5.4 (Holmes, 2006).

Stavudine, resembling **(2)**, had a high aqueous solubility value and negative log D value, and gave the highest flux value of all the compounds in PBS. In PBS, as the alkyl chain length for the stavudine derivatives increased, the aqueous solubility decreased, the log D values increased and the median flux values decreased, the same phenomenon was observed for **(2)** and the amide esters of **(2)** in PBS. Stavudine-5'-buterate and stavudine-5'-propionate, had aqueous solubility values higher than 1 mg/ml, but their log D values were lower than 1 and not between 1 and 2, but still they gave the highest median flux values in Pheroid™. In Pheroid™, the more lipophilic esters of stavudine, i.e., stavudine-5'-hexanoate, stavudine-5'-octanoate and stavudine-5'-decanoate with log D values higher than 1, gave low median flux values. Hence, similar to **(1)**, **(2)** and **(4)**, the more hydrophilic stavudine compounds with higher aqueous solubility values, permeated better with Pheroid™ than the more lipophilic compounds.

In the study done by Holmes (2006), all the compounds, except stavudine and stavudine-5'-acetate (both had negative log D values), had higher median flux values in Pheroid™ than in PBS, this was not seen in **(2)** and the amide esters of **(2)**. Hence, the stavudine esters are single alkyl chain derivatives with predominantly lower log D values than the double alkyl chain amide esters of **(2)** with higher log D values, especially **(5)** and **(6)**, as well as **(7)** and **(8)** that are insoluble in an aqueous medium. Consequently, the less lipophilic compounds, in this study

and the study performed by Homes (2006), permeate better in Pheroid™ than the more lipophilic ones which have trouble leaving the stratum corneum.

Table 5.4: Aqueous solubility, log D and median flux values in PBS and Pheroid™ of stavudine and its esters (Holmes, 2006).

Compound	Aqueous solubility (mg/ml)	Log D	Median Flux in PBS ($\mu mol.cm^{-2}.h^{-1}$)	Median Flux in Pheroid™ ($\mu mol.cm^{-2}.h^{-1}$)
Stavudine	104.75	-0.85	14.6×10^{-3}	13.7×10^{-3}
Stavudine-5'-acetate	5.17	-0.41	0.6×10^{-3}	0.2×10^{-3}
Stavudine-5'-propionate	1.73	0.27	0.6×10^{-3}	18.6×10^{-3}
Stavudine-5'-buterate	1.05	0.89	0.5×10^{-3}	20.2×10^{-3}
Stavudine-5'-hexanoate	0.11	1.86	0.2×10^{-3}	0.5×10^{-3}
Stavudine-5'-octanoate	0.08	2.66	Insoluble	0.3×10^{-3}
Stavudine-5'-decanoate	Insoluble	3.06	Insoluble	Insoluble

A series of investigations have been done on the transdermal delivery of **(1)** and the following flux values were obtained: with the use of water on hairless rat skin, 3.19 $\mu g.cm^{-2}.h^{-1}$ (Kim & Chien, 1996a) and with the use of EtOH and oleic acid on hairless rat skin, 1.88 $mg.cm^{-2}.h^{-1}$ and through human cadaver skin, 0.61 $mg.cm^{-2}.h^{-1}$ (Kim & Chien, 1996b). In this study the average and median flux obtained was 198.34 $\mu g.cm^{-2}.h^{-1}$ and 93.36 $\mu g.cm^{-2}.h^{-1}$, respectively at pH 5. Kim & Chien (1996a) had an extremely low flux value for **(1)**, due to using water as medium which has a pH of approximately 7, in this study we used PBS at pH 5, thus **(1)** was more unionised and gave higher flux values. Kim & Chien (1996b) used penetration enhancers, i.e., EtOH and oleic acid that increased the flux of **(1)**, which in this study was not the case and may be the cause for poorer flux values obtained.

Kim & Chien (1995a) stated that the therapeutic blood level for **(1)** is 0.14 $mg.cm^{-2}.h^{-1}$. Hence, with the use of PBS, the median flux (0.09 $mg.cm^{-2}.h^{-1}$) will not give therapeutic blood levels (the average flux (0.20 $mg.cm^{-2}.h^{-1}$) as were used by Kim & Chien (1995a) will give therapeutic blood levels).

5.3.4 Transdermal permeation: Experimental vs. predicted flux

Table 5.5: Predicted flux values using the Potts and Guy equation.

Compound	Flux ($\mu mol.cm^{-2}.h^{-1}$)	
	Predicted [a]	**Predicted** [b]
(1)	1.0×10^{-3}	1.0×10^{-3}
(2)	1.6×10^{-3}	2.2×10^{-3}
(3)	1.2×10^{-4}	2.7×10^{-6}
(4)	2.2×10^{-3}	2.1×10^{-5}
(5)	1.9×10^{-4}	2.7×10^{-6}
(6)	8.6×10^{-7}	1.4×10^{-8}
(7)	Insoluble	Insoluble
(8)	Insoluble	Insoluble

[a] calculated using experimental log D and aqueous solubility values (pH 5) in the Potts and Guy equation (Equation 5.1 & 5.2)

[b] calculated using ACD predicted log P and experimental aqueous solubility (pH 5) values in the Potts and Guy equation (Equation 5.1 & 5.2)

Experimental values obtained for aqueous solubility (pH 5), log D (pH 5) and the molecular weight (MW) can also be used to estimate the flux values (J_{max}) for **(1)**, **(2)** and the amide esters of **(2)**. The Potts and Guy equation (Equation 5.1) can be used to calculate the log K_p, from where the permeability coefficient (K_p) may be obtained (Hadgraft *et al.*, 2000). The estimated flux ($\mu mol.cm^{-2}.h^{-1}$) can be obtained from the product of the permeability coefficient and the aqueous solubility at the same pH (Equation 5.2).

$$\log K_p = -2.7 + 0.71 \log P - 0.0061 MW \qquad \text{Equation 5.1}$$

$$J_{max} = K_p \times \text{aqueous solubility} \qquad \text{Equation 5.2}$$

The predicted flux values, using experimentally determined and predicted partition coefficient values (obtained from the ACD Labs prediction software), are presented in Table 5.5.

5.3.5 Discussion

While discussing transdermal permeation, the experimental-predicted data specify the flux values obtained by using experimental aqueous solubility and log D values (pH 5) in the Potts

and Guy equation and predicted-predicted indicates the flux values acquired from the Potts and Guy equation by using experimental aqueous solubility (pH 5) and ACD predicted log P values.

The experimental-predicted and predicted-predicted flux values correlate better with each other and had lower flux values than the experimentally determined median flux. **(4)** has the highest experimental-predicted flux value, which is the same as for the predicted-predicted flux of **(2)**. The predicted-predicted flux value of **(3)** and **(5)** is the same and the model could not distinguish between twelve and sixteen carbon atoms. The predicted data use the experimentally determined aqueous solubility and as **(7)** and **(8)** was insoluble it could not be calculated. The predicted flux values didn't correlate well with the experimental flux values obtained in this study, which proves that the only dependable way of determining data is by experimental means.

5.4 Flux vs. physicochemical properties

Table 5.6: Spearman correlations between median flux and the physicochemical properties of compounds **(1)** to **(6)** in PBS and Pheroid™.

Item	Physicochemical properties	Correlations			
		PBS		Pheroid™	
		Spearman	p	Spearman	p
1	**Molecular weight (g/mol)**	-0.9429	0.0048	-0.9429	0.0048
2	**Aqueous solubility pH 5 (mg/ml)**	0.9429	0.0048	0.9429	0.0048
3	**Aqueous solubility pH 7 (mg/ml)**	0.9429	0.0048	0.9429	0.0048
4	**Log D pH 5**	-0.9429	0.0048	-0.9429	0.0048
5	**Log D pH 7**	-0.9429	0.0048	-0.9429	0.0048
6	**Melting Point (°C)**	0.4286	0.3965	0.6571	0.1562
7	**Integrity Before (kΩ)**	0.2000	0.7040	-0.4286	0.3965
8	**Integrity After (kΩ)**	0.0857	0.8717	-0.2571	0.6228

Note: Although it seems highly improbable to obtain the very similar values for the Spearman correlation of such diverse properties as items 1 – 5 in Table 5.6 it was indeed found and

confirmed in this study. This may be attributed to the data following the same pattern and the ranking process of the Spearman procedure.

When studying the correlation between median flux and the physicochemical properties the Spearman rank correlation was used, since this is a more robust estimate of correlation. The Pearson correlation coefficient was not used due to large variations (big spread) in some of the variables. The Spearman correlation is inversely related (strongly negative) if it is close to -1 and has a direct relationship (strongly positive) if it is close to 1. Throughout we worked with a 5 % level of significance to test the hypothesis of zero correlation. Thus, if the p value was less than 0.05 the Spearman correlation can be seen as statistically significant, hence either a significant positive or negative value was found. The correlations between flux and the physicochemical properties for both PBS and Pheroid™, together with the p-values are reported in Table 5.6.

5.4.1 Median flux vs. molecular weight

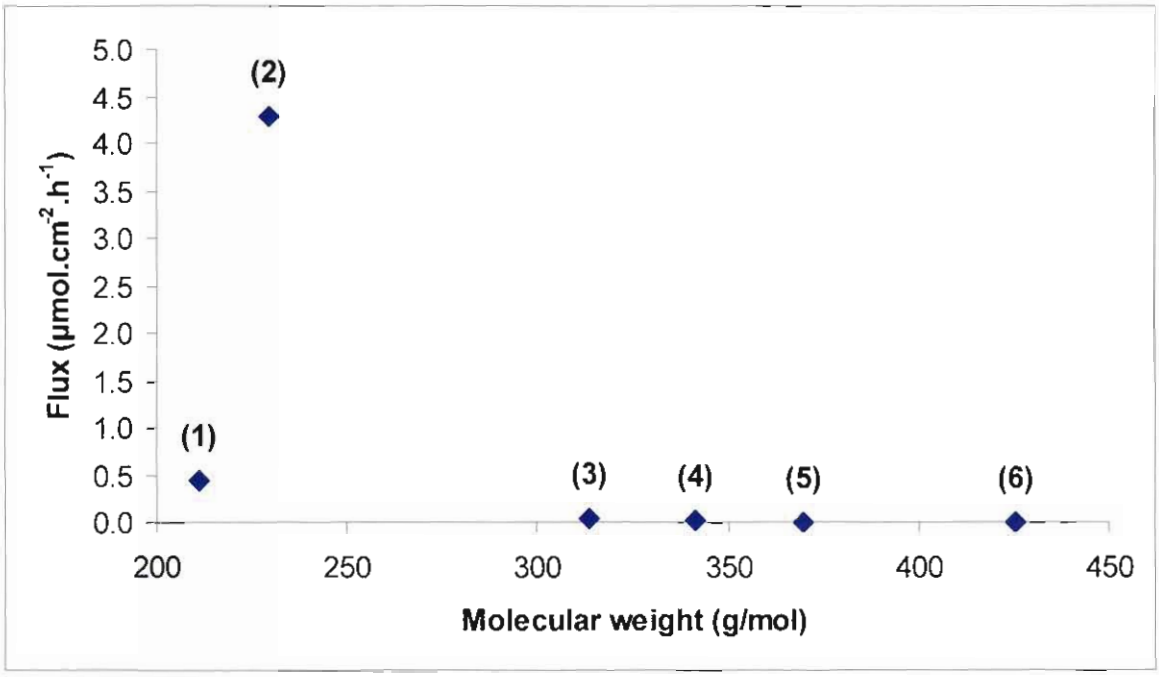

Figure 5.8: The relationship between median flux in PBS and molecular weight of compounds **(1)** to **(6)**.

The p value was smaller than 0.05, consequently the Spearman correlation between median flux and molecular weight is statistically significant. Hence, according to the Spearman correlation there is a strong inverse relationship (value close to -1) between molecular weight and median flux for both PBS and Pheroid™. Thus, smaller molecules in comparison to the larger molecules did penetrate effortlessly (Takahashi, 1993; Zatz, 1993) (§ 3.5.2.7) and as the

molecular size increased the median flux decreased in both PBS and Pheroid™ as seen in Figure 5.8 and Figure 5.9.

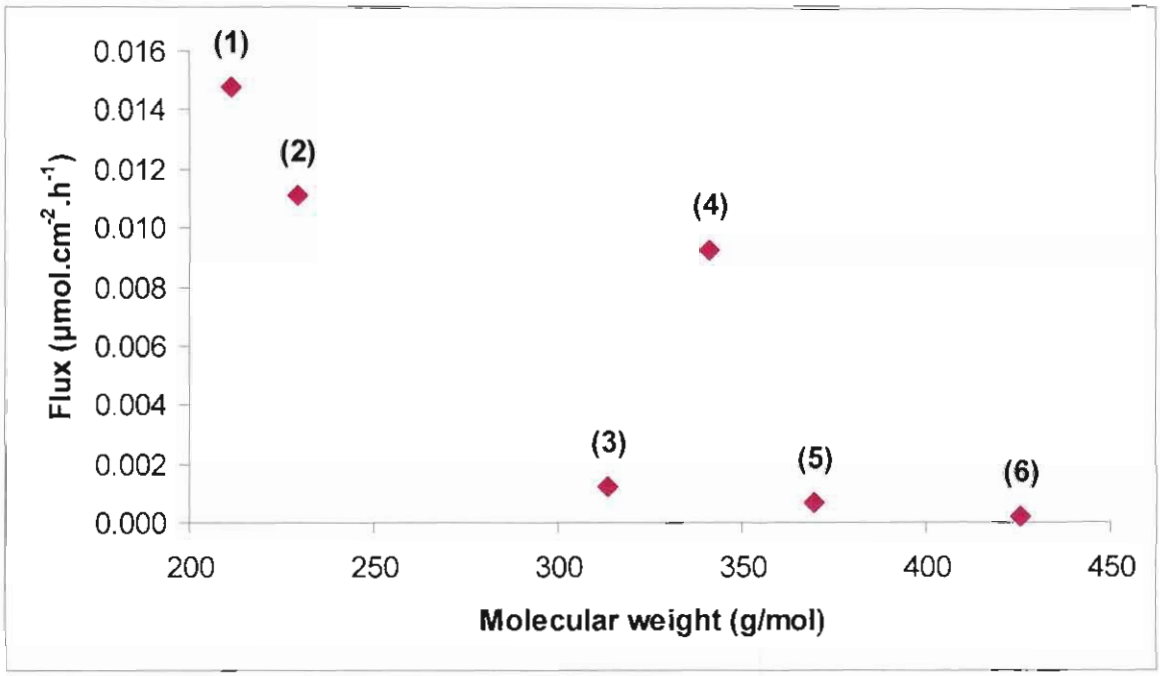

Figure 5.9: The relationship between median flux in Pheroid™ and molecular weight of compounds **(1)** to **(6)**.

5.4.2 Median flux vs. aqueous solubility

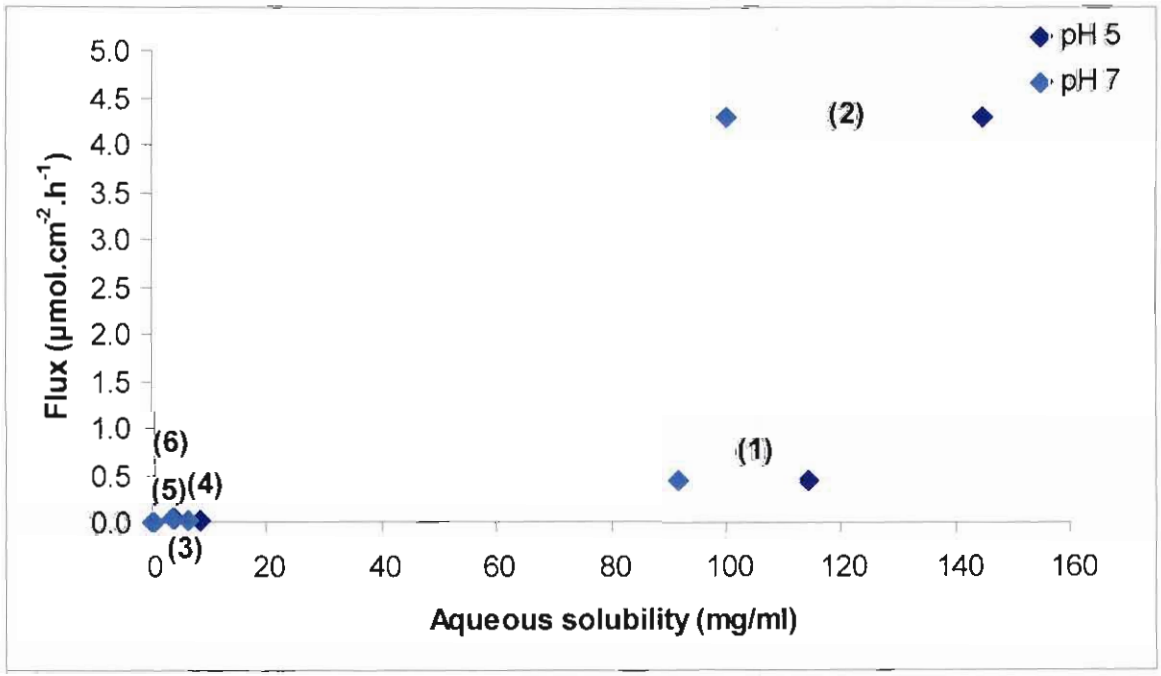

Figure 5.10: The relationship between median flux in PBS and aqueous solubility at pH 5 and 7 of compounds **(1)** to **(6)**.

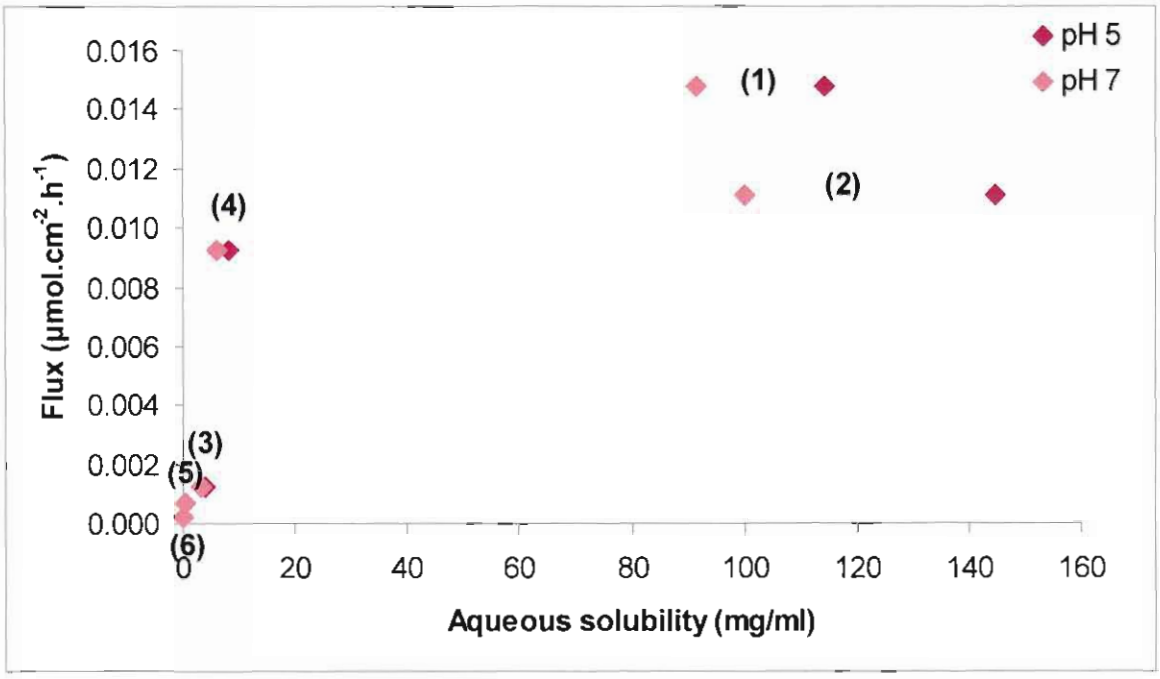

Figure 5.11: The relationship between median flux in Pheroid™ and aqueous solubility at pH 5 and 7 of compounds **(1)** to **(6)**.

The p value was smaller than 0.05, consequently the Spearman correlation between aqueous solubility and median flux is statistically significant. The Spearman correlation has a strong positive value close to one, consequently indicating a strong direct relationship between aqueous solubility and median flux in PBS and Pheroid™ at both pH 5 and 7. Thus, the hydrophilic compounds permeated more easily than the lipophilic compounds (Fourie, 2002; Gerber *et al.*, 2006; Goosen *et al.*, 2002) and as the aqueous solubility at pH 5 and 7 increased the median flux increased in both PBS and Pheroid™ as seen in Figure 5.10 and Figure 5.11.

5.4.3 Median flux vs. partition coefficient

The Spearman correlation has a strong significant negative value close to one, consequently indicating a strong inverse relationship between median flux and log D values in PBS and Pheroid™ at both pH 5 and 7. Thus, once again the hydrophilic compounds in comparison with the more lipophilic compounds had improved permeability (Fourie, 2002; Gerber *et al.*, 2006; Goosen *et al.*, 2002). A lipophilic drug may have difficulty leaving the stratum corneum and this might explain the low median flux values for the amide esters, although in Pheroid™ **(4)** had a higher median flux value than the other amide esters which is possibly because of having an aqueous solubility higher than 1 mg/ml and having a log D value between one and two (Hadgraft, 1996; Roberts & Sloan, 2000). As the log D values at pH 5 and 7 increased the median flux decreased in both PBS and Pheroid™ as seen in Figure 5.12 and Figure 5.13. The

p value was smaller than 0.05, consequently the Spearman correlation between median flux and log D values is statistically significant.

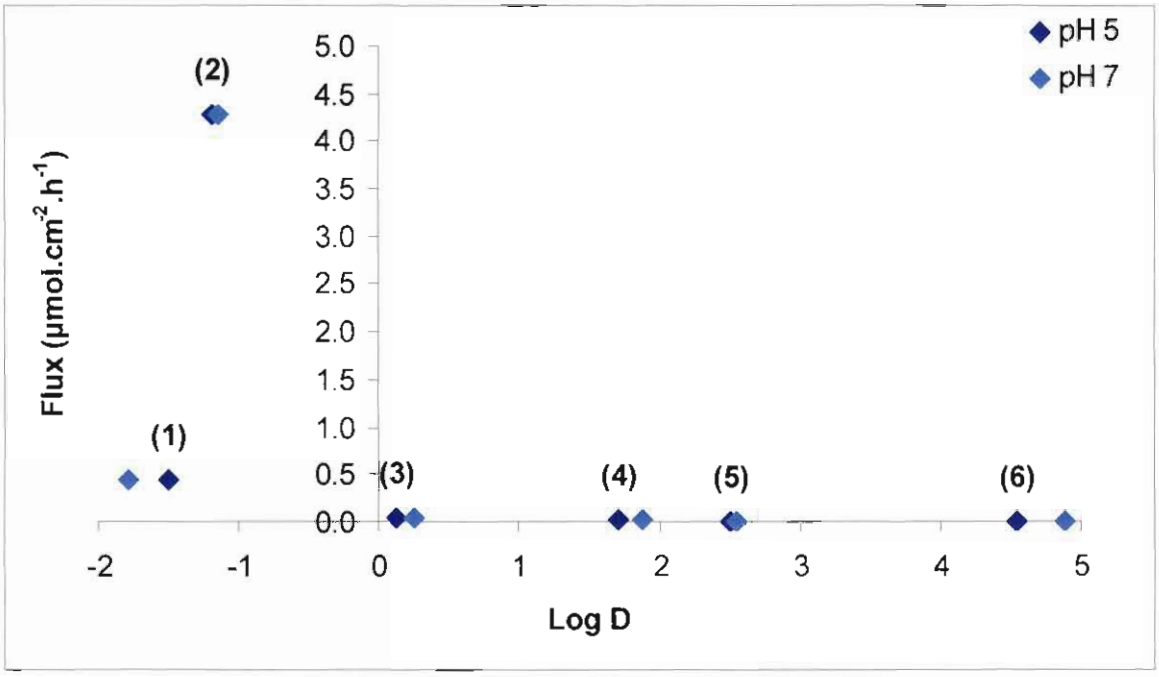

Figure 5.12: The relationship between median flux and log D in PBS at pH 5 and 7 of compounds **(1)** to **(6)**.

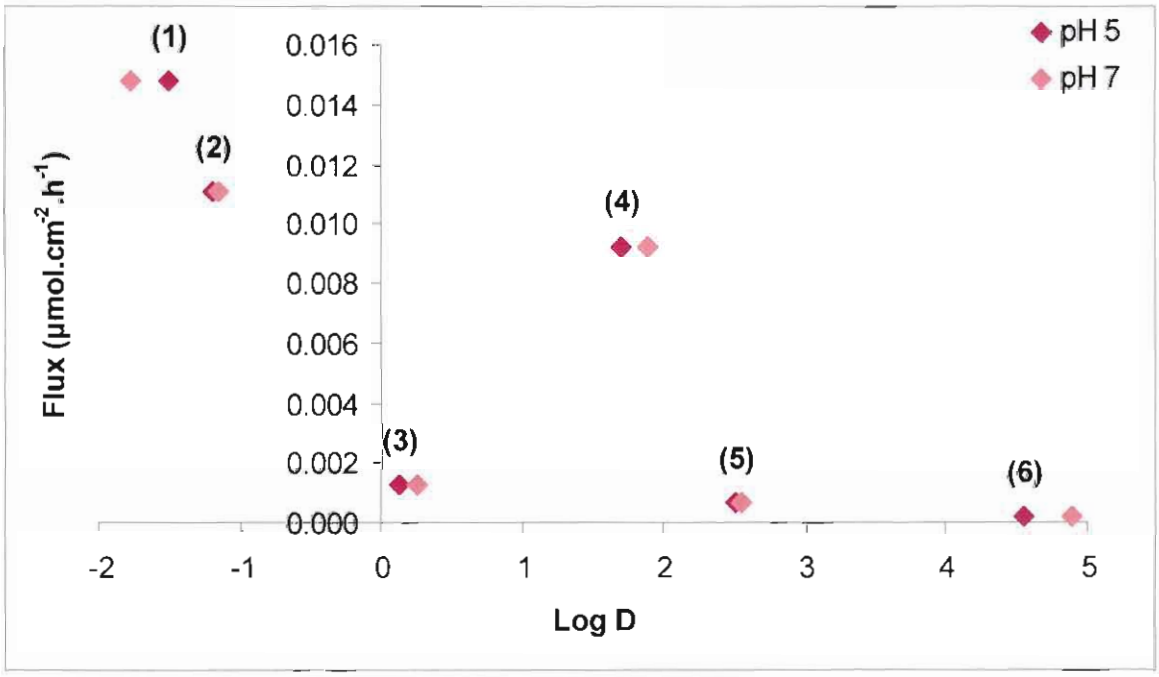

Figure 5.13: The relationship between median flux and log D in Pheroid™ at pH 5 and 7 of compounds **(1)** to **(6)**.

5.4.4 Median flux vs. melting point

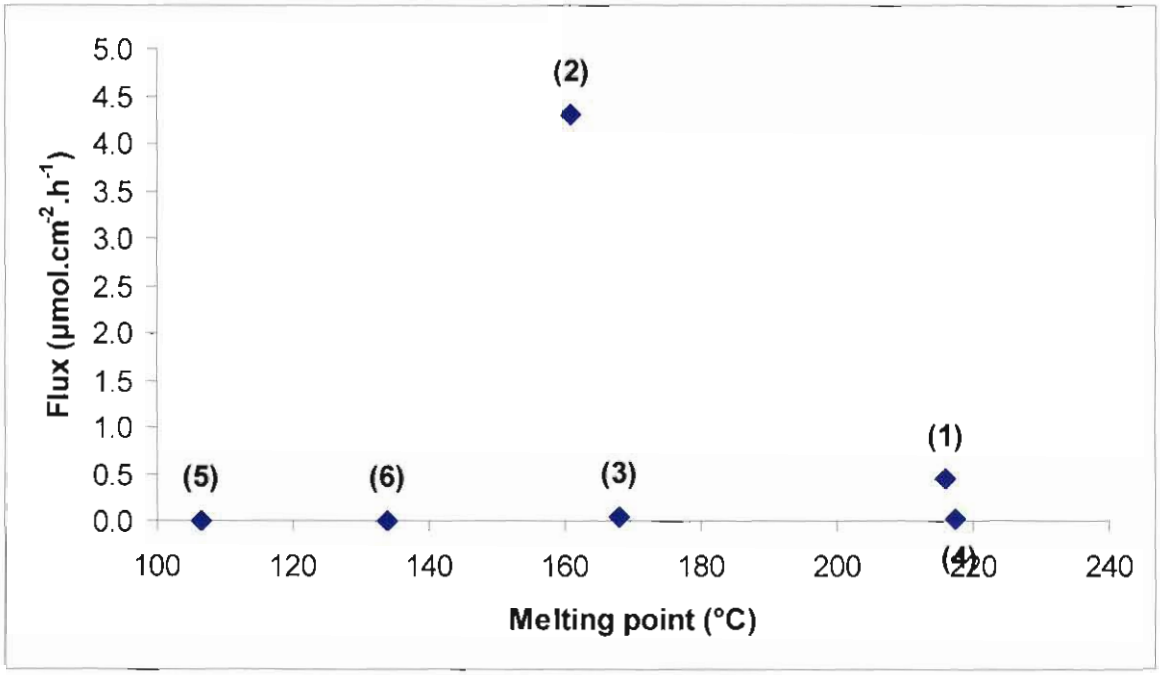

Figure 5.14: The relationship between median flux in PBS and melting point of compounds **(1)** to **(6)**.

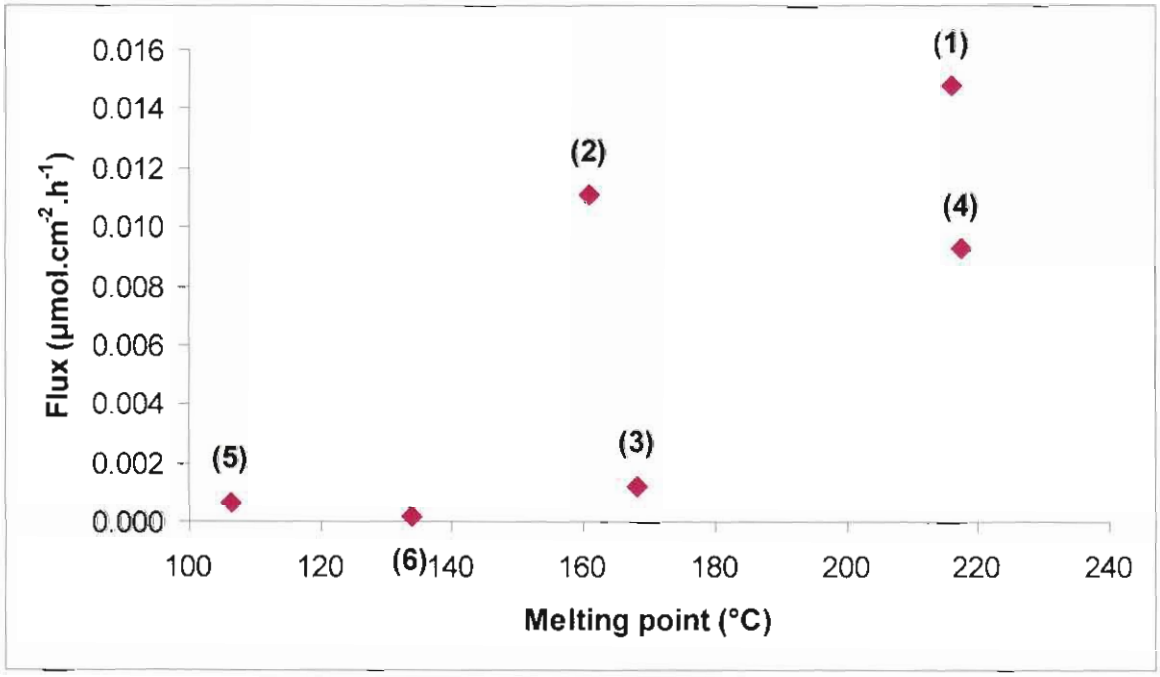

Figure 5.15: The relationship between median flux in Pheroid™ and melting point of compounds **(1)** to **(6)**.

The correlations between median flux and melting point were not statistically significant for both PBS and Pheroid™. However, the observed Spearman correlation for the Pheroid™ group

produced a stronger positive value than that of the PBS group. The median flux vs. melting point scatterplots for the PBS and Pheroid™ groups are presented in Figure 5.14 and Figure 5.15, respectively.

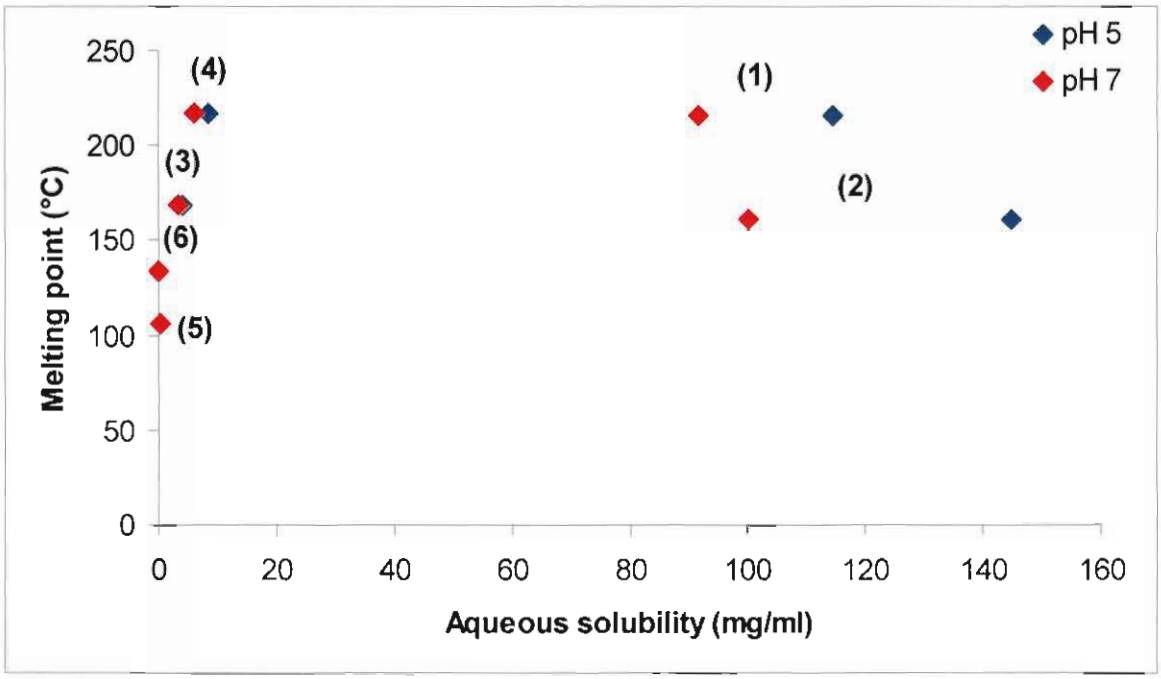

Figure 5.16: The relationship between melting point and aqueous solubility at pH 5 and 7 of compounds **(1)** to **(6)**.

According to Cleary (1993) and Stott *et al.* (1998) a drug will have a direct effect on solubility if the melting point is reduced causing increased transdermal permeation (§ 3.5.2.5). In Figure 5.16 melting point was plotted against aqueous solubility at pH 5 and 7 to see if there was any relationship as stated in the literature. If **(2)** and **(1)** is not taken into account, a direct relationship is found between melting point and aqueous solubility in pH 5 and 7, which confirms the literature.

5.4.5 Median flux vs. integrity

Neither the Pheroid™, nor PBS had significant correlation between median flux and integrity (before and after). The p values for integrity (before and after) in both PBS and Pheroid™ were extremely higher than 0.05.

A previous study done by Davies *et al.* (2004) found that an inverse relationship exists between skin integrity and the permeability coefficients of tritiated water (pH 7). In this study, however, there was no correlation between skin integrity and permeability coefficients of PBS (pH 5) and Pheroid™ (Figure 5.17 and Figure 5.18). The medium used could therefore offer a possible (but implausible) explanation for the difference in correlation between skin integrity and median flux.

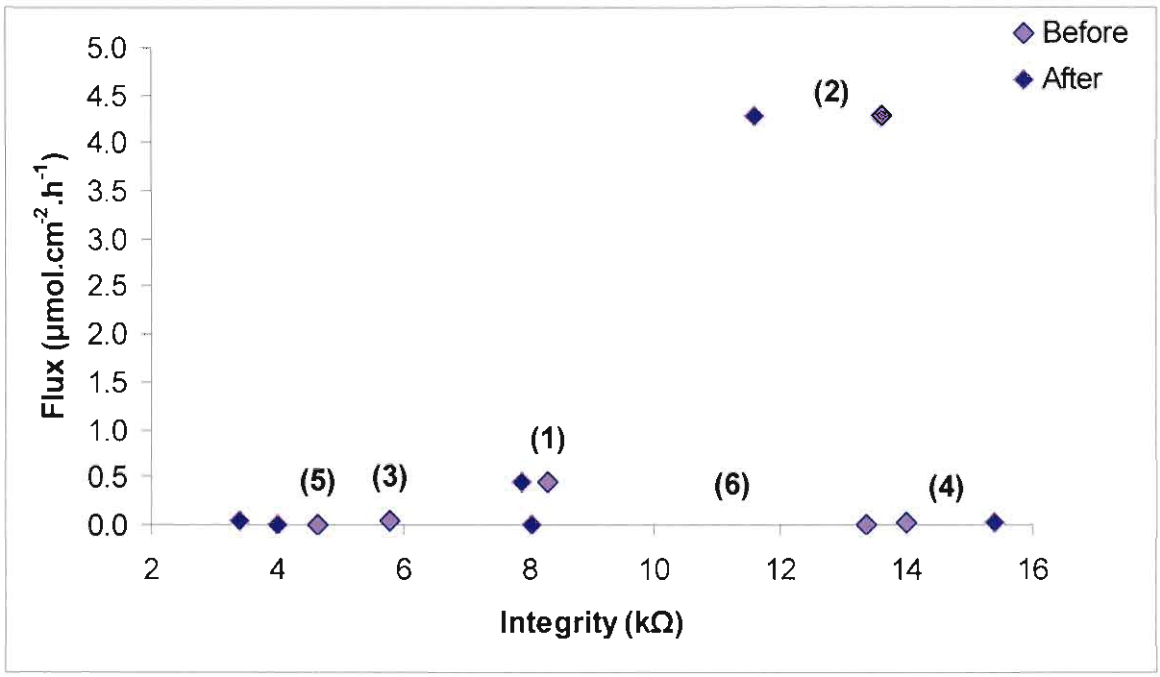

Figure 5.17: The relationship between median flux in PBS and the integrity (before and after) of compounds **(1)** to **(6)**.

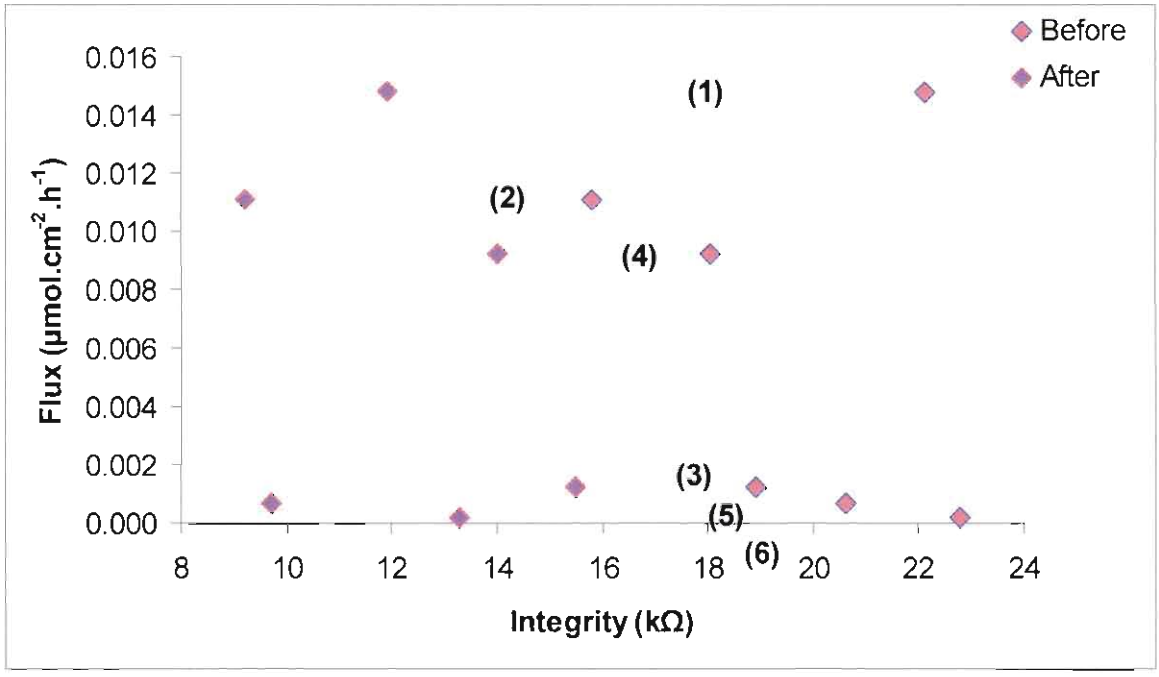

Figure 5.18: The relationship between median flux in Pheroid™ and the integrity (before and after) of compounds **(1)** to **(6)**.

5.5 Confocal laser scanning microscopy

5.5.1 Size and morphology of microsponge PheroidTM

CLSM micrographs were captured to see if compounds **(1)** to **(8)** were entrapped in the Pheroid™. A CLSM micrograph was captured of the microsponge Pheroid™ as control, therefore the difference in size and morphology could be examined between the microsponge Pheroid™ and the compounds. Liposomes were discussed to see if compounds **(1)** to **(8)** entrapped in microsponge Pheroid™ had the same morphology as used for liposomes (§ 3.7.1). CLSM micrographs and digitally zoomed CLSM micrographs are presented in Figure 5.20 and Figure 5.21 and the difference in microsponge size between the control and the compounds are shown in Figure 5.19.

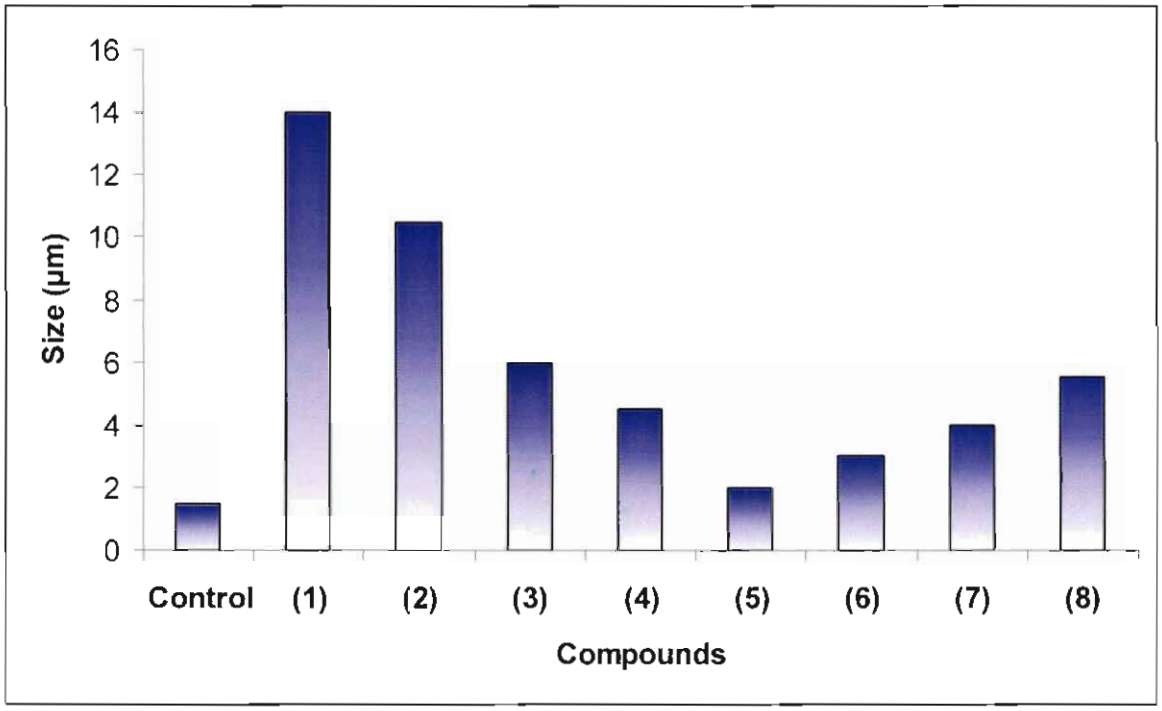

Figure 5.19: A representation of the difference in microsponge size between the control and compounds **(1)** to **(8)** in microsponge Pheroid™ formulation.

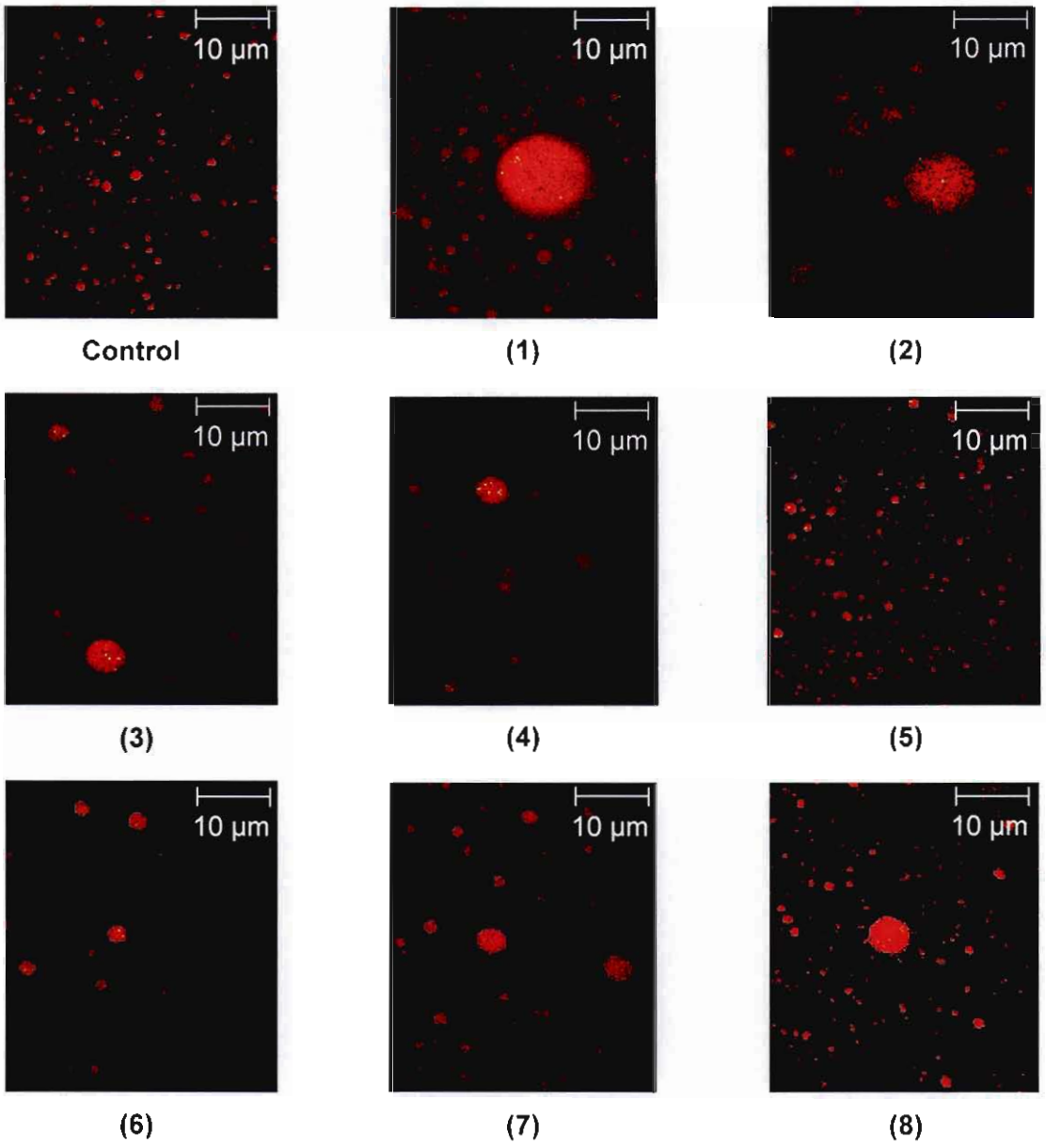

Figure 5.20: The CLSM micrographs of the microsponge Pheroid™ (control) and compounds **(1)** to **(8)** in entrapped in Pheroid™ microsponges.

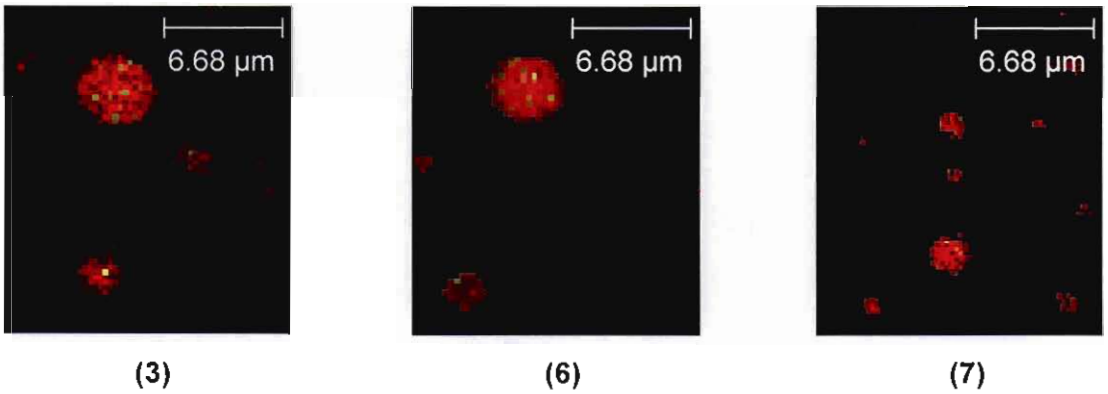

Figure 5.21: The digitally zoomed CLSM micrographs of **(3)**, **(6)** and **(7)** entrapped in the microsponges of the Pheroid™ formulation.

5.5.2 Discussion

All the CLSM micrographs had small (SUV) or large unilamellar vesicles (LUV), with a sponge-like appearance; none of them seem to be MLV or MVV. The microsponge Pheroid™ formulation and **(5)** had a large number of small vesicles on the micrograph, but the microsponge size of **(5)** was larger than that of the control. All of the compounds in comparison to the control had an increase in microsponge size and caused a decrease in the quantity of Pheroid™ in the preparation, which is an indication that entrapment occurred. The microsponge size of **(1)** in Pheroid™ was the largest; the microsponge size decreased from **(2)** to **(5)** and thereafter had an increase from **(5)** to **(8)**. The microsponge size of **(3)** and **(8)**, as well as **(4)** and **(7)** was almost the same. All the compounds were entrapped in Pheroid™, as can be deduced from the yellow spots seen on the micrographs. The entrapped **(7)** in Pheroid™ isn't clear, but is observed in the digitally zoomed CLSM micrographs. The best flux values were seen with **(1)** and **(2)** and they had the largest microsponge sizes of all the compounds, as they are hydrophilic compounds they might have permeated easier into the aqueous buffer. The aqueous solubility and flux of **(4)** was the highest of all the amide esters, although it had a medium microsponge size, in comparison to the other compounds. Hence, it seems that hydrophilic drugs permeate easier when entrapped in Pheroid™ than lipophilic compounds.

CHAPTER 6

SUMMARY AND FINAL CONCLUSIONS

The skin, although an ideal site for drug administration, is also a major barrier to this process. Effective drug therapies must therefore overcome the challenge of finding a technology to administer, measure and deliver the required quantity of drug into or through the skin.

As at the end of 2005, approximately 40.3 million people were living with HIV/AIDS which is generally treated with compounds like zalcitabine **(1)** and lamivudine **(2)**. The most common adverse effects occurring with **(1)** and **(2)** are abdominal pain, insomnia, nausea, vomiting, diarrhoea and fatigue, as well as peripheral neuropathy, cardiomyopathy, pancreatitis and mouth ulcers with **(1)**.

The adverse effects encouraged this study into the development of a transdermal delivery system for **(1)** and **(2)** with the aim of avoiding the poor palatability (of the liquid **(2)** formulation) (Schiffman *et al.*, 1999) and hepatic first pass metabolism, improving patient compliance and bioavailability as well as decreasing the administered dose. Much attention has been given to the use of delivery systems, i.e., Pheroid™, to improve transdermal permeation. The development of compounds with enhanced physicochemical properties for greater transdermal delivery has been of interest.

Research has found that a drug should have optimal permeation if it has reasonable solubility in both water and oils and has an aqueous solubility of more than 1 mg/ml and a log P in the range of 1 – 2 (Hadgraft, 1996; Roberts & Sloan, 2000). According to Guy & Hadgraft (1989a) there are potential problems in achieving steady plasma concentrations if compounds have log P values higher than 2. A preferentially oil soluble drug may have difficulty leaving the stratum corneum and in contrast, an extremely polar drug will have trouble partitioning into the stratum corneum from its vehicle. Membranes are more permeable by the unionised forms, because of their greater lipid solubility (Abdou, 1989; Smith, 1990). In work done in our laboratories it was indicated that the compounds with the highest aqueous solubility presented with the greatest transdermal fluxes (Fourie, 2002; Gerber *et al.*, 2006; Goosen *et al.*, 2002).

During this study, the aim was to determine the transdermal permeation of **(1)**, **(2)** and the synthesised amide esters of **(2)**, with and without the use of Pheroid™ as delivery system and to establish a correlation, if any, with selected physicochemical properties.

The following objectives were set:

- Synthesise amide esters of **(2)** and verify their structures by use of NMR, IR and MS.
- Experimentally determine the aqueous solubility and the partition coefficients of **(1)**, **(2)** and the synthesised amide esters of **(2)** at both pH 5 and 7 and compare it with values calculated from commonly used prediction software.
- Experimentally determine the transdermal flux of **(1)**, **(2)** and the amide esters of **(2)** in both PBS (pH 5) and Pheroid^{TM} and compare it with values calculated from commonly used theoretical equations.
- Determine if transdermal application of these compounds will reach therapeutic drug concentrations with respect to transdermal flux.
- Determine whether a correlation existed between selected physicochemical properties and transdermal flux data of **(1)**, **(2)** and the derivatives of **(2)**.
- Determine whether **(1)**, **(2)** and the synthesised amide esters of **(2)** have been entrapped in Pheroid^{TM} by use of CLSM.

The amide esters of **(2)** were successfully synthesised and the structures were verified by ^{1}H and ^{13}C NMR, MS and IR spectroscopy.

The aqueous solubility of all the compounds was lower at pH 7 (44.84 % unionised) than at pH 5 (98.78 % unionised). Hence, pH 5 was selected for diffusion studies since unionised compounds are more lipophilic and penetrate the stratum corneum with less difficulty than the ionised species (§ 3.5.2.4). The aqueous solubility on a mass basis (mg/ml) of **(1)** at both pH 5 and 7 (144.78 mg/ml and 110.16 mg/ml, respectively) was higher than that of **(2)** (114.36 mg/ml and 91.57 mg/ml, respectively). However, aqueous solubility on a molar basis of **(2)** at both pH 5 and 7 (631.53 mM and 436.90 mM, respectively) was higher than that of **(1)** (541.42 mM and 433.53 mM, respectively). The aqueous solubility of **(2)** at pH 5 and 7 was noticeably higher than that of compounds **(3)** to **(6)** (ranging from 1.00×10^{-4} to 8.34 mg/ml or 2.00×10^{-4} to 24.43 mM and 1.00×10^{-4} to 6.16 mg/ml or 2.00×10^{-4} to 18.04 mM, respectively). This was in accordance with data in the literature (§ 3.5.2.8), which proved that the solubility in general decreases with an increase in chain length. The highest aqueous solubility observed for all the amide esters was that of **(4)**. The experimental aqueous solubility values were also compared to values obtained from IA prediction software, but it did not correlate with each other, which might be attributed to the method of calculation, the fact that the software does not specify the buffers used or the pH at which they were calculated.

The octanol-PBS partition coefficient (log D) of compounds **(2)** to **(6)** was lower at pH 5 than at pH 7. Of all the compounds **(1)** had the lowest log D at both pH 5 and 7 (-1.50 and -1.78, respectively). The log D of **(2)** at both pH 5 and 7 (-1.19 and -1.15, respectively) was lower than that of compounds **(3)** to **(6)** (ranging from 0.12 to 4.55 and 0.25 to 4.88, respectively) and correlated with the aqueous solubility and the literature (§ 3.5.2.8). The log D of **(4)** is between 1 and 2, therefore it is the best candidate for transdermal permeation. The experimentally determined log D of **(1)** at pH 5 and the predicted log P calculated by ACD of **(1)** had the same values, while the experimentally determined log D of **(1)** at pH 7 and the predicted log P calculated by K_{ow}Win of **(1)** had almost the same values. ACD's log P and the experimental log D for **(2)** at both pH 5 and 7 were almost the same. The prediction sofware and experimentally determined data seem to correlate better with patent drugs. The amide esters of **(2)** did not correlate with any of the prediction software. Hence, the predicted software does not specify any of the physicochemical properties that may influence log P.

A comparison between average and median flux values of the amide esters of **(2)** show that there is a good correlation between the flux values in PBS and Pheroid™, (except for **(5)** in PBS). Compounds with higher flux values, like **(1)** and **(2)**, seem to be prone to larger differences between average and median flux. In the occurrence of large variation and skewed distributions of experimental values, the median flux is a more robust measurement. Therefore median flux is a more accurate method for determining flux.

Comparing the median flux values of **(1)** with that of **(2)** it is observed that the median flux of **(2)** (4.289 $\mu mol.cm^{-2}.h^{-1}$) in PBS is 10 times higher than that of **(1)** (0.442 $\mu mol.cm^{-2}.h^{-1}$), but in Pheroid™, the median flux (0.011 $\mu mol.cm^{-2}.h^{-1}$) of **(2)** is slightly lower than that of **(1)** (0.015 $\mu mol.cm^{-2}.h^{-1}$). In both PBS and Pheroid™, the median flux of **(2)** was higher than that of the amide esters (ranging from 2.0×10^{-4} to 0.046 $\mu mol.cm^{-2}.h^{-1}$ in PBS and 2.0×10^{-4} to 9.3×10^{-3} $\mu mol.cm^{-2}.h^{-1}$ in Pheroid™). Of all the amide esters of **(2)**, **(3)** in PBS and **(4)** in Pheroid™ presented the highest flux. In PBS, the flux values of the amide esters decreased as the alkyl chain length increased. Hence, it seems that as the compound became more lipophilic and its aqueous solubility decreased, it had trouble leaving the stratum corneum and permeating into the aqueous receptor phase. In Pheroid™, the same phenomenon as in PBS occurred with the amide esters of **(2)**, except for **(4)** that had an increase in flux (with almost the same flux value as **(2)**), this was expected, since **(4)** was the perfect candidate for transdermal permeation with an aqueous solubility value (8.34 mg/ml) higher than 1 mg/ml and a log D (1.70) between 1 and 2.

When comparing flux in Pheroid™ with that in PBS it is observed that all the compounds have lower flux values in Pheroid™ except **(6)** (which had the same value in both PBS and Pheroid™). Hence, Pheroid™ does not improve transdermal flux of this series of compounds.

It is interesting to note that the three compounds, i.e., **(1)**, **(2)** and **(4)** which had the highest median flux values in Pheroid™, also had the highest aqueous solubility values. Hence, it seems that when using Pheroid™ as delivery system to increase transdermal permeation, a more hydrophilic drug should be used.

In this study, it seems that there is a direct correlation between aqueous solubility and transdermal permeation; this phenomenon was also found by other studies done in our laboratories.

Holmes (2006) synthesised six esters of stavudine and determined (at pH 7) the aqueous solubility, log D together with the transdermal permeation in both PBS and Pheroid™ of stavudine and its six esters. The following similarities between stavudine, lamivudine **(2)** and their derivatives were found: the parent drugs have high aqueous solubility values and negative log D values, as well as the highest flux values of all the compounds; in PBS, as the alkyl chain length for the derivatives increased, the aqueous solubility decreased, the log D values increased and the median flux values decreased; in Pheroid™, the more lipophilic derivatives with higher log D values had low median flux values; and the more hydrophilic compounds with higher aqueous solubility values, permeated better in Pheroid™ than the more lipophilic compounds. Compared to PBS, Pheroid™ enhanced median flux values of the stavudine esters (mono alkyl chain) whilst reducing it for amide esters (di alkyl chain) of **(2)**; hence, the stavudine esters are less lipophilic, whereas the amide esters are more lipophilic. Consequently, it appears that the more hydrophilic a compound in Pheroid™, the better the transdermal permeation.

Previous investigations on **(1)** done by Kim & Chien (1996b) found higher flux values than the flux values obtained in this study, due to the use of penetration enhancers such as EtOH and oleic acid. Kim & Chien (1996a) had an exceptionally lower flux value for **(1)** than their study in 1996b and this study, due to the use of water with a pH of almost 7 where **(1)** is more unionised.

The median flux (0.09 $mg.cm^{-2}.h^{-1}$) of **(1)** will not give therapeutic blood levels (0.14 $mg.cm^{-2}.h^{-1}$) (Kim & Chien, 1995a).

The predicted flux, attained from the two methods using the Potts & Guy equation (Hadgraft *et al.*, 2000), correlated well with each other, but didn't correlate well with the experimental flux values. The results clearly indicated that the degree of ionisation of intended transdermal candidates had to be considered when selecting the donor solution pH. Thus, the only reliable way of determining these data, i.e., aqueous solubility, log D and transdermal flux, is by experimental means.

The Spearman rank correlation was used to determine the correlation between the physicochemical properties and the median flux of the compounds. A strong statistically significant correlation was observed between flux in both PBS and in Pheroid™ and each of molecular weight, aqueous solubility (at pH 5 and 7), and log D (at pH 5 and 7). The integrity of the skin (before and after) did not correlate with median flux in either PBS or Pheroid™. No correlations were found between median flux and melting point in both Pheroid™ and PBS.

In the CLSM micrographs it is observed, through the yellow spots, that all the compounds were entrapped in Pheroid™. All the compounds presented with SUV or LUV with a sponge-like appearance. The microsponge sizes of the compounds in Pheroid™ decreased from **(1)** to **(5)** and subsequently increased from **(5)** to **(8)**. The more hydrophilic compounds, i.e., **(1)**, **(2)** and **(4)**, gave the highest flux values. Hence, it seems that hydrophilic drugs permeate easier when entrapped in Pheroid™ than lipophilic compounds.

The aqueous solubility, log D and flux values of **(7)** and **(8)** could not be determined, because these two compounds are highly lipophilic and don't dissolve in PBS in either pH 5 or 7. With CLSM it is observed that **(7)** and **(8)** were entrapped in Pheroid™ and therefore if the receptor phase was milky, due to damaged skin, and injected on the HPLC the chromatograms showed small peaks in the first six hours. Hence, during normal diffusion studies in Pheroid™ no peaks were visible for **(7)** and **(8)** and we can speculate that these compounds had trouble leaving the epidermis.

This study has confirmed that transdermal flux is dependant on several factors including optimum solubility, partitioning, diffusion and the degree of ionisation in the stratum corneum in addition to a suitable partition coefficient and high aqueous solubility. The solution to the increased transdermal delivery of lipophilic drugs does not simply lie in producing a derivative with a higher aqueous solubility and more ideal partition coefficient or by use of a transdermal delivery system, i.e., Pheroid™. Further studies may be done on **(2)** to increase transdermal permeation, i.e., synthesising esters of the primary hydroxyl group or mono alkyl chain amides, alone, as well as mono-, di- and tri-phosphate derivatives.

REFERENCES

ABDOU, H.M. 1989. Dissolution, bioavailability and bioequivalence. Easton, Pennsylvania: Mack Publishing Company. 554 p.

ABRAHAM, M.H., CHADHA, H.S. & MITCHELL, R.C. 1995. The factors that influence skin penetration of solutes. *Journal of pharmacy and pharmacology,* 47: 8-16.

ADLER, M.W. 1993. Development of the epidemic. (*In* Adler, M.W., *ed.* ABC of AIDS. 3rd ed. Great Britain: Eyre & Spottiswoode Ltd. p. 1.)

ADKINS, J.C., PETERS, D.H. & FAULDS, D. 1997. Zalcitabine: An update of its pharmacodynamic and pharmacokinetic properties and clinical efficacy in the management of HIV infection. *Drugs,* 53: 1054-1080.

ALVAREZ-ROMÁN, R., NAIK, A., KALIA, Y.N., FESSI, H. & GUY, R.H. 2004. Visualization of skin penetration using confocal laser scanning microscopy. *European journal of pharmaceutics and biopharmaceutics,* 58 (2): 301-316.

ANDERSON, B.D. & RAYKAR, V.P. 1989. Solute structure permeability relationships in human stratum corneum. *The journal of investigative dermatology,* 93: 280-286.

ANON. 2002. Interactive Log Kow (KowWin) Demo. http://www.syrres.com/esc/est_kowdemo.htm [Date of access: 13 Sep. 2006].

ANSEL, H.C. 1981. Introduction to pharmaceutical dosage forms. 3rd ed. Philadelphia: Lea & Febiger. p. 63-64.

ASBILL, C.S. & MICHNIAK, B.B. 2000. Percutaneous penetration enhancers: Local versus transdermal activity. *Pharmaceutical science & technology today,* 3: 36-41.

BABAR, A., SOLANKI, U.D., CUTIE, A.J. & PLAKOGIANNIS, F. 1990. Piroxicam release from dermatological bases: In vitro studies using cellulose membrane and hairless mouse skin. *Drug development and industrial pharmacy,* 16: 523-540.

BACH, M. & LIPPOLD, B.C. 1998. Percutaneous penetration enhancement and its quantification. *European journal of pharmaceutics and biopharmaceutics,* 46: 1-13.

BAGGALEY, R.F., BOILY, M.C., WHITE, R.G. & ALARY, M. 2006. Risk of HIV-1 transmission for parenteral exposure and blood transfusion: A systematic review and meta-analysis. *AIDS,* 20: 805-812.

BARR, M. 1962. Percutaneous absorption. *Journal of pharmaceutical sciences,* 61: 395-409.

BARRé-SINOUSSI, F., CHERMANN, J.C., REY, F., NUGEYRE, M.T., CHARMARET, S., GRUEST, J., DAUGUET, C., AXLER-BLIN, C., VEZINET-BRUN, F., ROUZIOUX, C., ROZENBAUM, W. & MONTAGNIER, L. 1983. Isolation of a T-lymphotropic retrovirus from a patient at risk for Acquired Immune Deficiency Syndrome (AIDS). *Science,* 220 (4599): 868-871.

BARRY, B.W. 1983. Dermatological formulations. (*In* Bronaugh, R.L. & Maibach, H.I., *eds.* Percutaneous Absorption: Mechanisms-methodology-drug delivery. New York: Marcel Dekker. 664 p.)

BARRY, B.W. 2001. Novel mechanisms and devices to enable successful transdermal drug delivery. *European journal of pharmaceutical sciences,* 14: 101-114.

BARRY, B.W. 2002. Transdermal drug delivery. (*In* Aulton, M.E., *ed.* Pharmaceutics: The science of dosage form design. 2nd ed. New York: Churchill Livingstone. p. 499-513.)

BARTLETT, J.A., BENOIT, S.L., JOHNSON, V.A., QUINN, J.B., SEPULVEDA, G.E., EHMANN, W.C., TSOUKAS, C., FALLON, M.A., SELF, P.L. & RUBIN, M. 1996. Lamivudine plus zidovudine compared with zalcitabine plus zidovudine in patients with HIV infection. A randomised, double-blind, placebo-controlled trail. North American HIV working party. *Annals of internal medicine,* 125: 161-172.

BECKETT, A.H. 1982. Possibilities and limitations of transdermal absorption. (*In* Aulton, M., *ed.* Pharmaceutics: The science of dosage from design. New York: Churchill Livingstone. p. 154-170.)

BLANK, I.H., SCHEUPLIEN, R.J. & MCFARLANE, D.J. 1967. Mechanism of percutaneous absorption III: the effect of temperature on transport of non electrolytes across the skin. *Journal of investigative dermatology,* 49: 582-589.

BOUYAC-BERTOIA, M., DVORIN, J.D. & FOUCHEIR, R.A. 2001. HIV-1 infection requires a functional integrase. *Molecular and cellular biology,* 7 (5): 1025-1035.

BRENNAN, R.O. & DURACK, D.T. 1981. Gay compromise syndrome. *The Lancet,* 2: 1338-1339.

BRINKMAN, K. & TER HOFSTEDE, H.J.M. 1999. Mitochondrial toxicity of nucleoside analogue reverse transcriptase inhibitors: Lactic acidosis, risk factors and therapeutic options. *AIDS reviews,* 1: 140-146.

BRONAUGH, R.L., STEWART, R.F. & SIMON, M. 1986. Methods for in vitro percutaneous absorption studies VII: Use of excised human skin. *Journal of pharmaceutical sciences,* 75: 1094-1097.

BUNGE, A.L. & CLEECK, R.L. 1995. A new method for estimation of dermal absorption from chemical exposure II: effect of molecular weight and octanol-water partition coefficient. *Pharmaceutical research*, 12: 88-95.

CATES, W. JR., CHESNEY, M.A. & COHEN, M.S. 1997. Primary HIV infection – a public health opportunity. *American journal of public health,* 87: 1928-1930.

CDC. *See* Centres for Disease Control and Prevention

CENTRES FOR DISEASE CONTROL AND PREVENTION. 1981. Kaposi's Sarcoma and Pneumocystis pneumonia among homosexual men – New York and California. *Morbidity and mortality weekly reports,* 30: 305-308.

CENTRES FOR DISEASE CONTROL AND PREVENTION. 1982. A cluster of Kaposi's Sarcoma and Pneumocystis carinii pneumonia among homosexual male residents of Los Angeles and Orange counties, California. *Morbidity and mortality weekly reports,* 31 (23): 305-307

CENTRES FOR DISEASE CONTROL AND PREVENTION. 1983. Epidemiologic notes and reports: Immunodeficiency among female sexual partners of males with Acquired Immune Deficiency Syndrome (AIDS) - New York. *Morbidity and mortality weekly reports,* 31 (52): 697-698.

CENTRES FOR DISEASE CONTROL AND PREVENTION. 1992. 1993 Revised classification system for HIV infection and expanded surveillance case definition for AIDS among adolescents and adults. *Morbidity and mortality weekly reports,* 41 (RR-17): 1–19.

CENTRES FOR DISEASE CONTROL AND PREVENTION. 2001. Updated U.S. Public Health Service guidelines for the management of occupational exposures to HBV, HCV, and HIV and recommendations for postexposure prophylaxis. *Morbidity and mortality weekly reports,* 50 (RR-11): 1-52.

CHAN, D.C., FASS, D., BERGER, J.M. & KIM, P.S. 1997. Core Structure of gp41 from the HIV envelope glycoprotein. *Cell,* 89: 263-273.

CHAN, D.C. & KIM, P.S. 1998. HIV entry and its inhibition. *Cell,* 93 (5): 681-684.

CLEARY, G.W. 1993. Biological factors in absorption and permeation. (*In* Zatz, J.L., *ed.* Skin permeation: Fundamentals and applications . Wheaton: Allured. 300 p.)

COOVADIA, H. 2004. Antiretroviral agents – how best to protect infants from HIV and save their mothers from AIDS. *New England journal of medicine,* 351 (3): 289-292.

COSTA, L.J., MUNERATO, P., DIAZ, R.S. & TANURI, A. 2000. Generation of intersubtype Human Immunodeficiency Virus type-1 recombinants in vitro: Influences in the biological behaviour and establishment of productive infection. *Virology,* 268: 440-451.

CULLANDER, C. & GUY, R.H. 1992. Visualization of iontophoretic pathway with confocal microscopy and the vibrating probe electrode. *Solid state ionics,* 53-56: 197-206.

DANCKWERTS, M.P. 1991. Advances in topical and transdermal drug delivery. Part 1: Percutaneous absorption and transdermal patches. *South African pharmaceutical journal,* p. 314-318.

DANIEL, M.D., LETVIN, N.L., KING, N.W., KANNAGI, M., SEHGAL, P.K., HUNT, R.D., KANKI, P.J., ESSEX, M. & DESROSIERS, R.C. 1985. Isolation of T-cell tropic HTLV-III-like retrovirus from macaques. *Science,* 228: 1201-1204.

DAVIES, D.J., WARD, R.J. & HEYLINGS J.R. 2004. Multi-species assessment of electrical resistance as a skin integrity marker for in vitro percutaneous absorption studies. *Toxicology in vitro,* 18: 351-358.

DAVIS, K.C., HORSBURGH, C.R. Jr., HASIBA, U., SCHOCKET, A.L. & KIRKPATRICK, C.H. 1983. Acquired Immunodeficiency Syndrome in patients with hemophilia. *Annals of internal medicine,* 98: 284-286.

DEAN, M., CARRINGTON, M., WINKLER, C., HUTTLEY, G.A.; SMITH, M.W.; ALLIKMETS, R., GOEDERT, J.J., BUCHBINDER, S.P., VITTINGHOF, E., GOMPERTS, E., DONFIELD, S., VLAHOV, D., KASLOW, R., SAAH, A., RINALDO, C., DETELS, R. & O'BRIEN, S.J. 1996. Genetic restriction of HIV-1 infection and progression to AIDS by a deletion allele of the CKR5 structural gene. *Science,* 273: 1856-1862.

DE CLERCQ, E. 2001. Antiviral drugs: current state of the art. *Journal of clinical virology,* 22 (1): 73-89.

DE CLERCQ, E. 2004a. HIV-chemotherapy and -prophylaxis: new drugs, leads and approaches. *The International journal of biochemistry & cell biology,* 36 (9): 1800-1822.

DE CLERCQ, E. 2004b. Antiviral drugs in current clinical use. *Journal of clinical virology,* 30 (2): 115-133.

DEORA, A. & RATNER, L. 2001. Viral protein u (vpu) – mediated enhancement of Human Immunodeficiency Virus type 1 particle release depends on the rate of cellular proliferation. *Journal of virology,* 75 (14): 6714-6718.

DONEGAN, E. 2003. Transmission of HIV by blood, blood products, tissue transplantation, and artificial insemination. http://hivinsite.ucsf.edu/InSite?page=kb-07-02-09#S2.2X [Date of access: 10 Nov. 2006].

ELIAS, P.M. 1983. Epidermal lipids, barrier function and desquamation. *The journal of investigative dermatology,* 80: 44s-49s.

EL TAYAR, N., TSAI, R.S., TESTA, B., CARRUPT, P.A., HANSCH, C. & LEO, A. 1991. Percutaneous penetration of drugs: A quantitative structure-permeability relationship study. *Journal of pharmaceutical sciences,* 80: 744-749.

FASANO, W.J., MANNING, L.A. & GREEN, J.W. 2002. Rapid integrity assessment of rat and human epidermal membranes for in vitro dermal regulatory testing: Correlation of electrical resistance with tritiated water permeability. *Toxicology in vitro,* 16: 731-740.

FAUCI, A.S. 1993. Immunopathogenesis of HIV Infection. *Journal of Acquired Immunodeficiency Syndromes,* 6: 655-662.

FEINBERG, M.B., JARRETT, R.F., ALDOVINI, A., GALLO, R.C. & WONG-STAAL, F. 1986. HTLV-III expression and production involve complex regulation at the levels of splicing and translation of viral RNA. *Cell,* 46 (6): 807-817.

FLEMING, D.T. & WASSERHEIT, J.N. 1999. From epidemiological synergy to public health policy and practice: The contribution of other sexually transmitted diseases to sexual transmission of HIV infection. *Sexually transmitted infections,* 75: 3-17.

FLEXNER, C. 2006. Antiretroviral agents and treatment of HIV infection. (*In* Brunton, L.L., Lazo, J.S. & Parker, K.L., *eds.* Goodman & Gilman's The pharmacological basis of therapeutics. 11th ed. New-York: McGraw-Hill. p. 1273-1314.)

FLYNN, G.L. 1979. Topical drug absorption and topical pharmaceutical systems. (*In* Baker, G.S. & Rhodes, C.T., *eds.* Modern Pharmaceutics. 2nd ed. New York: Marcel Dekker. p. 265-270.)

FLYNN, G.L. 1989. Mechanism of percutaneous absorption from physicochemical evidence. (*In* Bronaugh, R.L. & Maibach, H.I., *eds.* Percutaneous Absorption: Mechanism-methodology-drug delivery. New York: Marcel Dekker. 664 p.)

FLYNN, G.L. 1990. Topical drug absorption and topical pharmaceutical systems. (*In* Baker, G.S. & Rhodes, C.T., *eds.* Modern Pharmaceutics. 2nd ed. New York: Marcel Dekker. p. 263-325.)

FLYNN, G.L. & WEINER, N.D. 1993. Topical and transdermal delivery - provinces or realism. (*In* Gurny, R. & Teubner, A., *eds.* Dermal and transdermal drug delivery: New insights and perspectives: Second International Symposium of the International Association for Pharmaceutical Technology (APV), 11-13 November 1991, Frankfurt. Stuttgart: Wissenschaftliche Verlagsgesellschaft. 193 p.)

FLYNN, G.L. & YALKOWSKY, S.H. 1972. Correlation and prediction of mass transport across membranes I: Influence of alkyl chain length on flux determining properties of barrier and diffusant. *Journal of pharmaceutical science,* 61 (6): 838-852.

FOLDVARI, M. 2000. Non-invasive administration of drugs through the skin: Challenges in delivery system design. *Pharmaceutical science and technology today,* 3: 417-425.

FOURIE, L. 2002. Physicochemical properties and transdermal delivery of carbamazepine and its N-alkyl and N-hydroxyalkyl analogues. Potchefstroom: PU for CHE. (Dissertation – M.Sc.) 84 p.

FRANKEL, A.D. & YOUNG, J.A.T. 1998. HIV-1: Fifteen proteins and an RNA. *Annual review of biochemistry,* 67: 1-25.

FREED, E.O. & MARTIN M.A. 1995. The role of Human Immunodeficiency Virus Type 1 envelope glycoproteins in virus infection. *The journal of biological chemistry,* 270 (41): 23883-23886.

FRIEDLAND, G., KAHL, P., SALTZMAN, B., ROGERS, M., FEINER, C., MAYERS, M., SCHABLE, C. & KLEIN, R.S. 1990. Additional evidence for lack of transmission of HIV infection by close interpersonal (casual) contact. *AIDS,* 4: 639-644.

FRIEDLAND, G.H. & KLEIN, R.S. 1987. 101 Non-sexual household contacts. *New England journal of medicine,* 317: 1125.

GABUZDA, D.H., LEVER, A., TERWILLIGER, E. & SODROSKI, J. 1992. Effects of deletions in the cytoplasmic domain on biological functions of Human Immunodeficiency Virus type 1 envelope glycoproteins. *Journal of virology,* 66 (6): 3306-3315.

GALLAY, P., SWINGLER, S., SONG, J., BUSHMAN, F. & TRONO, D. 1995. HIV nuclear import is governed by the phosphotyrosine-mediated binding of matrix to the core domain of integrase. *Cell,* 83: 569-576.

GAO, W.Y., SHIRASAKA, T., JOHNS, D.G., BRODER, S. & MITSUYA, H. 1993. Differential phosphorylation of azidothymidine, dideoxycytidine, dideoxyinosine in resting and activated peripheral blood mononuclear cells. *Journal of clinical investigation,* 91: 2326-2333.

GARCIA, P.M., KALISH, L.A., PITT, J., MINKOFF, H., QUINN, T.C., BURCHETT, S.K., GOTTLIEB, M.S., SCHROFF, R., SCHANKER, H.M., WEISMAN, J.D., FAN, P.T., WOLF, R.A. & SAXON, A. 1981. Pneumocystis carinii pneumonia and mucosal candidiasis in previously healthy homosexual men: Evidence of a new acquired cellular immunodeficiency. *New England journal of medicine,* 305: 1425-1431.

GERBER, M., BREYTENBACH, J.C., HADGRAFT, J. & DU PLESSIS, J. 2006. Synthesis and transdermal properties of acetylsalicylic acid and selected esters. *International journal of pharmaceutics,* 310: 31-36.

GOOSEN, C., LAING, T.J., DU PLESSIS, J., GOOSEN, T.C., LU, G. & FLYNN, G.L. 2002. Percutaneous delivery of thalidomide and its N-alkyl analogs. *Pharmaceutical research,* 19: 434-439.

GREENE, W.C. & PETERLIN, B.M. 2002. Charting HIV's remarkable voyage through the cell: Basic science as a passport to future therapy. *Nature medicine,* 8 (7): 673-680.

GREGG, C.R. 1999. Drug interactions and anti-infective therapies. *The American journal of medicine,* 106: 227-237.

GROBLER, A.F. 2004. Emzaloid™ Technology. Potchefstroom: North-West University. 20 p. [Confidential: Concept document].

GUPTA, S.K., SATHYAN, G. & HWANG, S.S. 1997. Clinical assessment of transdermal drug delivery systems. (*In* Gosh, T.K., Pfister, W.R. & Yum, S.I., *eds.* Transdermal and topical drug delivery systems. Buffalo Grove, Ill: Interpharm Press. p. 215-248.)

GUY, R.H. 1996. Currant status and future prospects of transdermal drug delivery. *Pharmaceutical research*, 14: 1765-1769.

GUY, R.H. & HADGRAFT, J. 1989a. Selection of drug candidates for transdermal drug delivery. (*In* Hadgraft, J. & Guy, R.H., *eds.* Transdermal drug delivery: Developmental issues and research initiatives. New York: Marcel Dekker. 324 p.)

GUY, R.H. & HADGRAFT, J. 1989b. Structure-activity correlations in percutaneous absorption. (*In* Bronaugh, R.L. & Maibach, H.I., *eds.* Percutaneous Absorption: Mechanisms-methodology-drug delivery. New York: Marcel Dekker. 664 p.)

HADGRAFT, J. 1991. Structure-activity relationships and percutaneous absorption. *Journal of controlled release,* 15 (3): 221-226.

HADGRAFT, J. 1996. Recent developments in topical and transdermal delivery. *European journal of drug metabolism and pharmacokinetics,* 21 (2): 165-173.

HADGRAFT, J. 2001. Skin, the final frontier. *International journal of pharmaceutics,* 224: 1-18.

HADGRAFT, J., CORDES, G. & WOLFF, M. 1990. Prediction of the transdermal delivery of β-blockers. (*In* Rietbrock, N., Hrsg. Die Haut als transportorgan fur Arzneistoffe. Steinkopff Verslag Darmstadt. p. 133-143.)

HADGRAFT, J., DU PLESSIS, J. & GOOSEN, C. 2000. The selection of non-steroidal anti-inflammatory agents for dermal delivery. *International journal of pharmaceutics,* 207: 31-37.

HADGRAFT, J., PECK, J., WILLIAMS, D.G., PUGH, W.J. & ALLAN, G. 1996. Mechanisms of action of skin penetration enhancers/retarders: Azone and analogues. *International journal of pharmaceutics,* 141: 17-25.

HADGRAFT, J.W. & SOMERS, G.F. 1956. Percutaneous absorption. *Journal of pharmacy and pharmacology,* 8: 625-631.

HADGRAFT, J. & VALENTA, C. 2000. pH, pKa and dermal delivery. *International journal of pharmaceutics,* 200: 243-247.

HADGRAFT, J. & WOLFF, M. 1993. Physicochemical and pharmacokinetic parameters affecting percutaneous absorption. (*In* Gurny, R. & Teuber, A., *eds.* Dermal and transdermal drug delivery: New insights and perspectives: Second International Symposium of the International Association for Pharmaceutical Technology (APV), 11-13 November 1991, Frankfurt. Stuttgart: Wissenschaftliche Verlagsgesellschaft. 193 p.)

HARRISON, E.J., GROUNDWATER, P.W., BRIAN, K.R. & HADGRAFT, J. 1996. Azone induced fluidity in human stratum corneum. A Fourier transform infrared spectroscopy investigation using the perdeuterated analogue. *Journal of controlled release,* 41: 283-290.

HAYDEN, F.G. 2001. Antimicrobial agents: Antiretroviral agents. (*In* Hardman, J.G., Limbird, L.E., Molinoff, P.B., Ruddon, W.R. & Gillman, A.G., *eds.* Goodman & Gilman's The pharmacological basis of therapeutics. 10th ed. New York: McGraw-Hill. 2148 p.)

HEALTH AND HUMAN SERVICES. 2005. Testing HIV positive – Do I have HIV? AIDSinfo, http://www.aidsinfo.nih.gov/ContentFiles/TestingPositive_FS_en.pdf [Date of access: 10 Nov. 2006].

HEYMANN, K.B. & BRUBAKER, J. 1997. Breast feeding and HIV infection. (*In* Cotton, D. & Watts, D.H., *eds.* The medical management of AIDS in women. New York: John Wiley & Sons. p. 55-66.)

HHS. *See* Health and Human Services

HILDEBRAND, J.H., PRAUSNITZ, J.M. & SCOTT, R.L. 1970. Regular and related solutions. New York: Van Nostrand Reinhold. p. 3-6.

HILDEBRAND, J.H. & SCOTT, R.L. 1950. The solubility of nonelectrolytes. 3rd ed. London: Dover Publishers. p. 289-303.

HISCOTT, J., KWON, H. & GENIN, P. 2001. Hostile takeovers: Viral appropriation of the NF-kappa B pathway. *Journal of clinical investigation,* 107 (2): 143-151.

HOLBROOK, K.A. & WOLFF, K. 1993. The structure of development of skin. (*In* Fitzpatrick, T.B., Eisen, A.Z., Wolff, K., Feedberg, I.M. & Austen, K.F., *eds.* Dermatology in general medicine. 4th ed. New York: McGraw Hill. 1: 97-145.)

HOLMES, E. 2006. The synthesis and transdermal delivery of stavudine derivatives. Potchefstroom: North-West University. (Dissertation – M.Sc.) 91 p.

HUNTER, J.A.A., SAVIN, J.A. & DAHL, M.V. 1996. Clinical Dermatology. 2nd ed. London: Blackwell Science. 316 p.

HYMES, K.B., CHEUNG, T., GREENE, J.B., PROSE, N.S., MARCUS, A., BALLARD, H., WILLIAMS, D.C. & LAUBENSTEIN, L.J. 1981. Kaposi's Sarcoma in homosexual men. *The Lancet,* 2: 598-600.

IDSON, B. 1975. Percutaneous Absorption. *Journal of pharmaceutical sciences,* 64 (6): 901-924.

IDSON, B. 1983. Vehicle effects in percutaneous absorption. *Drug metabolism reviews,* 14: 207-222.

JACK, L., CAMERON, B.D., SCOTT, R.C. & HADGRAFT, J. 1991. In vitro percutaneous absorption of salicylic acid: Effect of vehicle pH. (*In* Scott, R.C., Guy, R.H., Hadgraft, J. & Bodde, H.E., *eds.* Prediction of percutaneous penetration. London: IBC Technical. p. 515-518.)

JACKSON, E.W. 1993. Toxicological aspects of percutaneous absorption. (*In* Zats, J.L., *ed.* Skin permeation, fundamentals and application. Wheaton, Ill: Allured Publishing Corporation. p. 177-192.)

JET, A.E., YU, H. & KARLMANN, G.J. 2000. High rate of recombination throughout the Human Immunodeficiency Virus type 1 genome. *Journal of virology,* 74 (3): 1234-1240.

JOSSINET, F., PAILLART, J.C. & WESTHOF, E. 1999. Dimerization of HIV-1 genome RNA subtypes A and B: RNA loop structure and magnesium binding. *RNA,* 5 (9): 1222-1234.

JUNGINGER, H.E., HOFLAND, H.E.J. & BOWSTRA, J.A. 1991. Liposomes and niosomes : Interactions with human skin. *Cosmetics and toiletries,* 106 (8): 45-46.

KAHN, J.O. & WALKER, B.D. 1998. Acute Human Immunodeficiency Virus type 1 infection. *The New England journal of medicine,* 339: 33-39.

KAI, T., ISAMI, T., KOBATA, K., KUROSAKI, Y., NAKAYAMA, T. & KIMURA, T. 1992. Ceratinised epithelial transport of β-blocking agents. *Chemical and pharmaceutical bulletin,* 40 (9): 2498-2504.

KALIA, Y.N. & Guy, R.H. 2001. Modelling transdermal drug release. *Advanced drug delivery reviews,* 48: 159-172.

KATZ, M. & POULSON, R.T. 1971. Absorption of drugs through the skin. (*In* Brodie, B.B. & Gillette, J.R., *eds.* Handbook of experimental pharmacology: Concepts in biomedical pharmacology. Part 1. New York: Springer Verslag. 28: 103-162.)

KEMKEN, J., ZILGER, A. & MULLER, B.W. 1992. Influence of supersaturation on the pharmacodynamic effect of bupranolol after dermal administration using micro-emulsions as vehicle. *Pharmaceutical research,* 9 (4): 554-558.

KIM, D.D. & CHIEN, Y.W. 1995a. Transdermal delivery of zalcitabine: in vitro skin permeation study. *Aids,* 9 (12): 1331-1336.

KIM, D.D. & CHIEN, Y.W. 1995b. Transdermal delivery of dideoxynucleoside-type anti-HIV drugs. 1. Stability studies for hairless rat skin permeation. Journal of Pharmaceutical *Sciences,* 84 (9): 1061-1066.

KIM, D.D. & CHIEN, Y.W. 1996a. Simultaneous skin permeation of dideoxynucleoside-type anti-HIV drugs. *Journal of controlled release,* 40: 67-76.

KIM, D.D. & CHIEN, Y.W. 1996b. Transdermal delivery of dideoxynucleoside-type anti-HIV drugs. 2. The effect of vehicle and enhancer on skin permeation. *Journal of Pharmaceutical Sciences,* 85 (2): 214-219.

KLIGMAN, A.M. & CHRISTOPHERS, E. 1963. Preparation of isolated sheets of human stratum corneum. *Archives of dermatology,* 88: 702-705.

KOHL, N.E., EMINI, E.A., SCHLEIF, W.A., DAVIS, L.J., HEIMBACH, J.C., DIXON, R.A.F., SCOLNICK, E.M. & SIGAL, I.S. 1988. Active Human Immunodeficiency Virus protease is required for viral inactivity. *Proceedings of the National Academy of Sciences the United States of America,* 85: 4686-4690.

KOMMURU, T.R., KHAN, M.A. & REDDY, I.K. 1998. Racemate and enantiomers of ketoprofen: Phase diagram, thermodynamic studies, skin permeability and use of chiral permeation enhancers. *Journal of pharmaceutical sciences,* 87 (7): 833-840.

LEWIS, J.S., TERRIF, C.M., COULSTON, D.R. & GARRISON, M.W. 1997. Protease inhibitors: A therapeutic breakthrough for the treatment of patients with Human Immunodeficiency Virus. *Clinical therapeutics,* 19: 187-214.

LIEN, E.J. & TONG, G.L. 1973. Physicochemical properties and percutaneous absorption of drugs. *Journal of the society of cosmetic chemists,* 24: 371-384.

LIRON, Z.V.I. & COHEN, S. 1984. Percutaneous absorption of alkonoic acids II: Application of regular solution theory. *Journal of pharmaceutical sciences,* 73 (4): 538-542.

LIU, J.C. & WISNIEWSKI, S.J. 1997. Recent advances in topical drug delivery systems. (*In* Ghosh, T.K., Pfister, W.R. & Yum, S.I., *eds.* Transdermal and topical drug delivery systems. Buffalo Grove, Ill: Interpharm Press. p. 593-609).

LOVEDAY, C. 2001. International perspectives on antiretroviral resistance. Nucleoside reverse transcriptase inhibitor resistance. *Journal of Acquired Immunodeficiency Syndromes,* 26: S10-S24.

LUND, W., *ed.* 1994. The Pharmaceutical Codex. 12th ed. London: The Pharmaceutical Press. 1117 p.

LUSSO, P., DI MARZO VERONESE, F., ENSOLI, B., FRANCHINI, G., JEMMA, C., DEROCCO, S.E., KALYANARAMAN, V.S. & GALLO, R.C. 1990. Expanded HIV-1 cellular tropism by phenotypic mixing with murine endogenous retroviruses. *Science,* 247: 848-852.

MARTIN, A., SWARBRICK, J. & CAMMARATA, A. 1983. Physical Pharmacy. 3rd ed. Philadelphia: Lea & Febiger. 664p.

MARX, L.J. 1985. A virus by any other name? *Science,* 227 (4693): 1449-1451.

MASUR, H., MICHELIS, M.A., GREENE, J.B., ONORATO, I., STOUWE, R.A., HOLZMAN, R.S., WORMSER, G., BRETTMAN, L., LANGE, M., MURRAY, H.W. & CUNNIGHAM-RUNDLES, S. 1981. An outbreak of community acquired Pneumocystis carinii pneumonia: Initial manifestation of cellular immune dysfunction. *The New England journal of medicine,* 305: 1431-1438.

MCGOVERN, S.L., CASELLI, E., GRIGORIEFF, N. & SHOICHET, B.K. 2002. A common mechanism underlying promiscuous inhibitors from virtual and high-throughput screening. *Journal of medicinal chemistry,* 45 (8): 1712-1722.

MERIGAN, T.C., SKOWRON, G., BOZZETTE, S.A., RICHMAN, D., UTTAMCHANDANI, R., FISCHL, M., SCHOOLEY, R., HIRSCH, M., SOO, W., PETTINELLI, C. 1989. Circulating p24 antigen levels and responses to dideoxycytidine in Human Immunodeficiency Virus (HIV) infections. A phase I and II study. *Annals of internal medicine,* 110 (3): 189-194.

MITRAGOTRI, S. 2000. In situ determination of partition and diffusion coefficients in the lipid bilayers of stratum corneum. *Pharmaceutical research,* 17: 1026-1029.

MOHAN, P. 1992. Anti-AIDS drug development: Challenges and strategies. *Pharmaceutical research,* 9: 703-714.

MONTAGA, W. 1965. The skin. *Scientific American,* 212: 56-66.

MORGANTI, P., RUOCCO, E., WOLF, R. & ROUCCO, V. 2001. Percutaneous absorption and delivery systems. *Clinics in dermatology,* 19: 489-501.

MORRIS, L., CILLIERS, T. & BREDELL, H. 2001. CCR5 is a major co-receptor used by HIV-1 subtype C isolates from patients with active tuberculosis. *AIDS research and human retroviruses,* 17 (8): 697-701.

MUKHTAR, H. 1992. Pharmacology of the skin. Florida: CRC Press. 416 p.

MYERS, G., FOLEY, B., MELLORS, J.W., KORBER, B., JEANG, K. & WAIN-HOBSON, S., eds. 1996. Human retroviruses and AIDS 1996. http://www.hiv.lanl.gov/content/hiv-db/COMPENDIUM/1996/INTRO.pdf [Date of access: 11 Nov. 2006].

NAIK, A., KALIA, Y.N. & GUY, R.H. 2000. Transdermal drug delivery: Overcoming the skin's barrier function. *Pharmaceutical science and technology today,* 3: 318-325.

NAKASHIMA, A.K. & FLEMING, P.L. 2003. HIV/AIDS surveillance in the United States 1981-2001. *Journal of Acquired Immune Deficiency Syndrome,* 32: 68-85.

NARISHETTY, S.T.K. & PANCHAGNULA, R. 2004. Transdermal delivery system for zidovudine: In vitro, ex vivo and in vivo evaluation. *Biopharmaceutics and drug disposition,* 25: 9-20.

NUGROHO, A.K., LI, L., DIJKSTRA, D., WIKSTRÖM, H., DANHOF, M. & BOUWSTRA, J.A. 2005. Transdermal iontophoresis of the dopamine agonist 5-OH-DPAT in human skin in vitro. *Journal of controlled release,* 103 (2): 393-403.

OH, S.Y, JEONG, S.Y., PARK, T.G. & LEE, J.H. 1998. Enhanced transdermal delivery of AZT (zidovudine) using iontophoresis and penetration enhancer. *Journal of controlled release,* 51 (2): 161-168.

OSTRENGA, J., STEINMETZ, C. & POULSEN, B. 1971. Significance of vehicle composition: Relationship between topical vehicle composition, skin permeability and clinical efficacy. *Journal of pharmaceutical sciences,* 60: 1175-1179.

OURIEMCHI, E.M. & VERGNAUD, J.M. 2000. Process of drug transfer with three different polymeric systems with transdermal drug delivery. *Computational and theoretical polymer science,* 10: 391-401.

PADIAN, N., SHIBOSKI, S.C. & JEWELL, N.P. 1991. Female-to-male transmission of Human Immunodeficiency Virus. *The journal of the American medical association,* 266: 1664-1667.

PARDO, A., SHIRI, Y. & COHEN, S. 1992. Kinetics of transdermal penetration of an organic ion pair: Physostigmine salicylate. *Journal of pharmaceutical sciences,* 81 (10): 990-995.

PARHAM, M. 2000. Log P Interactive Analysis. http://www.logp.com [Date of access: 13 Sep. 2006].

PEDLEY, K.C. 1997. Applications of confocal and fluorescence microscopy. *Digestion,* 58 (2): 62-68.

PEFILE, S. & SMITH, E.W. 1997. Transdermal drug delivery: Vehicle design and formulation. *South African journal of science,* 93: 147-151.

PERRY, C.M. & FAULDS, D. 1997. Lamivudine: A review of its antiviral activity, pharmacokinetic properties and therapeutic efficacy in the management of HIV infection. *Drugs,* 53: 657-680.

POIGNARD, P., SAPHIRE, E.O., PARREN, P.W. & BURTON, D.R. 2001. Gp 120: Biologic aspects of structural features. *Annual review of immunology,* 19: 253-274.

POLLARD, V.W. & MALIM, M.H. 1998. The HIV-1 Rev protein". *Annual review of microbiology,* 52: 491-532.

POPOVIC, M., SARNGADHARAN, M.G., READ, E. & GALLO, R.C. 1984. Detection, isolation, and continuous production of cytopathic retroviruses (HTLV-III) from patients with AIDS and pre-AIDS. *Science,* 224 (4648): 497-500.

POTTS, R.O. & GUY, R.H. 1992. Predicting skin permeability. *Pharmaceutical research,* 9 (5): 663-669.

POTTS, R.O. & GUY, R.H. 1995. A predictive algorithm for skin permeability: The effects of molecular size and hydrogen bond activity. *Pharmaceutical research,* 12 (11): 1628-1633.

PRAUSNITZ, M.R., MITRAGOTRI, S. & LANGER, R. 2004. Current status and future potential of transdermal drug delivery. *Nature reviews drug discovery,* 3: 115-124.

PUGH, W.J., DEGIM, I.T. & HADGRAFT, J. 2000. Epidermal permeability: Penetrant structure relationships. 4. QSAR of permeant diffusion across human stratum corneum in terms of molecular weight, H-bonding and electronic charge. *International journal of pharmaceutics,* 197 (1-2): 203-211.

PUGH, W.J., ROBERTS, M.S. & HADGRAFT, J. 1996. Epidermal permeability: Penetrant structure relationships. 3. The effect of hydrogen bonding interactions and molecular size on diffusion through the stratum corneum. *International journal of pharmaceutics,* 138: 149-165.

RAYKAR, V.P., FUNG, M.C. & ANDERSON, B.D. 1988. The role of protein and lipid domains in the uptake of solutes by human stratum corneum. *Pharmaceutical research,* 5: 140-150.

REEVES, J.D. & DOMS, R.W. 2002. Human Immunodeficiency Virus Type 2. *Journal of general virology,* 83: 1253-1265.

RIEGER, M.M. 1993. Factors affecting sorption of topically applied substances. (*In* Zatz, J.L., *ed.* Skin permeation. fundamentals and applications. Wheaton: Allured. 300 p.)

RITSCHEL, W.A. 1988. Pharmacokinetic and biopharmaceutical aspects in drug delivery. (*In* Tyle, P., *ed.* Drug delivery devices: Fundamentals and applications. New York: Marcel Dekker. p. 17-79.)

RITSCHEL, W.A. & HUSSAIN, A.S. 1988. The principles of skin permeation. *Methods and findings in experimental and clinical pharmacology,* 10: 39-56.

RIVIERE, J.M. 1993. Biological factors in absorption and permeation. (*In* Zatz, J.L., *ed.* Skin permeation. fundamentals and applications. Wheaton: Allured. 300 p.)

ROBERTS, M.S., PUGH, W.J., HADGRAFT, J. & WATKINSON, A.C. 1995. Epidermal permeability – penetrant structure relationships I. An analysis of methods of predicting penetration of monofunctional solutes from aqueous solutions. *International journal of pharmaceutics,* 126: 219-233.

ROBERTS, W.J. & SLOAN, K.B. 2000. Prediction of transdermal flux of prodrugs of 5-fluorouracil, theophylline, and 6-mercaptopurine with a series/parallel model. *Journal of pharmaceutical sciences,* 89: 1415-1431.

ROBEY, W.G., SAFAI, B., OROSZLAN, S., ARTHUR, L.O., GONDA, M.A., GALLO, R.C. & FISCHINGER, P.J. 1985. Characterization of envelope and core structured gene products of HTLV-III with sera from HIV patients. *Science,* 228 (4699): 593-595.

RONGEN, H.A.H., BULT, A. & VAN BENNEKOM, W.P. 1997. Liposomes and immunoassays. *Journal of immunological methods,* 204 (2): 105-133.

ROTHMAN, S. 1954. Physiology and biochemistry of the skin. *The University of Chicago Press,* 1954: 27-53.

ROUSSEAU, C.M., NDUATI, R.W., RICHARDSON, B.A., STEELE, M.S., JOHN-STEWART, G.C., MBORI-NGACHA, D.A., KREISS, J.K. & OVERBAUGH, J. 2003. Longitudinal analysis of Human Immunodeficiency Virus type 1 RNA in breast milk and of its relationship to infant infection and maternal disease. *The journal of infectious diseases,* 187: 741-747.

ROY, S.D. 1997. Preformulation aspects of transdermal drug delivery systems. (*In* Ghosh, T.K. & Pfister, W.R. & Yum, S.I., *eds.* Transdermal and topical drug delivery systems. Buffalo Grove: Interpharm. 713 p.)

ROY, S.D. & FLYNN, G.L. 1988. Solubility and related physicochemical properties of narcotic analgesics. *Pharmaceutical research,* 5: 580-586.

ROY, S.D. & FLYNN, G.L. 1989. Transdermal delivery of narcotic analgesics: Comparative permeabilities of narcotic analgesics through human cadaver skin. *Pharmaceutical research,* 6: 825-832.

SAFAI, B. & WEISS, H. 1984. Clinical manifestations of Kaposi's Sarcoma. (*In* Ma, P. & Armstrong, D., *eds.* The Acquired Immune Deficiency Syndrome and infections of homosexual men. 1st ed. United States of America: Yorke Medical Books. p. 210-224.)

SAUNDERS, J.C.J., DAVIS, H.J., COETZEE, L., BOTHA, S., KRUGER, A.E. & GROBLER, A. 1999. A novel skin penetration enhancer: Elevation by membrane diffusion and confocal microscopy. *Journal of pharmacy and pharmaceutical sciences,* 2 (3): 99-107.

SAWANPIDOKKUL, N., THONGNOPNUA, P. & UMPRAYN, K. 2004. Transdermal delivery of zidovudine (AZT): The effects of vehicles, enhancers, and polymer membranes on permeation across cadaver pig skin. *AAPS PharmSciTech,* 5 (3): 1-8.

SCHACKER, T., COLLIER, A.C., HUGHES, J., SHEA, T. & COREY, L. 1996. Clinical and epidemiologic features of primary HIV infection. *Annals of internal medicine,* 125: 257-264.

SCHAEFFER, E., GLEZIUNAS, R. & GREENE, W.C. 2001. Human Immunodeficiency Virus type 1 nef function at the level of virus entry by enhancing cytoplasmic delivery of the virion. *Journal of virology,* 75 (6): 2993-3000.

SCHAEFER, H. & HENSBY, C. 1990. Skin permeability and models of percutaneous absorption. (*In* Galli, C.L., Hensby, C.N. & Marinovich, M., *eds.* Skin pharmacology and toxicology: Recent advances. New York: Plenum. 318 p.)

SCHAEFER, H., ZESCH, A. & STÜTTGEN, G. 1982. Skin permeability. Berlin: Springer-Verlag. p. 739-740

SCHALLA, W. & SCHAEFER, H. 1982. Mechanisms of penetration of drugs into the skin. (*In* Brandau, R. & Lippold, B.H., *eds.* Dermal and transdermal absorption: First international symposium from 12-14 January 1981, Munich. Stuttgart: Wissenschaftliche Verlagsgesellschaft. 257 p.)

SCHEUPLEIN, R.J. 1986. *Journal of investigative dermatology,* 47: 344-346.

SCHEUPLEIN, R.J. & BLANK, I.H. 1971. Permeability of the skin. *Physiology reviews,* 51: 702-747.

SCHIFFMAN, S.S., ZERVAKIS, J., SHAIO, E. & HEALD, A.E. 1999. Effect of nucleoside analogs zidovudine, didanosine, stavudine, and lamivudine on the sence of taste. *Nutrition,* 15 (11/12): 854-859.

SCHLEBUSCH, J. 2002. A briefing document on the use of the MeyerZall therapeutic system, based on Emzaloid™ technology, to increase the absorption of active ingredients, with special reference to MeyerZall Laboratories Tuberculosis Medicine Project. (Briefing document as tribute to the colleagues at MeyerZall.) George. 139 p. (Unpublished.)

SEKI, T., KAWAGUCHI, T. & JUNI, K. 1990. Enhanced delivery of zidovudine through rat and human skin via ester prodrugs. *Pharmaceutical research,* 7 (9): 948-952.

SHOTTON, D.M. 1989. Confocal scanning optical microscopy and its applications for biological specimens. *Journal of cell sciences,* 94: 175-206.

SKALSKI, V., CHANG, C.N., DUTSCHMAN, G. & CHENG, Y.C. 1993. The biochemical basis for the differential anti-Human Immunodeficiency Virus activity of two cis enantiomers of 2',3'-dideoxy-3'-thiacytidine. *Journal of biological chemistry,* 268: 23234-23238.

SMITH, K.L. 1990. Penetrant characteristics influencing skin absorption. (*In* Kemppainen, B.W. & Reifenrath, W.G., *eds.* Methods for skin absorption. Boca Raton: CRC Press. 219 p.)

SMITH, N. & SPITTLE, M. 1993. Tumours. (*In* Adler, M.W., *ed.* ABC of AIDS. 3rd ed. Great Britain: Eyre & Spottiswoode Ltd. p. 19)

SOVA, P., VOLSKY, D.J., WARY, L. & CHAO, W. 2001. Vif is largely absent from Human Immunodeficiency Virus type-1 mature virions and associate mainly with viral particles containing unprocessed gag. *Journal of virology,* 75 (12): 5504-5517.

STOTT, R.W., WILLIAMS, A.C. & BARRY, B.W. 1998. Transdermal delivery from eutectic systems: Enhanced permeation of a model drug, ibuprofen. *Journal of controlled release,* 50: 297-308.

STÜTTGEN, G. 1982. Drug absorption by intact and damaged skin. (*In* Brandau, R. & Lippold, B.H., *eds.* Dermal and transdermal absorption: First international symposium from 12-14 January 1981, Munich. Stuttgart: Wissenschaftliche Verlagsgesellschaft. 257 p.)

SUBRAHMANYAM, C.V.S. & SARASIJA, S. 1997. Solubility behaviour of Carbamazepine in binary solvents: Extended Hildebrand solubility approach to obtain solubility and other parameters. *Pharmazie,* 52 (12): 939-942.

SUN, Y. 1997. Skin absorption enhancement by physical means: Heat, ultrasound and electricity. (*In* Gosh, T.K., Pfister, W.R. & Yum, S.I., *eds.* Transdermal and topical drug delivery systems. Buffalo Grove, Ill: Interpharm Press. p. 327-355.)

SURBER, C., WILHELM, K. & MAIBACH, H.I. 1993. In vitro and in vivo percutaneous absorption of structurally related phenol and steroid analogs. *European journal of pharmacy and biopharmaceutics,* 39: 244-248.

SWEETMAN, S.C., *ed.* 2002. Martindale: The complete drug reference. 33rd ed. London: Pharmaceutical Press. p. 635-636.

TAKAHASHI, K., TAMAGAWA, S., KATAGI, T., RYTTING, H., NISHIHATA, T. & MIZUNO, N. 1993. Percutaneous permeation of basic compounds through shed snake skin as a model membrane. *Journal of pharmacy and pharmacology,* 45: 882-886.

TäUBER, U. 1982. Mechanism of penetration of drugs into the skin. (*In* Brandau, R. & Lippold, B.H., *eds.* Dermal and transdermal absorption: First international symposium from 12-14 January 1981, Munich. Stuttgart: Wissenschaftliche Verlagsgesellschaft. 257 p.)

TäUBER, U. 1989. Microbial metabolism of topically applied drugs. (*In* Hadgraft, J. & Guy, R.H., *eds.* Transdermal drug delivery: Developmental issues and research initiatives. New York: Marcel Dekker. 324 p.)

TENJARLA, S.N., PURANAJOTI, P., KASINA, R. & MANDAL, T. 1996. Terbutaline transdermal delivery: Preformulation studies and limitations of in vitro predictive parameters. *Journal of pharmacy and pharmacology,* 48: 1138-1142.

THEILLEUX-DELANDE, V., GIRARD, F., HUYNH-DINH, T., LANCELOT, G. & POALETTI, J. 2000. The HIV - 1 (Lai) RNA dimerization. Thermodynamic parameters associated with the transition from jissing complex to the extended dimer. *European journal of biochemistry,* 267 (9): 2711-2719.

TOJO, K. 1997. The prediction of transdermal permeation: Mathematical models. (*In* Ghosh, T.K. & Pfister, W.R. & Yum, S.I., *eds.* Transdermal and topical drug delivery systems. Buffalo Grove: Interpharm. 713 p.)

TOUITOU, E., JUNGINGER, H.E., WEINER, N.D., NAGAI, T. & MEZEI, M. 1994. Liposomes as carriers for topical and transdermal delivery. *Journal of pharmaceutical sciences,* 83 (9): 1189-1203.

TREGEAR, R.T. 1966. The permeability of skin to albumin, dextrans and polyvinyl pyrrolidone. Journal of investigative dermatology, 46: 24S-27S

UNAIDS. 2006. Report on global AIDS epidemic 2006. http://www.unaids.org/en/HIV_data/2006GlobalReport/default.asp. [Date of access: 10 Nov. 2006].

VERONESE, F.D., DEVICO, A.L., COPELAND, T.D., OROSZLAN, S., GALLO, R.C. & SARNGADHARAN, M.G. 1985. Characterization of gp41 as a trans-membrane protein coded by the HTLV-III/LAV envelope gene. *Science,* 229 (4720): 1402-1405.

WASHINGTON, C. & WASHINGTON, N. 1989. Physiological pharmaceutics. London: Taylor & Francis. 195 p.

WATKINSON, A.C., JOUBIN, H., GREEN, D.M., BRAIN, K.R. & HADGRAFT, J. 1995. The influence of vehicle on permeation from saturated solutions. *International journal of pharmaceutics,* 121: 27-35.

WEST, D.P. & NOWAKOWSKI, P.A. 1996. Dermatologic products. (*In* Covington, T.R., Berardi, R.R. & Young L.L., *eds.* Handbook of nonprescription drugs. 11th ed. Washington: American Pharmaceutical Press. 774 p.)

WIECHERS, J.W. 1989. The barrier function of the skin in relation to percutaneous absorption of drugs. *Pharmaceutisch weekblad, scientific edition,* 11 (6): 185-198.

WILD, C.T., SHUGARS, D.C., GREENWELL, T.K., MCDANAL, C.B. & MATTHEWS, T.J. 1994. Peptides corresponding to a predictive alpha-helical domain of Human Immunodeficiency Virus type 1 gp41 are potent inhibitors of virus infection. *Proceedings of the National Academy of Sciences the United States of America,* 91: 9770-9774.

WILLARD-GALLO, K.E., FUITADO, M., BURNY, A. & WOLINSKY, S.M. 2001. Down modulation of TCR/CD3 surface complexes after HIV-1 infection is associated with differential expression of the viral regulatory gene. *European journal of immunology,* 31 (4): 969-979.

WILLIAMS, A.C. 2003. Transdermal and topical drug delivery: From theory to clinical practice. London: Pharmaceutical Press. 242 p.

WILLIAMS, A.C. & BARRY, B.W. 1992. Skin absorption enhancers. *Critical reviews in therapeutic drug carrier systems,* 9: 305-353.

WINKELSTEIN, W. Jr, WILEY, J.A., PADIAN, N.S., SAMUEL, M., SHIBOSKI, S., ASCHER, M.S. & LEVY, J.A. 1988. The San Francisco men's health study: Continued decline in HIV seroconversion rates among homosexual/bisexual men. *American journal of public health,* 78: 1472-1474.

WRIGHT, S.J., CENTONZE, V.E., STRICKER, S.A., DE VRIES, P.J., PADDOCK, S.W. & SCHATTEN, G. 1993. An introduction to confocal microscopy and three-dimensional reconstruction. (*In* Matsumoto, B., *ed.* Cell biology applications of confocal microscopy. USA: Academic Press. p. 2-43.)

WURSTER, D.E. & KRAMER, S.F. 1961. Investigation of some factors influencing percutaneous absorption. *Journal of pharmaceutical sciences,* 50: 288-293.

YALKOWSKY, S.H., FLYNN, G.L. & SLUNICK, T.G. 1972. Importance of chain length on physicochemical and crystalline properties of organic homologs. *Journal of pharmaceutical sciences,* 61: 852-857.

YALKOWSKY, S.H. & VALVANI, S.C. 1980. Solubility and partitioning I: Solubility of nonelectrolytes in water. *Journal of pharmaceutical sciences,* 69 (8): 912-922.

YOUNG, S.D., BRITCHER, S.F., TRAN, L.O., PAYNE, L.S., LUMMA, W.C., LYLE, T.A., HUFF, J.R., ANDERSON, P.S., OLSEN, D.B., CARROLL, S.S., PETTIBONE, D.J., O'BRIEN, J.A., BALL, R.G., BALANI, S.K., LIN, J.H., CHEN, I., SCHLEIF, W.A., SARDANA, V.V., LONG, W.J., BYRNES, V.W. & EMINI, E.A. 1995. L-743,726 (DMP-266): A novel, highly potent non-nucleoside inhibitor of the Human Immunodeficiency Virus type 1 reverse transcriptase. *Antimicrobiol agents and chemotherapy,* 39: 2602-2605.

ZATZ, J.L. 1993. Scratching the surface: Rationale and approaches to skin permeation. (*In* Zatz, J.L., *ed.* Skin permeation: Fundamentals and application. Wheaton: Allured Publishing Corp. 300 p.)

ZHENG, Y.H., LOVSIN, N. & PETERLIN, B.M. 2005. Newly identified host factors modulate HIV replication. *Immunology letters,* 97 (2): 225-234.

ZHOU, J. & AIKEN, C. 2001. Nef enhances Human Immunodeficiency Virus type 1 infectivity resulting from intervirion fusion: Evidence supporting a role for nef at the virion envelop. *Journal of virology,* 75 (13): 5851-5859.

ZHU, T., KORBER, B.T., NAHMIAS, A.J., HOOPER, E., SHARP, P.M. & HO, D.D. 1998. An African HIV-1 sequence from 1959 and implications for the origin of the epidemic. *Nature,* 391 (6667): 594-597.

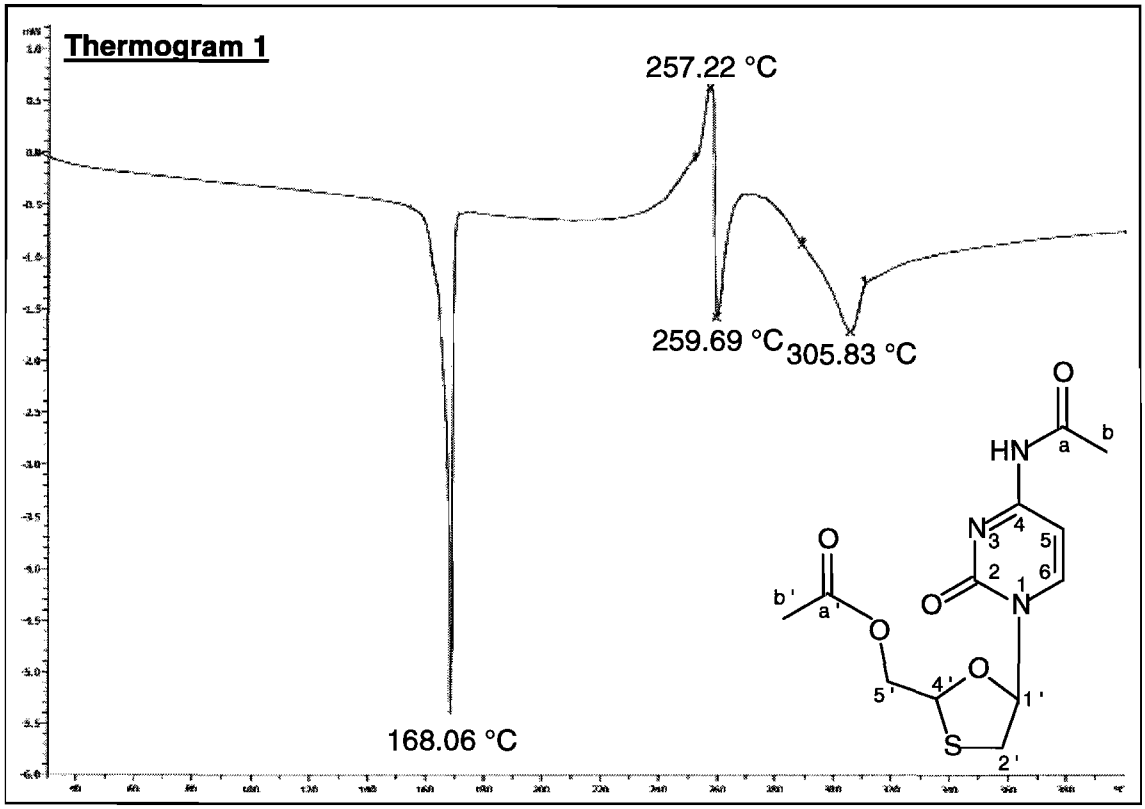
Thermogram 1
257.22 °C
259.69 °C
305.83 °C
168.06 °C

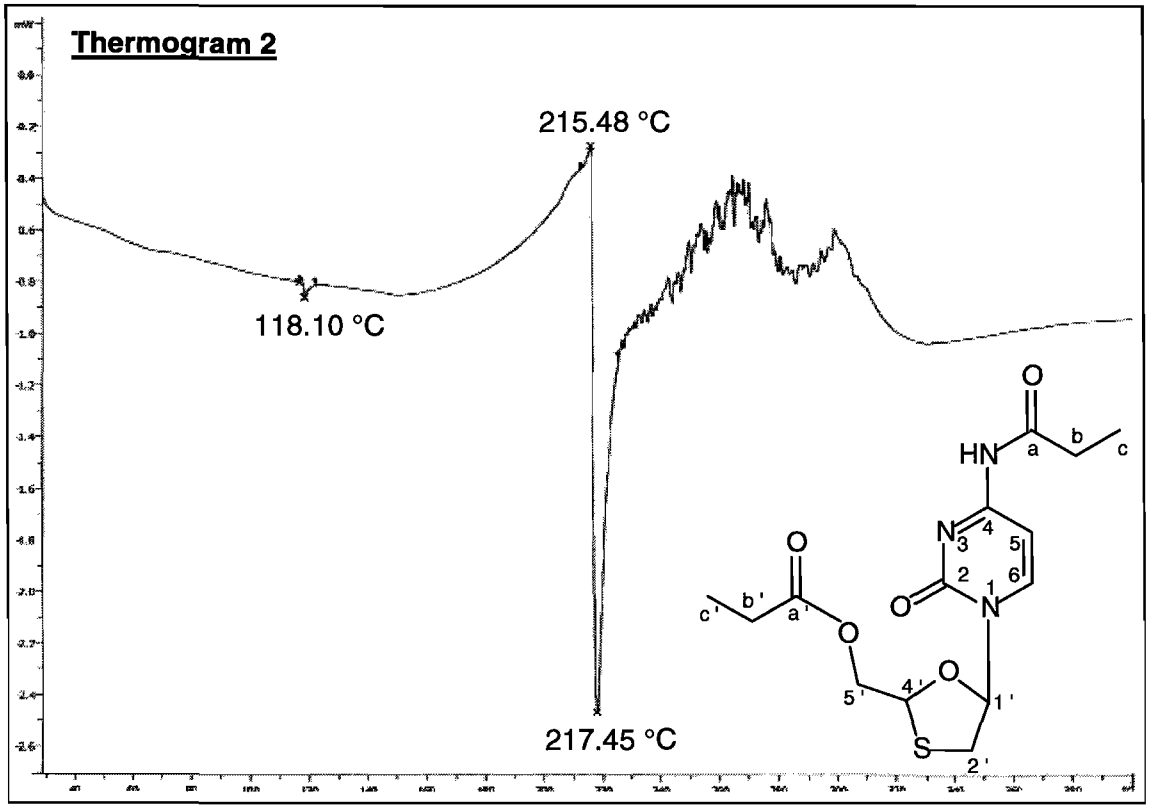
Thermogram 2
215.48 °C
118.10 °C
217.45 °C

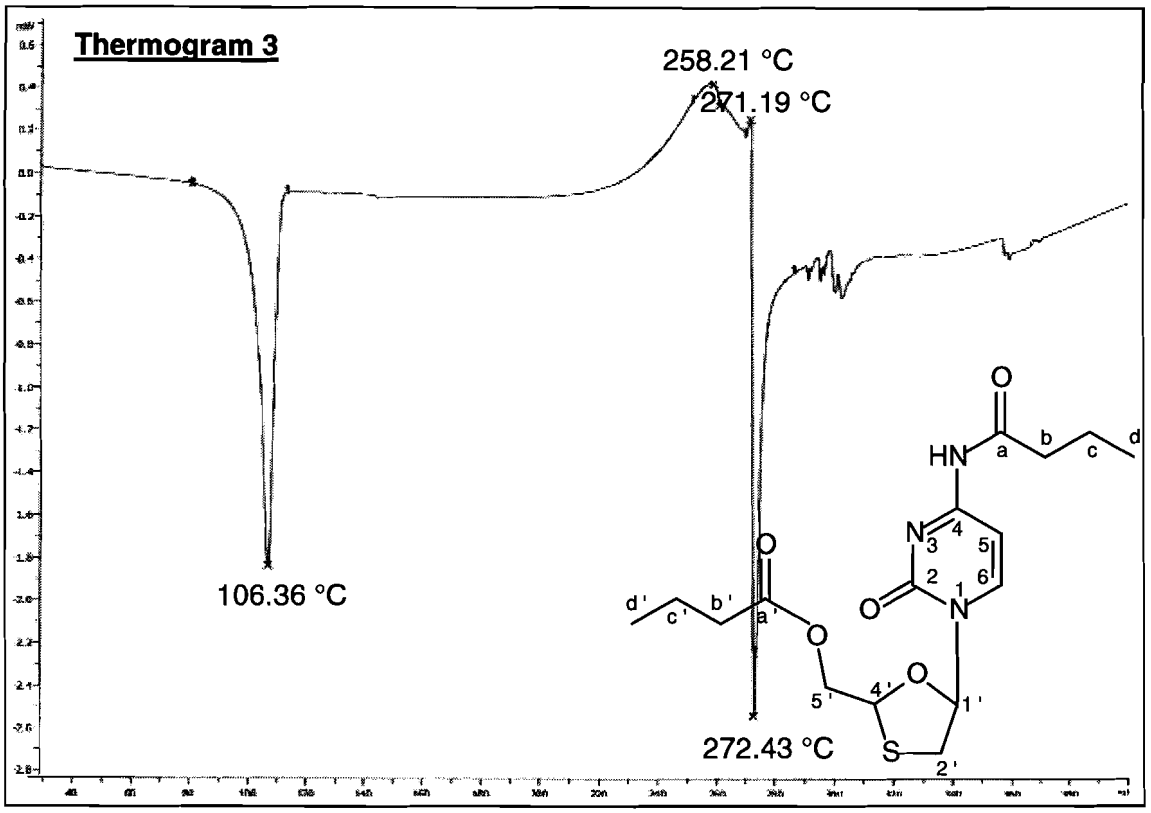
Thermogram 3
258.21 °C
271.19 °C
106.36 °C
272.43 °C

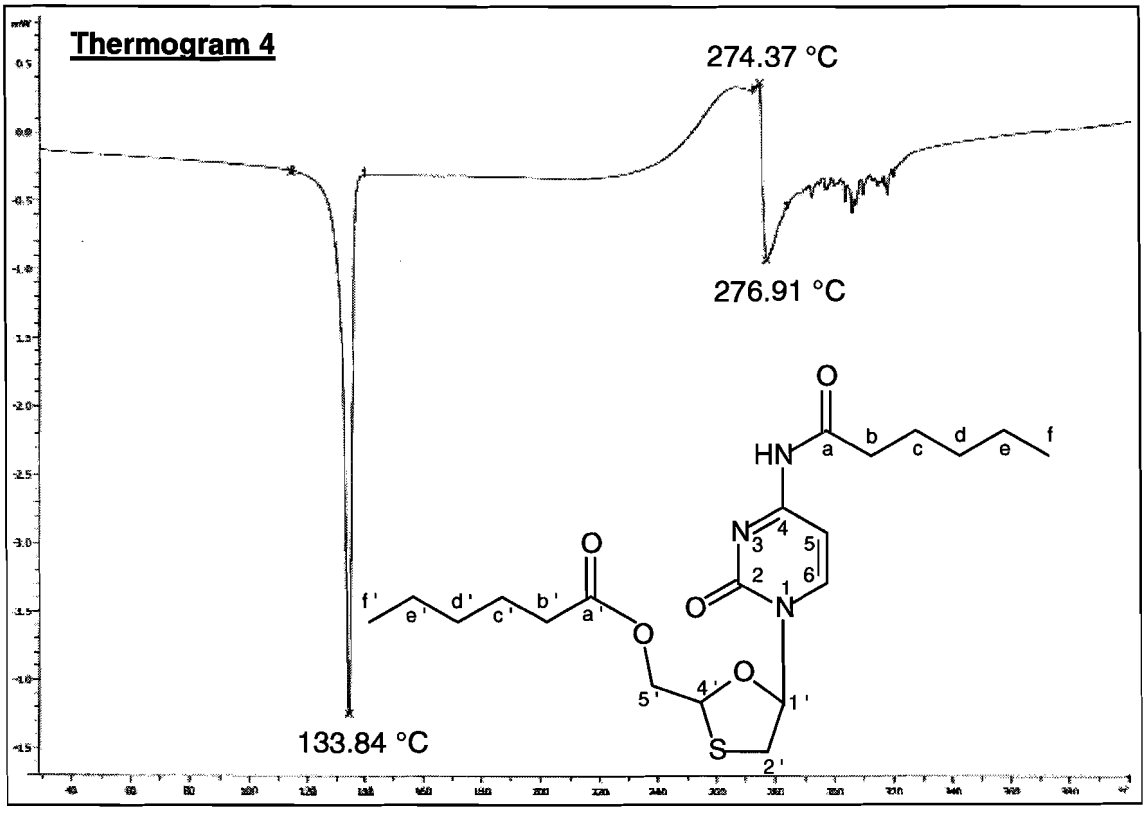
Thermogram 4
274.37 °C
276.91 °C
133.84 °C

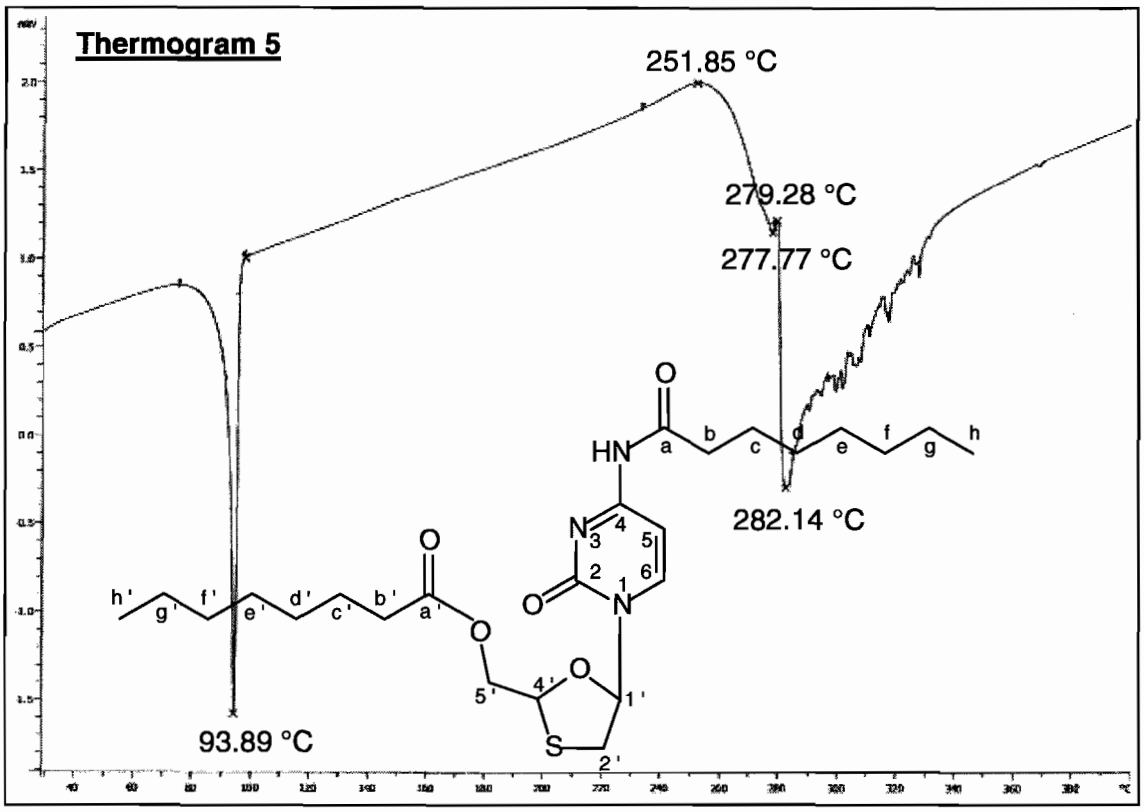
Thermogram 5
251.85 °C
279.28 °C
277.77 °C
282.14 °C
93.89 °C

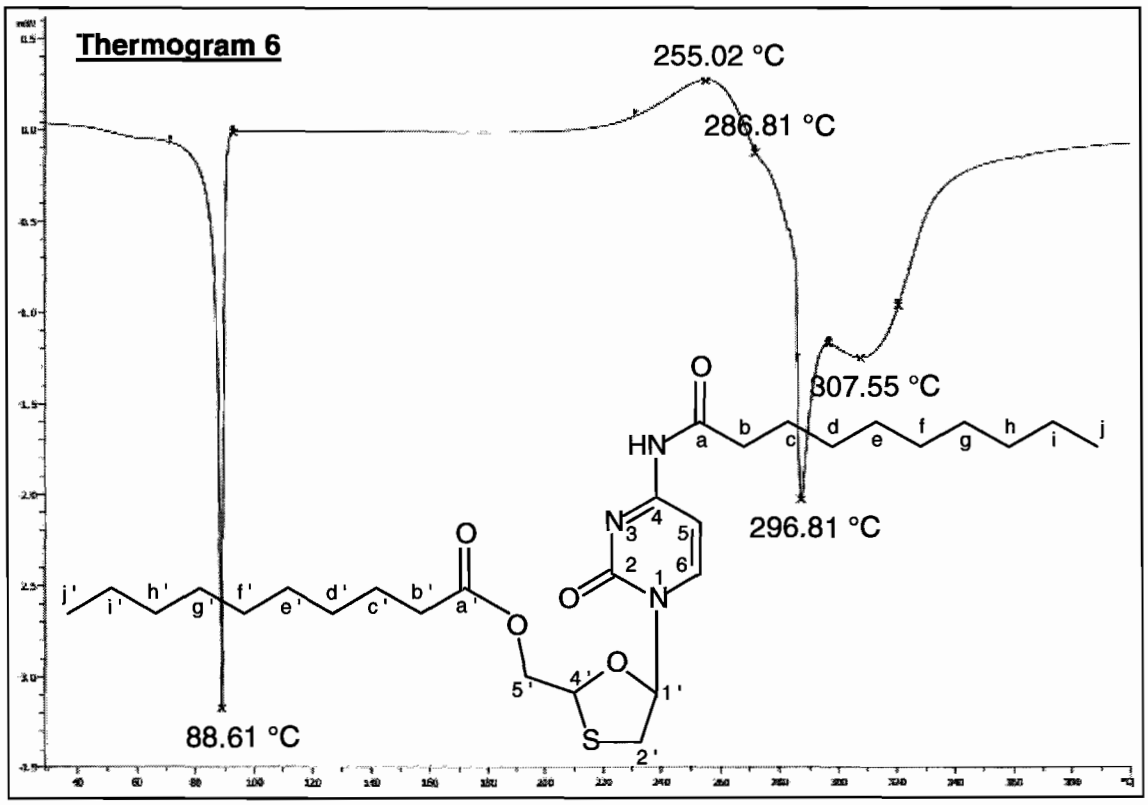
Thermogram 6
255.02 °C
286.81 °C
307.55 °C
296.81 °C
88.61 °C

Spectrum 1

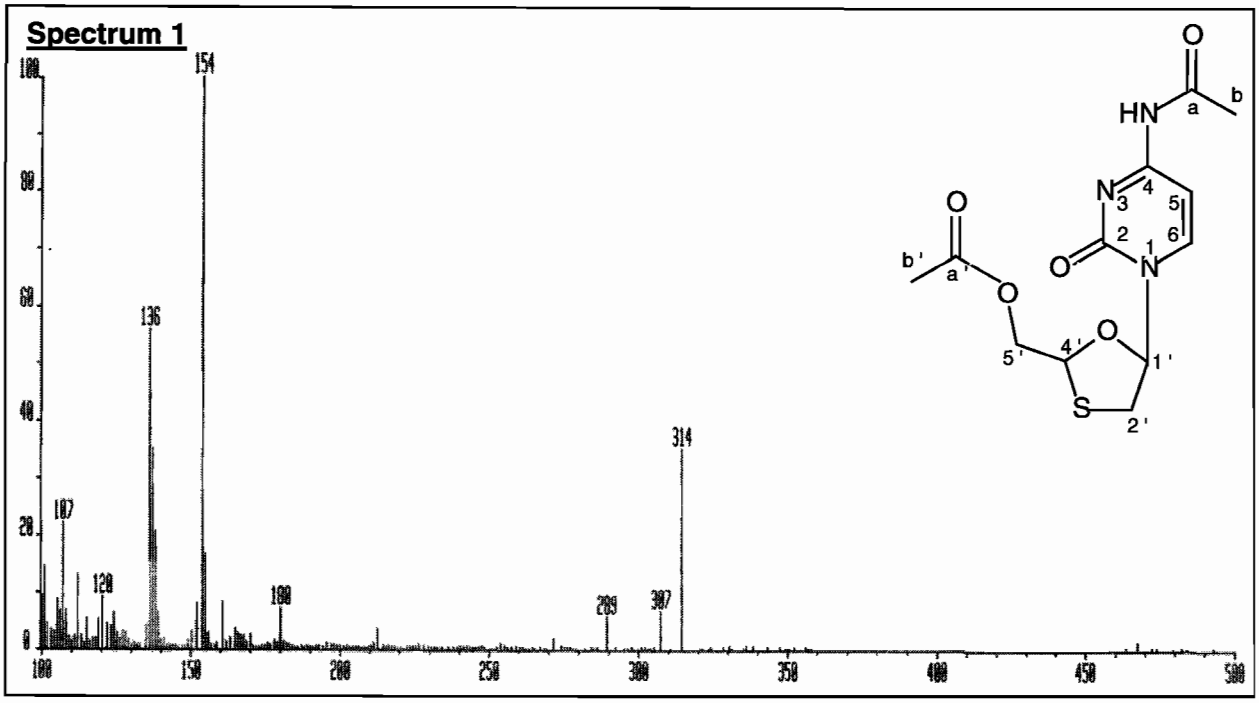

Spectrum 2

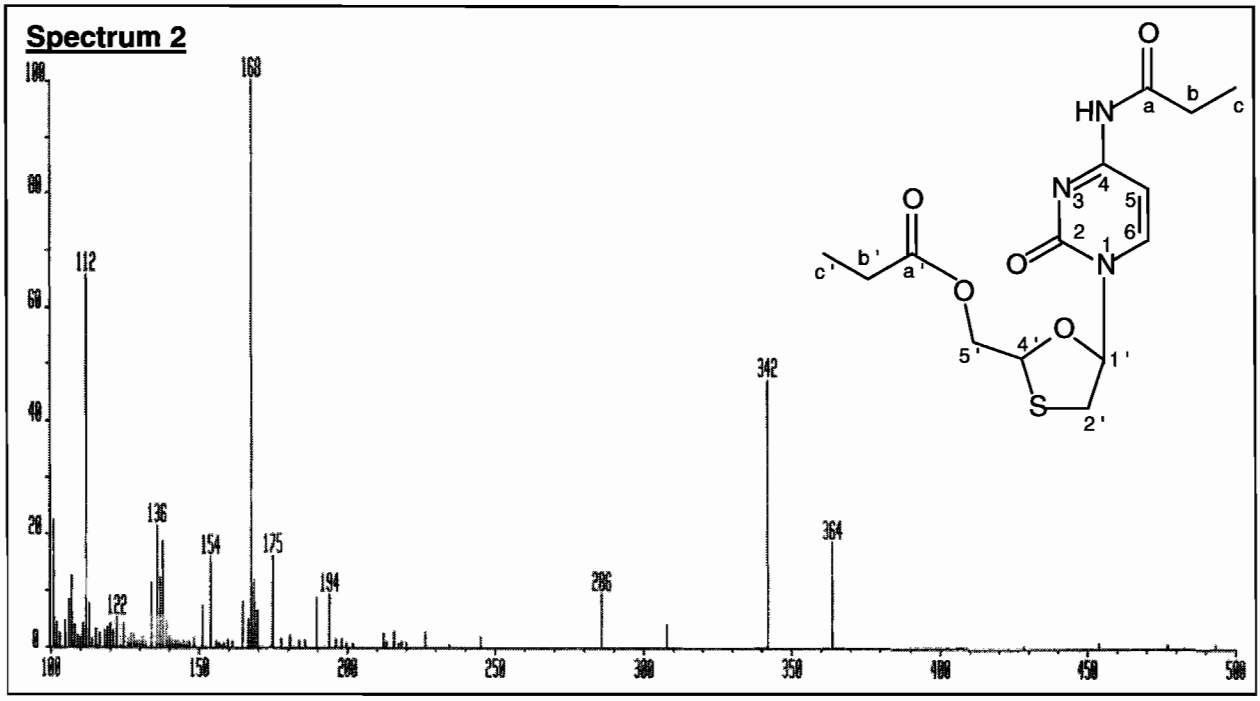

Spectrum 3

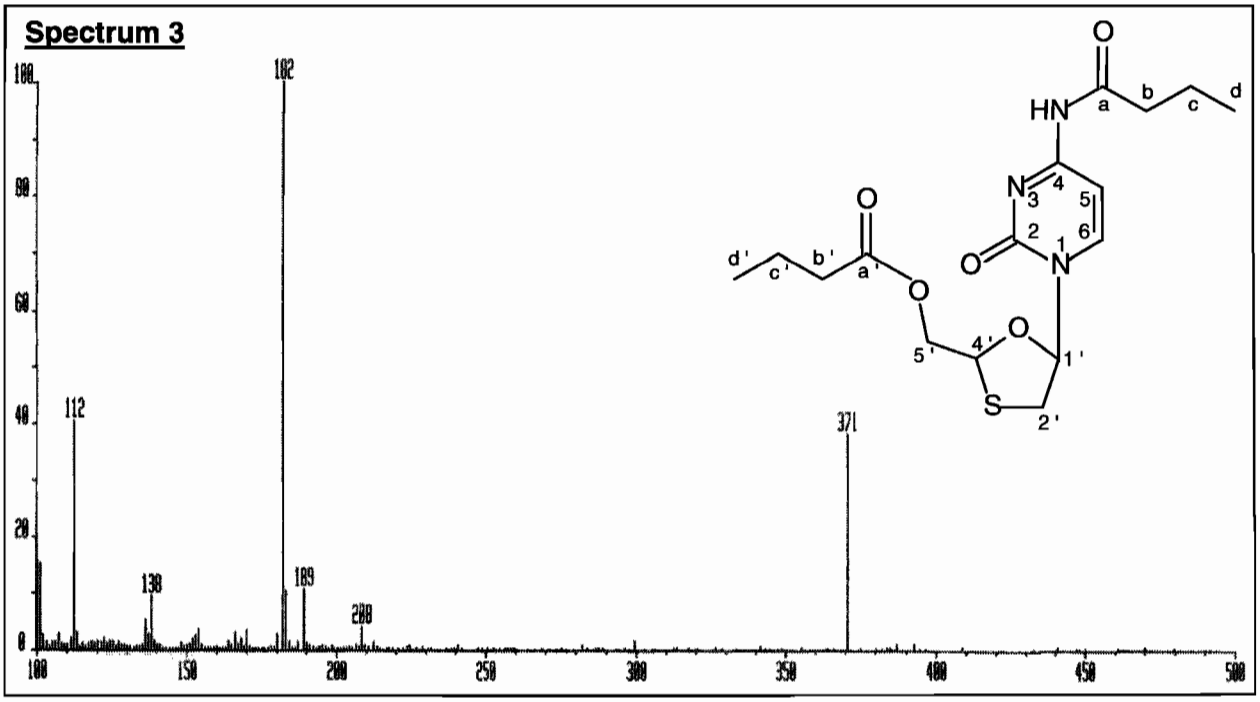

Spectrum 4

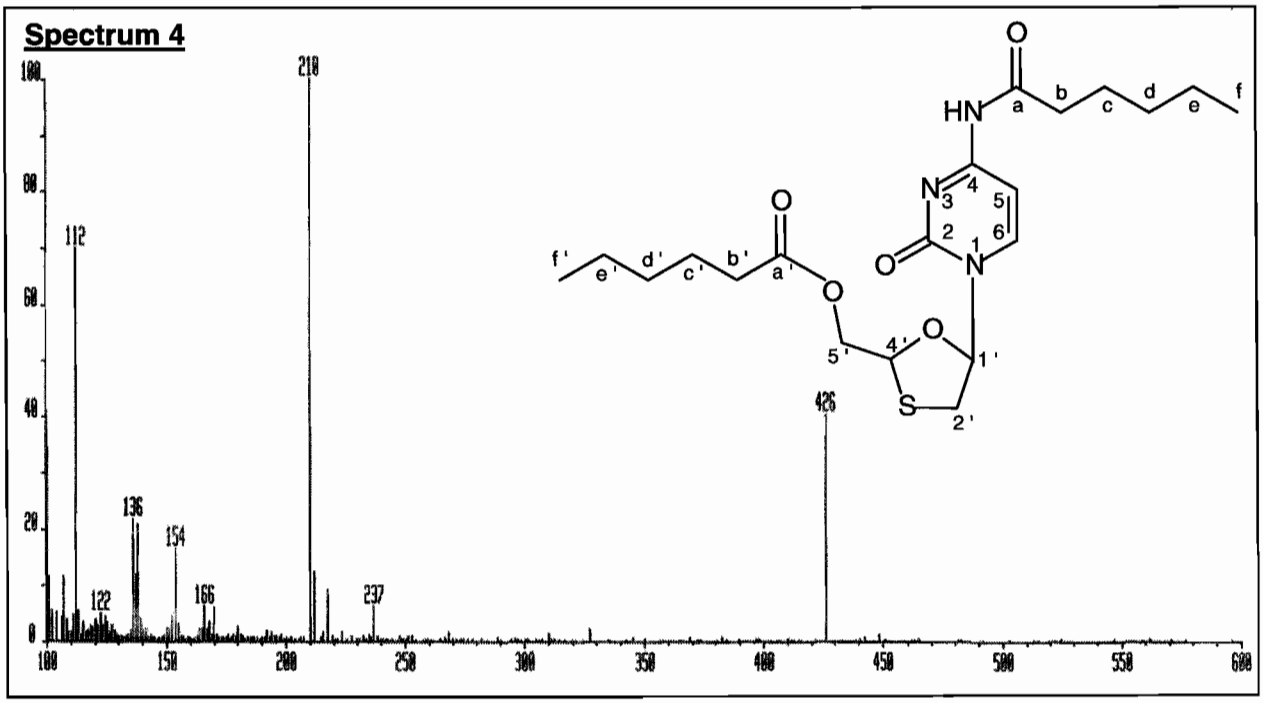

Spectrum 5

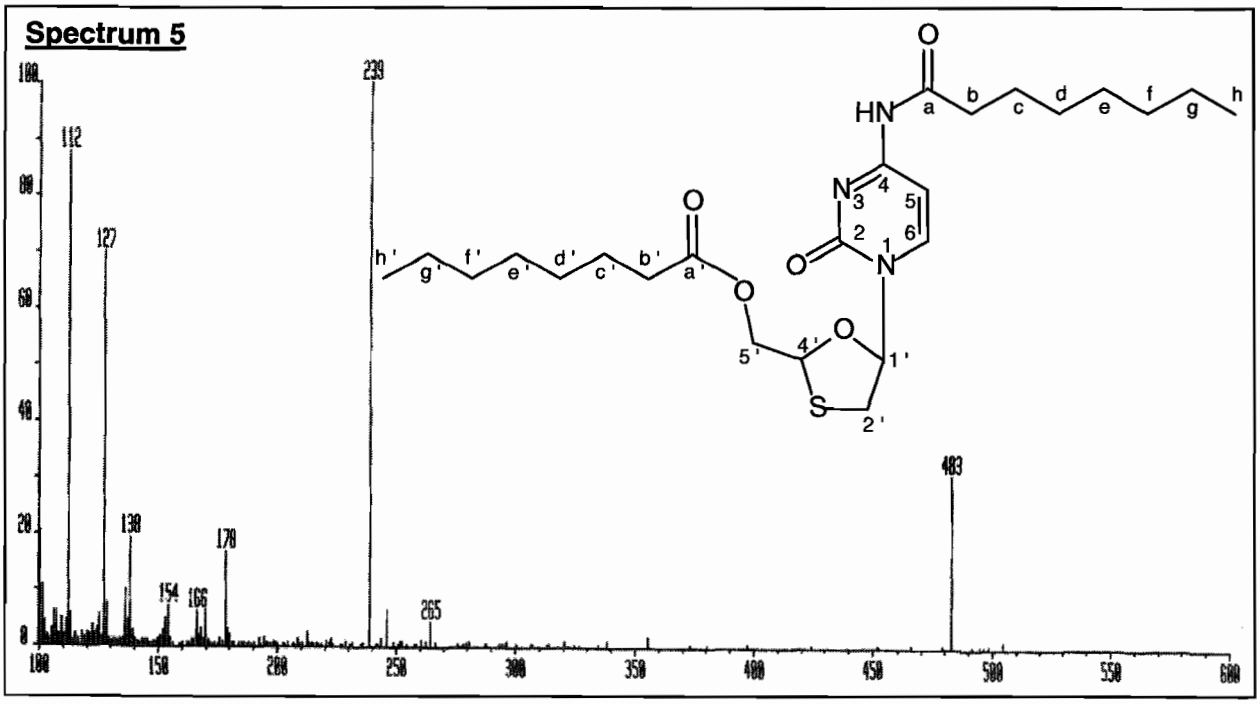

Spectrum 6

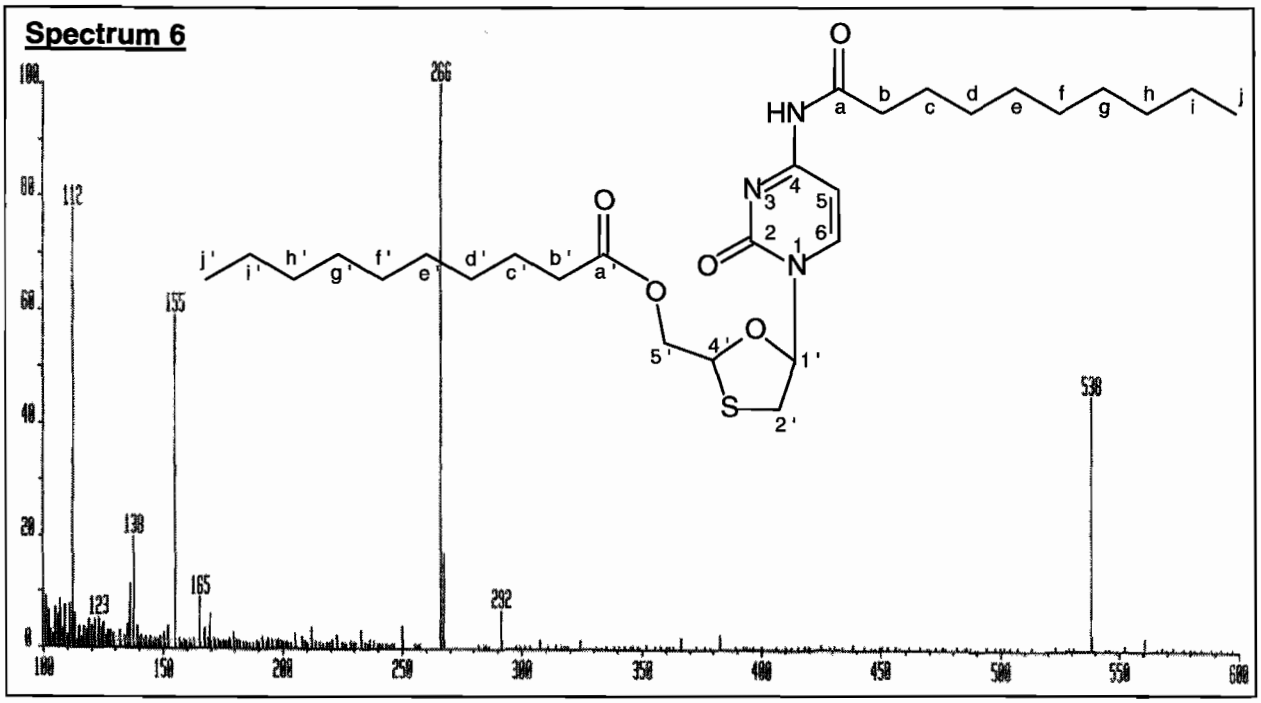

Spectrum 7

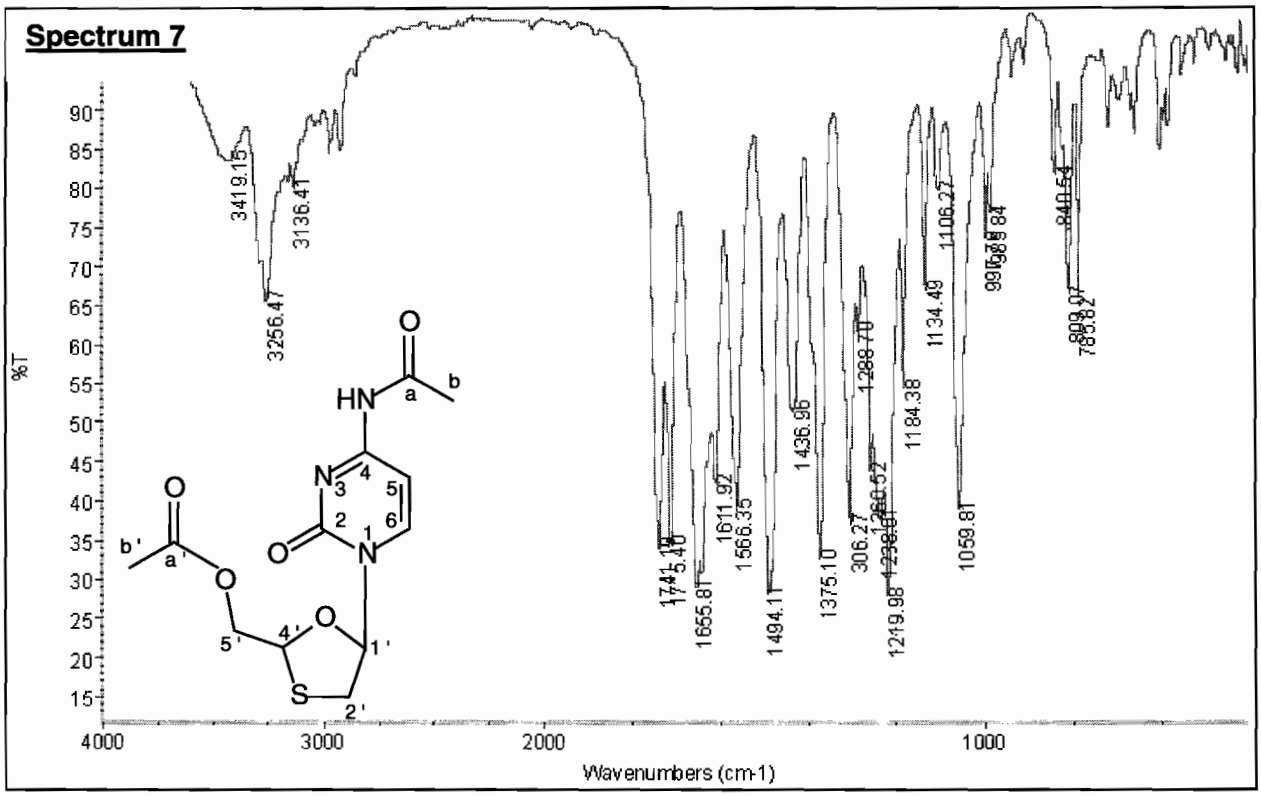

Spectrum 8

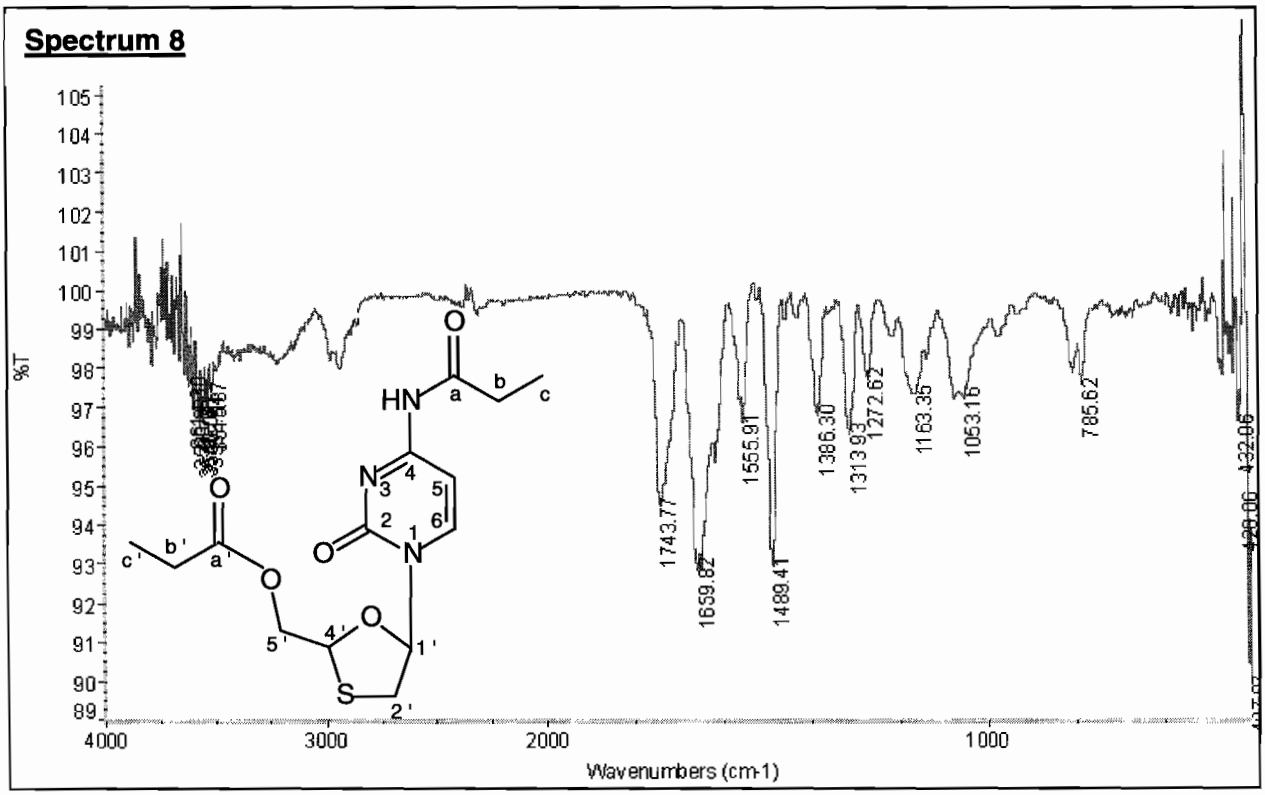

Spectrum 9

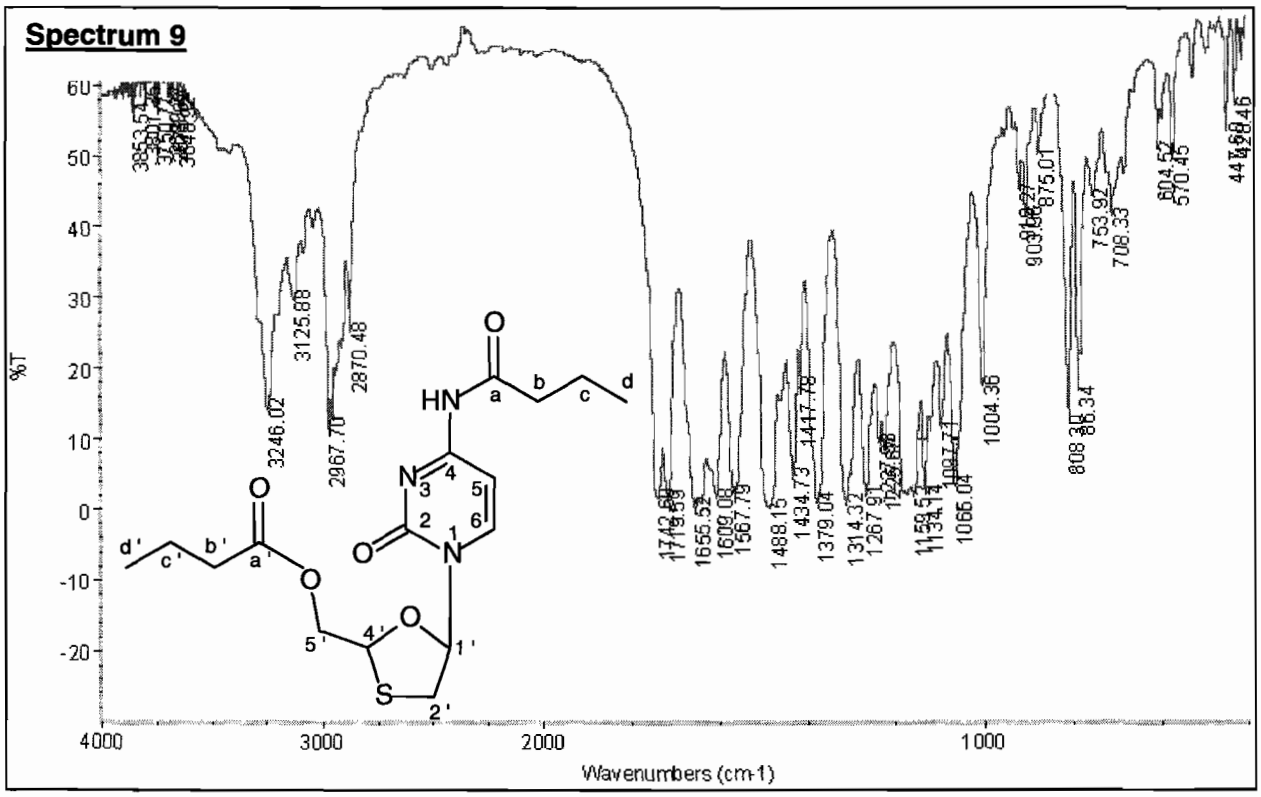

Spectrum 10

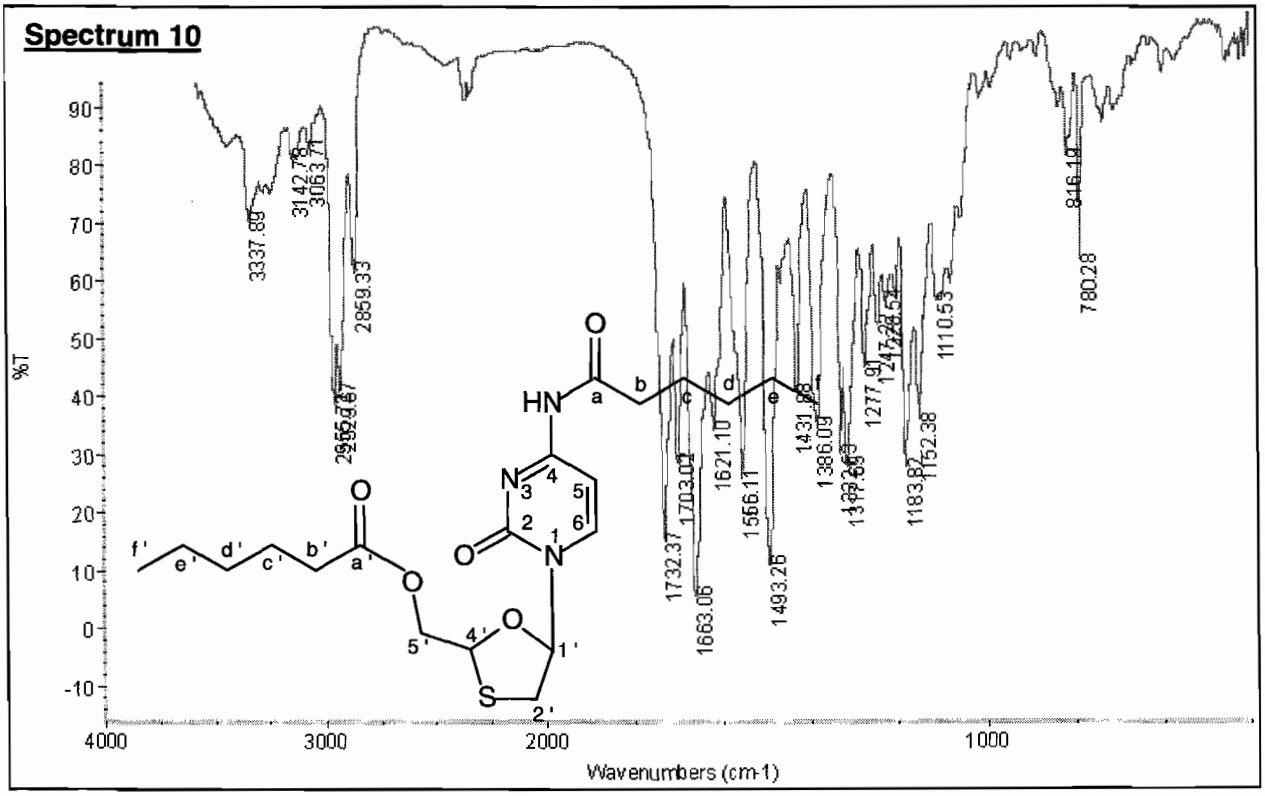

Spectrum 11

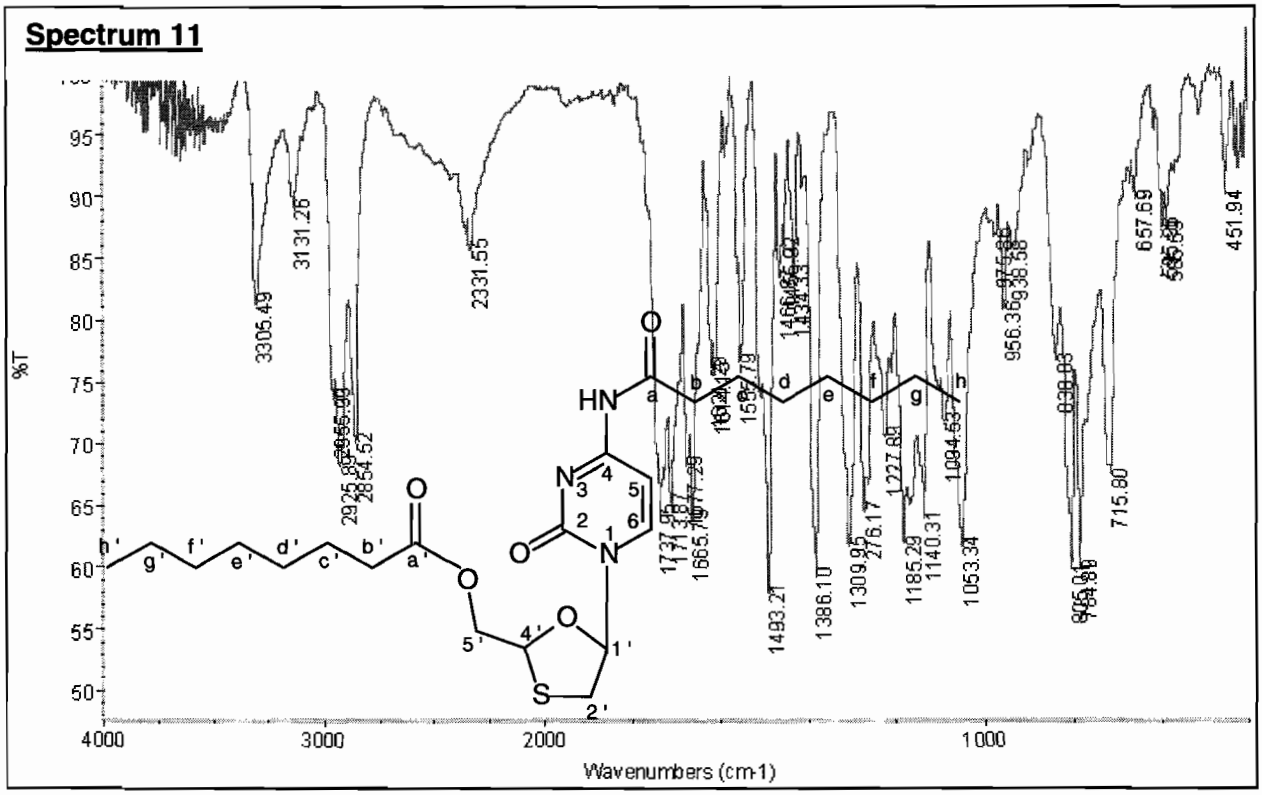

Spectrum 12

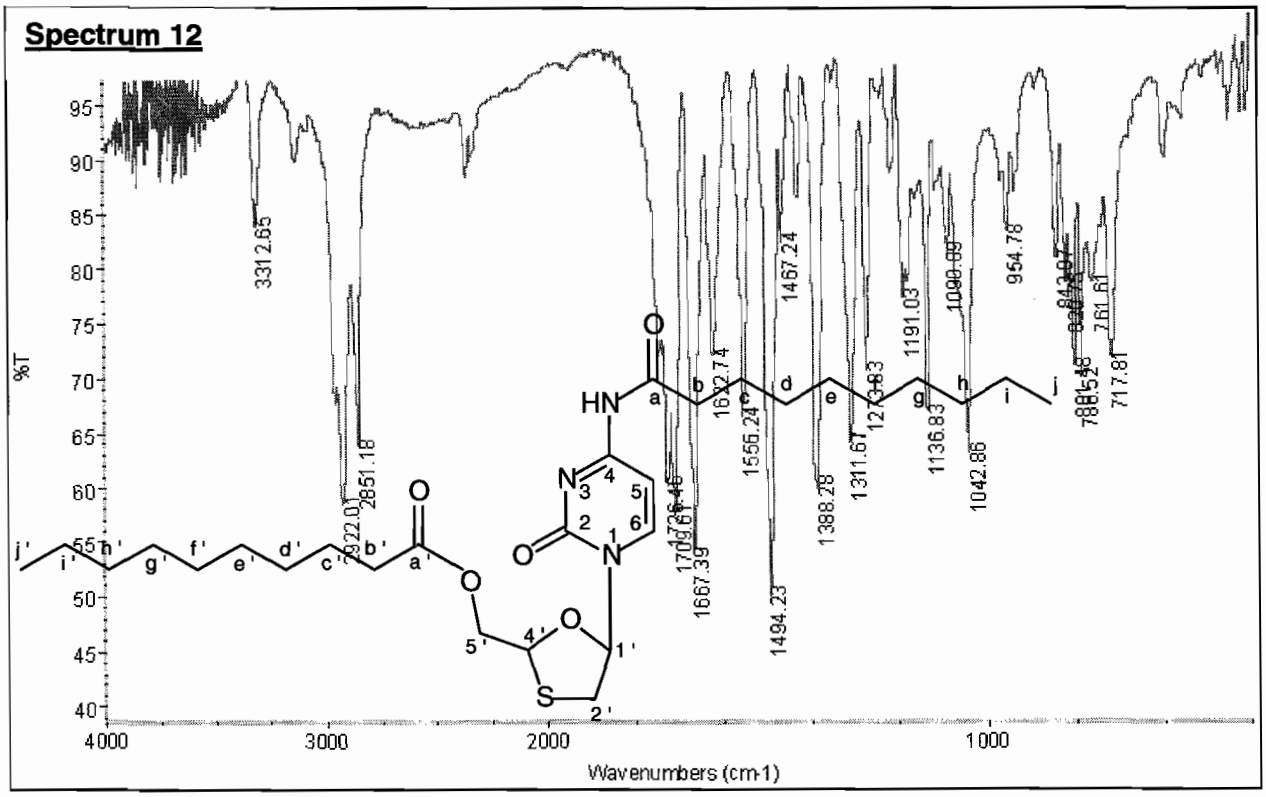

Spectrum 13

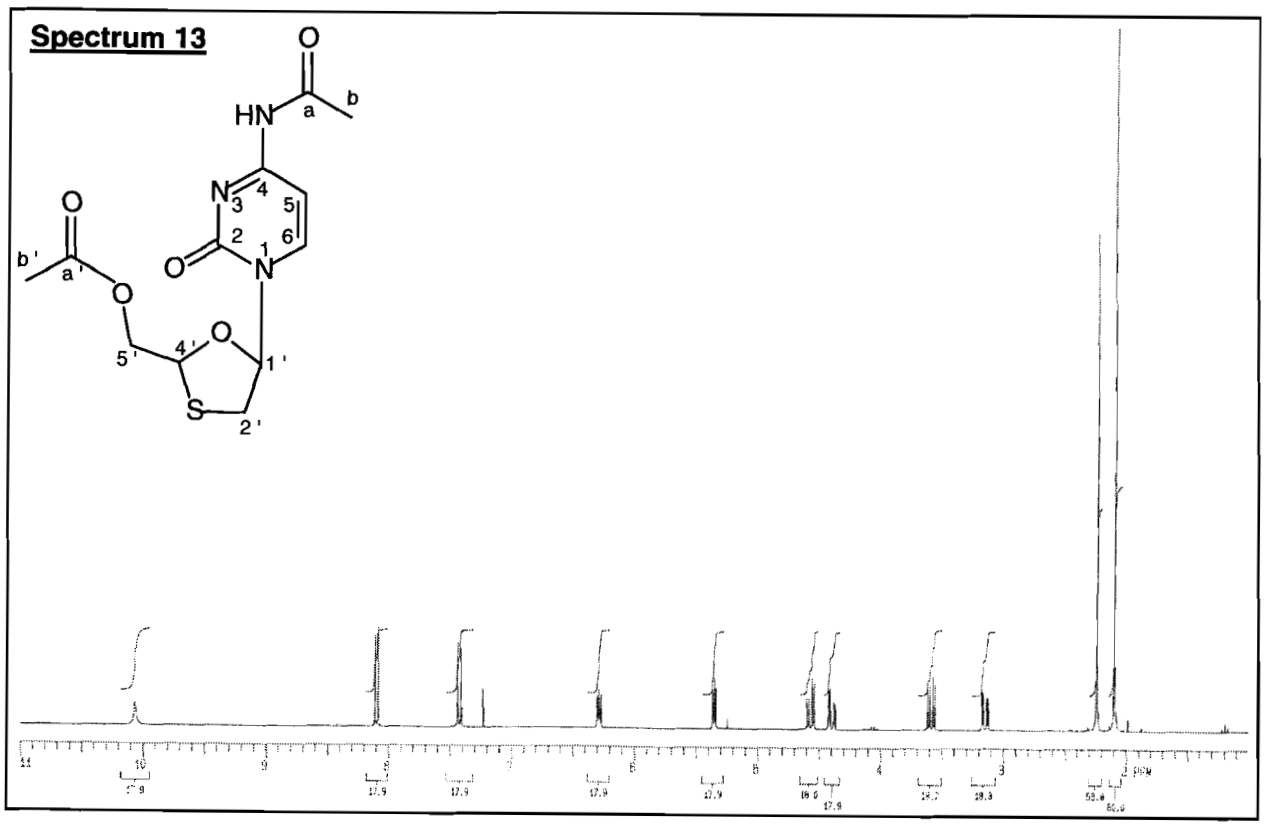

Spectrum 14

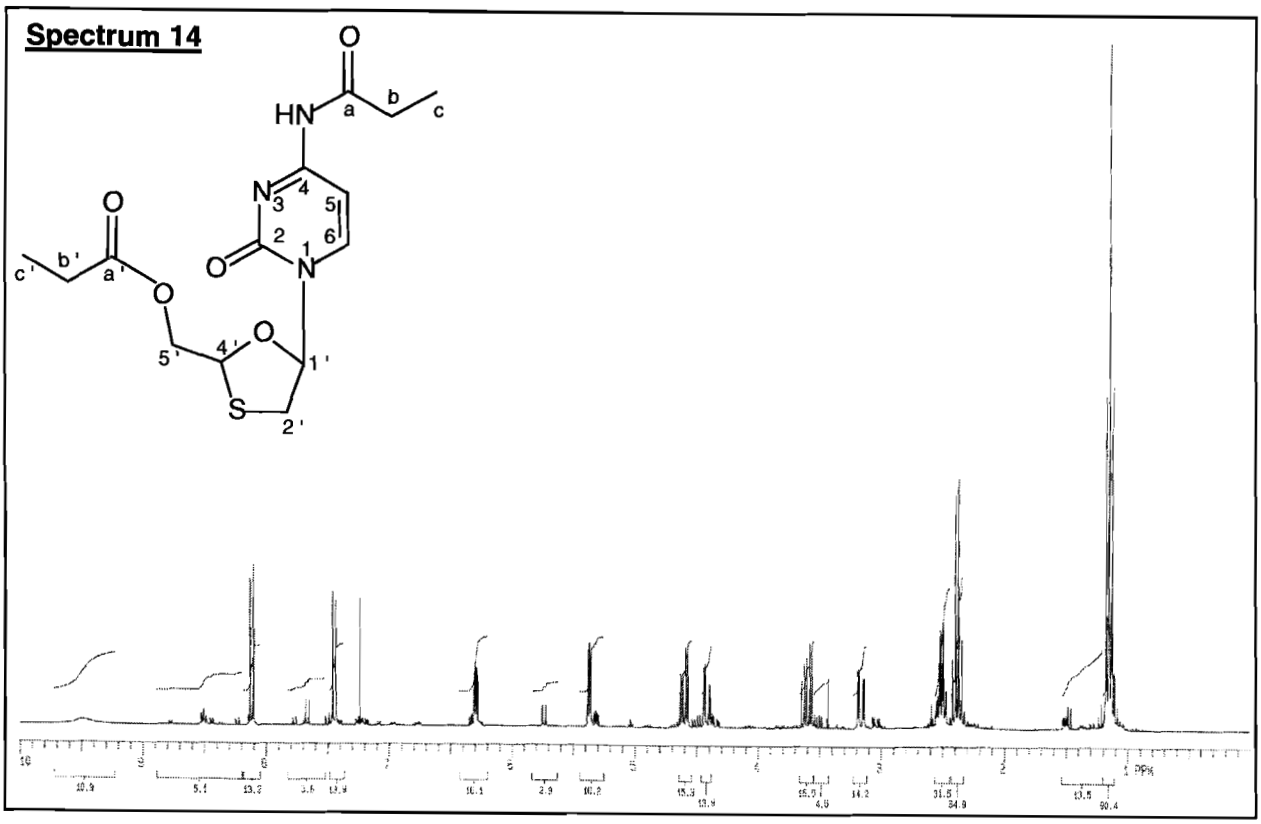

Spectrum 15

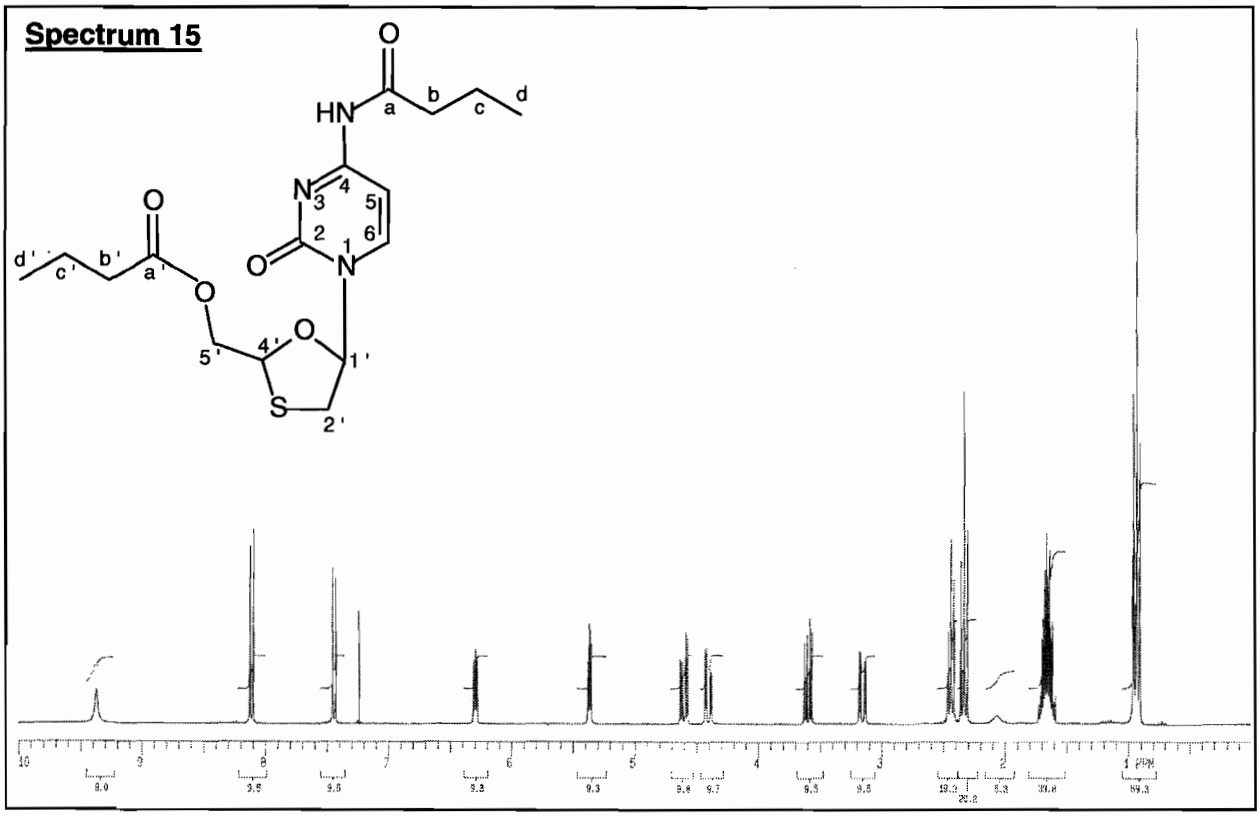

Spectrum 16

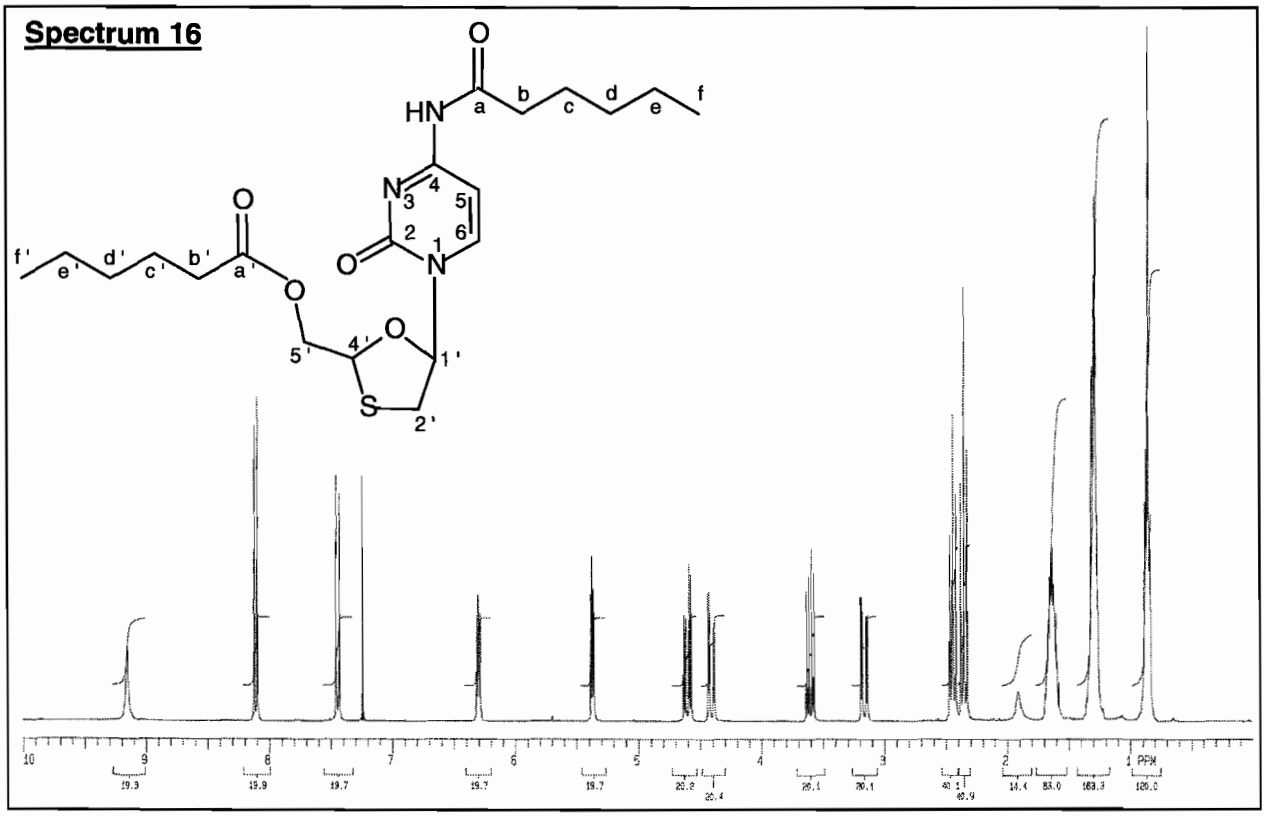

Spectrum 17

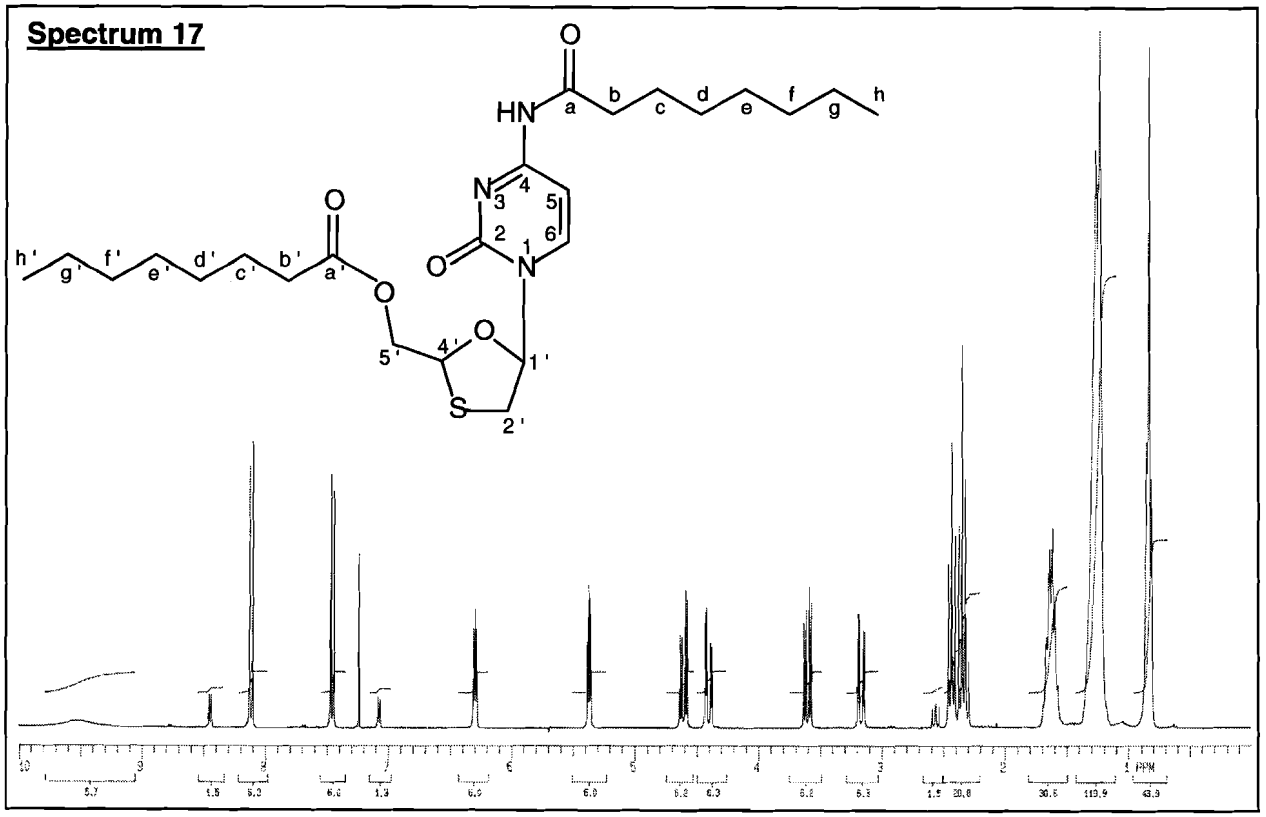

Spectrum 18

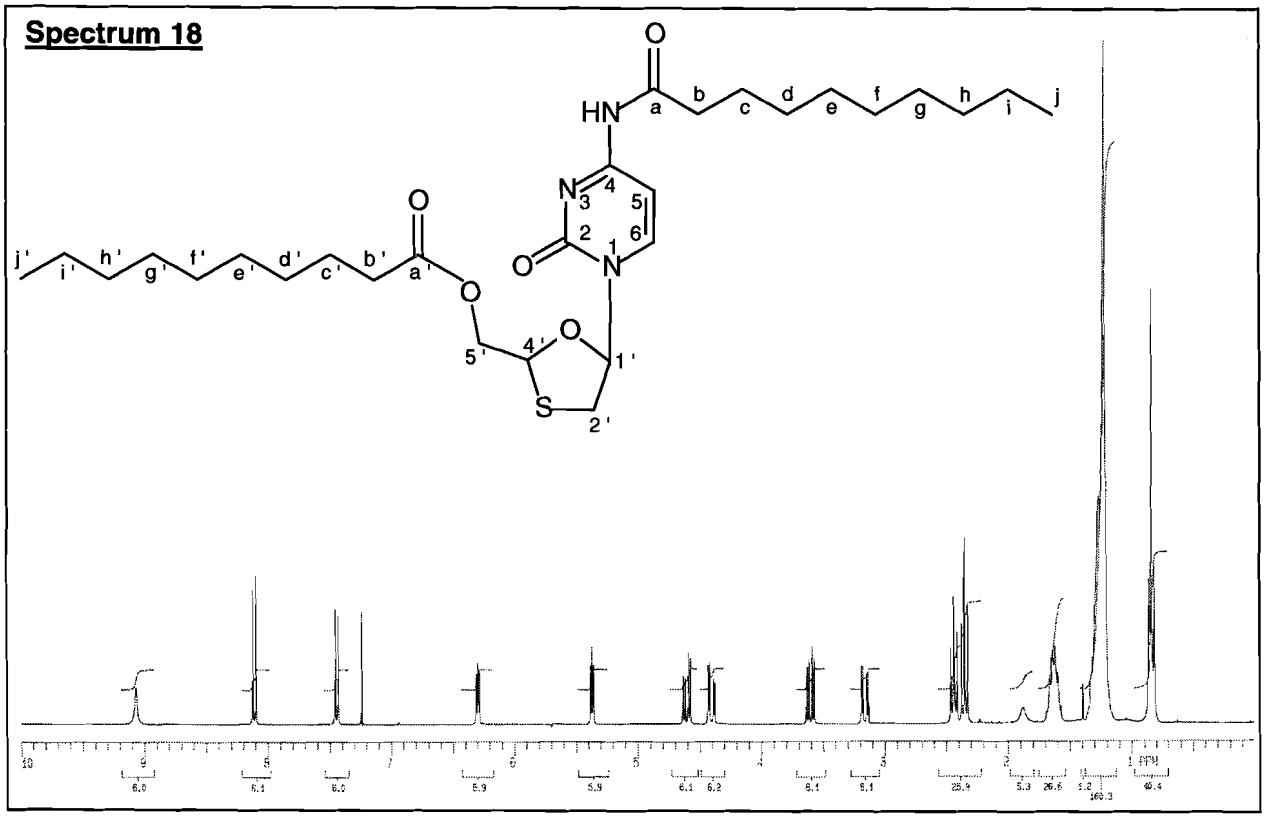

Spectrum 19

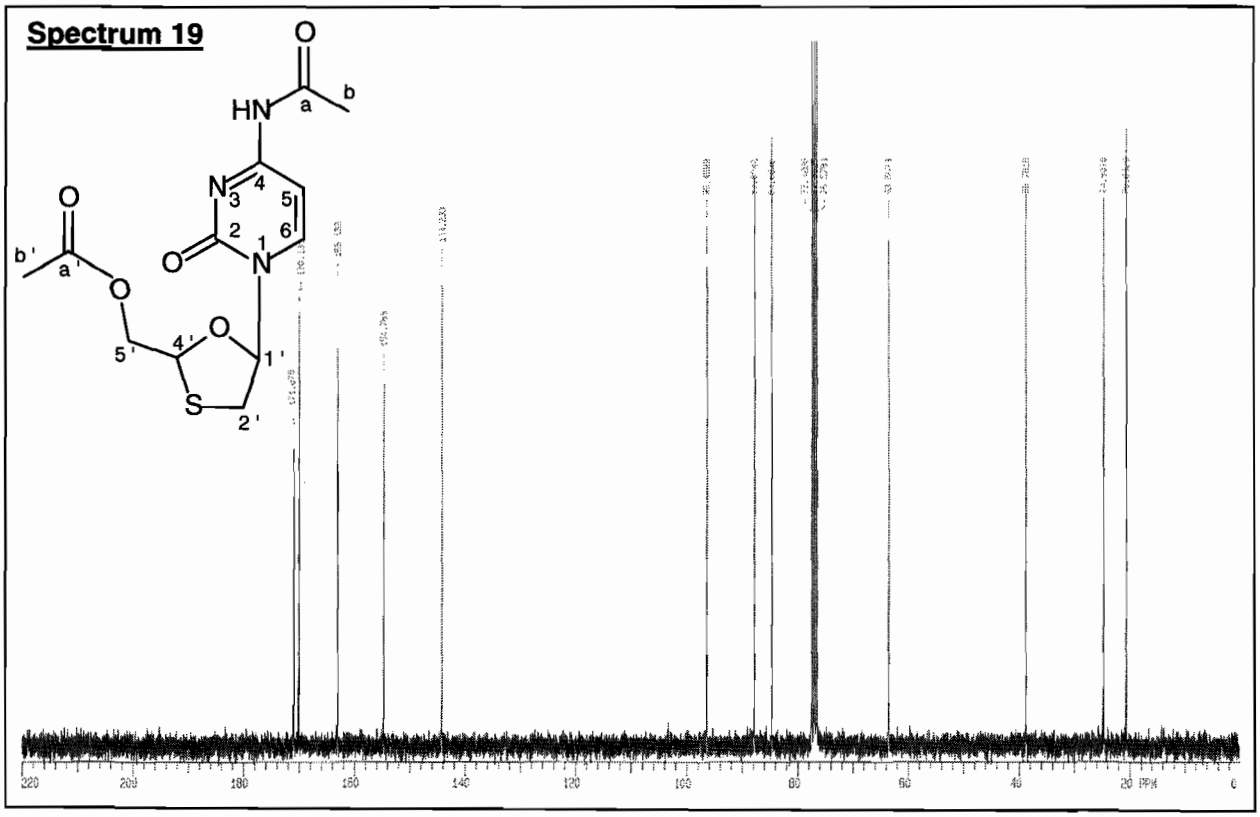

Spectrum 20

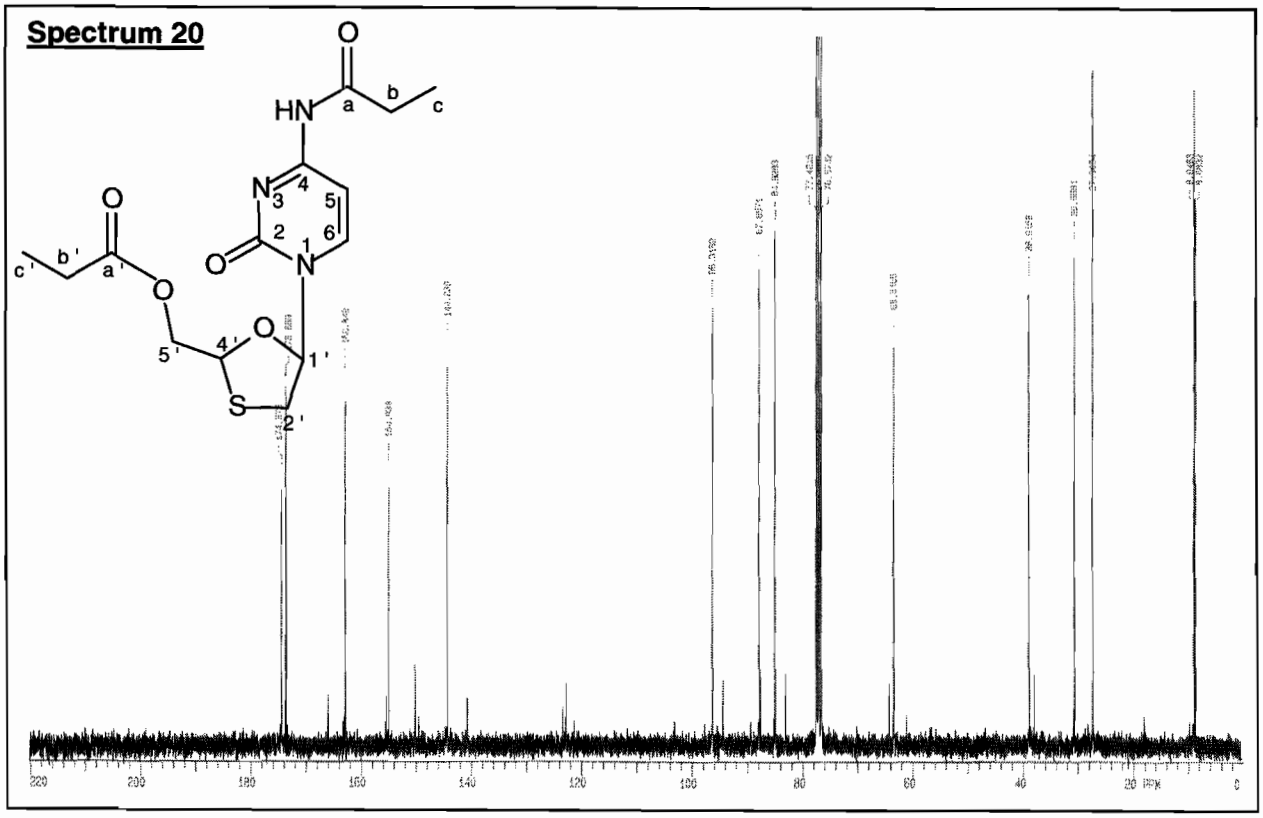

Spectrum 21

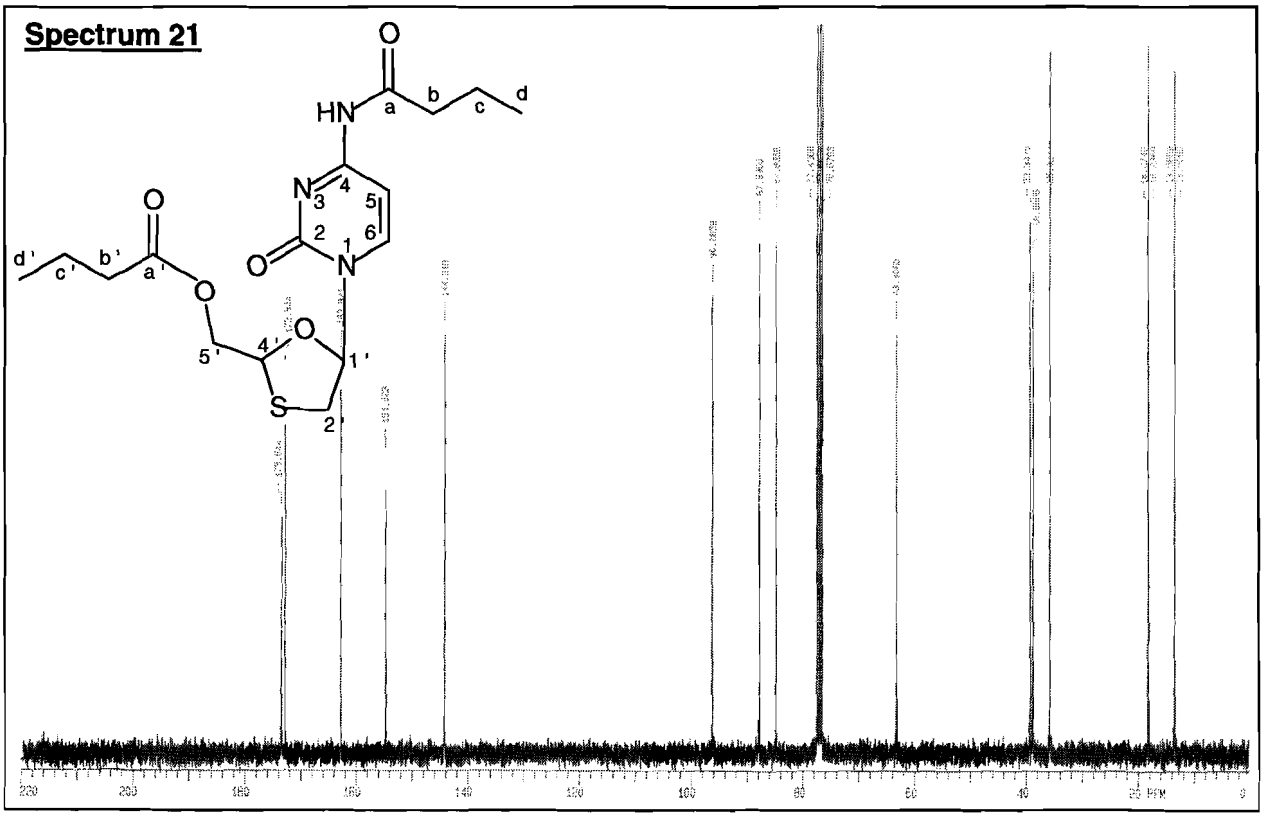

Spectrum 22

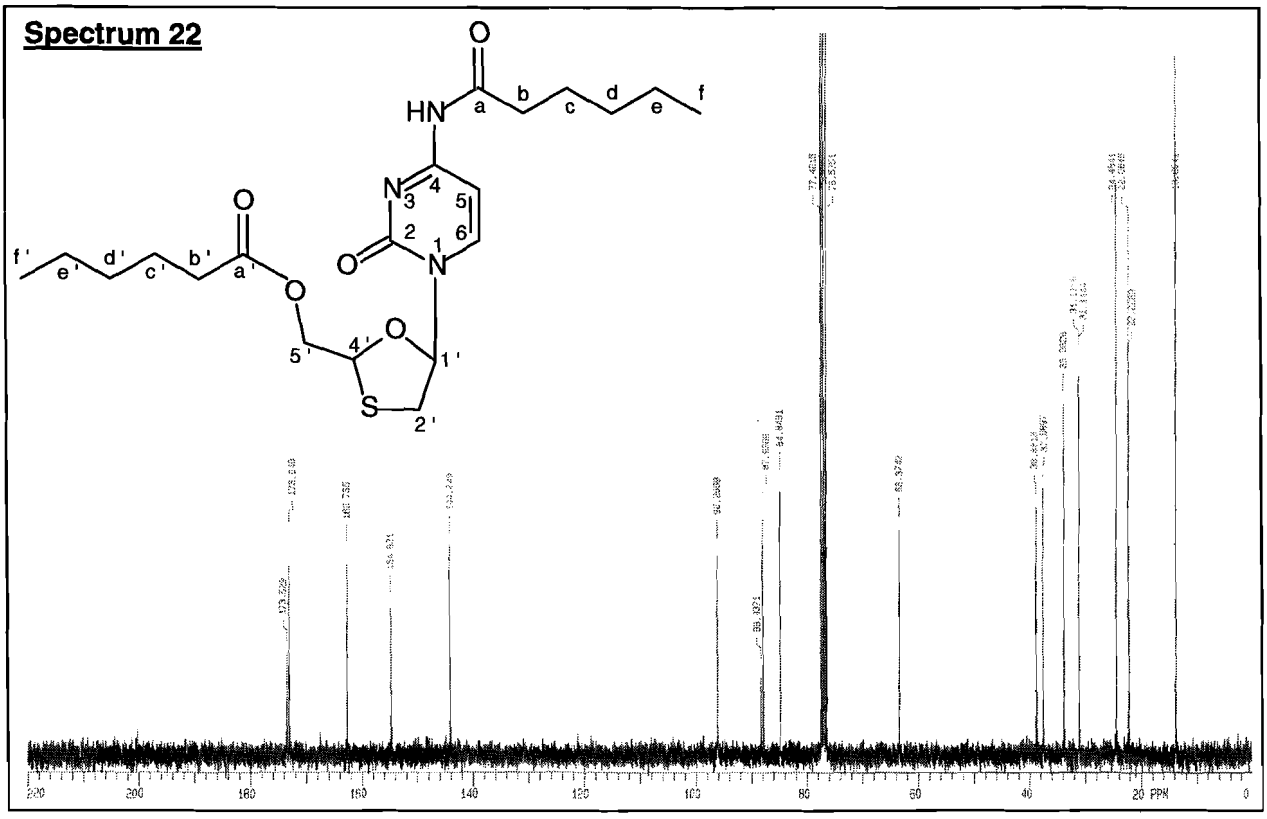

Spectrum 23

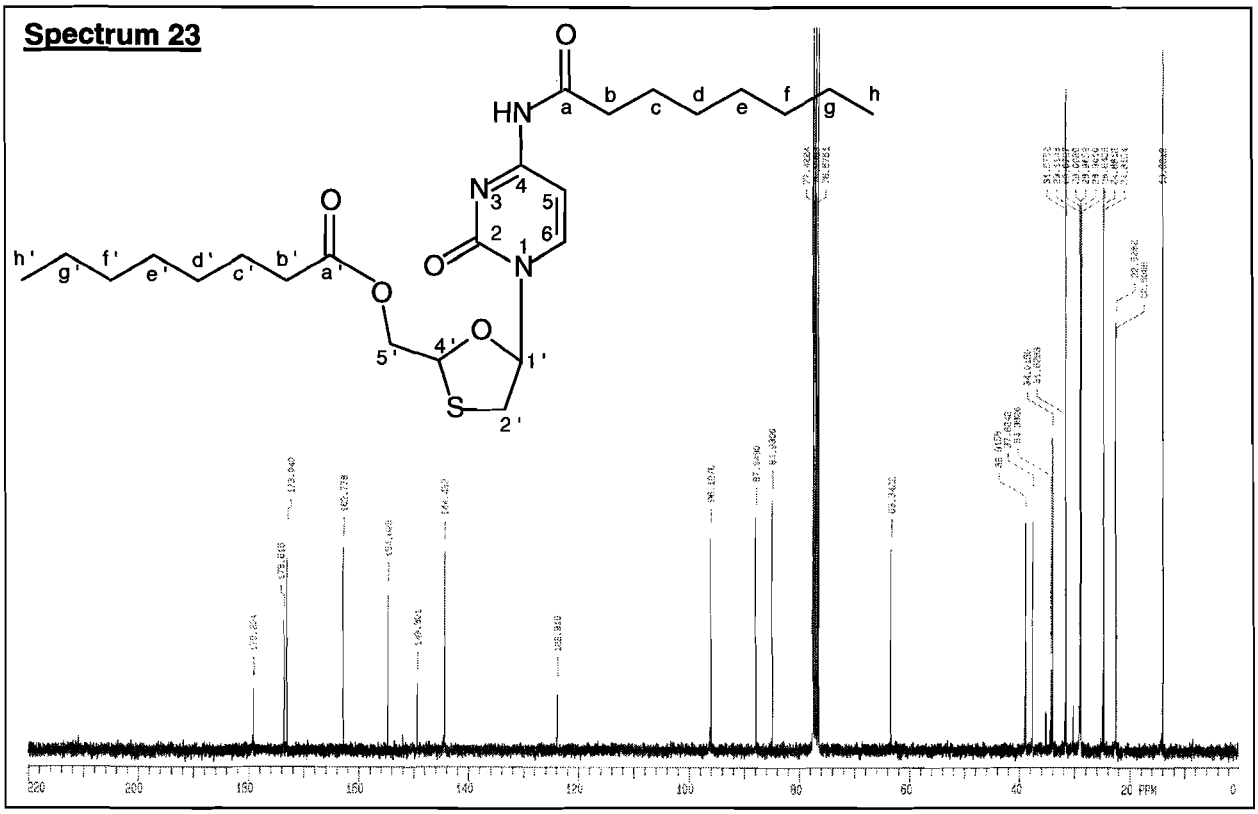

Spectrum 24

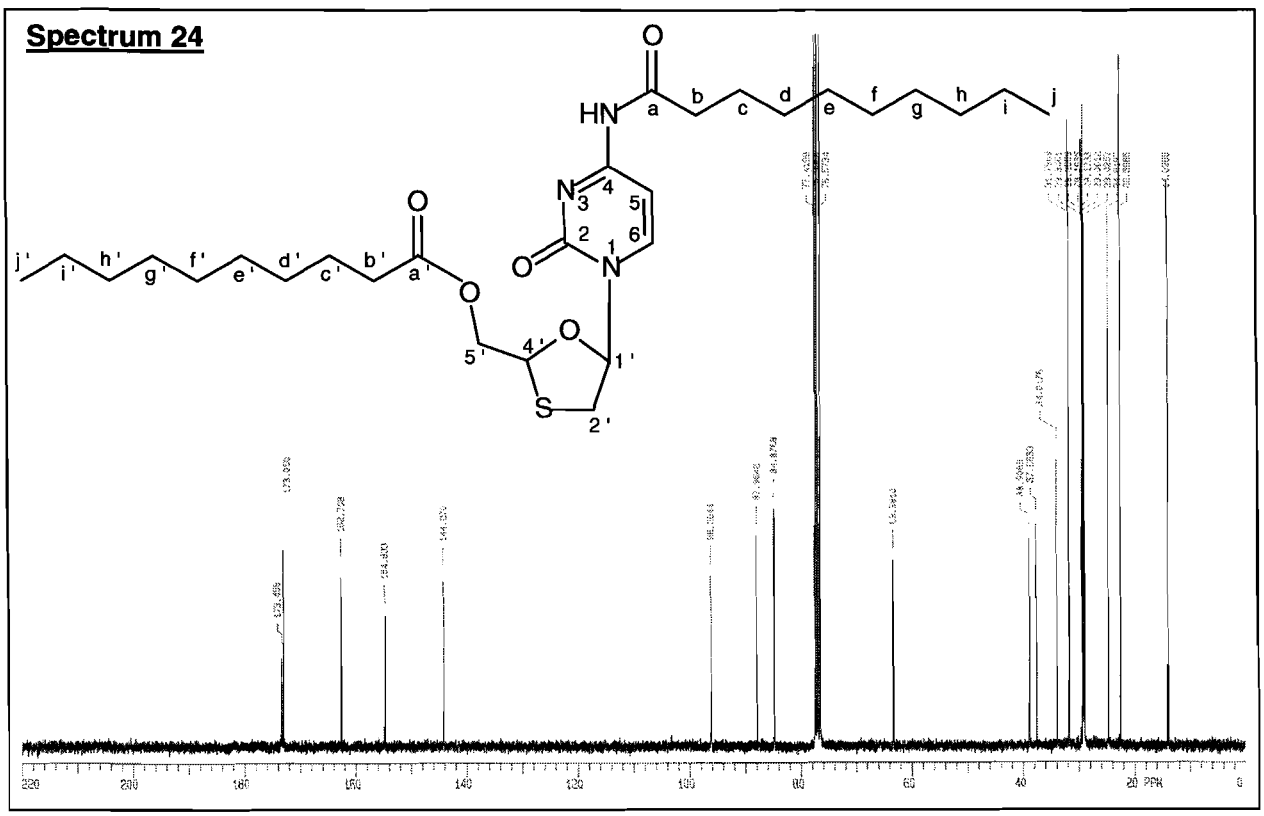

APPENDIX 1

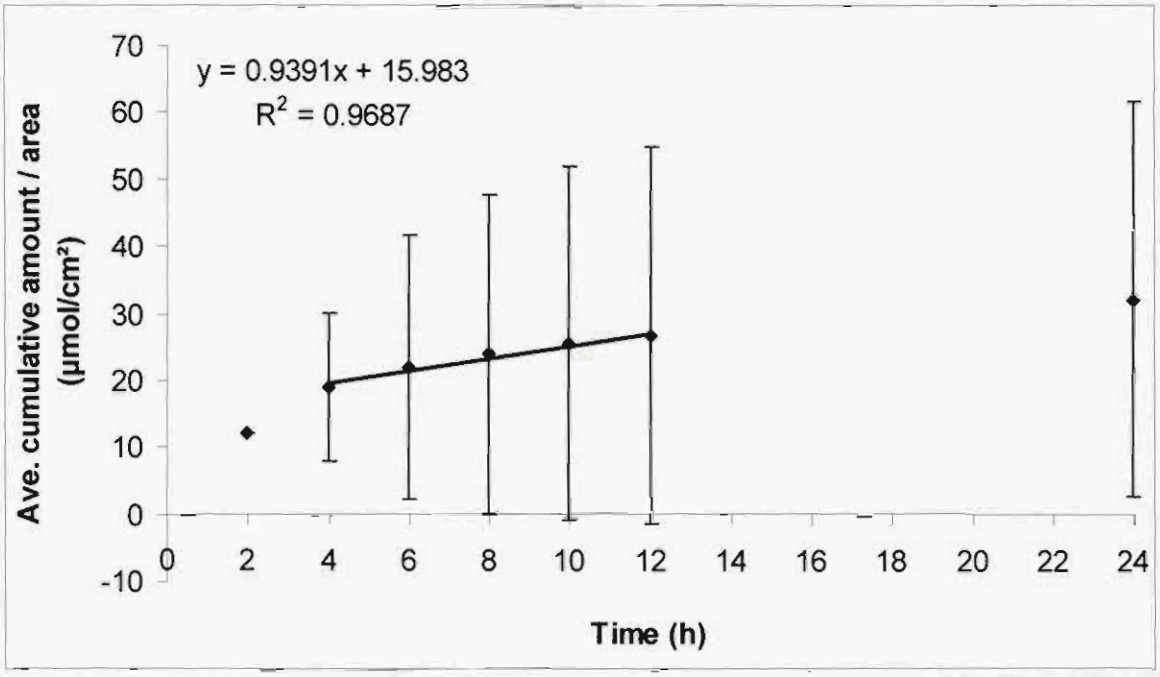

Figure A.1: Average cumulative amount of **(1)** in PBS that penetrated through the skin as a function of time to illustrate the average flux of **(1)**.

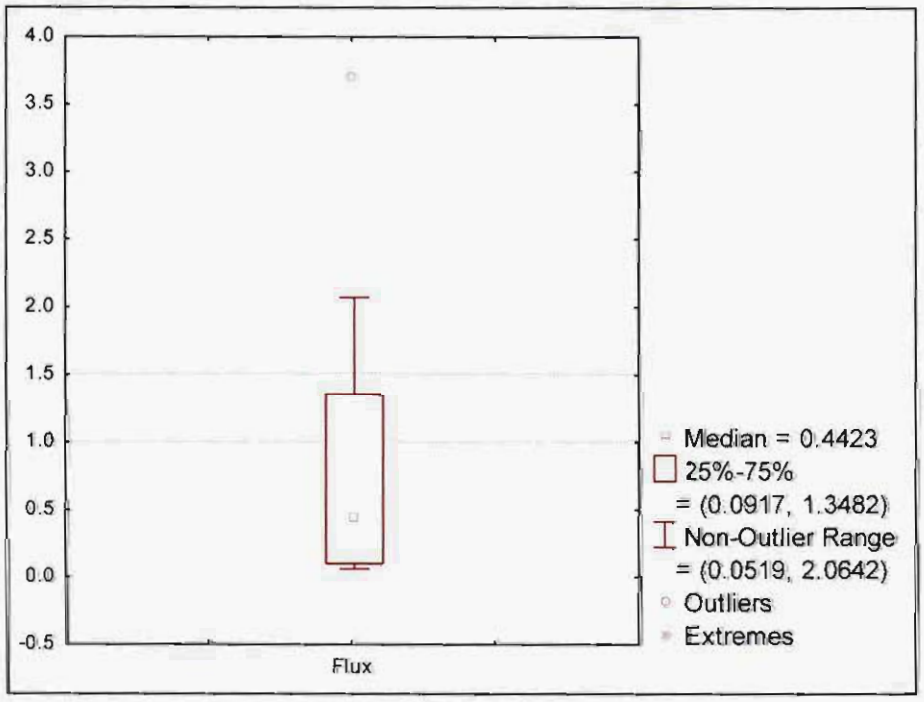

Figure A.2: Box-plot of the flux of **(1)** in PBS to illustrate the median flux and the skewness of data.

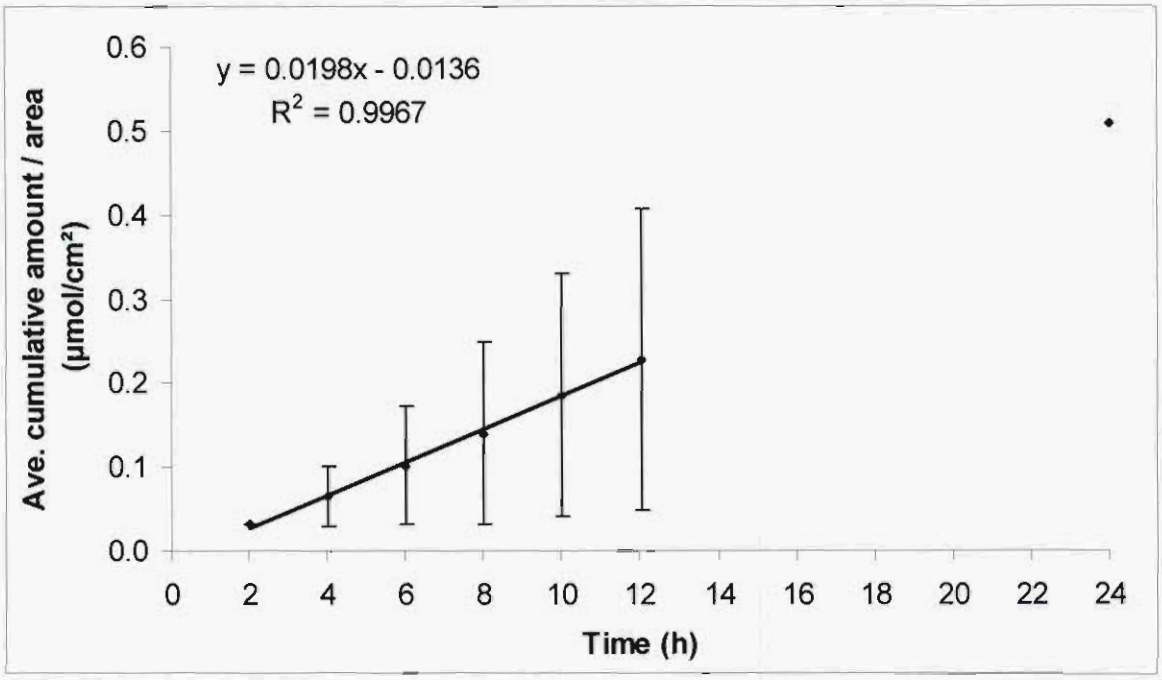

Figure A.3: Average cumulative amount of **(1)** in Pheroid™ that penetrated through the skin as a function of time to illustrate the average flux of **(1)**.

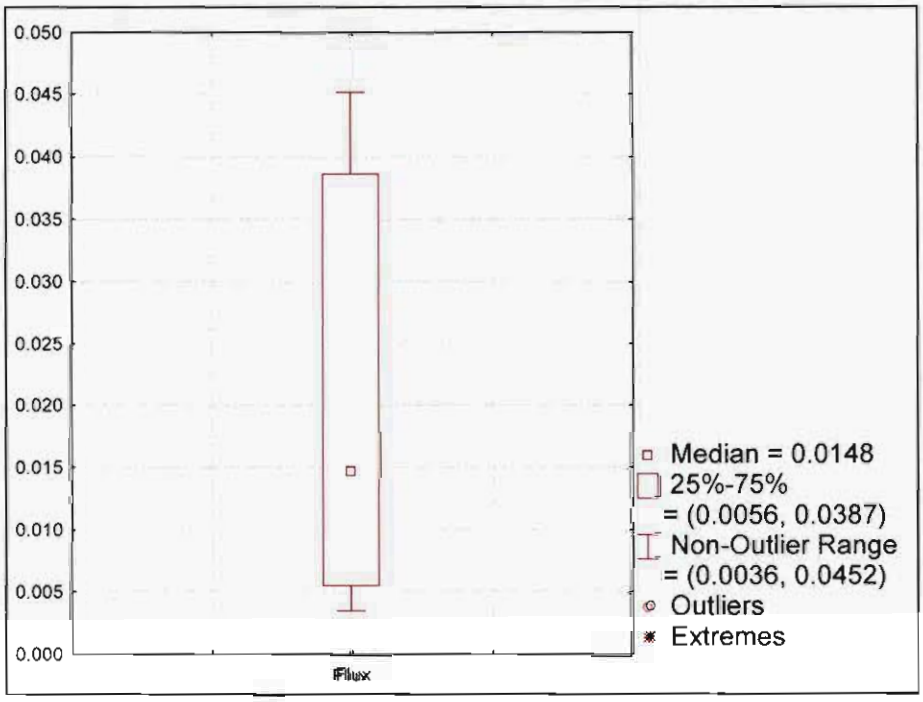

Figure A.4: Box-plot of the flux of **(1)** in Pheroid™ to illustrate the median flux and the skewness of data.

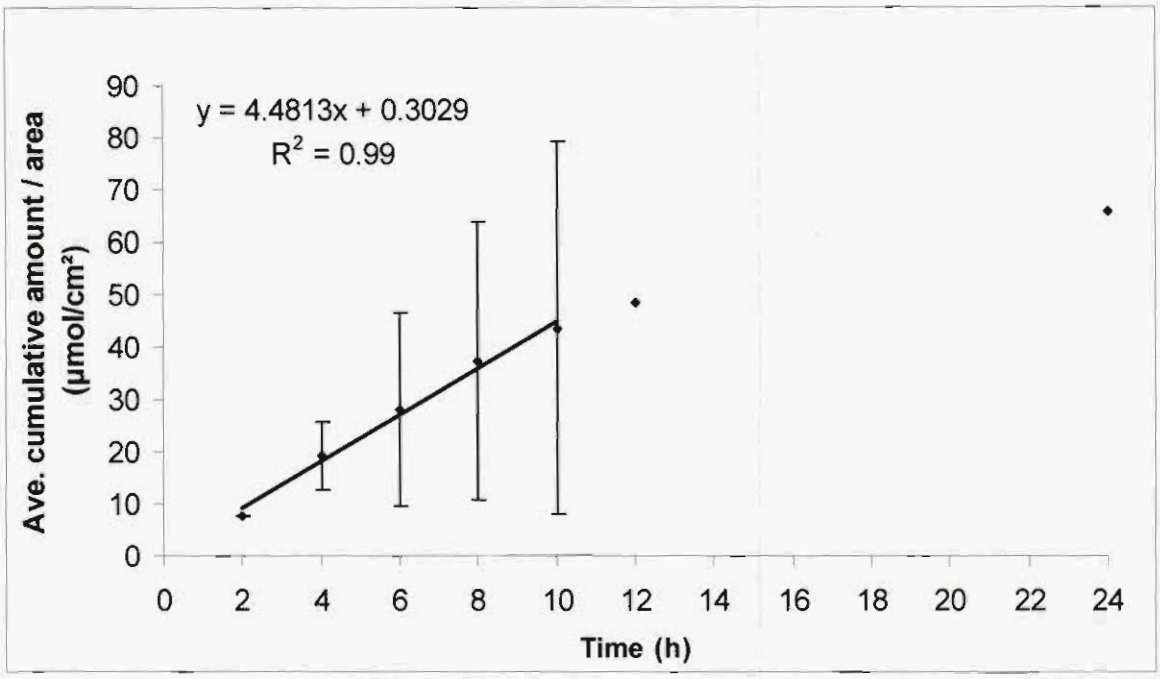

Figure A.5: Average cumulative amount of **(2)** in PBS that penetrated through the skin as a function of time to illustrate the average flux of **(2)**.

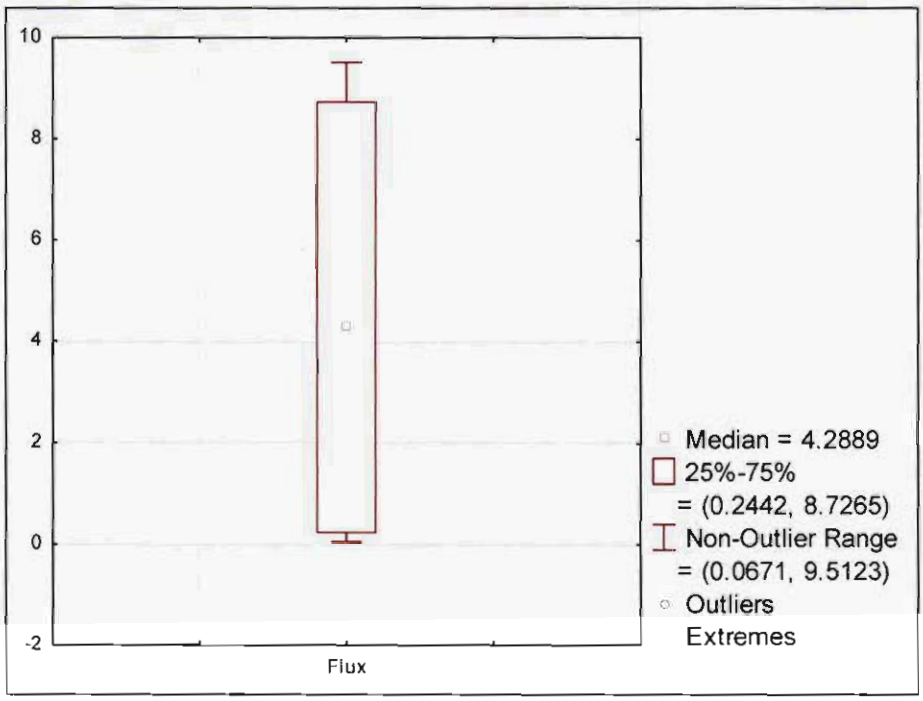

Figure A.6: Box-plot of the flux of **(2)** in PBS to illustrate the median flux and the skewness of data.

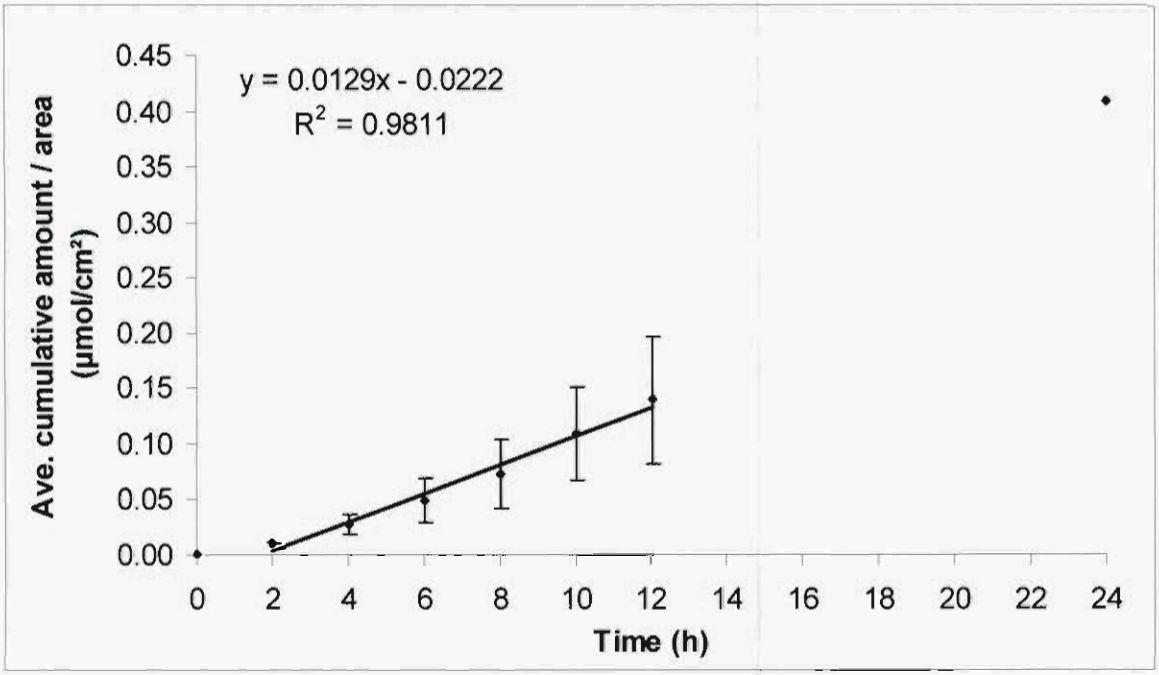

Figure A.7: Average cumulative amount of **(2)** in Pheroid™ that penetrated through the skin as a function of time to illustrate the average flux of **(2)**.

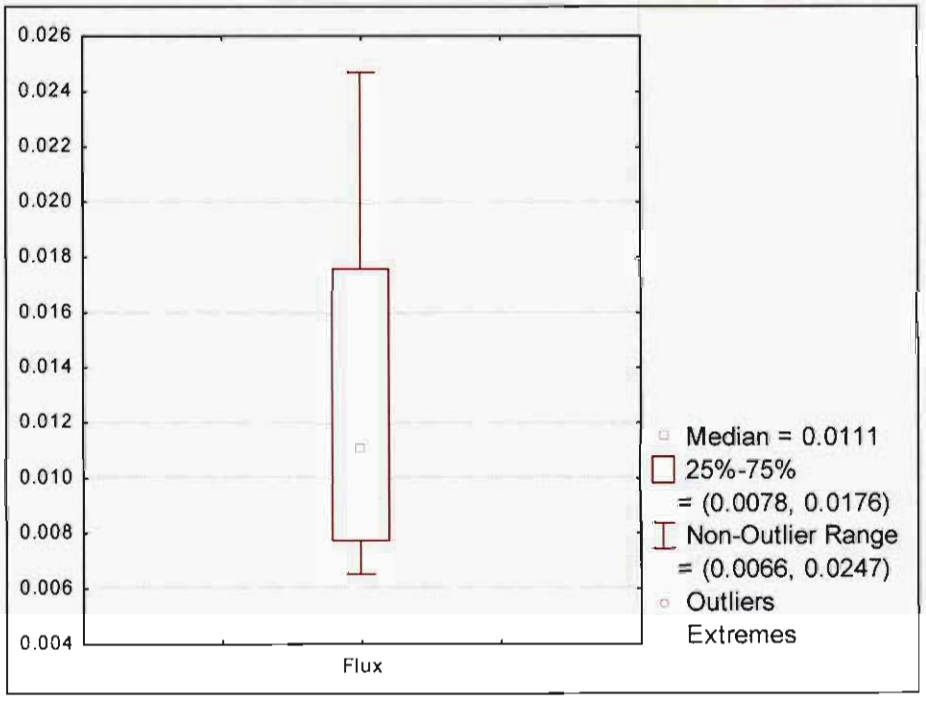

Figure A.8: Box-plot of the flux of **(2)** in Pheroid™ to illustrate the median flux and the skewness of data.

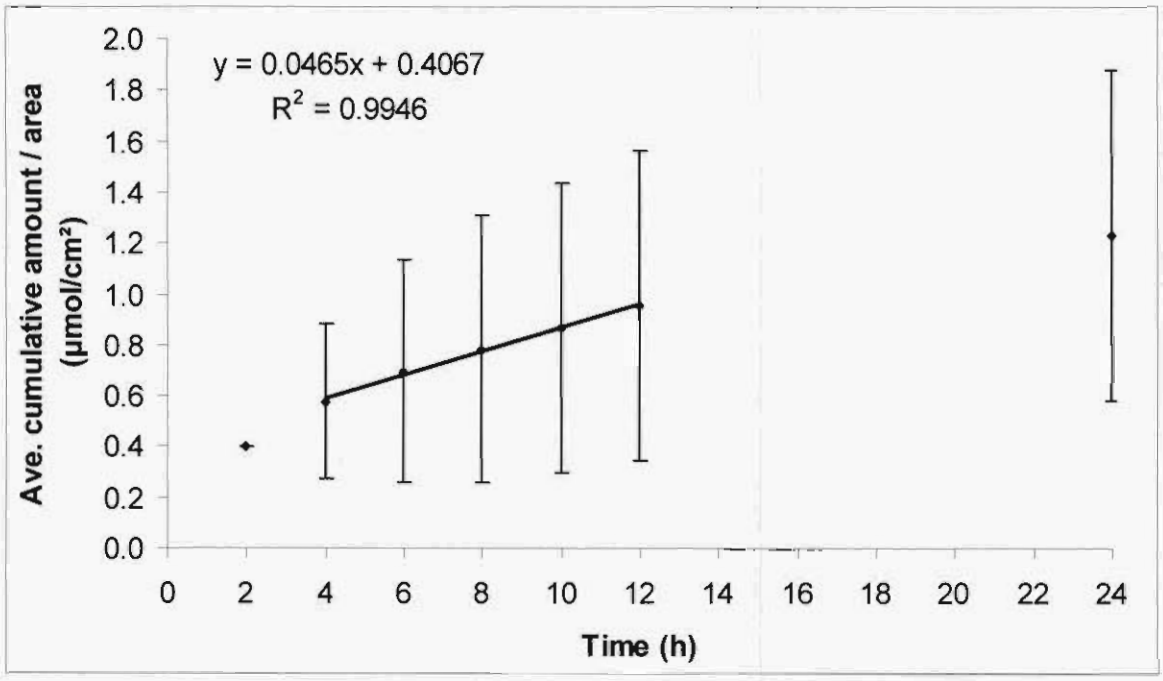

Figure A.9: Average cumulative amount of **(3)** in PBS that penetrated through the skin as a function of time to illustrate the average flux of **(3)**.

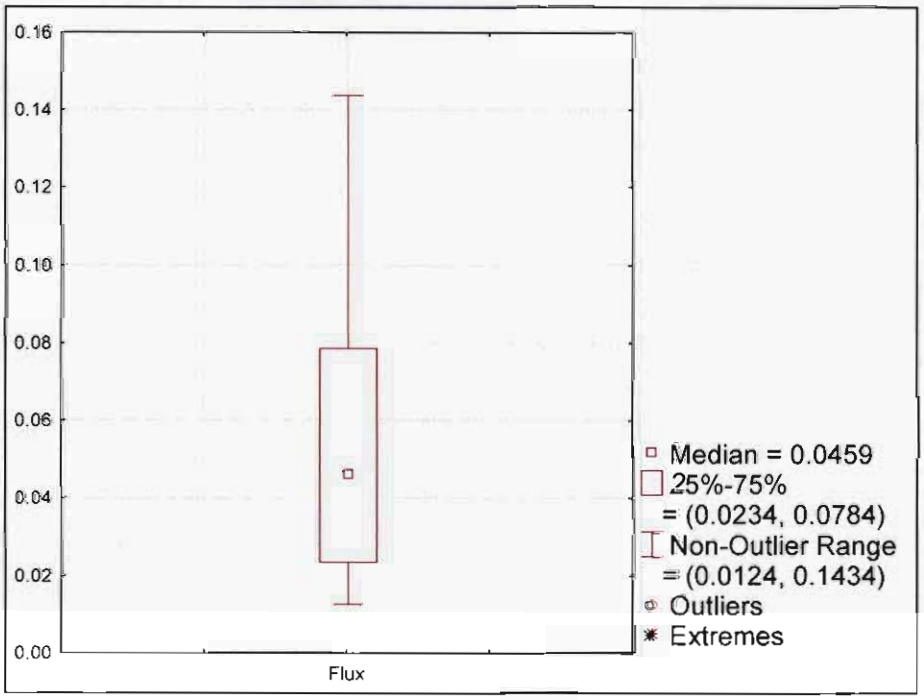

Figure A.10: Box-plot of the flux of **(3)** in PBS to illustrate the median flux and the skewness of data.

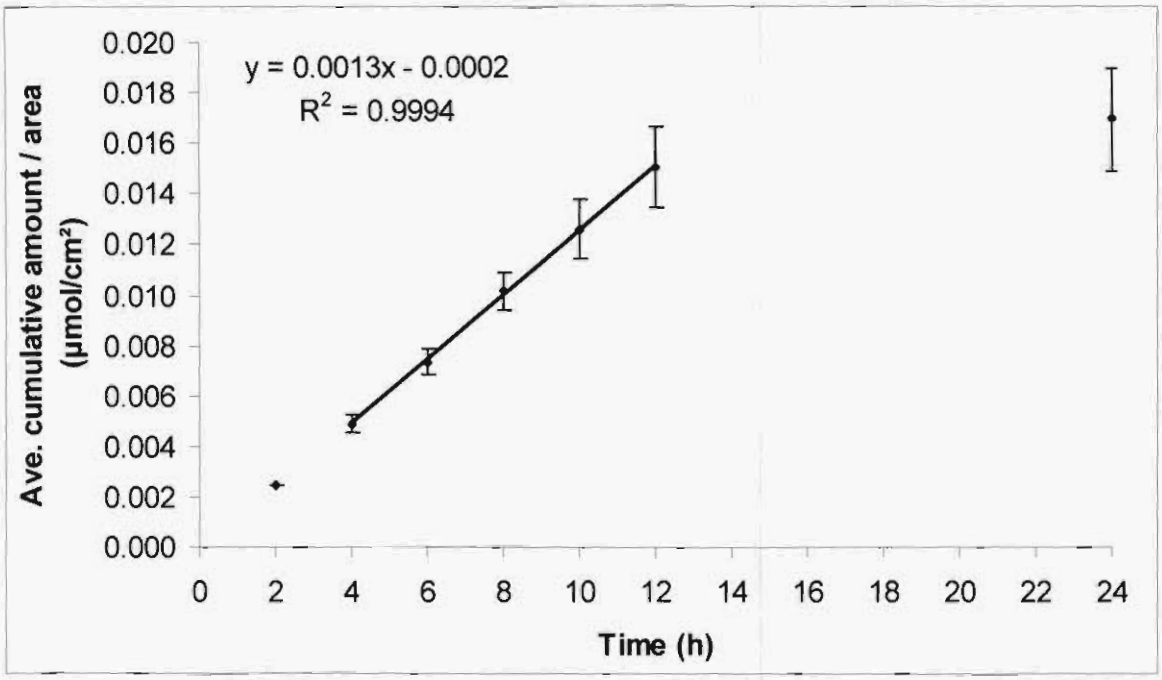

Figure A.11: Average cumulative amount of **(3)** in Pheroid™ that penetrated through the skin as a function of time to illustrate the average flux of **(3)**.

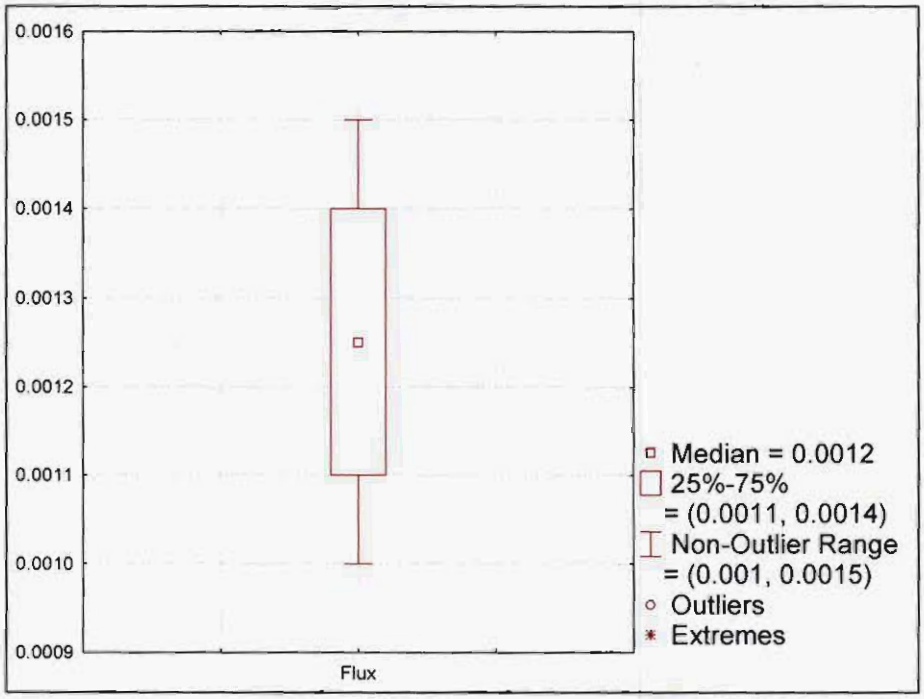

Figure A.12: Box-plot of the flux of **(3)** in Pheroid™ to illustrate the median flux and the skewness of data.

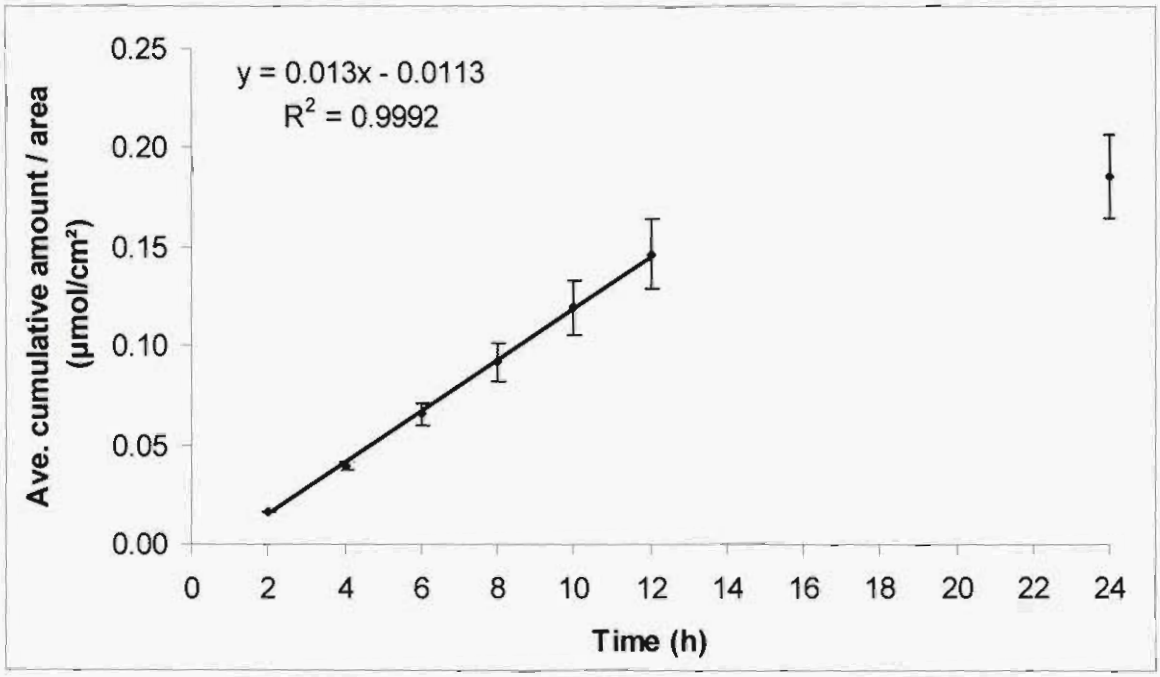

Figure A.13: Average cumulative amount of **(4)** in PBS that penetrated through the skin as a function of time to illustrate the average flux of **(4)**.

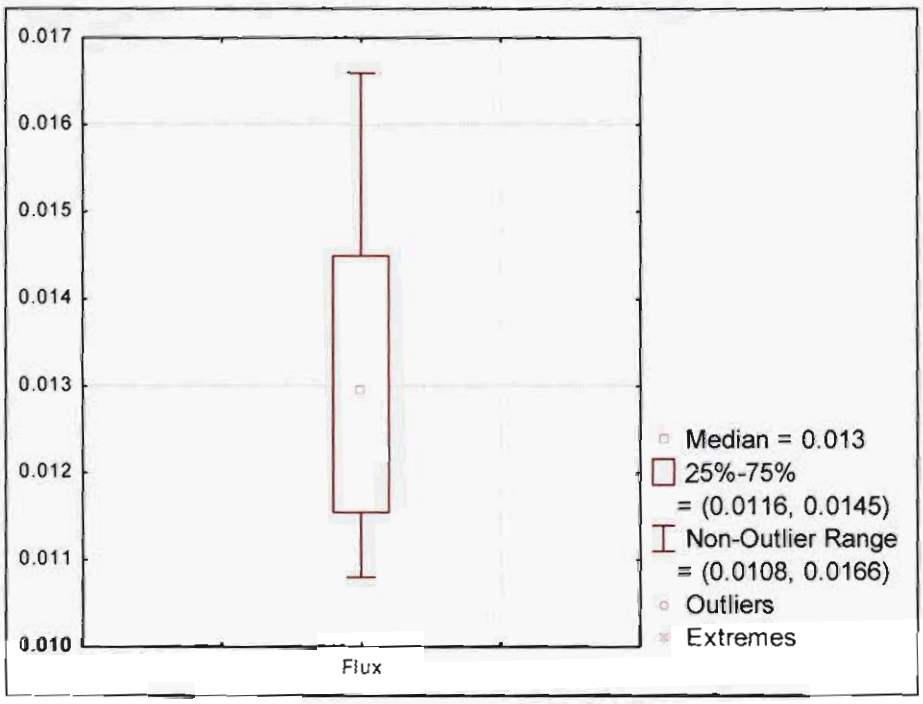

Figure A.14: Box-plot of the flux of **(4)** in PBS to illustrate the median flux and the skewness of data.

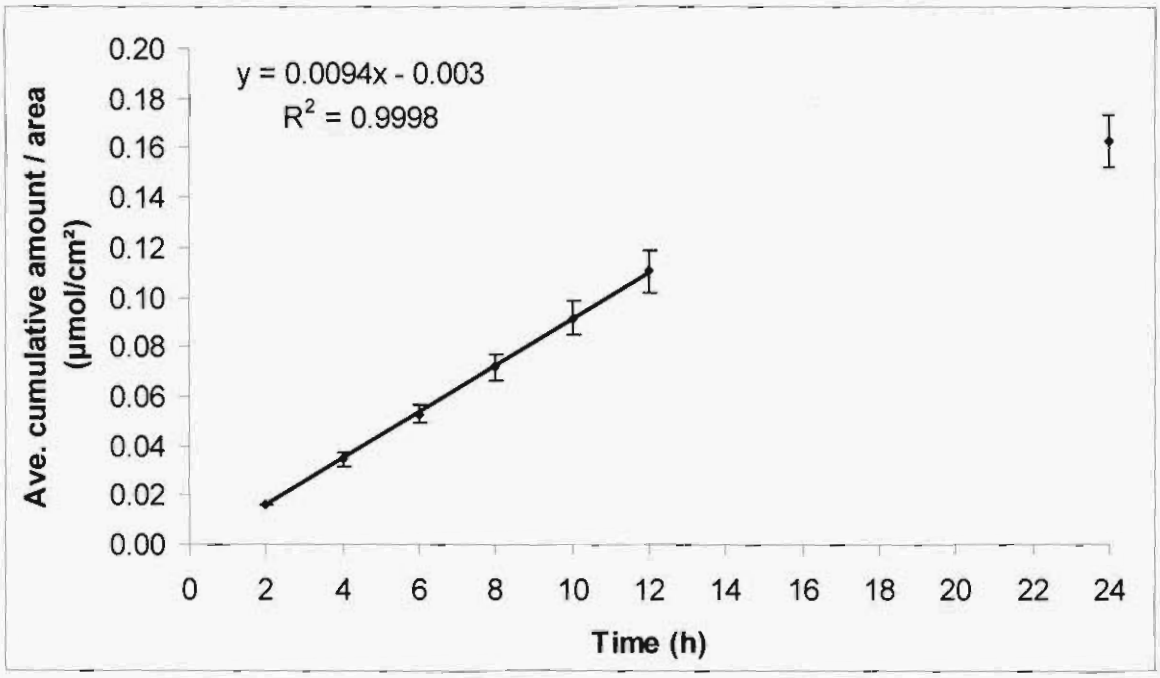

Figure A.15: Average cumulative amount of **(4)** in Pheroid™ that penetrated through the skin as a function of time to illustrate the average flux of **(4)**.

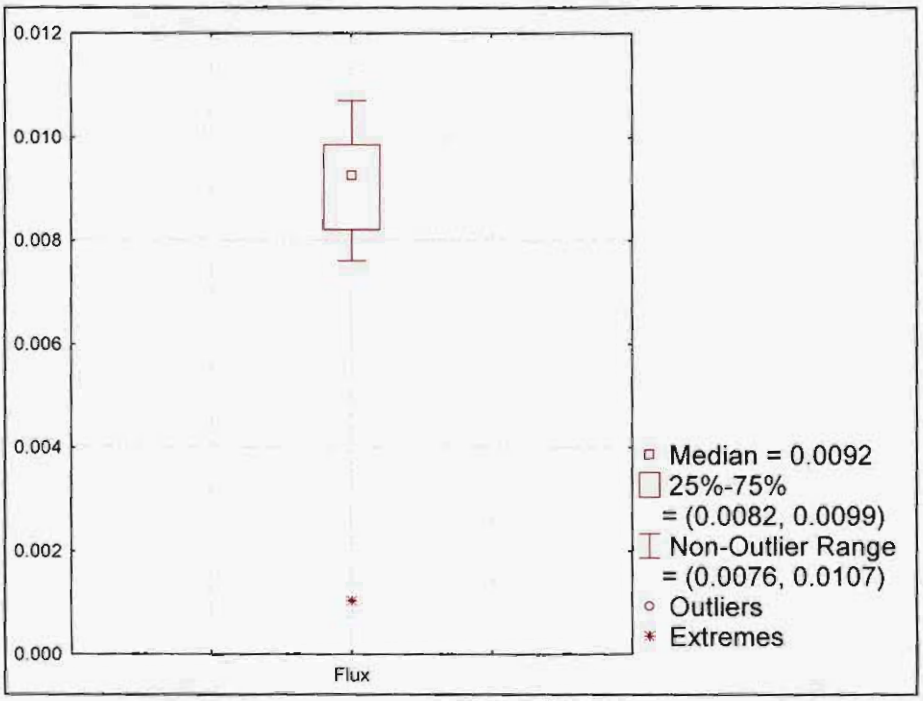

Figure A.16: Box-plot of the flux of **(4)** in Pheroid™ to illustrate the median flux and the skewness of data.

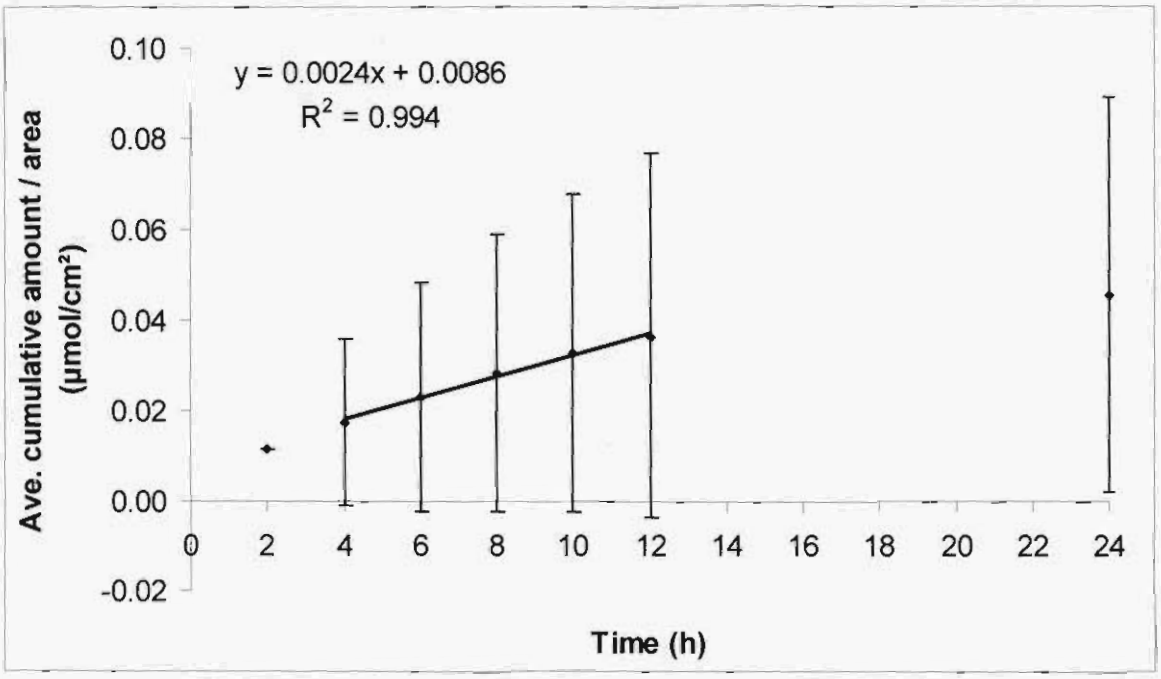

Figure A.17: Average cumulative amount of **(5)** in PBS that penetrated through the skin as a function of time to illustrate the average flux of **(5)**.

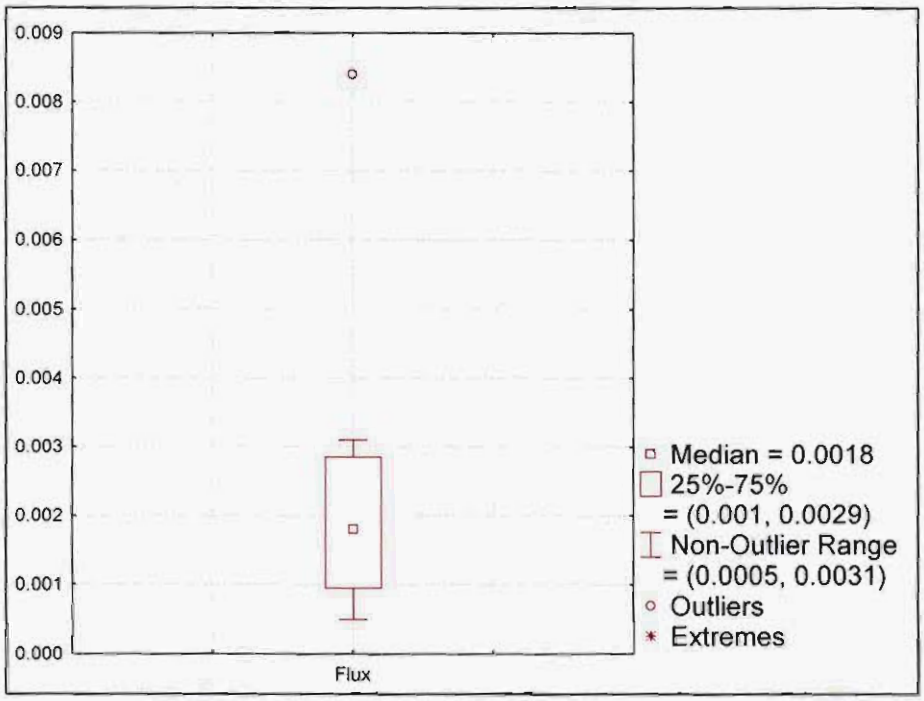

Figure A.18: Box-plot of the flux of **(5)** in PBS to illustrate the median flux and the skewness of data.

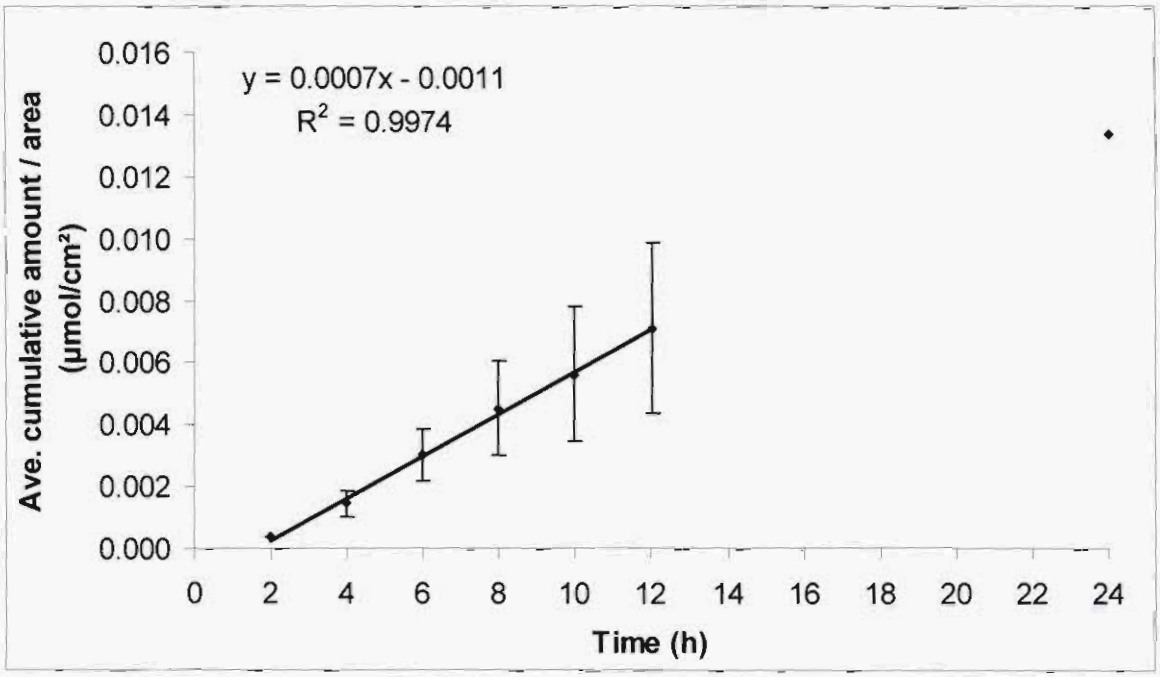

Figure A.19: Average cumulative amount of **(5)** in Pheroid™ that penetrated through the skin as a function of time to illustrate the average flux of **(5)**.

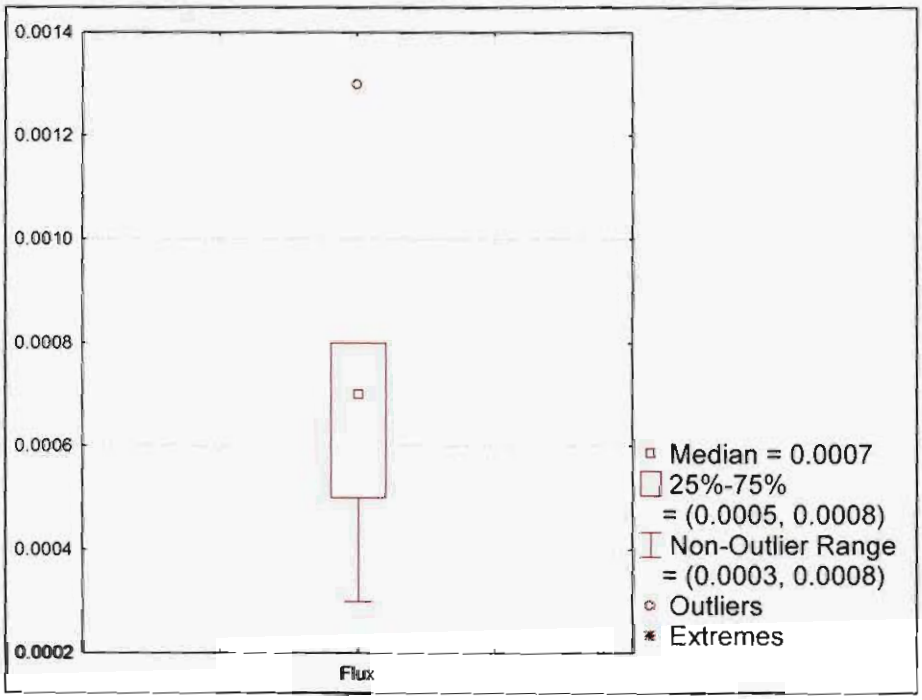

Figure A.20: Box-plot of the flux of **(5)** in Pheroid™ to illustrate the median flux and the skewness of data.

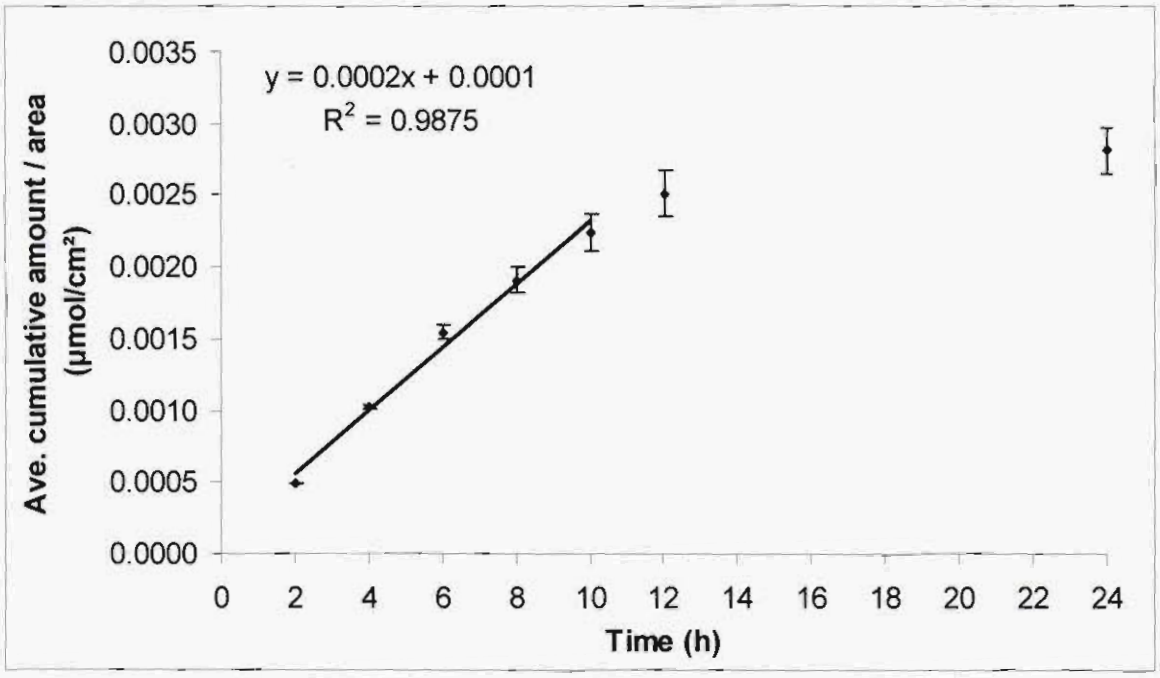

Figure A.21: Average cumulative amount of **(6)** in PBS that penetrated through the skin as a function of time to illustrate the average flux of **(6)**.

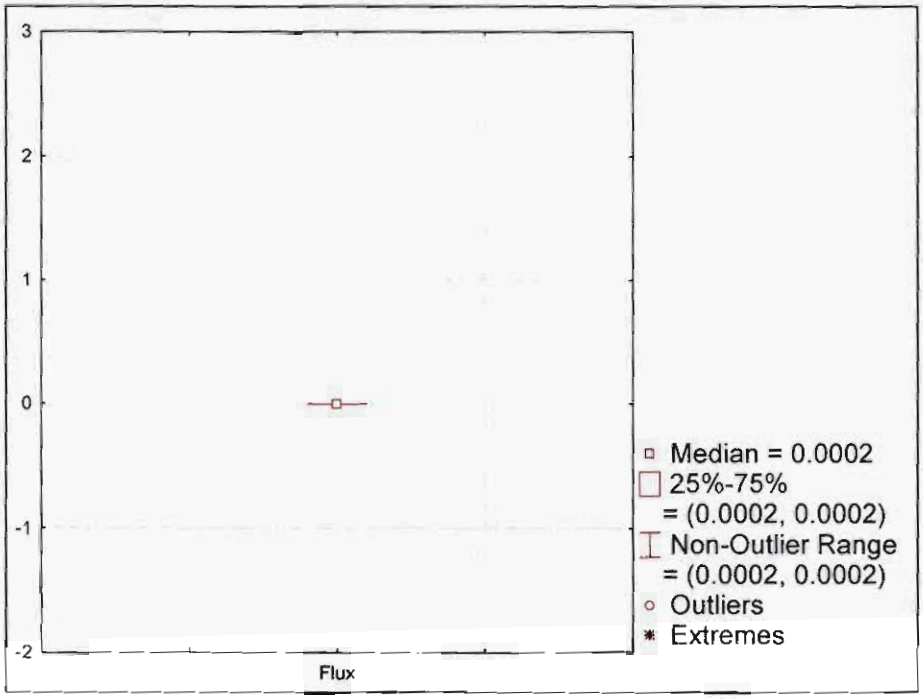

Figure A.22: Box-plot of the flux of **(6)** in PBS to illustrate the median flux and the skewness of data.

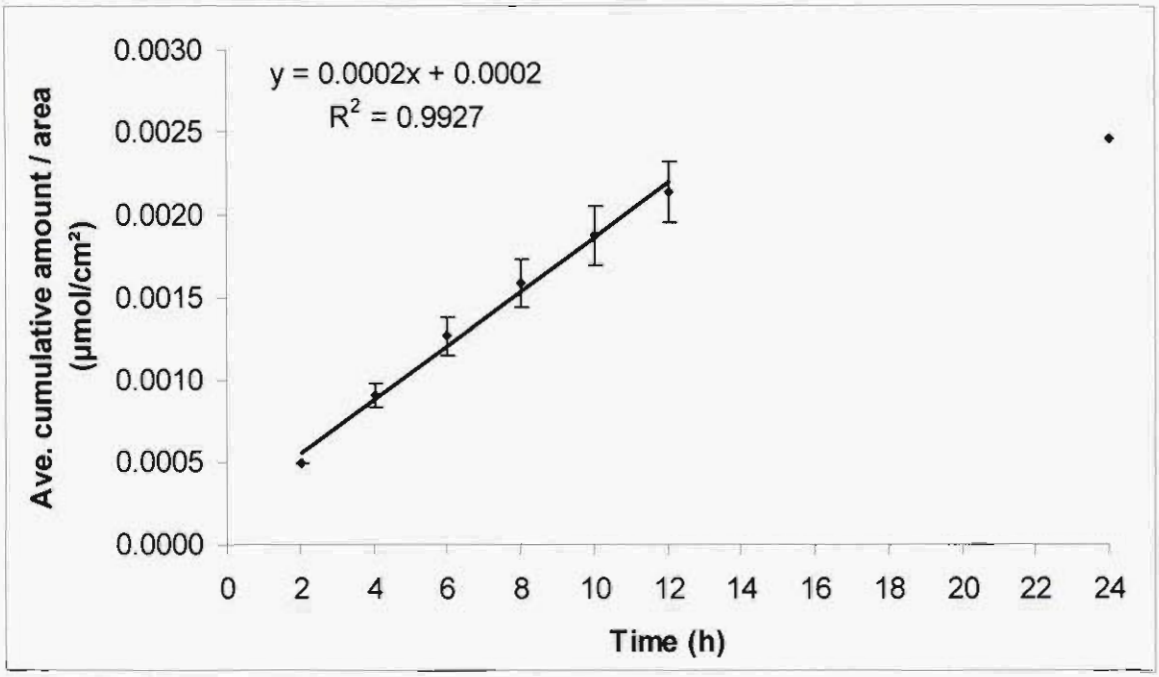

Figure A.23: Average cumulative amount of **(6)** in Pheroid™ that penetrated through the skin as a function of time to illustrate the average flux of **(6)**.

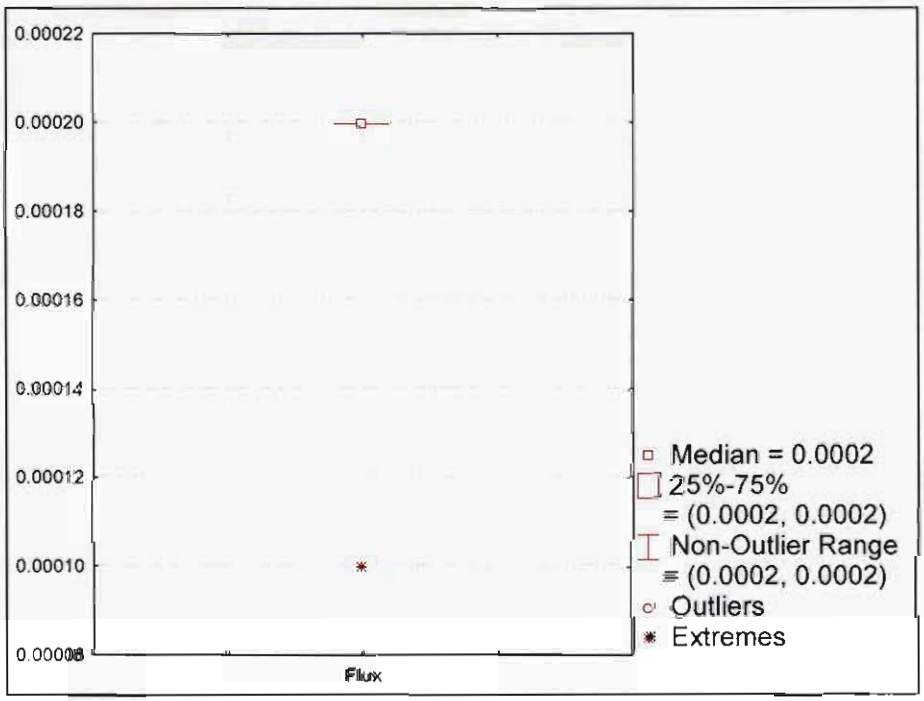

Figure A.24: Box-plot of the flux of **(6)** in Pheroid™ to illustrate the median flux and the skewness of data.